Nickel Catalyzed Cross-Electrophile-Coupling of Thioesters with Alkyl Bromides under Mechanochemical Conditions

SUPPORTING INFORMATION

Ivo H. Lindenmaier[*a], Robert C. Richter[*a], Liesa Renz[a], Mattis T. Vochezer[a], Marius Schier[a], Pascal Faßnacht[a], Markus Ströbele[b] and Ivana Fleischer[a]

[a] Institute of Organic Chemistry, Faculty of Science,
Eberhard Karls Universität Tübingen, Auf der Morgenstelle 18, 72076 Tübingen, Germany
ivana.fleischer@uni-tuebingen.de

[b] Institute of Inorganic Chemistry, Faculty of Science,
Eberhard Karls Universität Tübingen, Auf der Morgenstelle 18, 72076 Tübingen, Germany.

Table of Contents

1. General Information 3
1.1 Chemicals and General Techniques 3
1.2 Analytical Techniques 3
2. General Procedures 5
3. Screening Information 7
3.1 Ligand Screening 7
3.1 LAG Additive Screening 9
3.1 Nickel-Source Screening 10
3.1 Reductant Screening 11
3.1 Additive Screening 12
3.1 Reaction Time Screening 16
4. Mechanistic Studies 17
4.1 Radical Clock Experiment 17
4.2 Radical Scavengers 17
4.3 Side Products 18
4.4 Oxidative addition complex 19
4.5 Nickel Zincate Complex 20
5. Analytical Data 21
5.1 Synthesis of Nickel Complexes. 21
5.2 Synthesis of Thioester 28
5.3 Synthesis of Ketones 73
6. Unsuccessful Substrates 154
7. Crystallographic Data 155
8. GC-FID Calibration Data 156
9. References 159

1. General Information

1.1 Chemicals and General Techniques

With exception of mechanochemical XEC reactions, which were conducted without taking special precautions towards the reaction atmosphere, substrate syntheses and mechanistic experiments were carried out under an argon atmosphere unless denoted otherwise using standard Schlenk techniques or an argon atmosphere Glovebox (GS MEGA E-Line, Glovebox Systemtechnik) and pre-dried glassware. Dry solvents (THF, *n*-hexane, DCM) were prepared using a solvent-purification-system (MB-SPS5, MBraun) and stored over 3 Å molsieves. Column chromatography was carried out on a Puriflash system (Interchim XS420) using pre-packed columns (30 or 50 µm) from Büchi. Thin Layer Chromatography was performed on silica gel coated glass plates (0.25 mm) with fluorescence indicator UV254 (Macherey-Nagel, TLC plates SIL G-25 UV254). For detection of spots, irradiation of UV light at 254 nm or a stain of $KMnO_4$ was used. Chemicals were purchased from abcr, Acros, Alfa Aesar, BLDChem, Carbolution Chemicals, Carl Roth, Fluorochem, Sigma-Aldrich or TCI and used as received.

Mechanochemical reactions were carried out in a MM400 mixer mill from Retsch in stainless steel milling jars (10 mL) using two stainless steel balls (4 g). The temperature of the jars typically rose to approximately 35 °C during the reaction due to kinetic energy. No precautions to heat or cool the device were taken.

1.2 Analytical Techniques

NMR spectra were recorded using Bruker Avance III HD 400 or Bruker Avance III HDX 700 at room temperature (400 or 700 MHz for ^{1}H experiments; 101 or 176 MHz for ^{13}C experiments; 376 MHz for ^{19}F experiments) in commercially available deuterated solvents. ^{13}C NMR experiments were performed with broadband proton-decoupling. Chemical shifts (δ) are reported in ppm relative to the residual NMR solvent signals (chloroform: ^{1}H 7.26 ppm and ^{13}C 77.16 ppm).[1] Hetero-NMR chemical shifts are given relative to external standards (^{19}F: $CFCl_3$). The coupling constants (*J* values) are given in Hz and spin multiplicity with the usual designations for splitting patterns (s = singlet, d = doublet, t = triplet, q = quartet, m = multiplet).

HR-MS (ESI, APCI) measurements were carried out by the mass spectrometry department of the Institute of Organic Chemistry, University of Tübingen. Measurements were carried out using maXis 4G from Bruker (ESI, APCI) or Q-exactive HF from Thermo Scientific (ESI). The molecular ions $[M+H]^+$ and $[M+Na]^+$ respectively are given in m/z units.

GC-FID (flame ionization detection) analysis was carried out on an Agilent 7820A system using dry hydrogen as carrier gas. An Agilent 19091J-431 column (30 m × 320 µm × 0.25 µm) was used. Program: heating from 35 °C to 280 °C within 53 minutes (5 °C/min, 4 min hold time). Conversion and yield were determined *via* calibration against the internal standard *n*-pentadecane.

Melting point determination was achieved by using a Büchi B-540 machine with a visual detection (heating rate 5 °C/min).

FT-IR spectra were recorded using a Cary 630 FTIR by applying the sample neat on a diamond ATR sampler.

Elemental analyses were performed on an Elementar Vario MICRO cube.

2. General Procedures

General Procedure A1 (GP-A1): Synthesis of *S*-phenyl thioesters from acid chlorides.

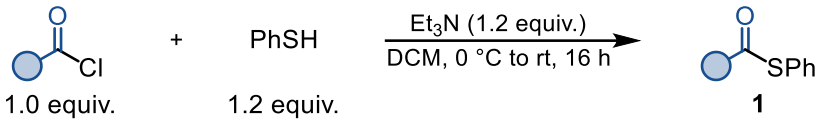

S-phenyl thioesters were synthesized according to literature.[2] In a RBF, Et_3N (1.2 equiv.) and the respective acid chloride (1.0 equiv.) were added to a stirred and cooled DCM (0.4 M) solution (0 °C) of thiophenol (1.2 equiv.). After 30 min, the mixture was allowed to warm to rt and stirred overnight. The reaction was quenched with water (20 mL) and the aqueous phase was extracted with DCM (2 × 30 mL). The combined organic phases were washed with $HCl_{(aq.)}$ (1 M, 20 mL), sat. $NaHCO_{3(aq.)}$ (20 mL), and brine (20 mL) and dried over $MgSO_4$. After solvent removal *in vacuo* the crude product was purified by recrystallization or flash column chromatography.

Note: Schlenk conditions were applied for alkyl acid chlorides.

General Procedure A2 (GP-A2): Synthesis of *S*-phenyl thioesters by Steglich esterification.

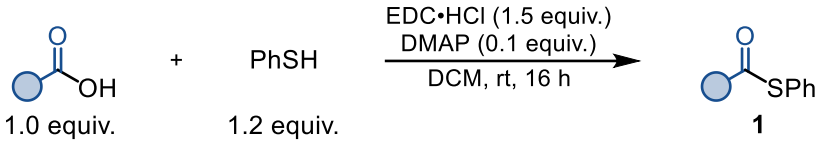

S-phenyl thioesters were synthesized according to literature with slight modifications.[3] In a Schlenk RBF, the respective carboxylic acid (10 mmol, 1.0 equiv.), EDC•HCl (1.5 equiv.), and DMAP (0.1 equiv.) were stirred in DCM (50 mL) for 10 min. Subsequently, thiophenol (1.2 equiv.) was added and the mixture was stirred overnight. The reaction was quenched with water (20 mL), and the aqueous phase was extracted with DCM (3 × 30 mL). The combined organic phases were dried over $MgSO_4$, concentrated *in vacuo* and purified by flash column chromatography.

General Procedure B (GP-B): Nickel-catalyzed XEC of *S*-phenyl thioesters with alkyl bromides under mechanochemical conditions (scope).

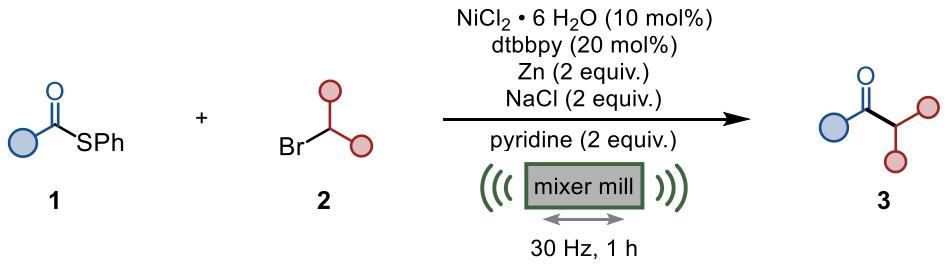

A 10 mL stainless steel milling jar was charged with $NiCl_2 \cdot 6H_2O$ (23.8 mg, 0.1 mmol, 10 mol%), 4,4'-(di-*tert*-butyl)-2,2'-bipyridine (dtbbpy, 53.7 mg, 0.2 mmol, 20 mol%), zinc (131 mg, 2.0 mmol, 2.0 equiv.), NaCl (117 mg, 2.0 mmol, 2.0 equiv.), *S*-phenyl thioester (1.0 mmol, 1.0 equiv.), alkyl bromide (2.0 mmol, 2.0 equiv.), pyridine (161 µL, 2.0 mmol, 2.0 equiv.) and two stainless steel balls (⌀ = 10 mm, m = 4 g). The milling jar was closed, placed in a MM 400 and shaken at 30 Hz for 1 h. Subsequently, the jar was opened and rinsed with EtOAc (10 mL). Volatiles were removed *in vacuo* and the residue was subjected to flash column chromatography (*n*-hexane/EtOAc) for purification.

General Procedure C (GP-C): Optimization of the nickel-catalyzed XEC of *S*-phenyl benzothioate with hydrocinnamyl bromide under mechanochemical conditions.

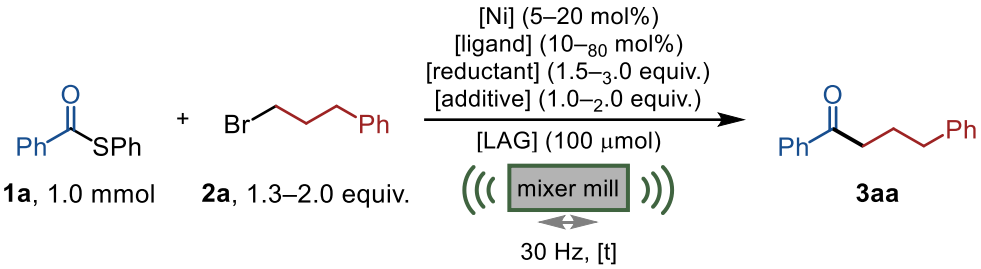

A 10 mL stainless steel milling jar was charged with the respective nickel source (5–20 mol%), ligand (10–80 mol%), *S*-phenyl benzothioate (1.0 mmol, 1.0 equiv.), reductant (1.5–3.0 equiv., if solid), potential additive (1.0–2.0 equiv., if solid) and two stainless steel balls (⌀ = 10 mm, m = 4 g). Subsequently, all liquid components: hydrocinnamyl bromide (1.3–2.0 equiv.), LAG additive (100 µL), reductant (3.0 equiv., if liquid) and potential additive (0.3–3.0 equiv., if liquid) were added. The milling jar was closed, placed in a MM 400 and shaken at 30 Hz for the respective time (0.25–2 h). After the reaction, the jar was opened and *n*-pentadecane and EtOAc were added. An aliquot was taken and filtered through Celite, Al_2O_3 and $MgSO_4$, before being analyzed by GC-MS/FID.

3. Screening Information

3.1 Ligand Screening

The optimization of the reaction was initiated with a ligand screening, evaluating a total of 16 nitrogen-based, two phosphine, and one *N*-heterocyclic carbene (NHC) ligands under mechanochemical conditions. Among the ligands tested, the bidentate nitrogen ligands dtbbpy (**L12**) and phen (**L7**) provided the highest yields, affording the desired ketone in 54% and 44% yield, respectively (Table S 1, entries 1 and 2).

Several other bidentate ligands from the phenanthroline and bipyridine families (**L8**, **L11** and **L13**–**L15**) gave low to moderate yields (20–34%) despite achieving high conversions of the thioester **8** (Table S 1, entries 3–5, 7, 8). In contrast, sterically demanding phen-type ligands such as bathocuproine (**L10**) and neocuprine (**L9**) led to severely diminished yields (Table S 1, entries 15 and 16), suggesting that increased bulk hinders catalyst performance. Related bidentate nitrogen ligands such as BOX (**L16**) and PyOX (**L17**) delivered comparable but limited yields (22% and 20%, respectively; Table S 1, entries 6 and 9). Tridentate ligands, including terpyridine (**L20**), along with PyBOX derivatives (**L18**, **L19**), showed uniformly poor reactivity, affording less than 20% yield (Table S 1, entries 10–12, 14). Furthermore, **L21** furnished no observable product (Table S 1, entry 20). Similarly, the monodentate pyridine (**L6**) failed to efficiently promote the transformation, resulting in a mere 4% yield (Table S 1, entry 13).

Phosphine-based ligands, including PPh_3 (**L23**) and dppf (**L24**), as well as the NHC ligand (**L22**), were ineffective under the reaction conditions, delivering only trace amounts of the desired product (<2%, Table S 1, entries 17–19).

Table S 1. Ligand screening for the nickel catalyzed XEC of an alkyl bromide with a *S*-phenyl thioester mediated by mechanochemistry.

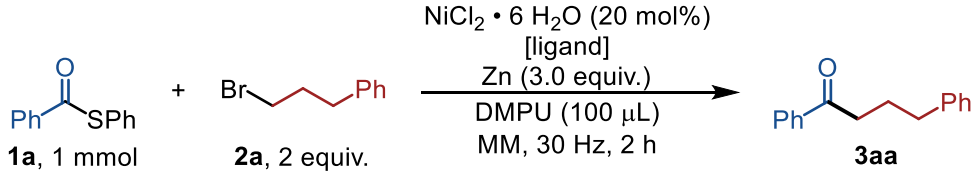

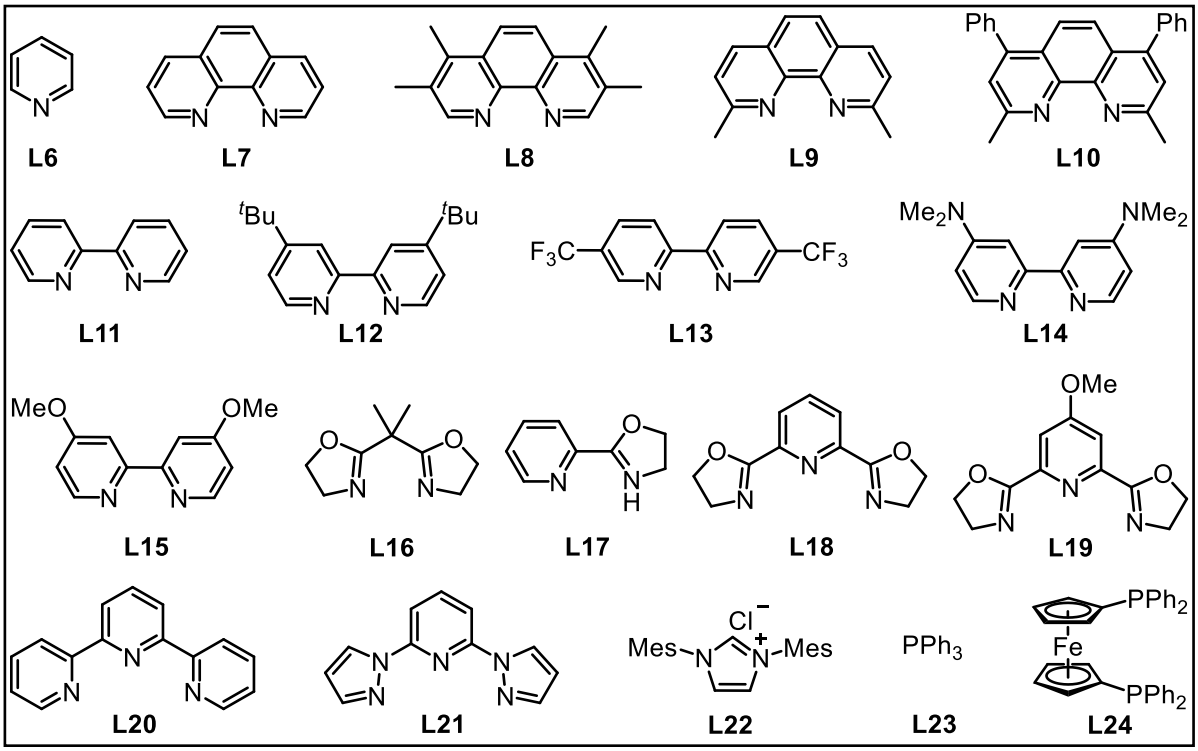

Entry	Ligand / Loading (mol%)		Yield (%)[a]	Conversion 1a / 2a (%)[a]	
1	dtbbpy (**L12**)	40	54	quant.	63
2	phen (**L7**)	40	44	55	36
3	$^{3,4,7,8\text{-Me}}$phen (**L8**)	40	34	43	36
4	$^{5,5'\text{-CF3}}$bpy (**L13**)	40	29	quant.	6
5	bpy (**L11**)	40	24	86	46
6	BOX (**L16**)	40	22	62	19
7	$^{4,4'\text{-NMe2}}$bpy (**L14**)	40	21	38	38
8	$^{4,4'\text{-OMe}}$bpy (**L15**)	40	20	25	21
9	PyOX (**L17**)	40	20	25	32
10	Terpy (**L20**)	40	19	52	81
11	Terpy (**L20**)	20	17	48	69
12	$^{4\text{-OMe}}$PyBOX (**L19**)	40	9	31	27
13	Pyridine (**L6**)	80	4	25	53
14	PyBOX (**L18**)	40	4	86	28
15	Neocuprine (**L9**)	40	2	59	31

16	Bathocuproine (**L10**)	40	1	53	23
17	IMes•HCl[b] (**L22**)	20	1	30	62
18	PPh_3 (**L23**)	40	1	33	40
19	dppf (**L24**)	20	1	34	36
20	bpp (**L21**)	40	0	31	19

Reaction conditions: **1a** (1 mmol, 1.0 equiv.), **2a** (2.0 equiv.), $NiCl_2(H_2O)_6$ (20 mol%), ligand (20 – 80 mol%), Zn (3 equiv.), DMPU (100 µL), MM (30 Hz, 2 h). [a]Determined by GC-FID using *n*-pentadecane as an internal standard. [b]Cs_2CO_3 (40 mol%).

3.1 LAG Additive Screening

Following the identification of **L7** and **L12** as the most effective ligands, a screening of liquid-assisted grinding (LAG) additives was conducted to assess their impact on reaction efficiency (Table S 2). Amide- and urea-derived solvents proved most effective for both ligands, with DMPU delivering the highest yields (24–54%;Table S 2, entries 1, 3, 6, 17).

MeOH also performed well: 31% with **L7** and 47% with **L12** (Table S 2, entries 4 and 23), prompting further investigations into alcoholic solvents. An inverse correlation between steric bulk and reactivity was observed. More hindered alcohols such as ^{i}PrOH and ^{t}BuOH resulted in lower yields (Table S 2, entries 8 and 10), while EtOH gave moderate results (27%; Table S 2, entry 5). Among other solvents, MeCN showed fair activity (22%; Table S 2, entry 7), whereas THF, toluene, H_2O, HFIP, and PhCN all led to poor yields (9–15%; Table S 2, entries 9, 11–14).

In solvent mixtures, a 1:1 ratio of DMA/MeOH with **L7** slightly improved the yield (49%; Table S 2, entry 15). However, all tested mixtures using **L12**, including MeOH/DMA, DMPU/MeOH, and DMA/EtOAc, led to marginally reduced yields compared to neat DMPU (Table S 2, entries 24–26).

Table S 2. LAG additive screening for the nickel catalyzed XEC of an alkyl bromide with a *S*-phenyl thioester mediated by mechanochemistry.

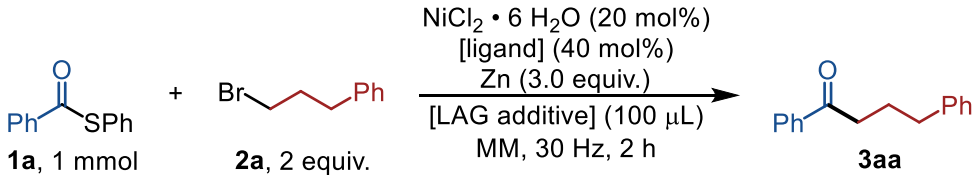

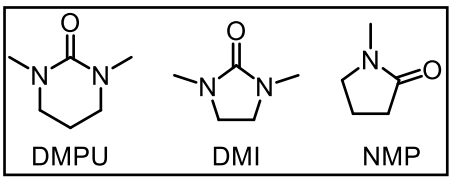

Entry	LAG	Ligand	Yield (%)[a]	Conversion 1a / 2a (%)[a]

1	DMPU	**L7**	44	55	36
2	NMP	**L7**	32	54	37
3	DMF	**L7**	32	67	35
4	MeOH	**L7**	31	62	25
5	EtOH	**L7**	27	54	26
6	DMI	**L7**	24	48	26
7	MeCN	**L7**	22	61	13
8	^{i}PrOH	**L7**	20	35	24
9	THF	**L7**	15	41	9
10	^{t}BuOH	**L7**	14	33	18
11	toluene	**L7**	11	29	9
12	H_2O	**L7**	9	27	9
13	HFIP	**L7**	9	19	23
14	PhCN	**L7**	9	39	8
15	DMA/MeOH (1:1)	**L7**	49	quant.	44
16	/	**L7**	8	23	/
17	DMPU	**L12**	54	quant.	63
18	DMA	**L12**	51	quant.	51
19[b]	DMA	**L12**	35	85	24
20[c]	DMA	**L12**	51	90	50
21[d]	DMA	**L12**	43	75	39
22[e]	DMA	**L12**	39	71	40
23	MeOH	**L12**	47	95	34
24	DMA/MeOH (1:1)	**L12**	45	quant.	44
25	DMPU/MeOH (1:1)	**L12**	43	85	44
26	DMA/EA (1:1)	**L12**	41	92	28

Reaction conditions: **1a** (1 mmol, 1.0 equiv.), **2a** (2.0 equiv.), $NiCl_2(H_2O)_6$ (20 mol%), ligand (40 mol%), Zn (3 equiv.), LAG additive (100 µL), MM (30 Hz, 2 h). [a]Determined by GC-FID using *n*-pentadecane as an internal standard. [b]DMA (50 µL). [c]DMA (200 µL). [d]**L12** (21 mol%). [e]**L12** (10 mol%).

3.1 Nickel-Source Screening

As **L12** consistently outperformed **L7**, subsequent screening of nickel(II) salts was conducted exclusively with **L12** (Table S 3). A marked decrease in yield was observed when deviating from $NiCl_2(H_2O)_6$, which remained the optimal Ni(II) source (Table S 3, entries 1–7). Notably, even the use of a pre-formed Ni(**L12**) complex, generated from $NiCl_2(H_2O)_6$, resulted in reduced yields. This loss in activity could only be partially recovered by the addition of extra **L12** (Table S 3, entries 8 and 9).

Table S 3. Nickel-source screening for the nickel catalyzed XEC of an alkyl bromide with a *S*-phenyl thioester mediated by mechanochemistry.

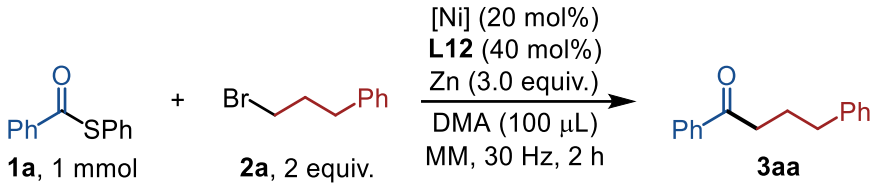

Entry	Ni Source	Ni loading	Yield (%)[a]	Conversion 1a / 2a (%)[a]	
1	$NiCl_2(H_2O)_6$	20	51	quant.	51
2	$NiBr_2$(diglyme)	20	29	84	36
3	$Ni(acac)_2$	20	18	63	51
4	$NiCl_2$(DME)	20	18	63	47
5	$NiCl_2$	20	17	70	61
6	$Ni(OTf)_2$	20	17	73	17
7	$Ni(OAc)_2(H_2O)_4$	20	13	quant.	59
8[b]	Ni(**L12**)$Cl_2(H_2O)_4$	40	12	96	16
9[c]	Ni(**L12**)$Cl_2(H_2O)_4$	40	23	quant.	32

Reaction conditions: **1a** (1 mmol, 1.0 equiv.), **2a** (2.0 equiv.), Ni source (20–40 mol%), **L12** (40 mol%), Zn (3 equiv.), DMA (100 µL), MM (30 Hz, 2 h). [a]Determined by GC-FID using *n*-pentadecane as an internal standard. [b]Without ligand. [c]Additional **L12** (20 mol%).

3.1 Reductant Screening

Substitution of zinc powder with alternative reductants led to reduced yields overall (Table S 4). Among the tested reductants, TDAE and manganese showed moderate performance (Table S 4, entries 2 and 3), whereas all other reductants resulted in poor outcomes.

Table S 4. Reductant screening for the nickel catalyzed XEC of an alkyl bromide with a *S*-phenyl thioester mediated by mechanochemistry.

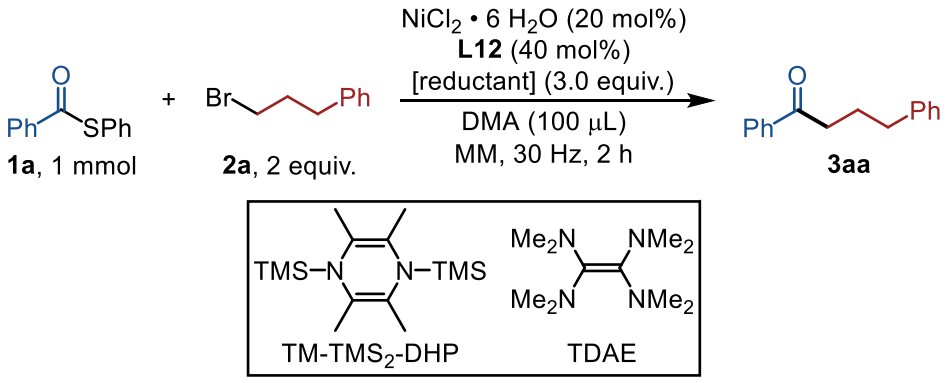

Entry	reductant	Yield (%)[a]	Conversion 1a / 2a (%)[a]	
1	Zn	51	quant.	51
2	TDAE	27	39	15
3	Mn	21	63	30

4	Mg	2	quant.	quant.
5	TM-TMS_2-DHP	0	43	20

Reaction conditions: **1a** (1 mmol, 1.0 equiv.), **2a** (2.0 equiv.), $NiCl_2(H_2O)_6$ (20 mol%), **L12** (40 mol%), reductant (3 equiv.), DMA (100 µL), MM (30 Hz, 2 h). [a]Determined by GC-FID using *n*-pentadecane as an internal standard.

3.1 Additive Screening

To further improve the reaction yield, a variety of additives were screened (Table S 5). Among them, pyridine and Ph_3PO provided the most promising results, each moderately increasing the yield of the desired ketone (Table S 5, entries 2 and 3). Both Lewis bases may act by coordinating *in situ* generated Lewis acidic zinc(II)-salts,[4] which appear to inhibit catalysis (Table S 5, entry 13).

Encouraged by the effect of pyridine, derivatives, including picoline, 2,4,6-collidine, and DMAP were evaluated. However, all led to diminished yields, likely due to steric or electronic mismatches (Table S 5, entries 4, 8, 9).

Given that Ph_3PO could potentially be reduced to PPh_3 under the reaction conditions, the latter was tested independently, clarifying which species was responsible for the observed effect. The sharp decrease in yield upon PPh_3 addition (Table S 5, entry 11) confirmed that Ph_3PO, and not its reduced form, was the active additive.

To assess whether water present in hydrated nickel salts played a beneficial role, excess H_2O was added to the reaction. As the yield remained largely unchanged, it was concluded that while water is not beneficial, the reaction is neither moisture sensitive (Table S 5, entry 5).

In an effort to scavenge liberated thiol byproducts, copper(I)-salts, namely CuCl and CuTc were tested (Table S 5, entries 6 and 14).[5] Both negatively affected the yield, likely due to their inherent Lewis acidity as thiol scavengers. Similarly, additives such as $Fe(acac)_3$ and $MgCl_2(H_2O)_6$ also reduced the reaction efficiency (Table S 5, entries 7, 12), reinforcing the conclusion that Lewis acidic metal salt are generally unfavorable additives.

Finally, inspired by the work of the MacMillan group, phthalimide was evaluated as an additive but showed no beneficial effect in this system (Table S 5, entry 10).[6]

Table S 5. Additive screening for the nickel catalyzed XEC of an alkyl bromide with a *S*-phenyl thioester mediated by mechanochemistry.

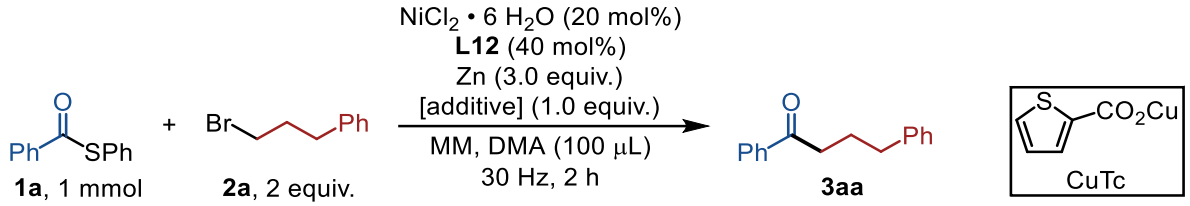

Entry	Additive	Yield (%)[a]	Conversion 1a (%)[a]	Conversion 2a (%)[a]
1	/	51	quant.	51
2	PyH	64	quant.	90
3	Ph_3PO	60	97	68
4	Picoline	53	94	79
5[b]	H_2O	47	quant.	43
6	CuCl	43	82	42
7	$Fe(acac)_3$	43	42	78
8	2,4,6-Collidine	41	88	50
9	DMAP	32	94	78
10	Phthalimide	28	89	29
11	PPh_3	19	58	54
12	$MgCl_2(H_2O)_6$	16	59	13
13	$ZnBr_2$	6	30	7
14	CuTc	4	38	85
15	LiI	2	11	38

Reaction conditions: **1a** (1 mmol, 1.0 equiv.), **2a** (2.0 equiv.), $NiCl_2(H_2O)_6$ (20 mol%), **L12** (40 mol%), Zn (3 equiv.), additive (1 equiv.), DMA (100 µL), MM (30 Hz, 2 h). [a]Determined by GC-FID using *n*-pentadecane as an internal standard. [b]H_2O (1.4 equiv.)

Building on the beneficial effect of Ph_3PO, further screening was carried out to evaluate its influence under modified reaction conditions (Table S 6). Increasing the amount of Ph_3PO proved advantageous, affording 71% of **3aa**, even at a reduced catalyst loading (Table S 6, entry 2).

In contrast, lowering the amount of zinc consistently reduced the yield, regardless of catalyst or alkyl halide loading (Table S 6, entries 3–5). Although MeOH had shown promise during the LAG additive screening, its usage under these conditions led to a reduction in yield (Table S 6, entry 6).

Table S 6. Ph_3PO additive screening for the nickel catalyzed XEC of an alkyl bromide with a *S*-phenyl thioester mediated by mechanochemistry.

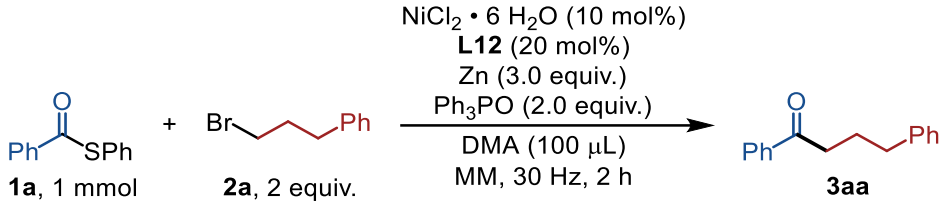

1a, 1 mmol + **2a**, 2 equiv. → **3aa**

Entry	Deviation from Conditions Above	Yield (%)[a]	Conversion 1a / 2a (%)[a]	
1[b]	[Ni] (20 mol%), Ph_3PO (3.0 equiv.)	60	97	68
2	None	71	88	69
3	Zn (2.0 equiv.)	52	66	50
4[c]	[Ni] (5 mol%), Zn (2.0 equiv.)	46	56	42
5	**2a** (1.3 equiv.), Zn (2.0 equiv.)	43	56	71
6	MeOH as LAG additive	47	77	44

Reaction conditions: **1a** (1 mmol, 1.0 equiv.), **2a** (2.0 equiv.), Ni source (10 mol%), **L12** (20 mol%), Zn (3 equiv.), Ph_3PO (2.0 equiv.), DMA (100 µL), MM (30 Hz, 2 h). [a]Determined by GC-FID using *n*-pentadecane as an internal standard. [b]**L12** (40 mol%). [c]**L12** (10 mol%).

Analogous to the screening with Ph_3PO, reaction conditions incorporating pyridine as an additive were further optimized (Table S 7). The reaction tolerated a reduction in zinc (Table S 7, entry 2) and catalyst loading (Table S 7, entry 3) without significant loss in yield. However, reducing the amount of alkyl halide or pyridine led to diminished performance (Table S 7, entries 4 and 5). In contrast, increasing the pyridine amount enhanced the yield (Table S 7, entry 6), and at elevated pyridine concentrations, lower ligand loadings became tolerable (Table S 7, entry 7). Under these conditions, reduction of zinc equivalents was also feasible without compromising efficiency (Table S 7, entry 8). A decrease in catalyst loading to 5 mol% was accompanied by a slight drop in yield (Table S 7, entry 9), and therefore 10 mol% was selected for subsequent studies. The observed tolerance to ligand reduction (Table S 7, entry 7) was specific to high catalyst loadings. At 10 mol% catalyst, reducing the ligand loading was accompanied by a decrease in yield (Table S 7, entry 10). Additionally, use of a preformed $Ni(phen)Cl_2$ complex resulted in slightly lower yields (entry 11).

Replacing DMA with MeOH led to comparable results (Table S 7, entry 12), but again, lowering the alkyl halide equivalents negatively impacted the outcome (Table S 7, entry 13). In this system, a 5 mol% catalyst loading remained effective (Table S 7, entry 14), and although further increasing pyridine did not improve the yield, it reduced alkyl halide consumption, thereby minimizing byproduct formation (Table S 7, entry 15).

A key finding was that pyridine could function as the LAG additive itself, eliminating the need for additional solvents, while even slightly improving the yield (Table S 7, entry 16). This discovery enabled further exploration of minimal conditions: reductions in ligand, catalyst, zinc, and halide equivalents were all tolerated (Table S 7, entries 17–20), though such minimization was avoided in the final protocol to retain operational freedom during scope investigations. Similarly, while lower pyridine loading was feasible (Table S 7, entry 21), the higher concentration was maintained to ensure robustness, given the prior observed sensitivity. Attempts to simultaneously minimize multiple variables led to decreased yields and reproducibility issues (Table S 7, entry 22), underscoring the optimization limits of the developed system. Finally, the addition of NaCl proved beneficial, delivering an improved yield and defining the optimized conditions used in subsequent scope studies (Table S 7, entry 23).[7]

Table S 7. Pyridine additive screening for the nickel catalyzed XEC of an alkyl bromide with a *S*-phenyl thioester mediated by mechanochemistry.

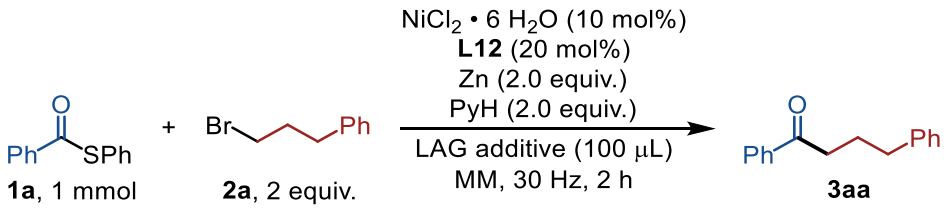

1a, 1 mmol + **2a**, 2 equiv. → **3aa**

Entry	LAG	Deviation from Conditions Above	Yield (%)[a]
1[b]	DMA	[Ni] (20 mol%), Zn (3 equiv.), PyH (1 equiv.)	64
2[b]	DMA	[Ni] (20 mol%), PyH (1 equiv.)	61
3	DMA	Zn (3equiv.), PyH (1 equiv.)	60
4[b]	DMA	[Ni] (20 mol%), **9** (1.3 equiv.), Zn (3 equiv.), PyH (1 equiv.)	48
5[b]	DMA	[Ni] (20 mol%), Zn (3equiv.), PyH (0.25 equiv.)	51
6[b]	DMA	[Ni] (20 mol%), Zn (3 equiv.)	76
7	DMA	[Ni] (20 mol%), **L12** (20 mol%)	75
8	DMA	None	72
9[c]	DMA	[Ni] (5 mol%)	51
10	DMA	**L12** (11 mol%)	62
11	DMA	$Ni(phen)Cl_2$ (10 mol%) instead of $NiCl_2(H_2O)_6$ and **L12**	63
12	MeOH	None	77
13	MeOH	**2a** (1.5 equiv.)	69
14[c]	MeOH	[Ni] (5 mol%)	81
15	MeOH	[Ni] (5 mol%), PyH (3 equiv.)	80
16	PyH[d]	None, PyH (2 equiv.)	87
17	PyH[d]	**L12** (11 mol%)	89

18	PyH[d]	**2a** (1.5 equiv.)	92
19	PyH[d]	Zn (1.5 equiv.)	86
20[c]	PyH[d]	[Ni] (5 mol%)	80
21	PyH	None	89
22[e]	PyH	**2a** (1.5 equiv.), **L12** (11 mol%)	70
23	PyH[d]	NaCl (2 equiv.) as additive	quant.
24	PyH[d]	Without $NiCl_2(H_2O)_6$	2

Reaction conditions: **1a** (1 mmol, 1.0 equiv.), **2a** (2.0 equiv.), Ni source (10 mol%), **L12** (20 mol%), Zn (2 equiv.), Pyridine (2.0 equiv.), DMA (100 µL), MM (30 Hz, 2 h). [a]Determined by GC-FID using *n*-pentadecane as an internal standard. [b]**L12** (40 mol%). [c]**L12** (10 mol%). [d]Pyridine (2 equiv.). [e]1 h.

3.1 Reaction Time Screening

A key advantage of mechanochemical XECs is their significantly reduced reaction time compared to conventional methods. Thus, the optimal reaction time for the model system was assessed. Notably, full conversion of the thioester was achieved within 30 min (Table S 8). However, to accommodate potentially more challenging substrates during scope studies, a 1 h reaction time was selected as the standard.

Table S 8. Reaction time screening for the nickel catalyzed XEC of an alkyl bromide with a *S*-phenyl thioester mediated by mechanochemistry.

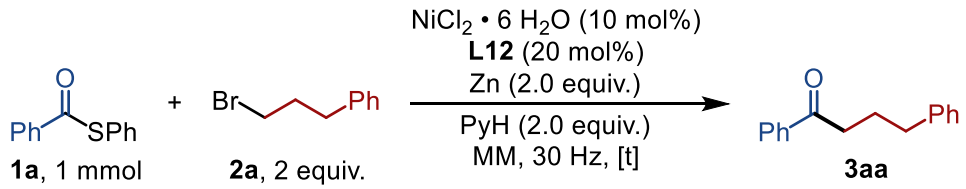

1a, 1 mmol **2a**, 2 equiv. **3aa**

Entry	Time (h)	Yield (%)[a]	Conversion 1a / 2a (%)[a]	
1	2	87	quant.	quant.
2	1	94	quant.	81
3	0.5	92	quant.	61
4	0.25	78	84	44

Reaction conditions: **1a** (1 mmol, 1.0 equiv.), **2a** (2.0 equiv.), $NiCl_2(H_2O)_6$ (10 mol%), **L12** (20 mol%), reductant (2 equiv.), Pyridine (2 equiv.), MM (30 Hz). [a]Determined by GC-FID using *n*-pentadecane as an internal standard.

4. Mechanistic Studies

4.1 Radical Reporter Experiment

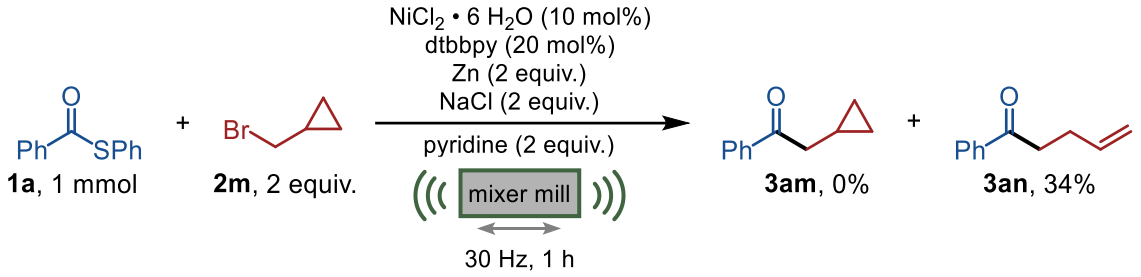

Scheme S 1. Radical reporter experiment for the nickel catalyzed XEC of **1a** with **2m** under mechanochemical conditions.

To evaluate whether the developed coupling involves radical species derived from the alkyl bromide, a radical reporter experiment utilizing **2m** was conducted according to **GP-B** (Scheme S 1). As the ring opened XEC product (**3an**) was isolated as a single isomer, a cyclopropyl methyl radical is most likely involved, excluding the potential Negishi type pathway.[8]

4.2 Radical Scavengers

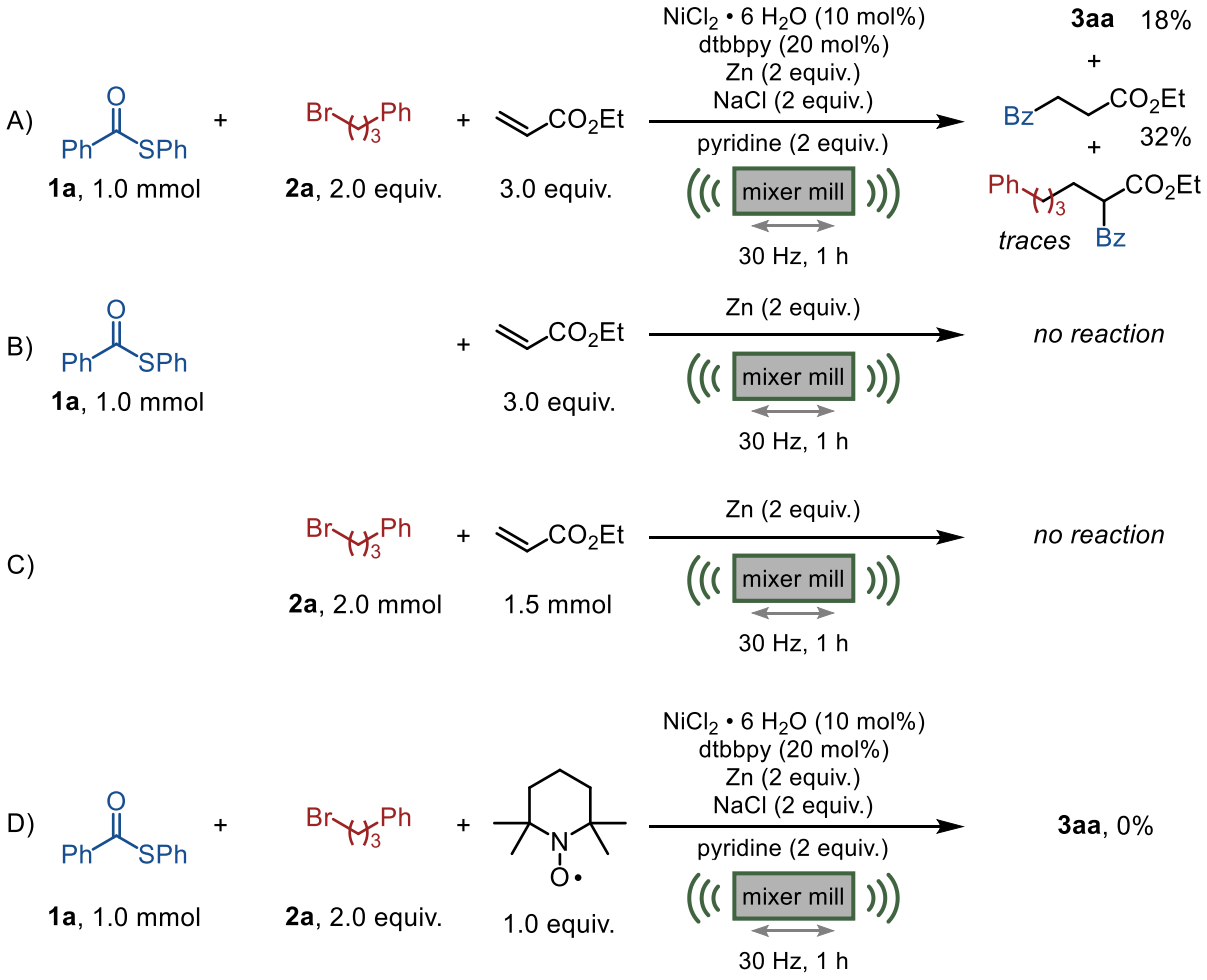

Scheme S 2. Mechanochemical reactions under reductive conditions in the presence of ethyl acrylate. A) standard conditions. B/C) Control reactions with only **1a** or **2a** respectively. D) TEMPO as radical scavenger.

Reactions with additional ethyl acrylate (1 equiv.), serving as a potential Giese-type acceptor, were conducted. Under standard conditions according to **GP-B**, the hydroacylation and mixed addition products were detected alongside the XEC product (Scheme S 2A). Control experiments omitting the nickel catalyst, employing only one starting material showed no formation of addition products (Scheme S 2B/C). These results demonstrate that activation of thioesters requires the nickel catalyst and that potential organozinc species do not undergo Michael addition with ethyl acrylate under the applied conditions. In another experiment, 2-2'-6-6'-tetramethylpiperidin-*N*-oxid (TEMPO) was added to standard conditions, effectively inhibiting product formation. Together with the radical reporter experiment, these findings support the involvement of alkyl radicals derived from the alkyl bromide and indicate that thioester activation by nickel could proceed *via* SET or a two-electron oxidative addition pathway.[9, 10]

4.3 Side Products

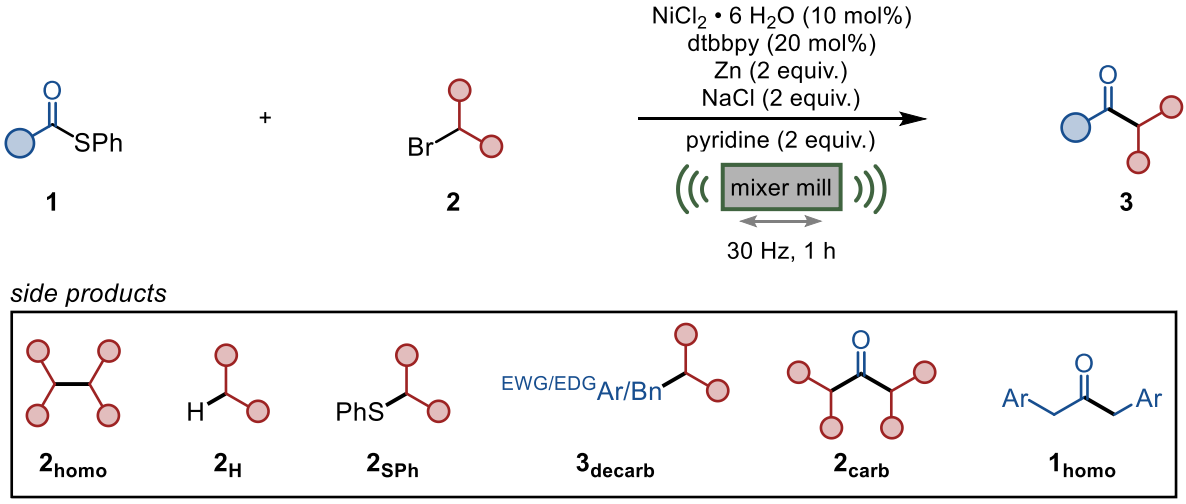

Scheme S 3. Observed side products for the nickel catalyzed XEC of **1** with **2** under mechanochemical conditions.

Throughout the project several side products have been observed (Scheme S 3). For instance, homocoupling (**2**$_{homo}$), protodehalogenation (**2**$_{H}$) and thiol substitution products (**2**$_{SPh}$) of **2** were observed throughout all reactions as major side products. Additionally, for various *S*-phenyl thioesters, the decarbonylated XEC product (**3**$_{decarb}$) was observed in up to 50% yield. Hereby especially benzylic, electron deficient and selected electron rich aryl *S*-phenyl thioesters facilitated the decarbonylation. For such substrates, the carbonylated homocoupling of **2** (**2**$_{carb}$) was also observed in minor quantities. Finally, for benzylic *S*-phenyl thioesters the single decarbonylated homocoupling product (**1**$_{homo}$) was detected in substantial quantities.

4.4 Oxidative addition complex

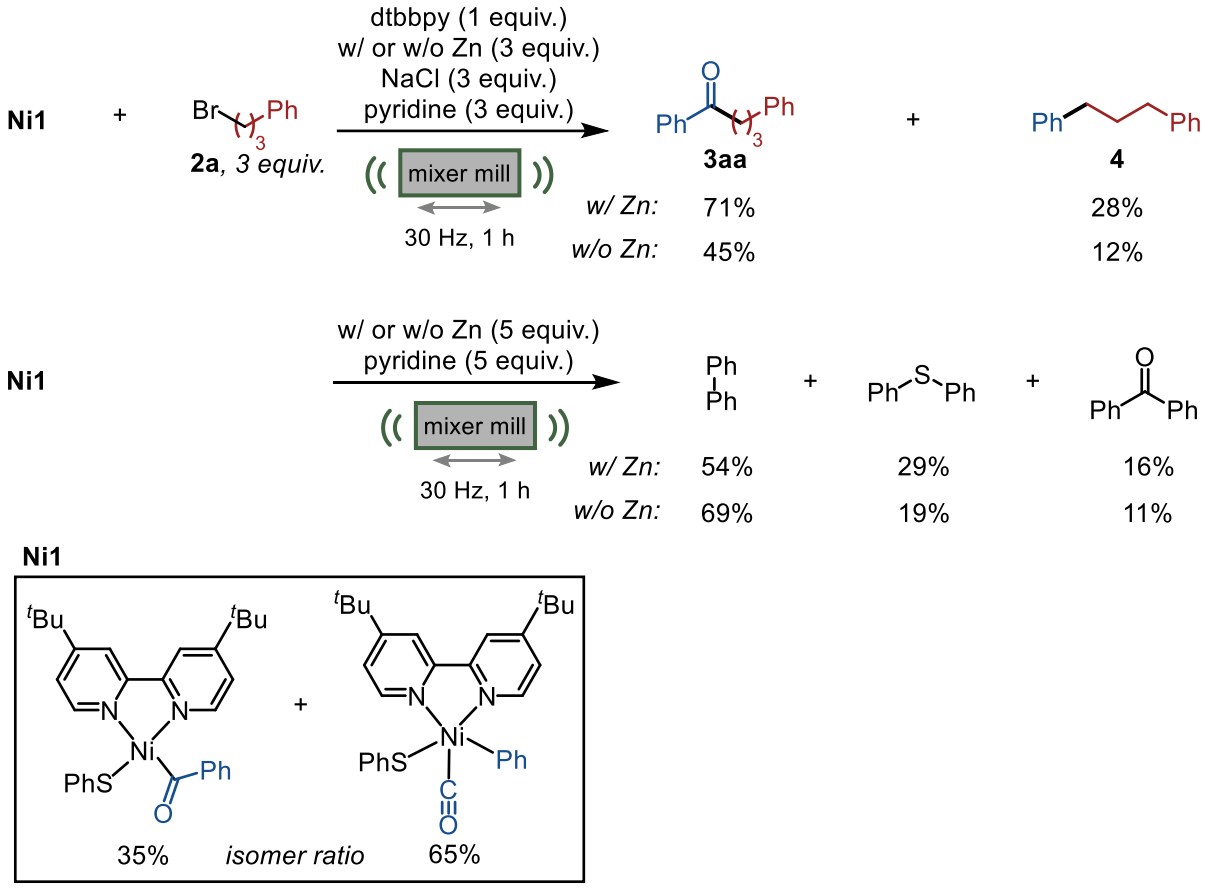

Scheme S 4. Stochiometric reactions of **Ni1** with and without **2a** in presence and absence of Zn under mechanochemical conditions. Yields of 3aa and 4 were determined by GC-FID and the ratio of biphenyl to diphenylsulfide to benzophenone was estimated by GC-MS.

A 10 mL stainless steel milling jar was charged with the respective amounts of **2a** (0–3 equiv.), NaCl (0–3 equiv.), Zn (0–5 equiv.), and pyridine (3–5 equiv.) alongside two stainless steel balls (⌀ = 10 mm, m = 4 g) and transferred to a glovebox. **Ni1** (see section 5.1) (10–30 mg, 1 equiv.), and dtbbpy (0–1 equiv.) were added and the milling jar was closed, placed in a MM 400 and shaken at 30 Hz for 1 h. After the reaction, the jar was opened and *n*-pentadecane and EtOAc were added. An aliquot was taken and filtered through Celite, Al_2O_3 and $MgSO_4$, before being analyzed by GC-MS/FID.

4.5 Nickel Zincate Complex

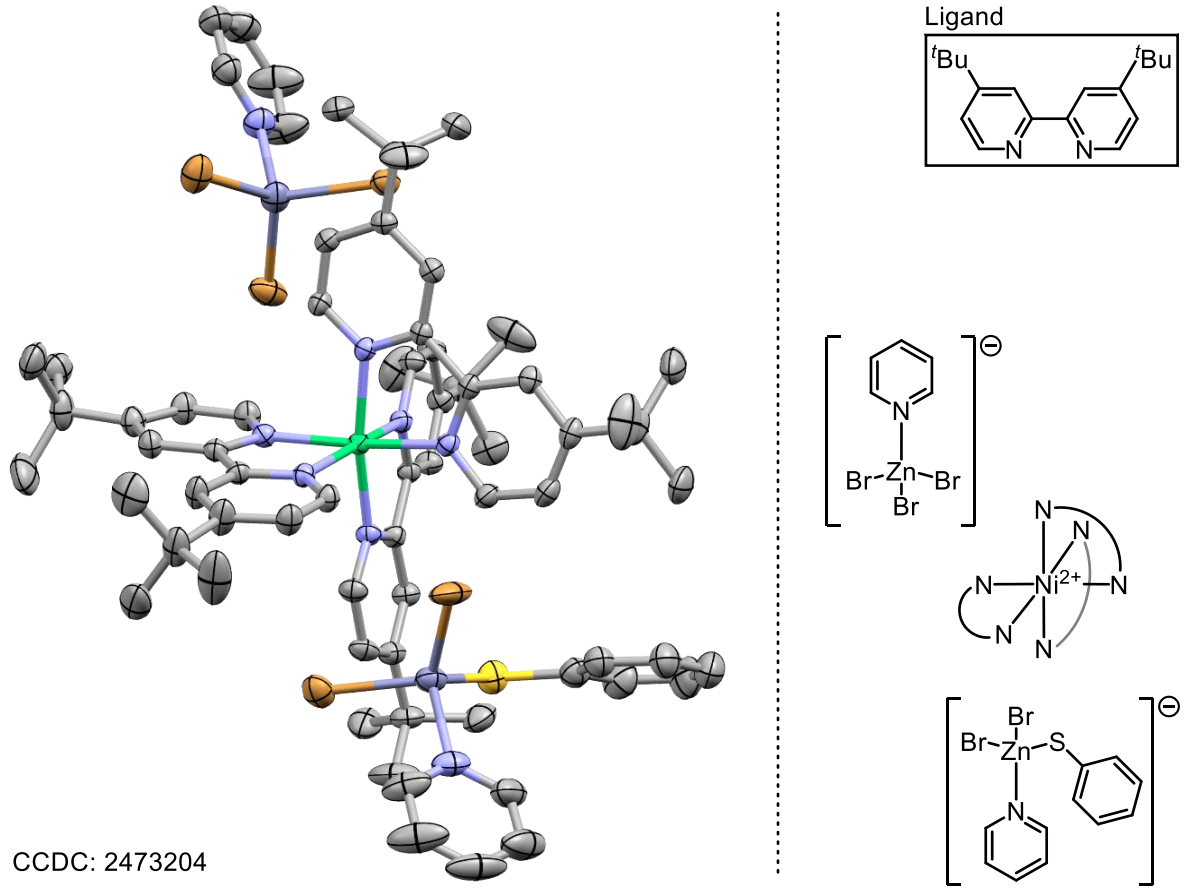

Figure S1. ORTEP representation of $[Ni(dtbbpy)_3][Zn(PyH)Br_3][Zn(PyH)(SPh)Br_2]$ (CCDC: 2473204) crystallized from crude reaction mixture obtained subsequent to aqueous workup of the nickel catalyzed XEC of **1a** with **2a** under mechanochemical conditions. Hydrogen atoms are omitted for clarity, and the thermal ellipsoids are drawn at 50% probability level.

Upon aqueous workup of the catalytic system, crystals suitable for single-crystal X-ray diffraction were obtained. The structure revealed a nickel(II) complex coordinated by three dtbbpy ligands and two zincate species, each bearing a pyridine ligand. Although the structure was isolated after aqueous workup, and it therefore remains uncertain whether this exact species is present under catalytic conditions, it clearly demonstrates that pyridine can coordinate to Zn(II) species. This observation provides a plausible rationale for the beneficial effect of pyridine, as optimization studies showed that addition of $ZnBr_2$ to the reaction was detrimental.

5. Analytical Data

5.1 Synthesis of Nickel Complexes

Synthesis of Ni1.

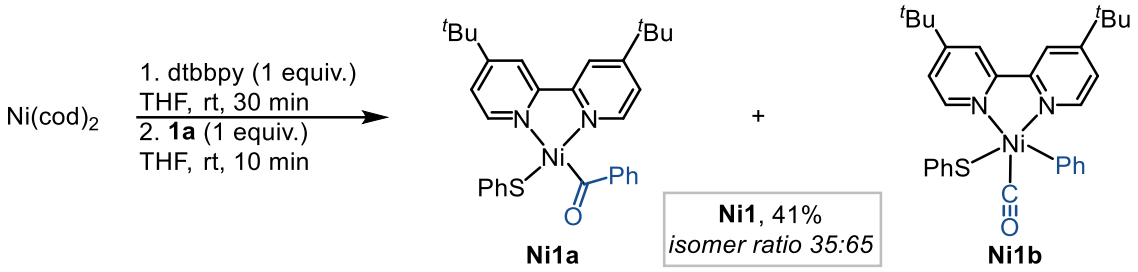

In a glovebox, $Ni(cod)_2$ (150 mg, 0.55 mmol, 1.0 equiv.) and dtbbpy (146 mg, 0.55 mmol, 1.0 equiv.) were dissolved in THF (2 mL) and stirred for 30 min at rt, resulting in a dark blue/violet solution. **1a** (117 mg, 0.55 mmol, 1.0 equiv.) was added and the mixture was stirred for another 10 min, quickly changing color to black. Subsequently, *n*-hexane (10 mL) was added, the precipitate was filtered, washed with *n*-hexane (3 × 2 mL) and dried *in vacuo* resulting in a dark solid (121 mg, 224 µmol, 41%).

*Analytical data of **Ni1**:*

HR-MS: Attempts to measure HR-MS for **Ni1** (ESI/APCI) remained unsuccessful.

IR (ATR, $\tilde{\nu}$ [cm^{-1}]): 3050 (w), 2954 (w), 2906 (w), 2868 (w), 1608 (s), 1571 (m), 1541 (w), 1468 (m), 1407 (m), 1366 (w), 1297 (w), 1247 (w), 1198 (w), 1183 (w), 1146 (m), 1083 (w), 1019 (w), 975 (w), 870 (m), 837 (m), 769 (w), 740 (m), 684 (s).

Elemental Analysis: Calc. for $C_{31}H_{34}N_2NiOS$: C, 68.78; H, 6.33; N, 5.17. Found: C, 68.65; H, 6.08; N, 5.05; S, 5.92.

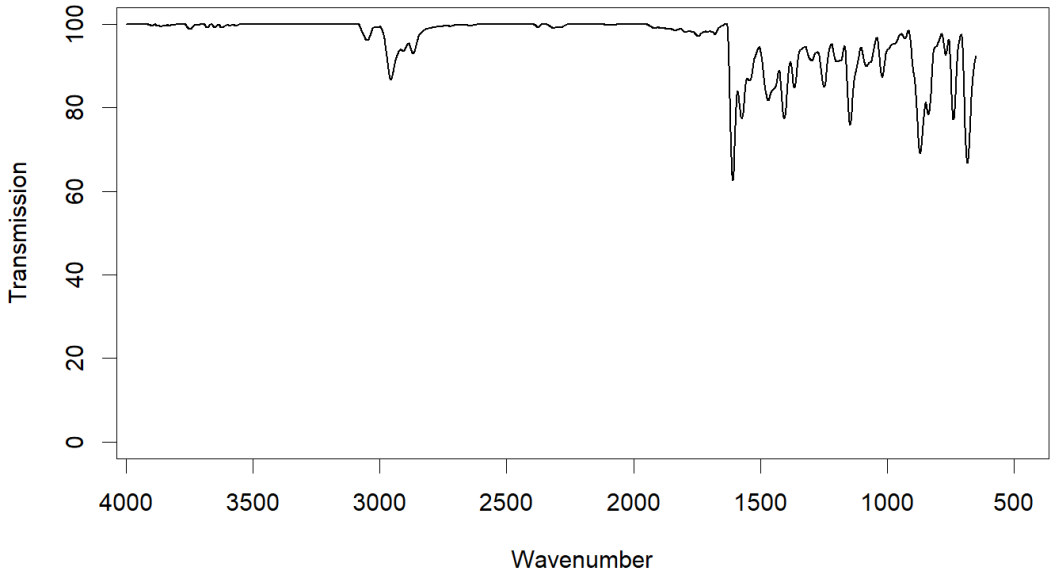

Figure S2. IR spectrum (neat, ATR) of **Ni1**.

*NMR data of **Ni1a**:*

^{1}H NMR (700 MHz, THF-d_8, δ): 9.16 (d, *J* = 5.8 Hz, 1H), 8.61 – 8.48 (m, 1H), 8.14 (m, 2H), 8.01 – 7.99 (m, 1H), 7.56 – 7.54 (m, 2H), 7.53 – 7.42 (m, 3H), 7.34 – 7.22 (m, 3H), 6.65 – 6.61 (m, 2H), 1.41 (s, 9H), 1.35 (s, 9H).

^{13}C{^{1}H} NMR (176 MHz, THF-d_8, δ): 188.9, 163.5, 162.5, 160.9, 158.7, 157.1, 156.1, 154.8, 152.4, 150.0, 149.6, 137.2, 135.7, 129.9, 129.7, 129.5, 125.8, 124.0, 122.5, 121.6, 121.1, 118.7, 118.3, 118.2, 30.7, 30.4, 30.1.

*NMR data of **Ni1b**:*

^{1}H NMR (700 MHz, THF-d_8, δ): 8.97 (d, *J* = 5.8 Hz, 1H), 8.23 (d, *J* = 7.5 Hz, 2H), 8.18 – 8.16 (m, 2H), 8.02 (d, *J* = 5.8 Hz, 1H), 7.57 – 7.56 (m, 2H), 7.41 – 7.37 (m, 2H), 7.22 – 7.18 (m, 2H), 6.75 – 6.70 (m, 2H), 6.69 – 6.64 (m, 2H), 1.40 (s, 9H), 1.36 (s, 9H).

^{13}C{^{1}H} NMR (176 MHz, THF-d_8, δ): 197.0, 163.8, 162.9, 155.9, 154.1, 150.7, 149.8, 149.6, 147.4, 139.1, 134.9, 134.6, 128.9, 127.9, 127.7, 127.0, 126.9, 124.7, 123.6, 121.9, 118.9, 118.1, 36.0, 30.4, 30.2, 30.0.

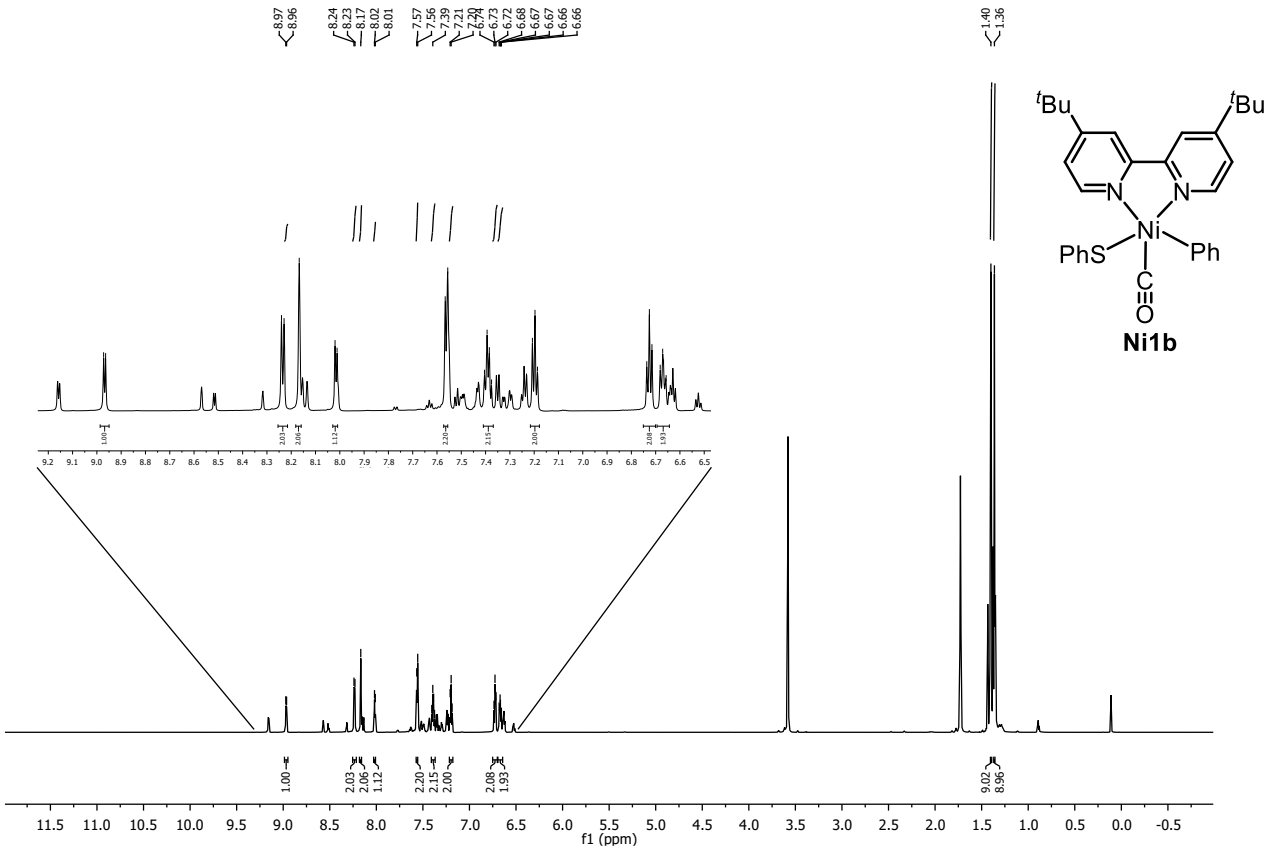

Figure S3. ^{1}H NMR spectrum (700 MHz, THF-d_8) of **Ni1**. Signals of **Ni1b** are indicated and integrated, while remaining signals belong to **Ni1a**.

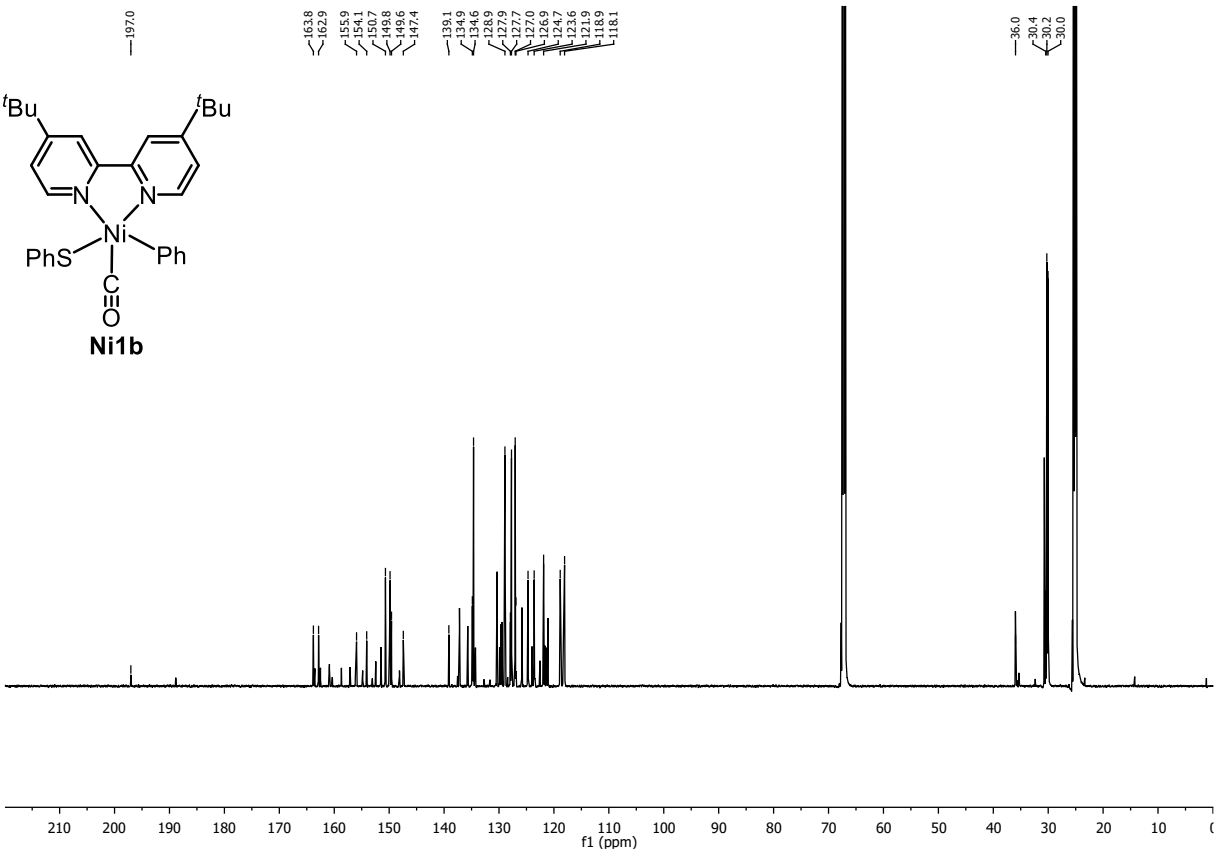

Figure S4. ^{13}C NMR spectrum (176 MHz, THF-d_8) of **Ni1**. Signals of **Ni1b** are indicated, while remaining signals belong to **Ni1a**.

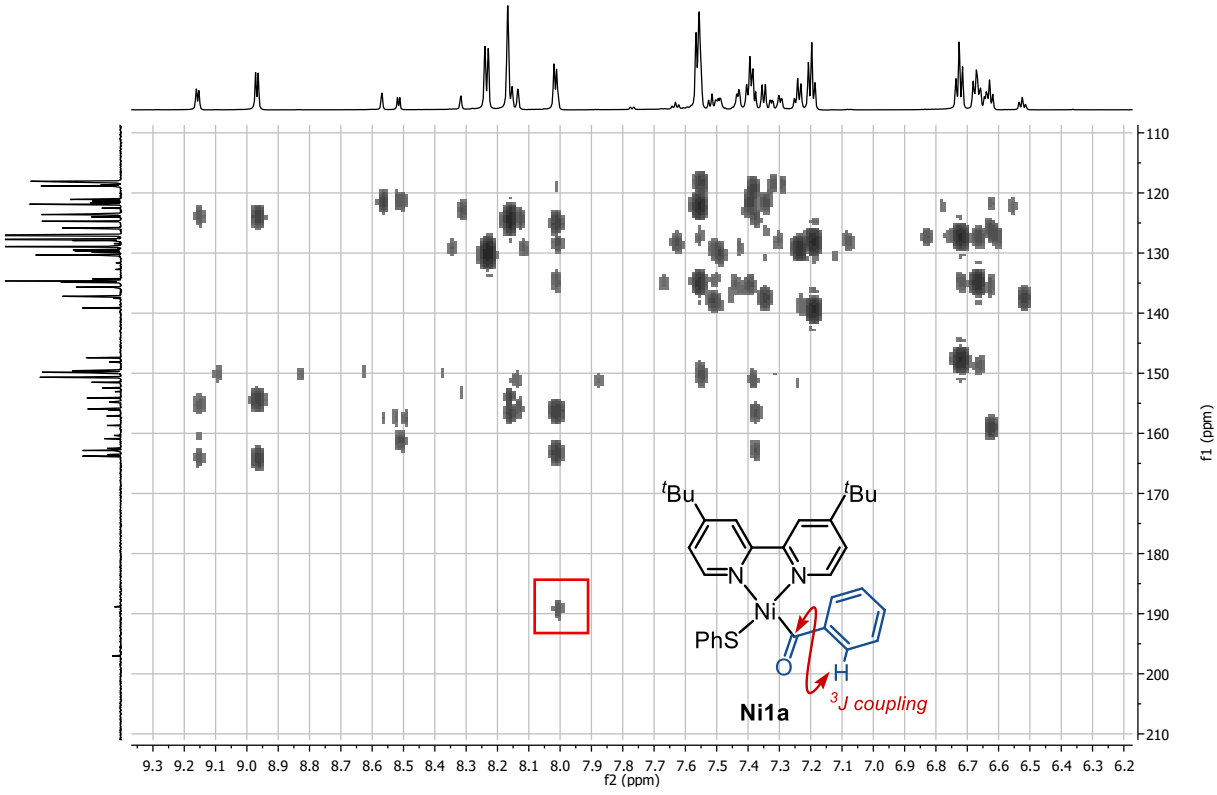

Figure S5. ^{1}H^{13}C-HMBC NMR spectrum (700MHz/176MHz, THF-d_8) of **Ni1**.

Synthesis of Ni2.

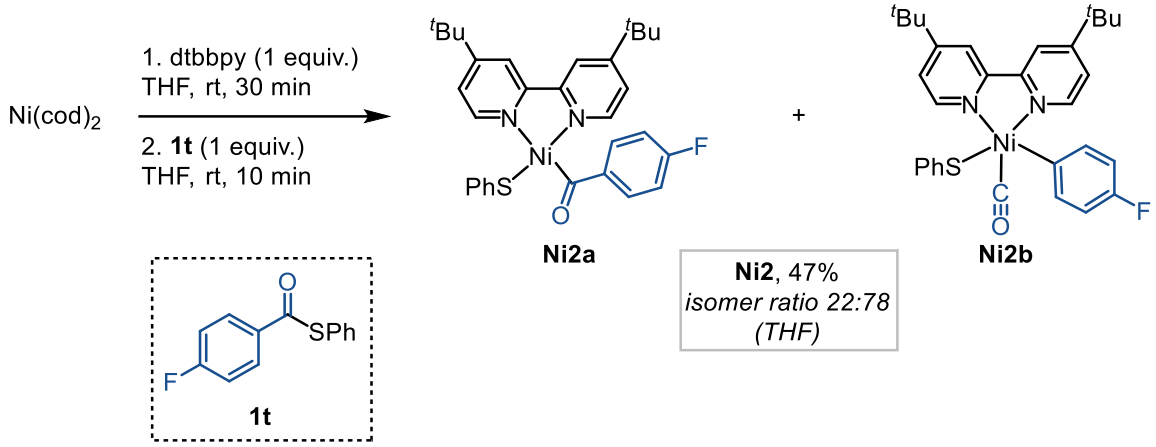

In a glovebox, $Ni(cod)_2$ (100 mg, 0.364 mmol, 1.0 equiv.) and dtbbpy (97.6 mg, 0.364 mmol, 1.0 equiv.) were dissolved in THF (2 mL) and stirred for 30 min at rt, resulting in a dark blue/violet solution. **1t** (84.4 mg, 0.364 mmol, 1.0 equiv.) was added and the mixture was stirred for another 10 min, quickly changing color to black. Subsequently, *n*-hexane (10 mL) was added, the precipitate was filtered, washed with *n*-hexane (3 × 2 mL) and dried *in vacuo* resulting in a dark solid **Ni2** (92.4 mg, 172 µmol, 47%).

A single crystal suitable for XRD was obtained from layering a THF solution with hexane at -40 °C.

*Analytical data of **Ni2**:*

^{1}H NMR (600 MHz, THF-d_8, δ): 9.13 – 8.87 (m, 1H), 8.60 – 8.23 (m, 4H), 8.15 – 7.93 (m, 1H), 7.65 – 7.58 (m, 1H), 7.56 – 7.45 (m, 2H), 7.44 – 7.25 (m, 2H), 7.01 – 6.94 (m, 1H), 6.78 – 6.44 (m, 3H), 1.45 – 1.25 (m, 18H).

^{13}C{^{1}H} NMR (151 MHz, THF-d_8, δ): 202.8, 187.6, 165.3, 163.9, 163.6, 163.0, 156.1, 155.9, 154.8, 154.0, 151.2, 150.5, 149.6, 149.5, 147.6, 146.9, 137.0, 135.8, 135.0, 134.7, 131.0, 131.0, 130.9, 130.8, 129.8, 129.0, 127.1, 127.0, 124.8, 124.1, 123.7, 123.6, 122.1, 122.0, 121.3, 119.3, 118.8, 118.5, 118.1, 114.5 (d, J = 20.8 Hz), 112.6 (d, J = 17.8 Hz), 89.9, 36.0, 31.1, 30.6, 30.2, 29.9.

^{19}F NMR (565 MHz, THF-d_8, δ): -112.3, -126.7.

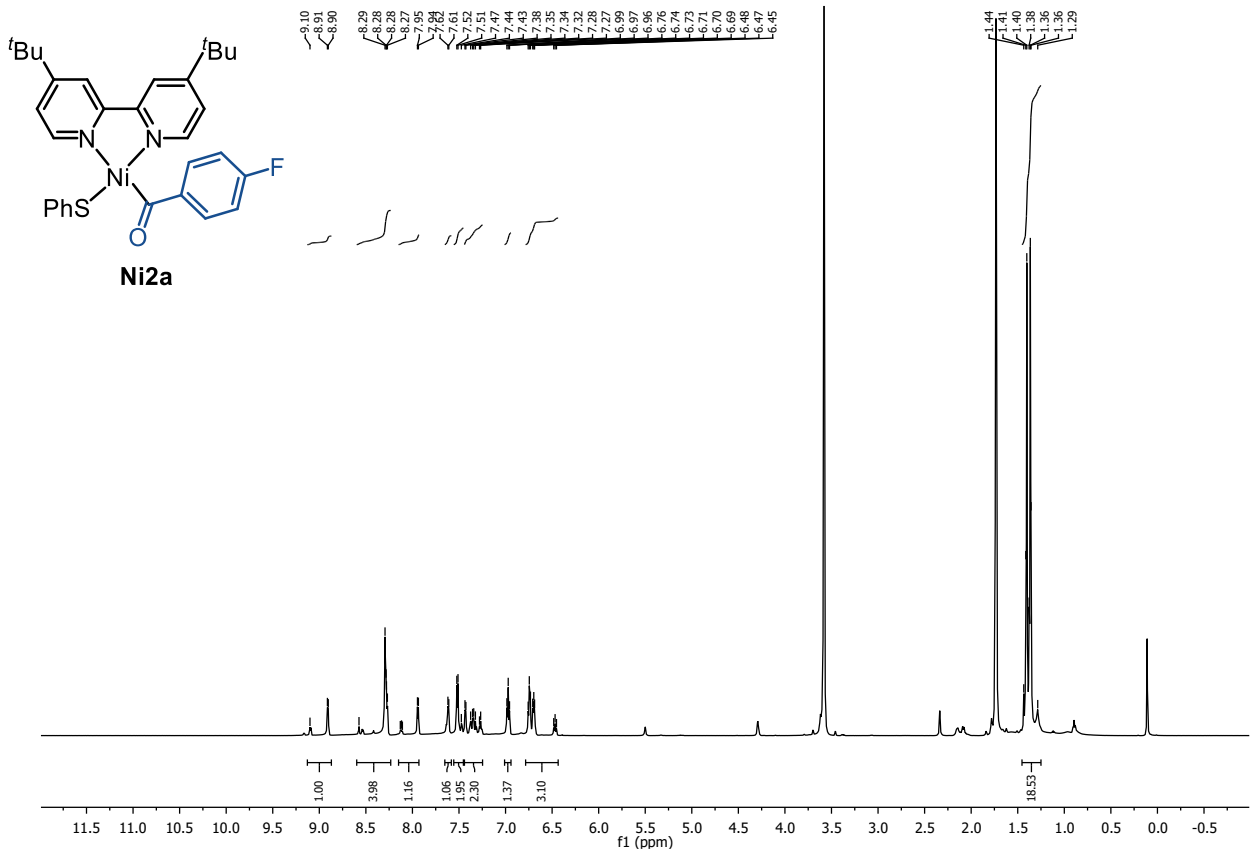

Figure S6. ^{1}H NMR spectrum (600 MHz, THF-d_8) of **Ni2**.

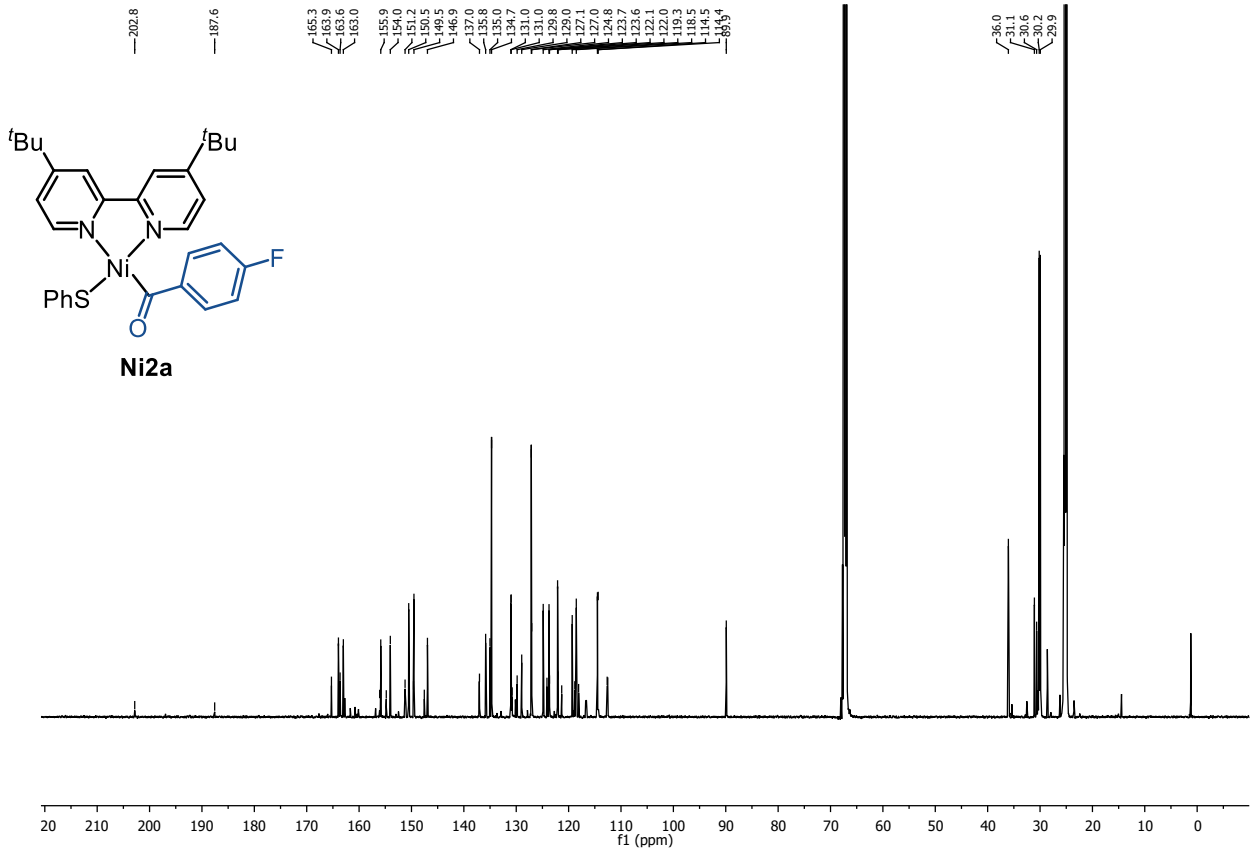

Figure S7. ^{13}C NMR spectrum (151 MHz, THF-d_8) of **Ni2**.

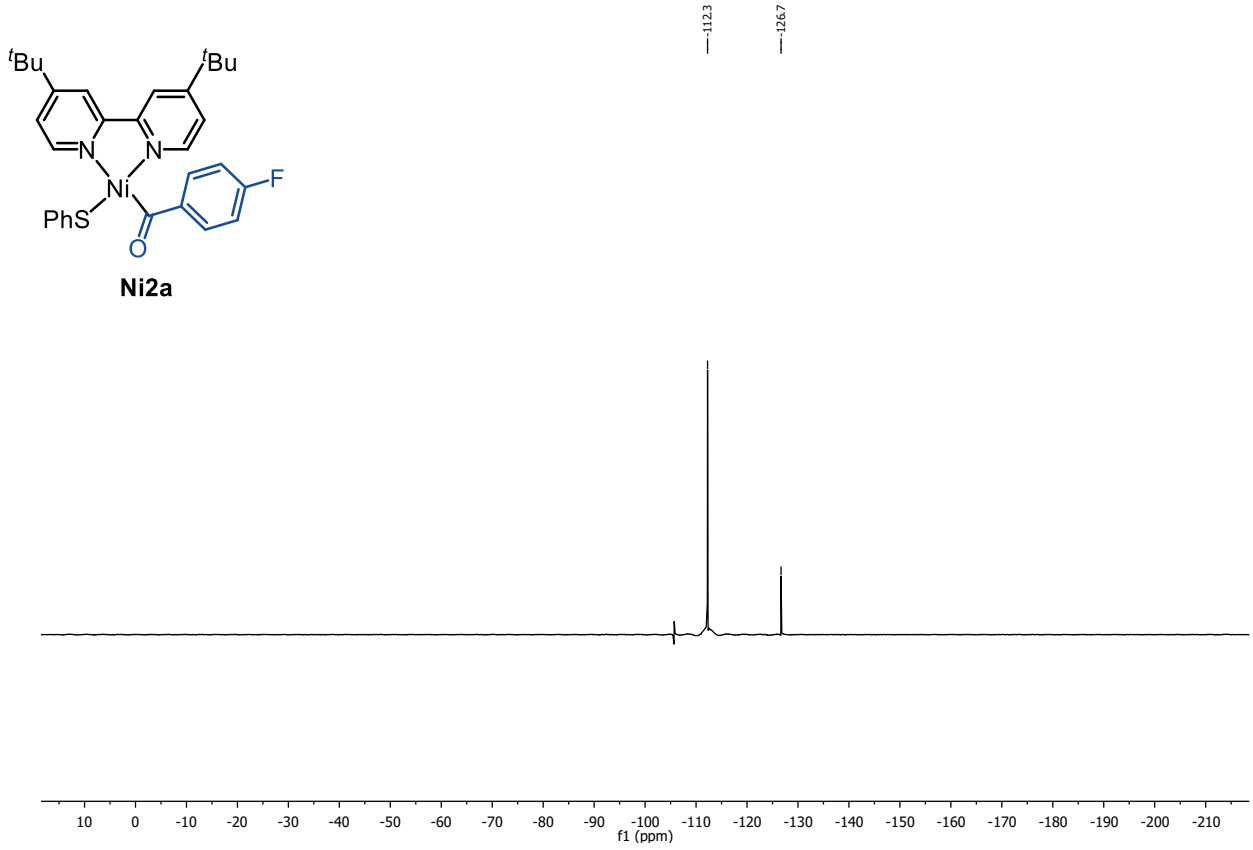

Figure S8. ^{19}F NMR spectrum (565 MHz, THF-d_8) of **Ni2**.

5.2 Synthesis of Thioester

S-phenyl benzothioate (1a):

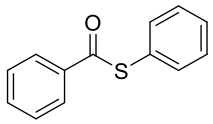

1a

$C_{13}H_{10}OS$ (214.28 g/mol)

Following **GP-A1**, **1a** was synthesized using benzoyl chloride (20.9 mL, 180 mmol, 1.0 equiv.), thiophenol (22.1 mL, 216 mmol, 1.2 equiv.) and triethylamine (25 mL, 180 mmol, 1.0 equiv.). Purification by crystallization (DCM/*n*-hexane) afforded **1a** (24.1 g, 113 mmol, 63%) as colorless solid. Conforms to reported analytical data.[11]

^{1}H NMR (400 MHz, $CDCl_3$, δ): δ 8.10 – 8.03 (m, 2H), 7.66 – 7.45 (m, 8H).

^{13}C{^{1}H} NMR (101 MHz, $CDCl_3$, δ): 190.2, 136.7, 135.2, 133.7, 129.6, 129.3, 128.8, 127.6, 127.5.

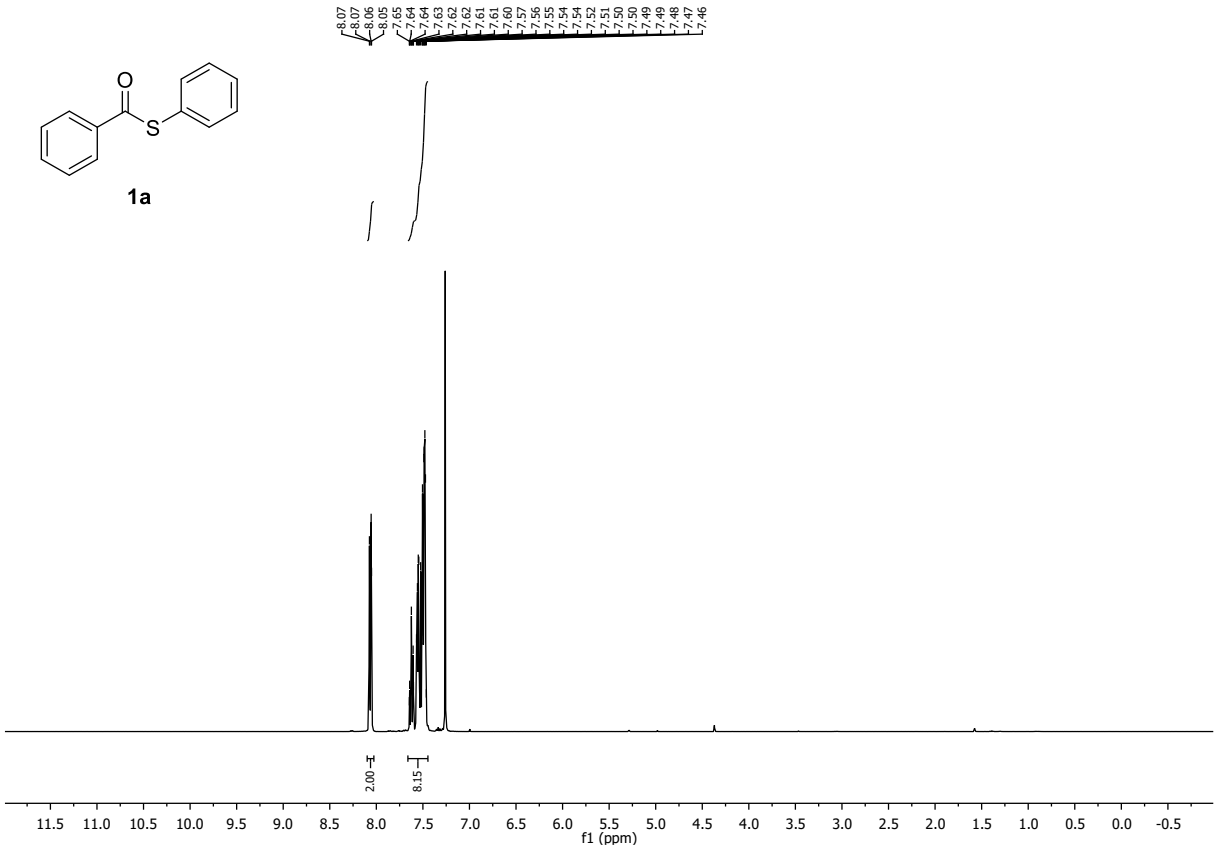

Figure S9. ^{1}H NMR spectrum (400 MHz, $CDCl_3$) of **1a**.

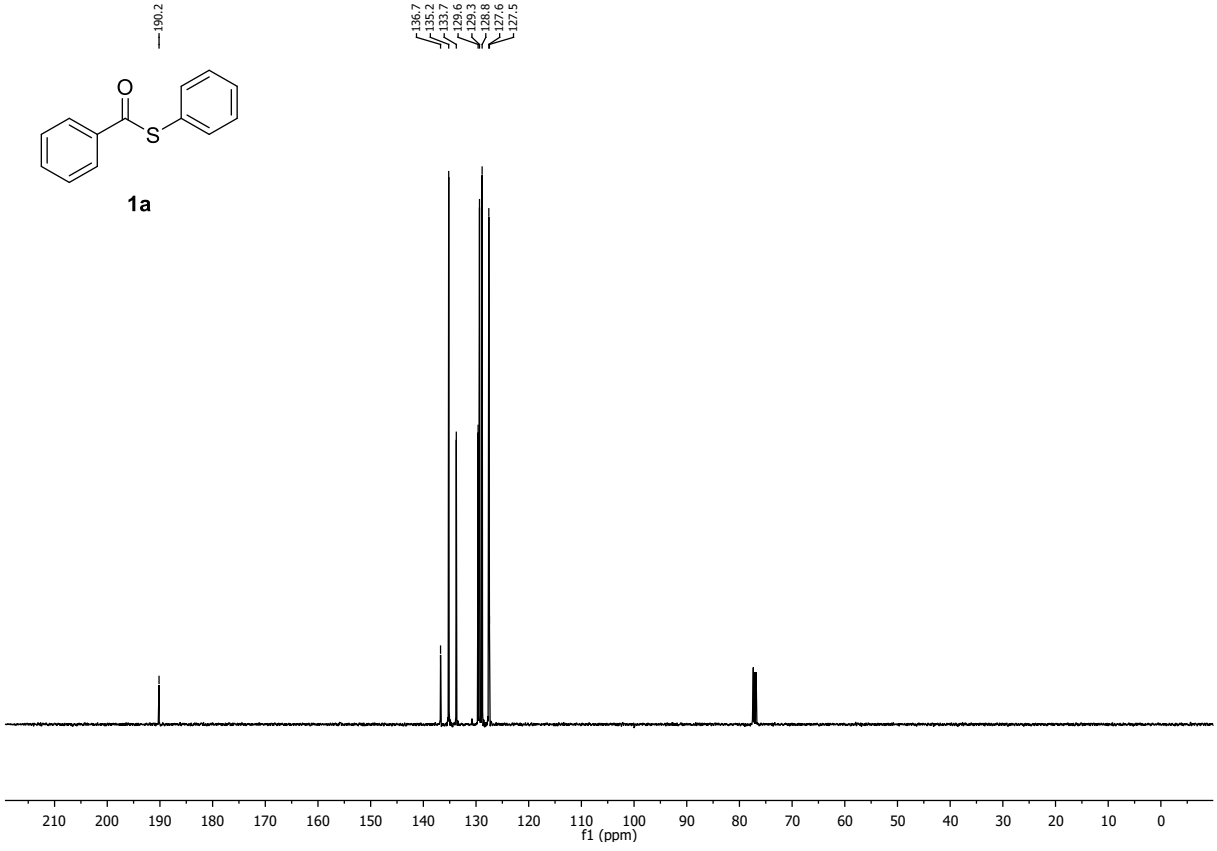

Figure S10. ^{13}C NMR spectrum (101 MHz, $CDCl_3$) of **1a**.

***S*-phenyl 2-methylbenzothioate (1b):**

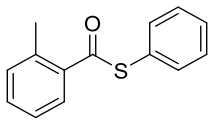

1b

$C_{14}H_{12}OS$ (228.31 g/mol)

Following **GP-A1**, **1b** was synthesized using 2-methylbenzoyl chloride (2.29 mL, 20.0 mmol, 1.0 equiv.), thiophenol (2.45 mL, 24.0 mmol, 1.2 equiv.) and triethylamine (3.34 mL, 24.0 mmol, 1.2 equiv.). Purification by crystallization (DCM/*n*-hexane) afforded **1b** (0.55 g, 2.40 mmol, 12%) as colorless solid. Conforms to reported analytical data.[11]

^{1}H NMR (400 MHz, $CDCl_3$, δ): 7.96 (dd, *J* = 7.8, 1.3 Hz, 1H), 7.56 – 7.40 (m, 6H), 7.35 – 7.26 (m, 2H), 2.51 (s, 3H).

^{13}C{^{1}H} NMR (101 MHz, $CDCl_3$, δ): 192.3, 137.6, 136.9, 135.0, 132.1, 131.9, 129.6, 129.4, 128.8, 128.4, 126.0, 20.9.

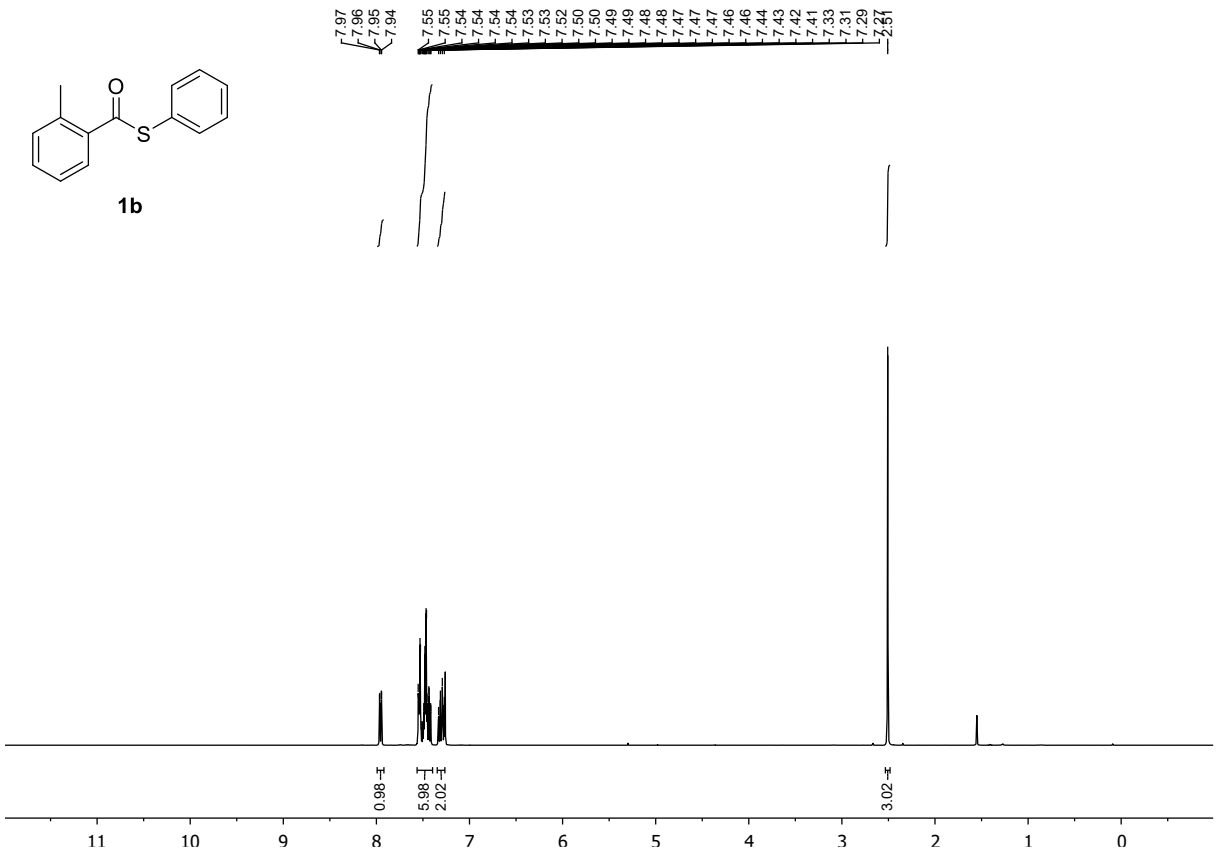

Figure S11. ^{1}H NMR spectrum (400 MHz, $CDCl_3$) of **1b**.

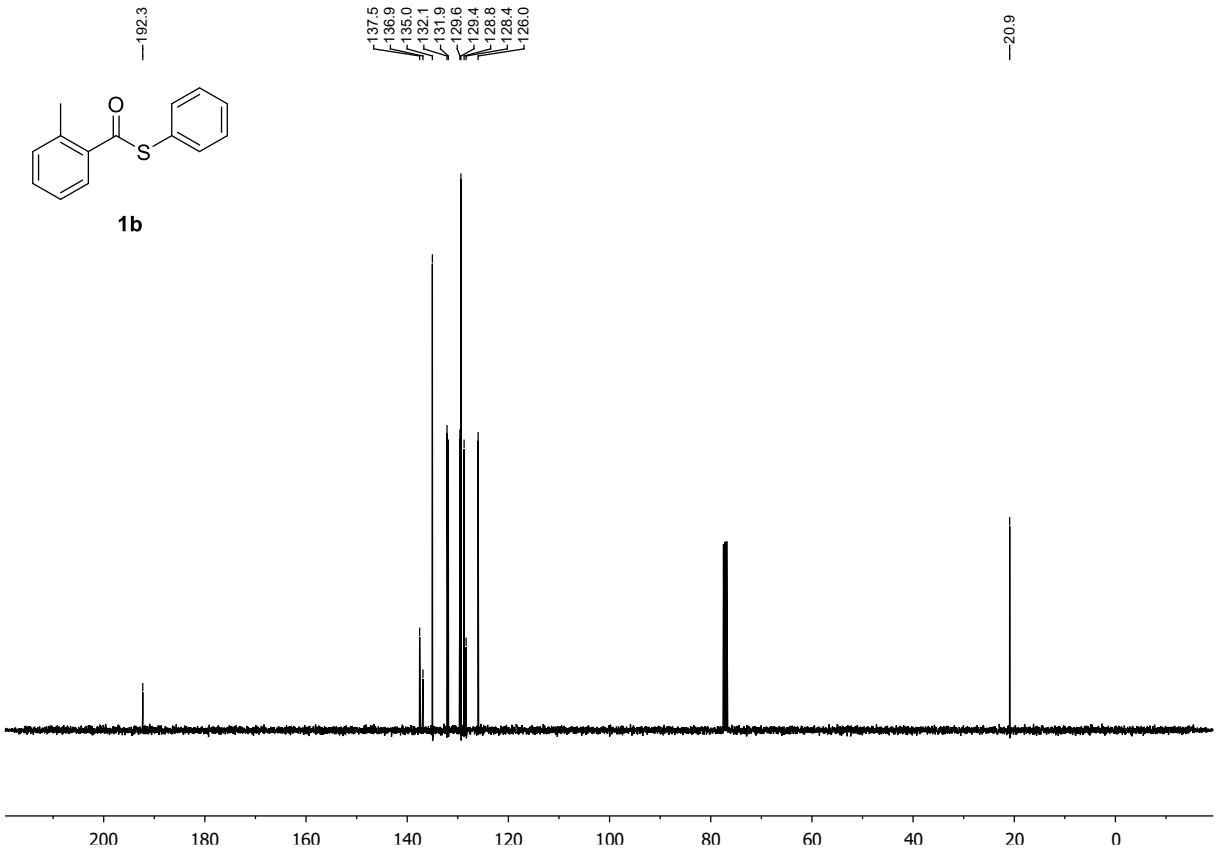

Figure S12. ^{13}C NMR spectrum (101 MHz, $CDCl_3$) of **1b**.

***S*-phenyl naphthalene-1-carbothioate (1c):**

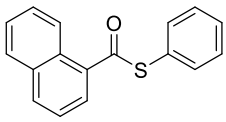

1c

$C_{17}H_{12}OS$ (264.34 g/mol)

Following **GP-A1**, **1c** was synthesized using 1-naphthoyl chloride (3.06 mL, 20.0 mmol, 1.0 equiv.), thiophenol (2.45 mL, 24.0 mmol, 1.2 equiv.) and triethylamine (3.34 mL, 24.0 mmol, 1.2 equiv.). Purification by crystallization (DCM/*n*-hexane) afforded **1c** (3.94 g, 14.9 mmol, 75%) as colorless solid. Conforms to reported analytical data.[12]

^{1}H NMR (400 MHz, $CDCl_3$, δ): 8.61 – 8.54 (m, 1H), 8.24 (dd, *J* = 7.2, 1.2 Hz, 1H), 8.09 – 8.01 (m, 1H), 7.94 – 7.87 (m, 1H), 7.68 – 7.49 (m, 8H).

^{13}C{^{1}H} NMR (101 MHz, $CDCl_3$, δ): 192.3, 135.0, 134.8, 134.0, 133.4, 129.7, 129.5, 129.4, 128.5, 128.4, 128.2, 128.1, 126.8, 125.4, 124.6.

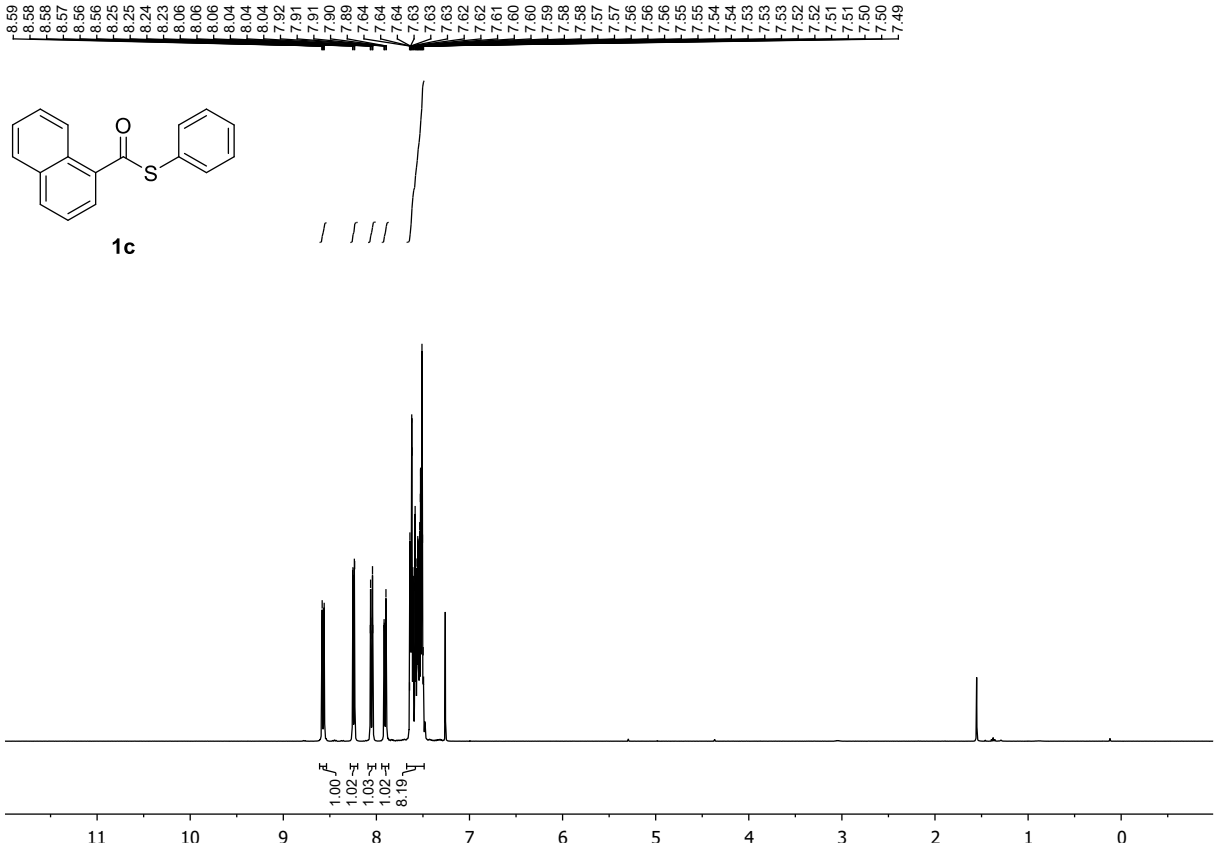

Figure S13. ^{1}H NMR spectrum (400 MHz, $CDCl_3$) of **1c**.

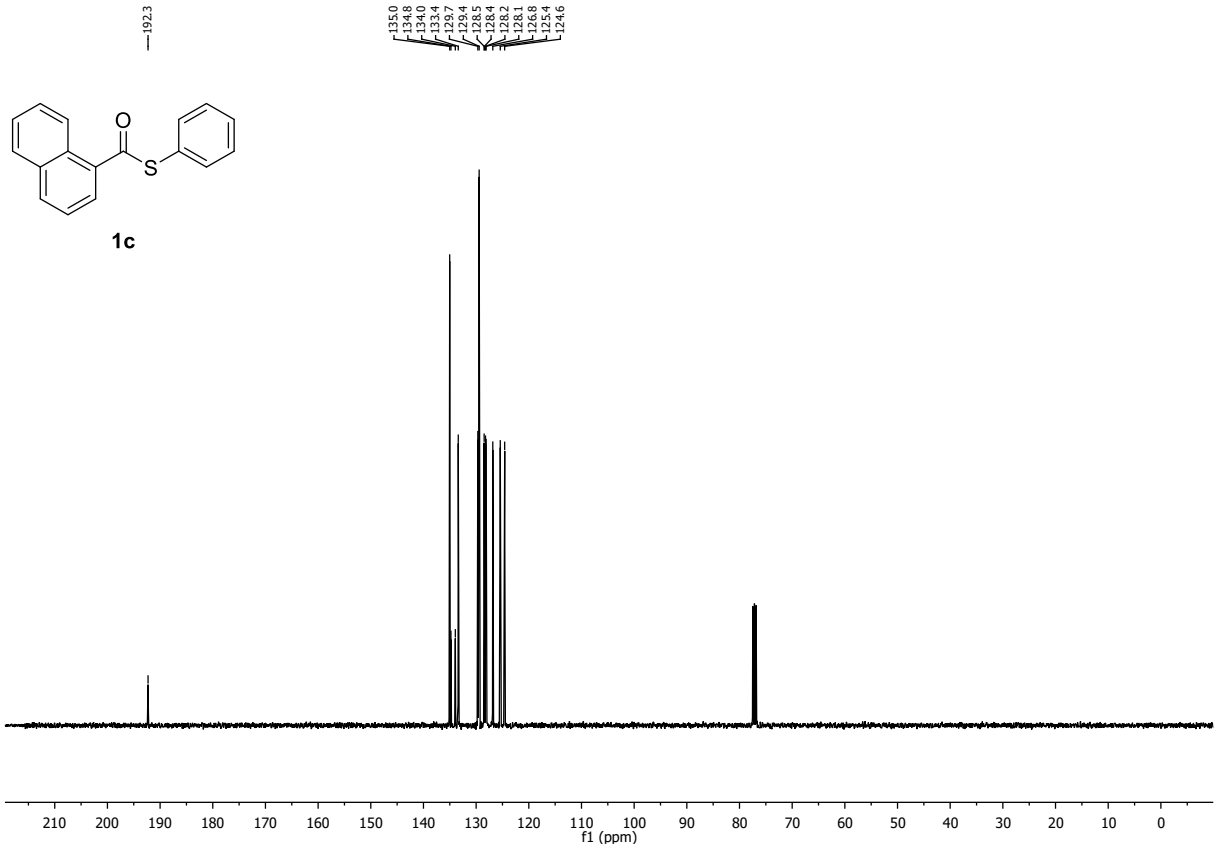

Figure S14. ^{13}C NMR spectrum (101 MHz, $CDCl_3$) of **1c**.

***S*-phenyl 3-chlorobenzothioate (1d):**

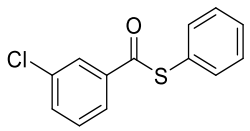

1d

$C_{13}H_9ClOS$ (248.72 g/mol)

Following **GP-A1**, **1d** was synthesized using 3-chlorobenzoyl chloride (2.57 mL, 20.0 mmol, 1.0 equiv.), thiophenol (2.45 mL, 24.0 mmol, 1.2 equiv.) and triethylamine (3.34 mL, 24.0 mmol, 1.2 equiv.). Purification by crystallization (DCM/*n*-hexane) afforded **1d** (2.53 g, 10.2 mmol, 51%) as colorless solid. Conforms to reported analytical data.[2]

^{1}H NMR (400 MHz, $CDCl_3$, δ): 8.00 (m, 1H), 7.92 (m, 1H), 7.58 (m, 1H), 7.55 – 7.40 (m, 6H).

^{13}C{^{1}H} NMR (101 MHz, $CDCl_3$, δ): 189.1, 138.3, 135.1, 133.7, 130.2, 129.9, 129.5, 127.6, 126.9, 125.7.

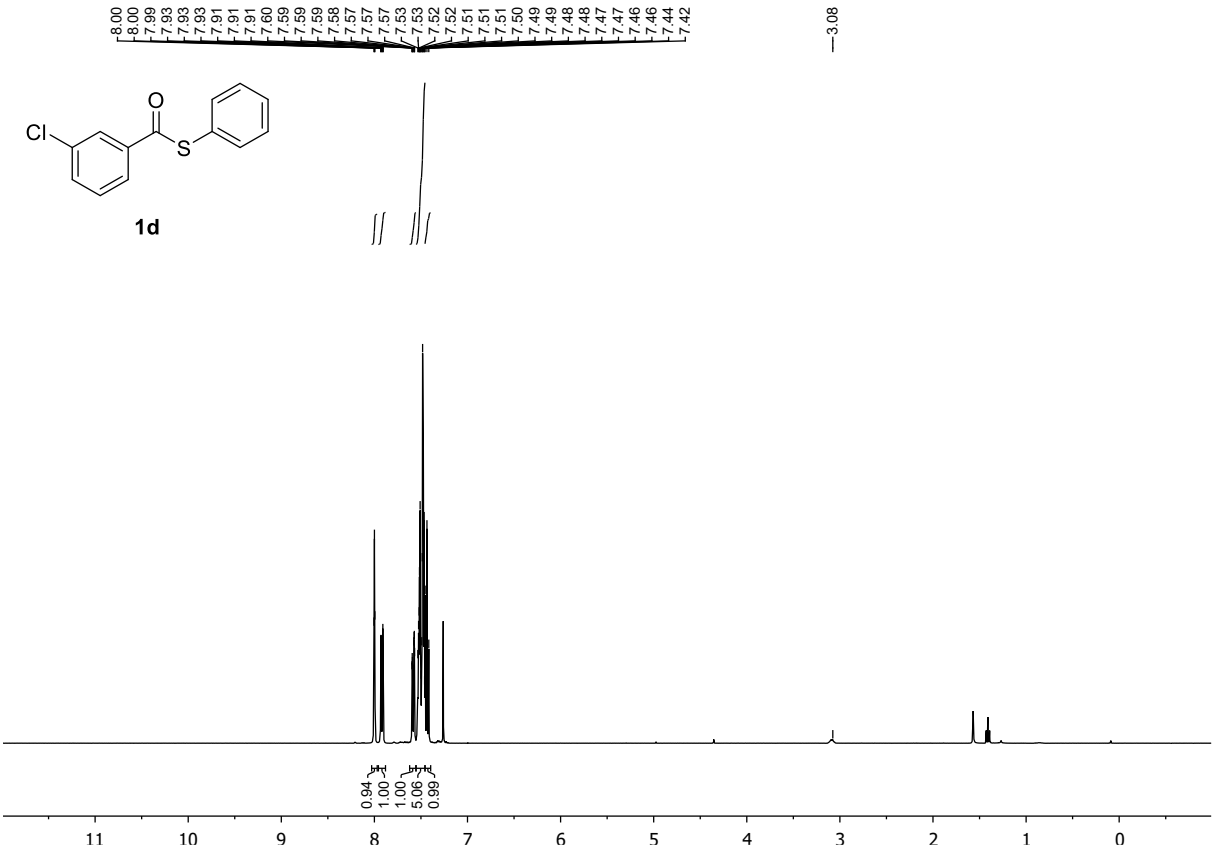

Figure S15. ^{1}H NMR spectrum (400 MHz, $CDCl_3$) of **1d**.

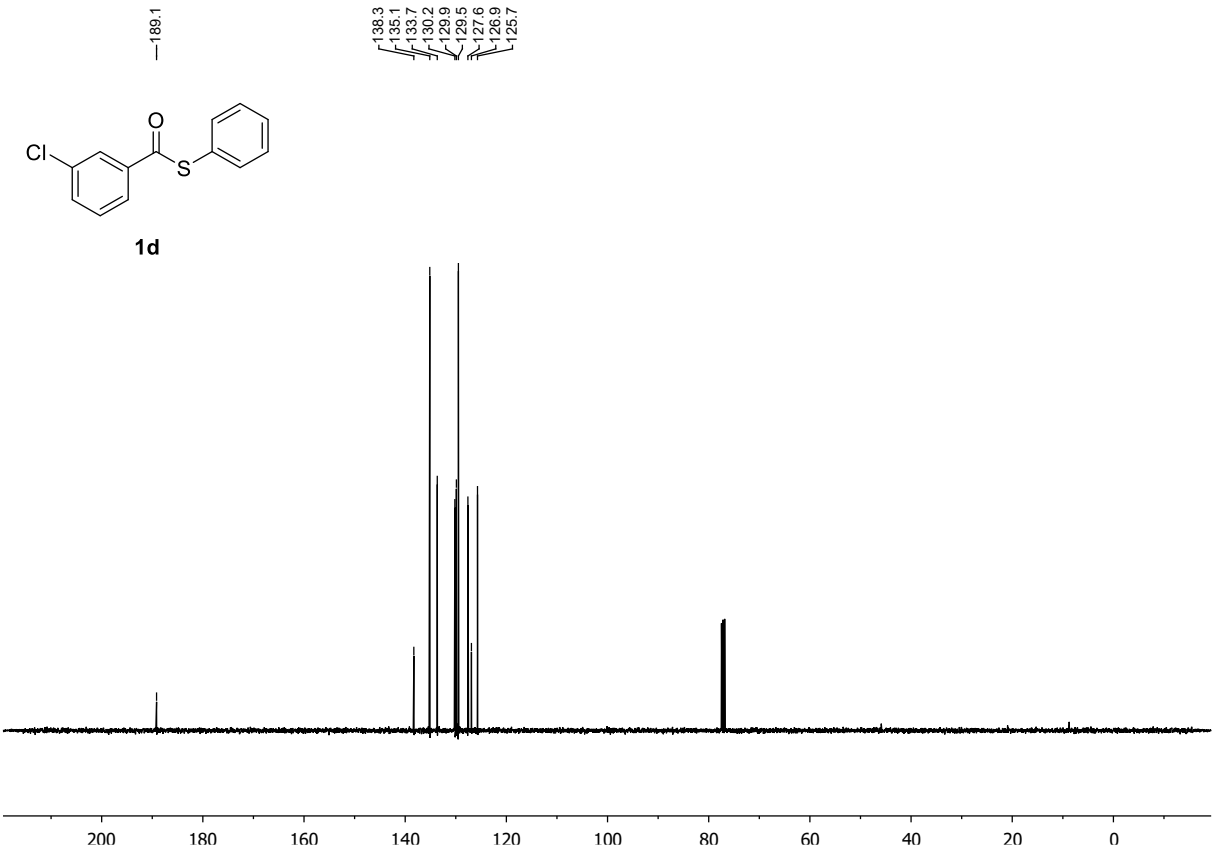

Figure S16. ^{13}C NMR spectrum (101 MHz, $CDCl_3$) of **1d**.

***S*-Phenyl 3-bromobenzothioate (1e):**

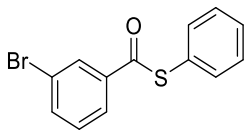

1e

$C_{13}H_9BrOS$ (293.18 g/mol)

Following **GP-1**, **1e** was synthesized using 3-bromobenzoyl chloride (2.20 g, 10.0 mmol, 1.0 equiv.), thiophenol (1.03 mL, 10.5 mmol, 1.05 equiv.) and triethylamine (1.53 mL, 11.0 mmol, 1.1 equiv.). Purification by crystallization (DCM/*n*-hexane) afforded **1e** (2.77 g, 9.45 mmol, 95%) as yellow oil. Conforms to reported analytical data.[13]

^{1}H NMR (400 MHz, $CDCl_3$, δ): 8.15 (dd, *J* = 1.8, 1.8 Hz, 1H), 8.00 – 7.92 (m, 1H), 7.77 – 7.70 (m, 1H), 7.54 – 7.46 (m, 5H), 7.37 (dd, *J* = 7.9, 7.9 Hz, 1H).

^{13}C{^{1}H} NMR (101 MHz, $CDCl_3$, δ): 189.0, 138.5, 136.6, 135.1, 130.5, 130.4, 129.9, 129.5, 126.9, 126.1, 123.1.

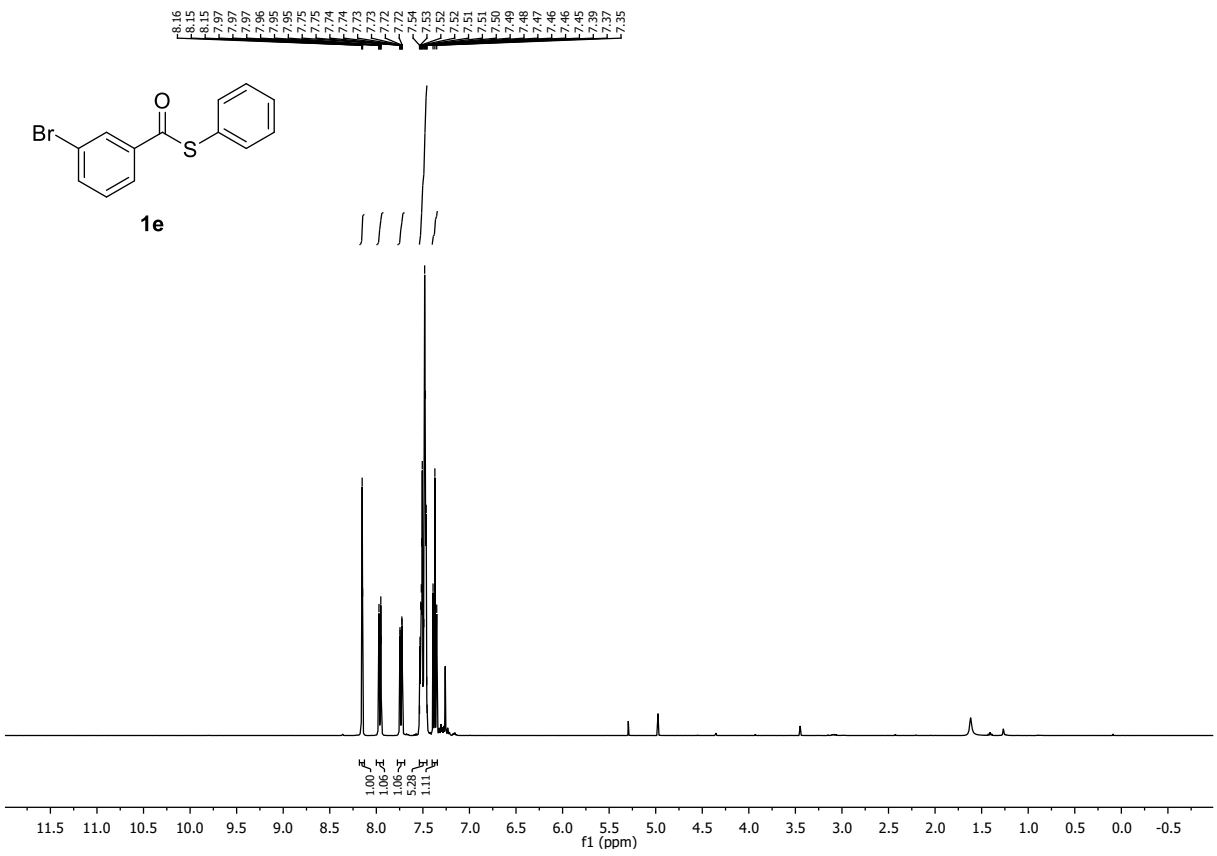

Figure S17. ^{1}H NMR (400 MHz, $CDCl_3$) spectrum of **1e**.

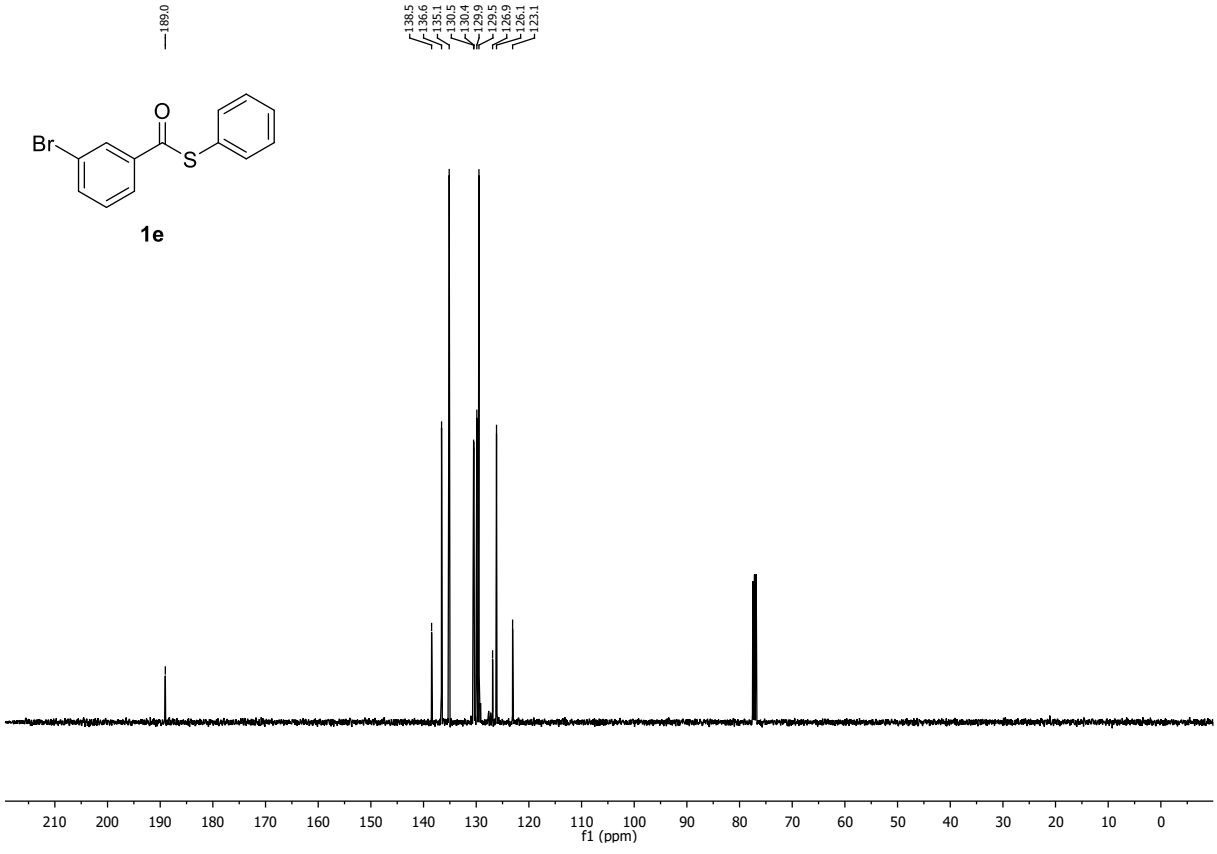

Figure S18. ^{13}C NMR (101 MHz, $CDCl_3$) spectrum of **1e**.

***S*-Phenyl 4-(trifluoromethyl)benzothioate (1f):**

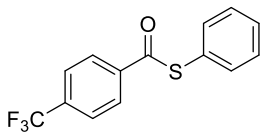

1f

$C_{14}H_9F_3OS$ (282.28 g/mol)

Following **GP-A1**, **1f** was synthesized using 4-(trifluoromethyl)benzoyl chloride (3.07 mL, 20.0 mmol, 1.0 equiv.), thiophenol (2.45 mL, 24.0 mmol, 1.2 equiv.) and triethylamine (3.34 mL, 24.0 mmol, 1.2 equiv.). Purification by crystallization (DCM/*n*-hexane) afforded **1f** (4.39 g, 15.6 mmol, 78%) as colorless solid. Conforms to reported analytical data.[14]

^{1}H NMR (400 MHz, $CDCl_3$, δ): 8.14 (d, *J* = 8.0 Hz, 2H), 7.76 (d, *J* = 8.2 Hz, 2H), 7.58 – 7.44 (m, 5H).

^{13}C{^{1}H} NMR (101 MHz, $CDCl_3$, δ): 189.5, 139.6, 135.1, 130.0, 129.6, 128.0, 126.7, 126.0 (q, *J* = 3.7 Hz), 123.6 (q, *J* = 272.7 Hz).

^{19}F NMR (376 MHz, $CDCl_3$, δ): -63.1.

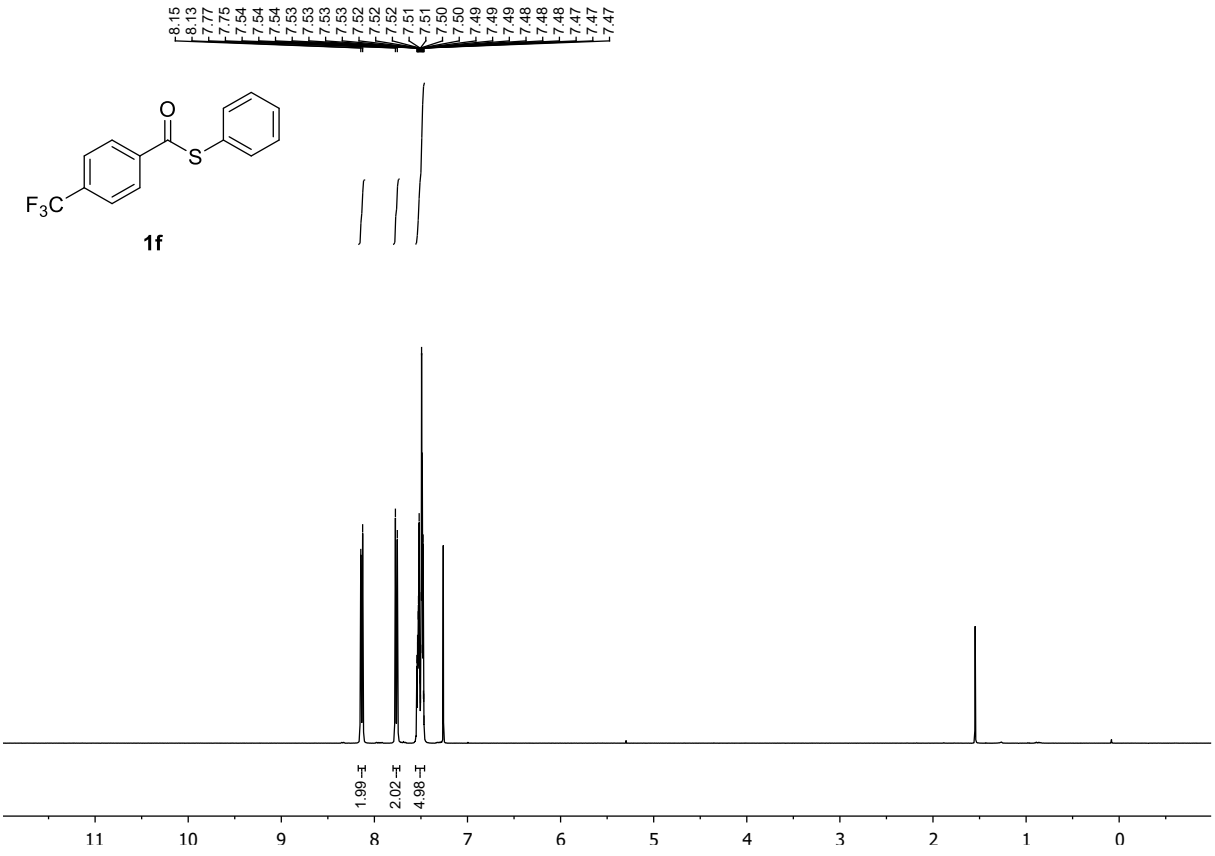

Figure S19. ^{1}H NMR spectrum (400 MHz, $CDCl_3$) of **1f**.

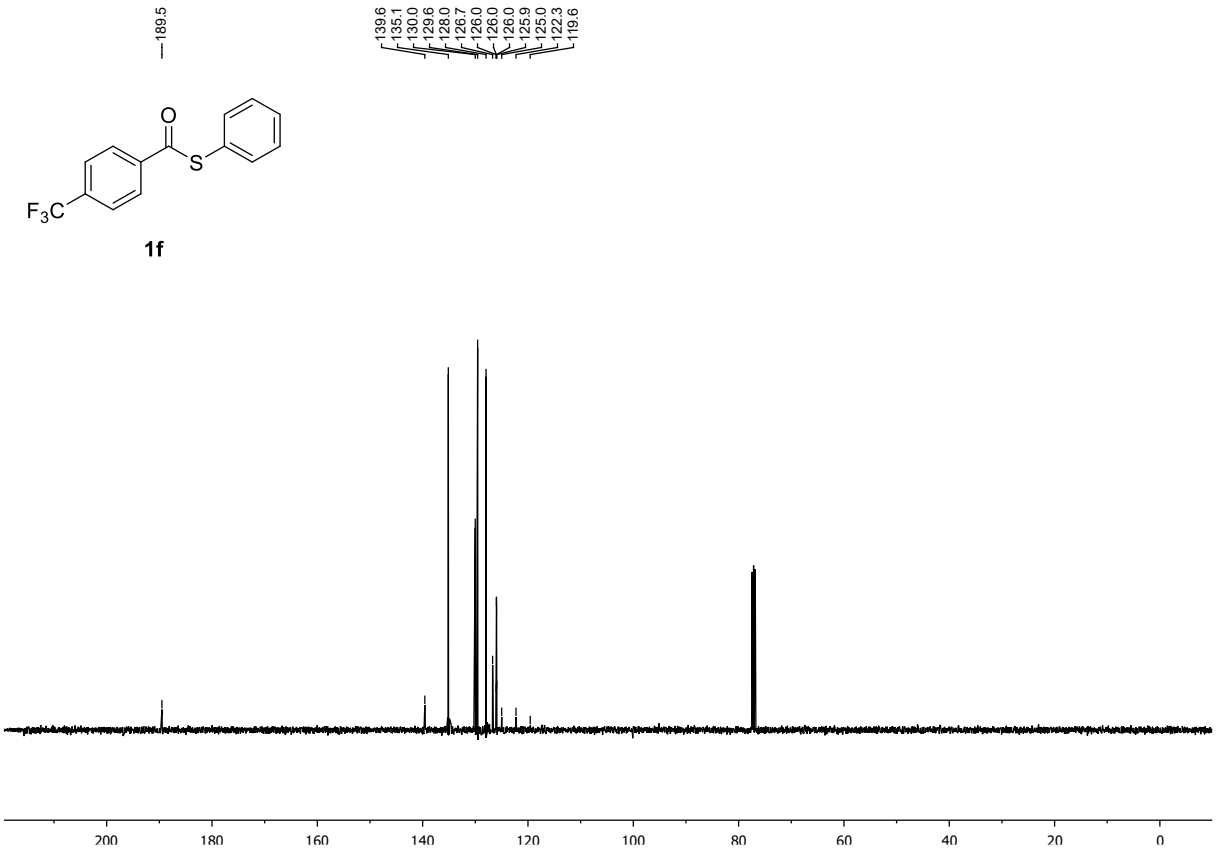

Figure S20. ^{13}C NMR spectrum (101 MHz, $CDCl_3$) of **1f**.

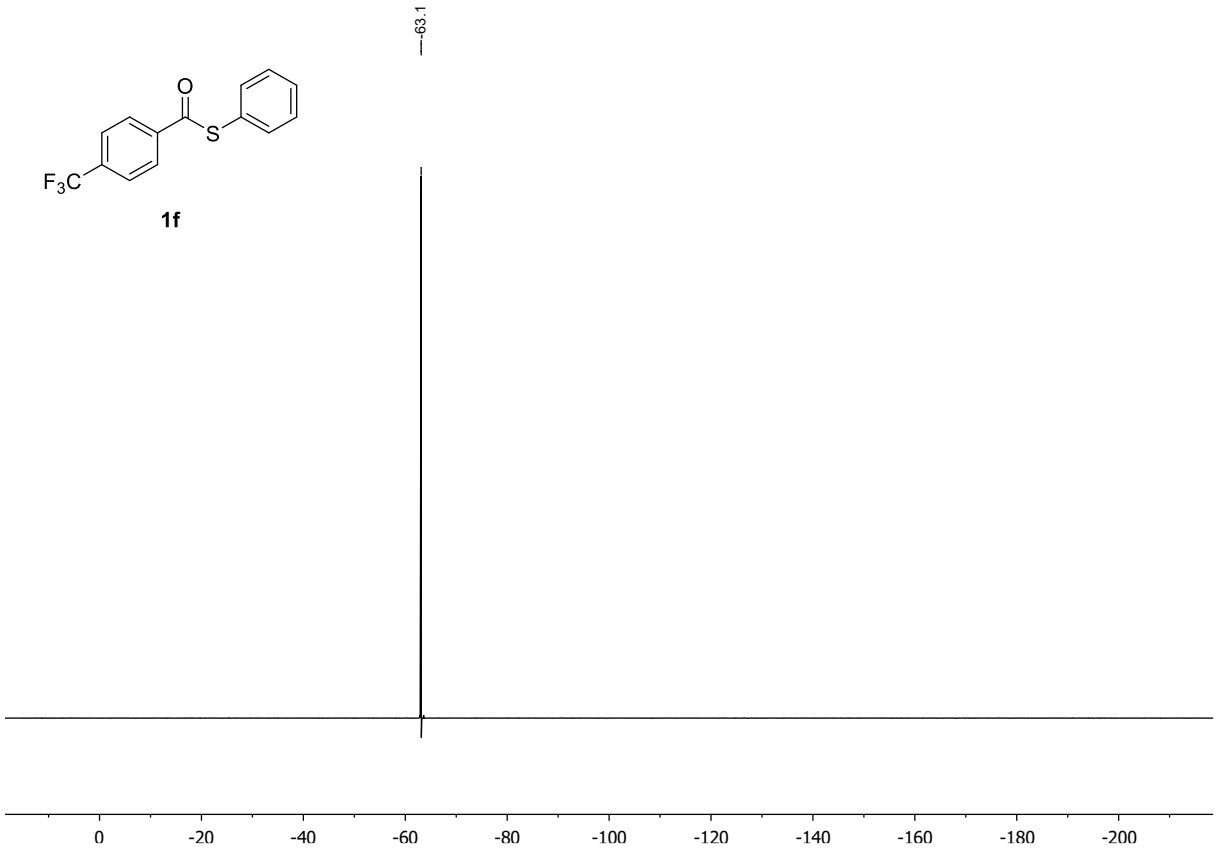

Figure S21. ^{19}F NMR spectrum (376 MHz, $CDCl_3$) of **1f**.

Methyl 4-((phenylthio)carbonyl)benzoate (1g):

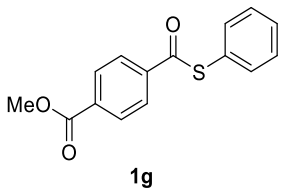

1g

$C_{15}H_{12}O_3S$ (272.32 g/mol)

Following **GP-A1**, **1g** was synthesized using methyl 4-(chlorocarbonyl)benzoate (3.03 mL, 20.0 mmol, 1.0 equiv.), thiophenol (2.45 mL, 24.0 mmol, 1.2 equiv.) and triethylamine (3.34 mL, 24.0 mmol, 1.2 equiv.). Purification by crystallization (DCM/*n*-hexane) afforded **1g** (4.92 g, 18.1 mmol, 90%) as colorless solid. Conforms to reported analytical data.[14]

^{1}H NMR (400 MHz, $CDCl_3$, δ): 8.19 – 8.05 (m, 4H), 7.55 – 7.45 (m, 5H), 3.96 (s, 3H).

^{13}C{^{1}H} NMR (101 MHz, $CDCl_3$, δ): 189.9, 166.2, 140.1, 135.1, 134.6, 130.1, 129.9, 129.5, 127.5, 127.0, 52.7.

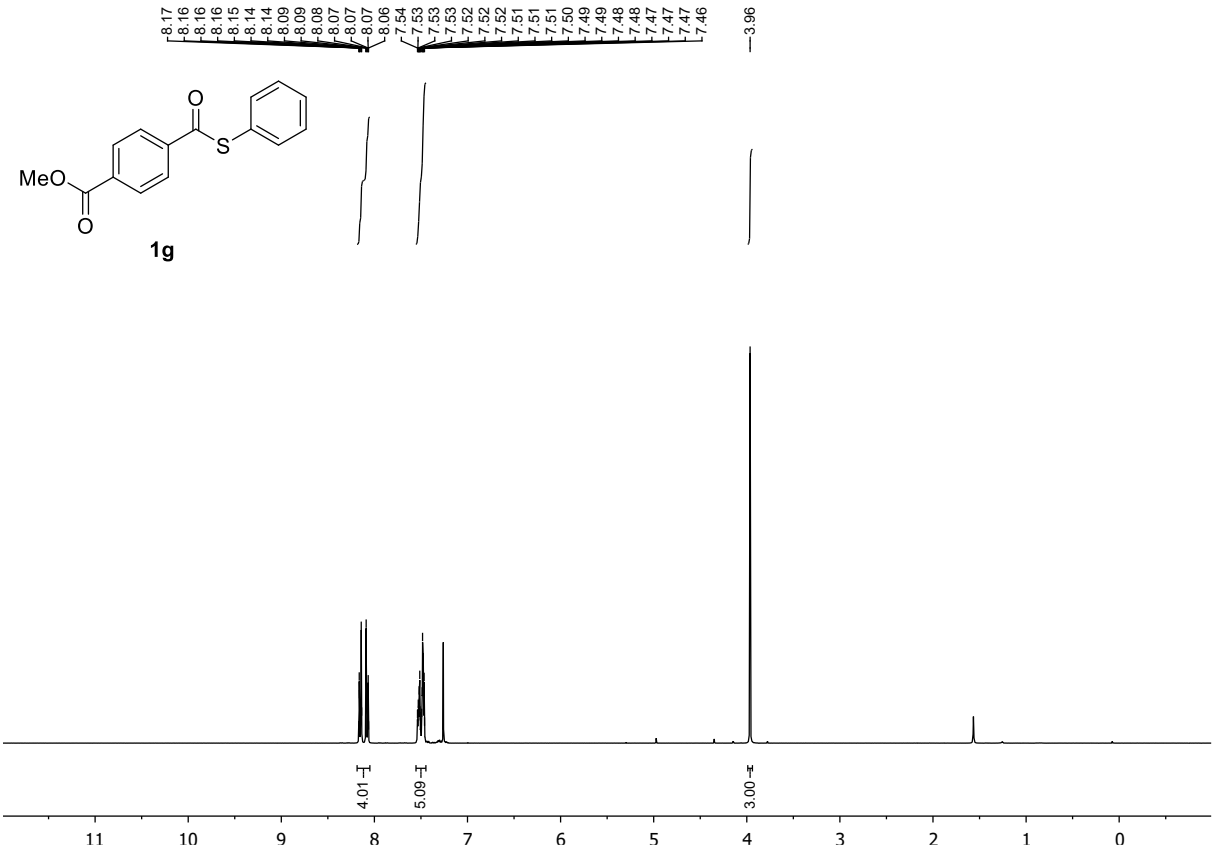

Figure S22. ^{1}H NMR spectrum (400 MHz, $CDCl_3$) of **1g**.

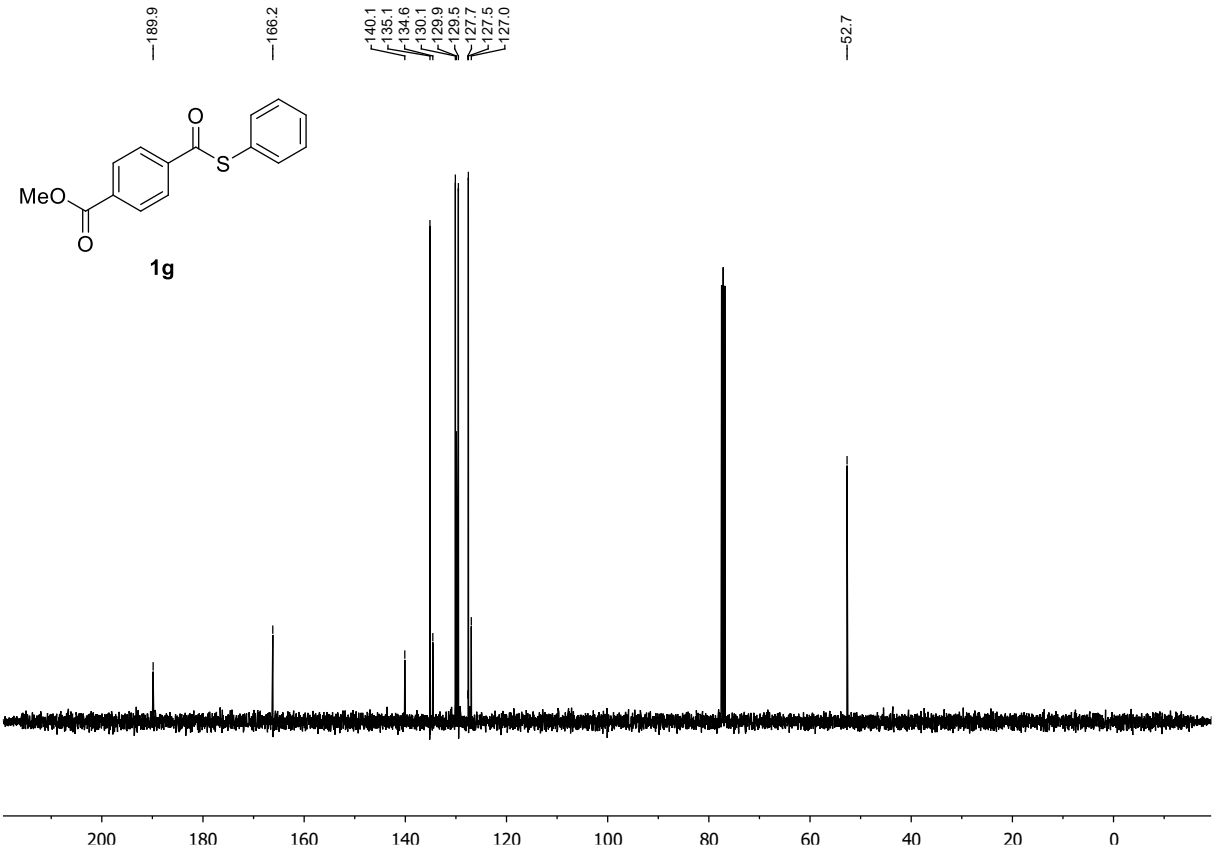

Figure S23. ^{13}C NMR spectrum (101 MHz, $CDCl_3$) of **1g**.

***S*-phenyl 4-methoxybenzothioate (1h):**

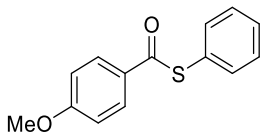

1h

$C_{14}H_{12}O_2S$ (244.31 g/mol)

Following **GP-A1**, **1h** was synthesized using methyl 4-(chlorocarbonyl)benzoate (2.74 mL, 20.0 mmol, 1.0 equiv.), thiophenol (2.45 mL, 24.0 mmol, 1.2 equiv.) and triethylamine (3.34 mL, 24.0 mmol, 1.2 equiv.). Purification by crystallization (DCM/*n*-hexane) afforded **1h** (4.41 g, 18.0 mmol, 90%) as colorless solid. Conforms to reported analytical data.[11]

^{1}H NMR (400 MHz, $CDCl_3$, δ): 8.07 – 7.97 (m, 2H), 7.56 – 7.49 (m, 2H), 7.49 – 7.39 (m, 3H), 7.01 – 6.92 (m, 2H), 3.88 (s, 3H).

^{13}C{^{1}H} NMR (101 MHz, $CDCl_3$, δ): 188.7, 164.1, 135.3, 129.8, 129.5, 129.5, 129.3, 127.8, 114.0, 55.7.

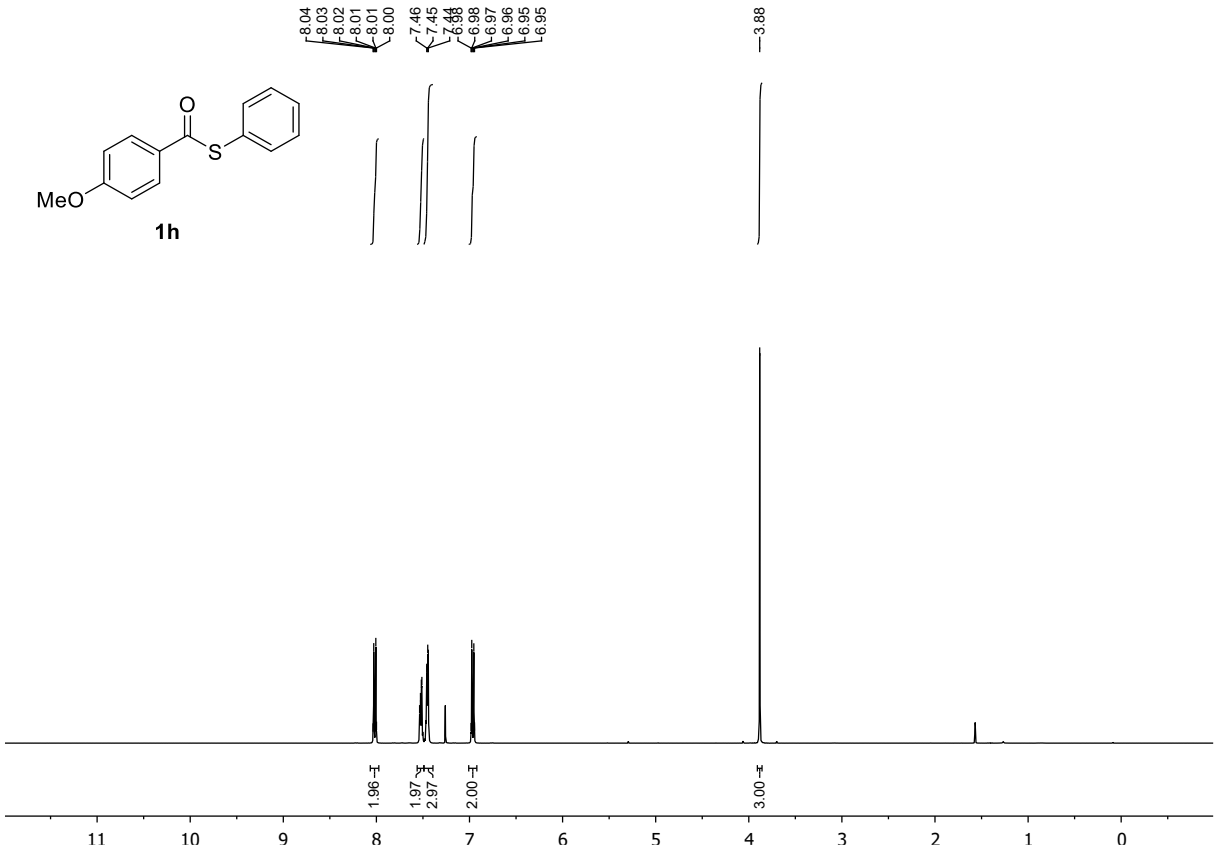

Figure S24. ^{1}H NMR spectrum (400 MHz, $CDCl_3$) of **1h**.

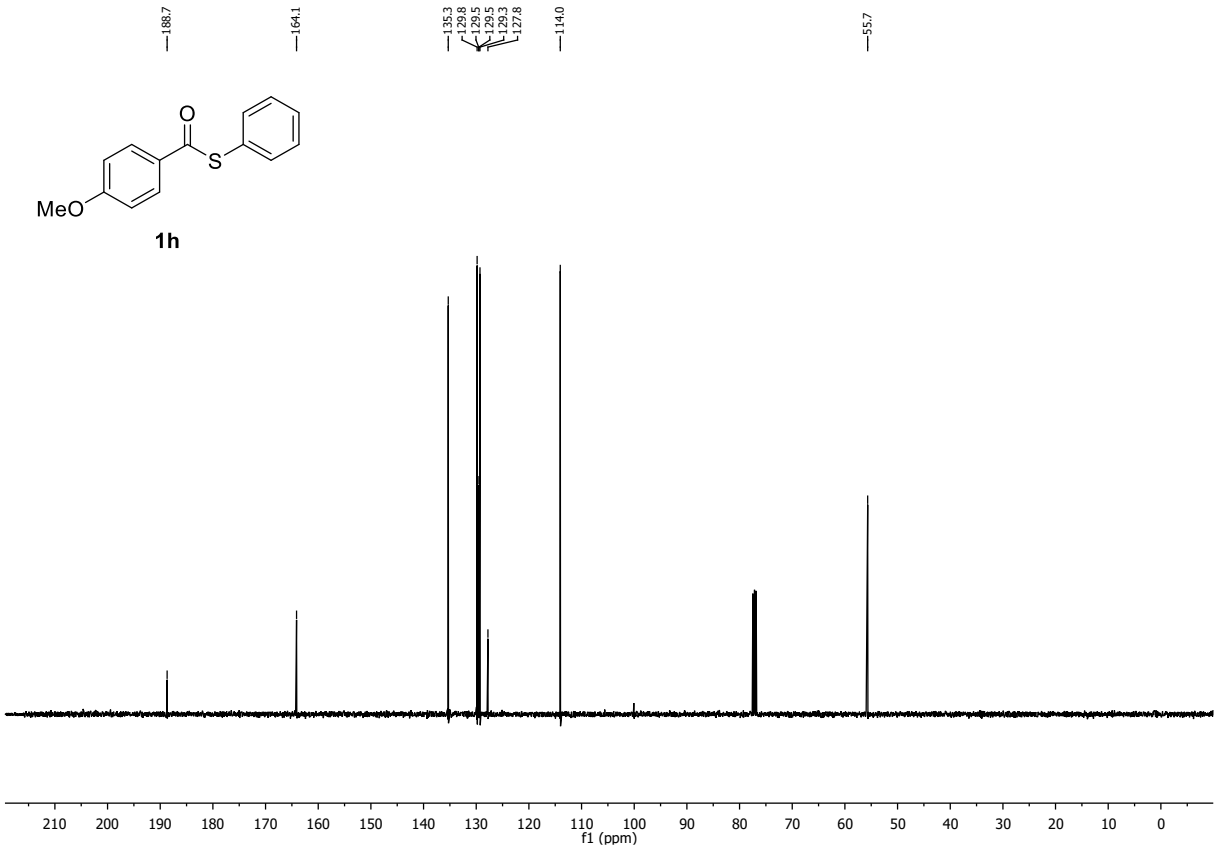

Figure S25. ^{13}C NMR spectrum (101 MHz, $CDCl_3$) of **1h**.

***S*-phenyl benzo*[d]*[1,3]dioxole-5-carbothioate (1i):**

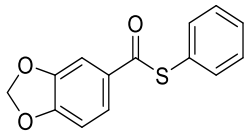

1i

$C_{14}H_{10}O_3S$ (258.29 g/mol)

Following **GP-A1**, **1i** was synthesized using 1,3-benzodioxole-5-carbonyl chloride (1.85 g, 10.0 mmol, 1 equiv.), thiopenol (1.32 g, 12.0 mmol, 1.2 equiv.), and triethylamine (1.21 g, 12 mmol, 1.2 equiv.). Purification by crystallization (DCM/n-hexane) afforded **1g** (863 mg, 3.34 mmol, 33%) as colorless solid. Conforms to reported analytical data.[15]

^{1}H NMR (400 MHz, $CDCl_3$, δ): 7.69 (dd, *J* = 8.2, 1.8 Hz, 1H), 7.53 – 7.48 (m, 2H), 7.48 – 7.42 (m, 4H), 6.88 (d, *J* = 8.2 Hz, 1H), 6.07 (s, 2H).

^{13}C{^{1}H} NMR (101 MHz, $CDCl_3$, δ): 188.5, 152.4, 148.3, 135.3, 131.2, 129.6, 129.3, 127.6, 123.8, 108.3, 107.6, 102.2.

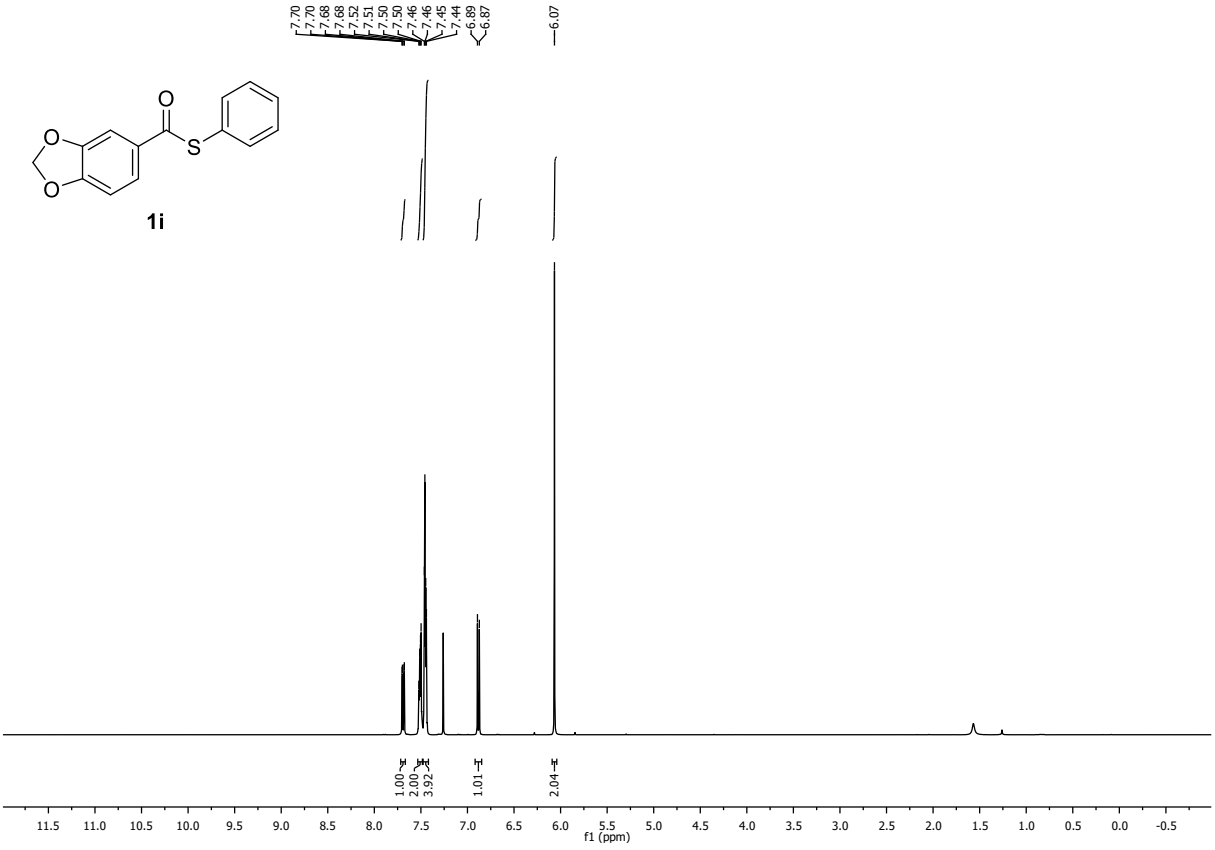

Figure S26. ^{1}H NMR spectrum (400 MHz, $CDCl_3$) of **1i**.

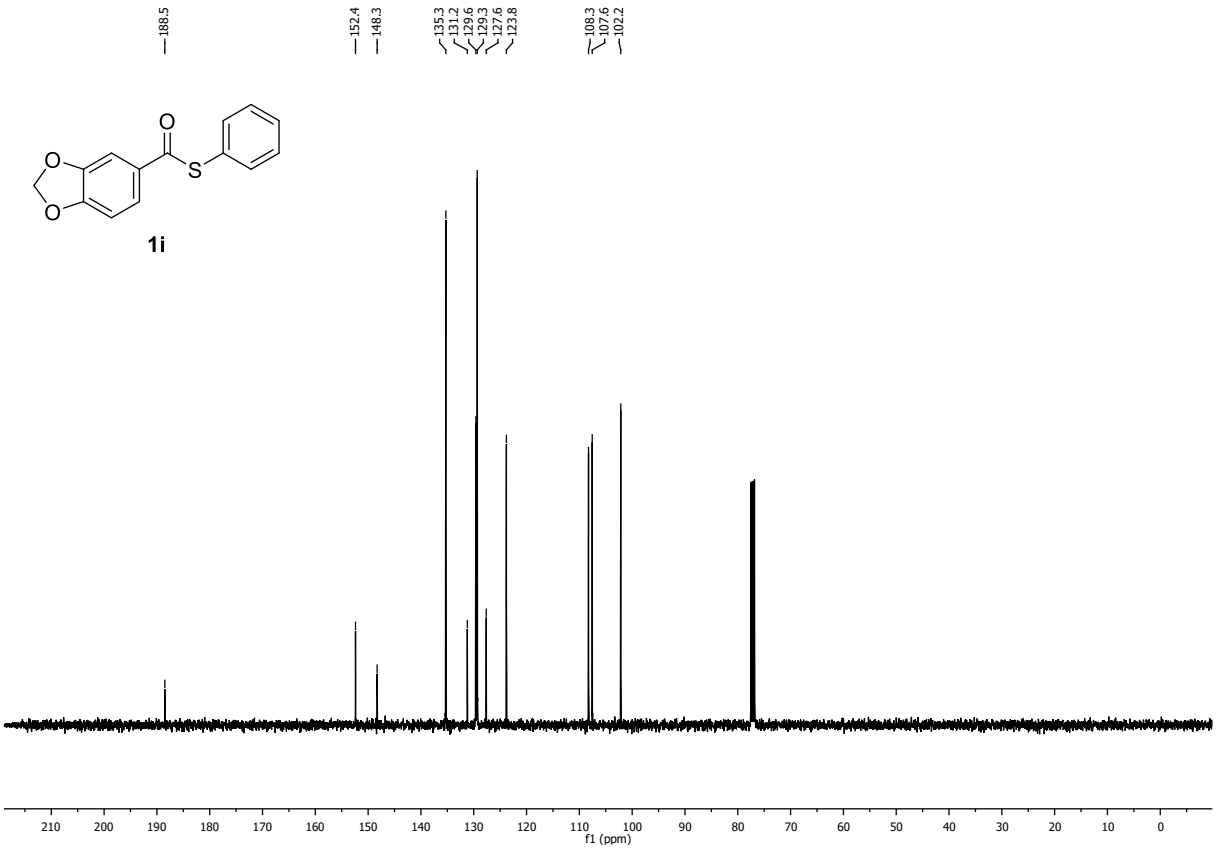

Figure S27. ^{13}C NMR spectrum (101 MHz, $CDCl_3$) of **1i**.

***S*-Phenyl 3-phenylpropanethioate (1j):**

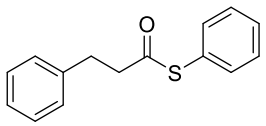

1j

$C_{15}H_{14}OS$ (242.34 g/mol)

Following **GP-A1**, **1j** was synthesized using 3-phenylpropanoyl chloride (8.43 g, 50.0 mmol, 1.0 equiv.), thiophenol (5.36 mL, 52.5 mmol, 1.05 equiv.) and triethylamine (7.32 mL, 52.5 mmol, 1.05 equiv.). Purification by crystallization (DCM/*n*-hexane) afforded **1j** (10.2 g, 42.1 mmol, 84%) as colorless solid. Conforms to reported analytical data.[13]

^{1}H NMR (400 MHz, $CDCl_3$, δ): 7.46 – 7.35 (m, 5H), 7.34 – 7.29 (m, 2H), 7.26 – 7.18 (m, 3H), 3.08 – 2.92 (m, 4H).

^{13}C{^{1}H} NMR (101 MHz, $CDCl_3$, δ): 196.8, 140.1, 134.6, 129.5, 129.3, 128.7, 128.5, 127.8, 126.6, 45.3, 31.5.

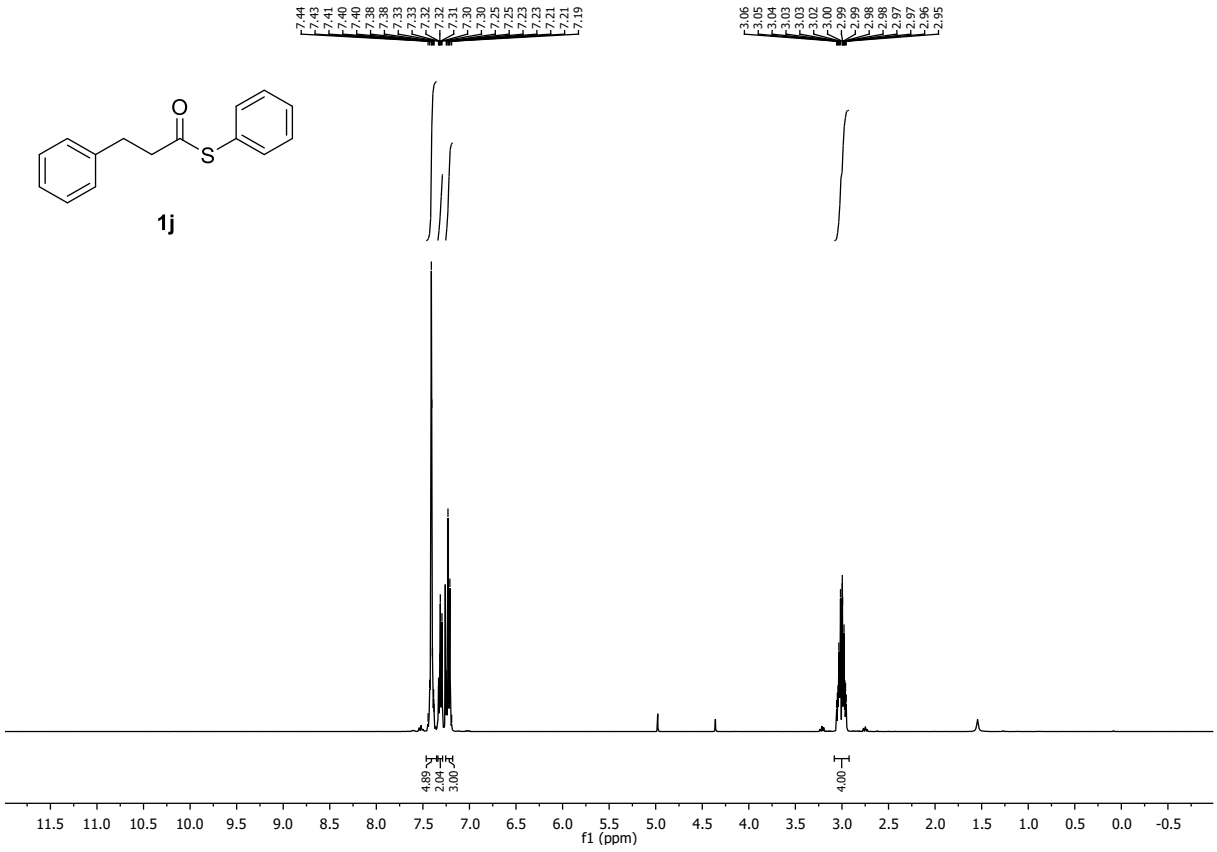

Figure S28. ^{1}H NMR spectrum (400 MHz, $CDCl_3$) of **1j**.

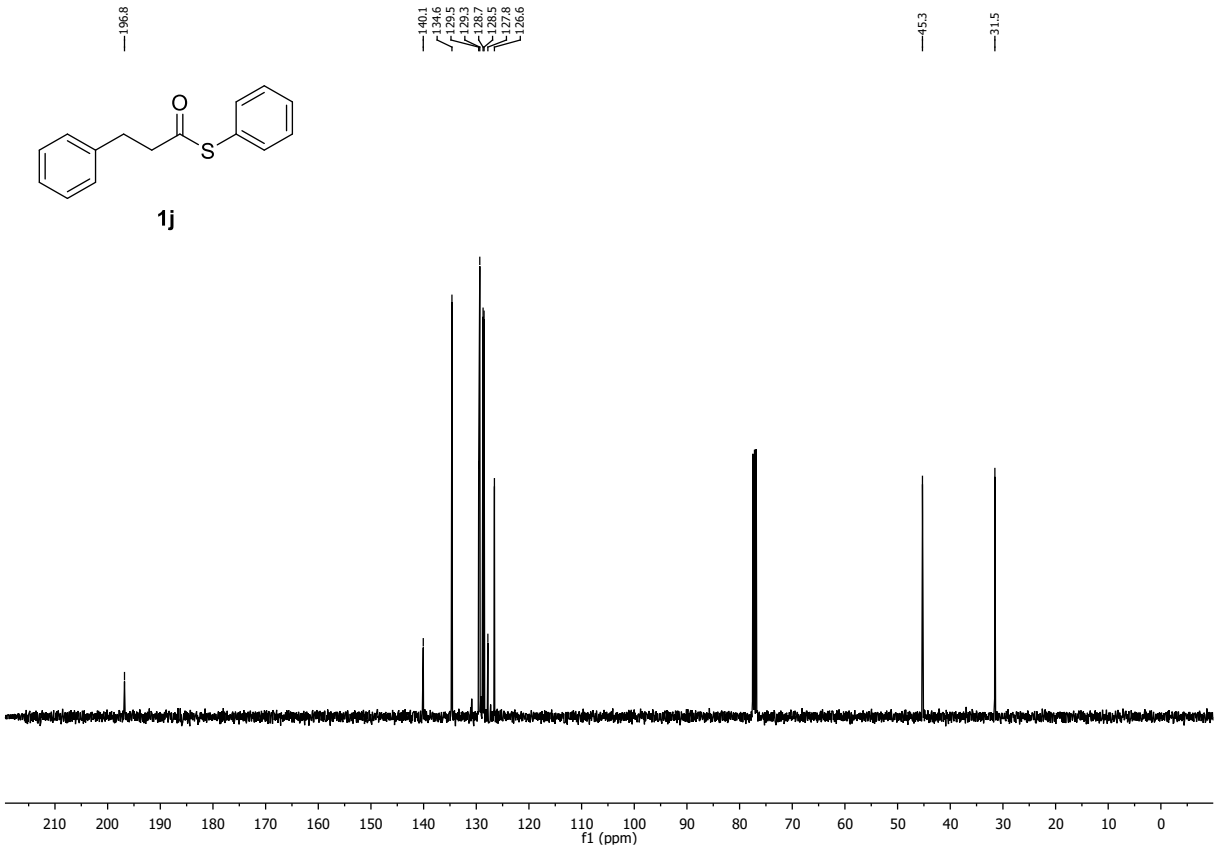

Figure S29. ^{13}C NMR spectrum (101 MHz, $CDCl_3$) of **1j**.

***S*-Phenyl 2-phenylethanethioate (1k):**

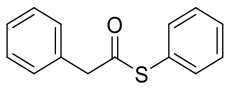

1k

$C_{14}H_{12}OS$ (228.31 g/mol)

Following **GP-A1**, **1k** was synthesized using 2-phenylacetyl chloride (2.67 mL, 20.0 mmol, 1.0 equiv.), thiophenol (2.45 mL, 24.0 mmol, 1.2 equiv.) and triethylamine (3.34 mL, 24.0 mmol, 1.2 equiv.). Purification by crystallization (DCM/*n*-hexane) afforded **1k** (1.23 g, 5.4 mmol, 27%) as colorless solid. Conforms to reported analytical data.[14]

^{1}H NMR (400 MHz, $CDCl_3$, δ): 7.46 – 7.27 (m, 10H), 3.93 (s, 2H).

^{13}C{^{1}H} NMR (101 MHz, $CDCl_3$, δ): 195.5, 134.6, 133.4, 129.8, 129.5, 129.3, 128.8, 127.9, 127.7, 50.3.

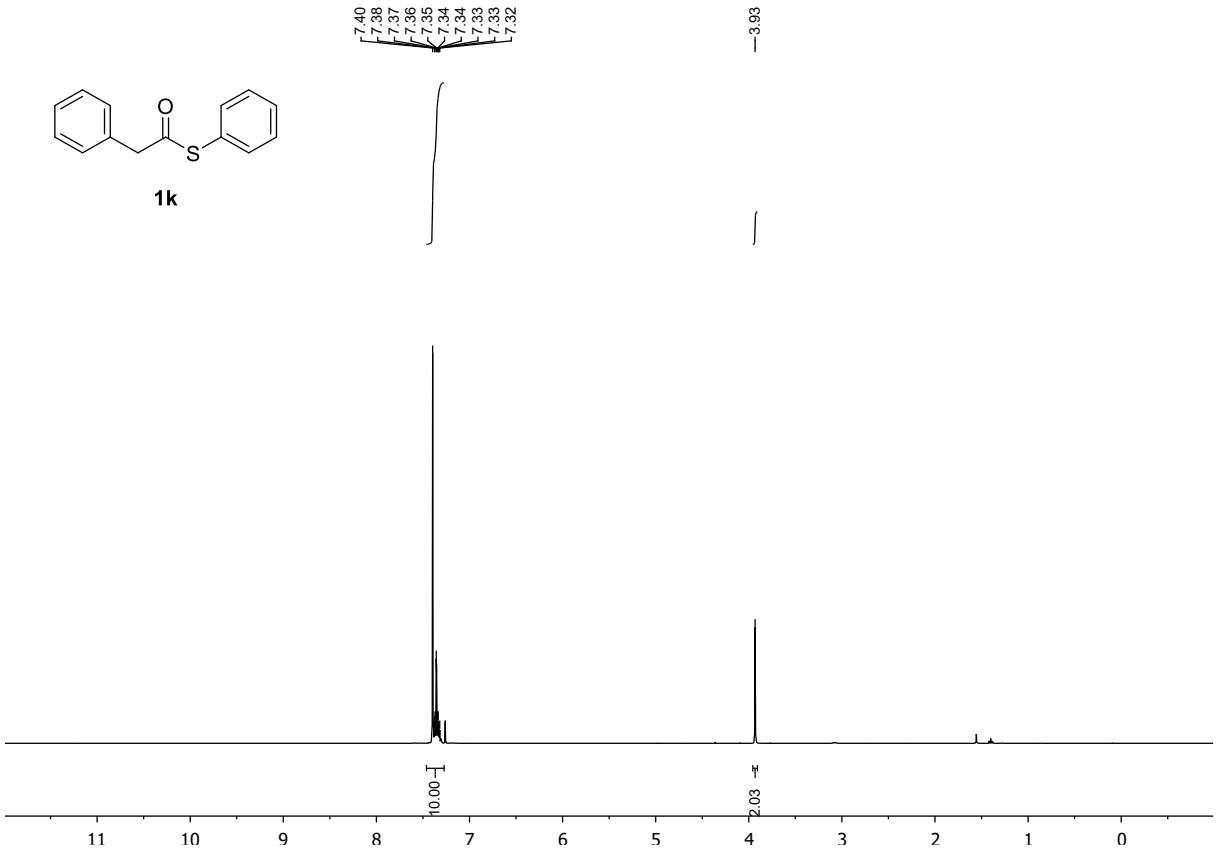

Figure S30. ^{1}H NMR spectrum (400 MHz, $CDCl_3$) of **1k**.

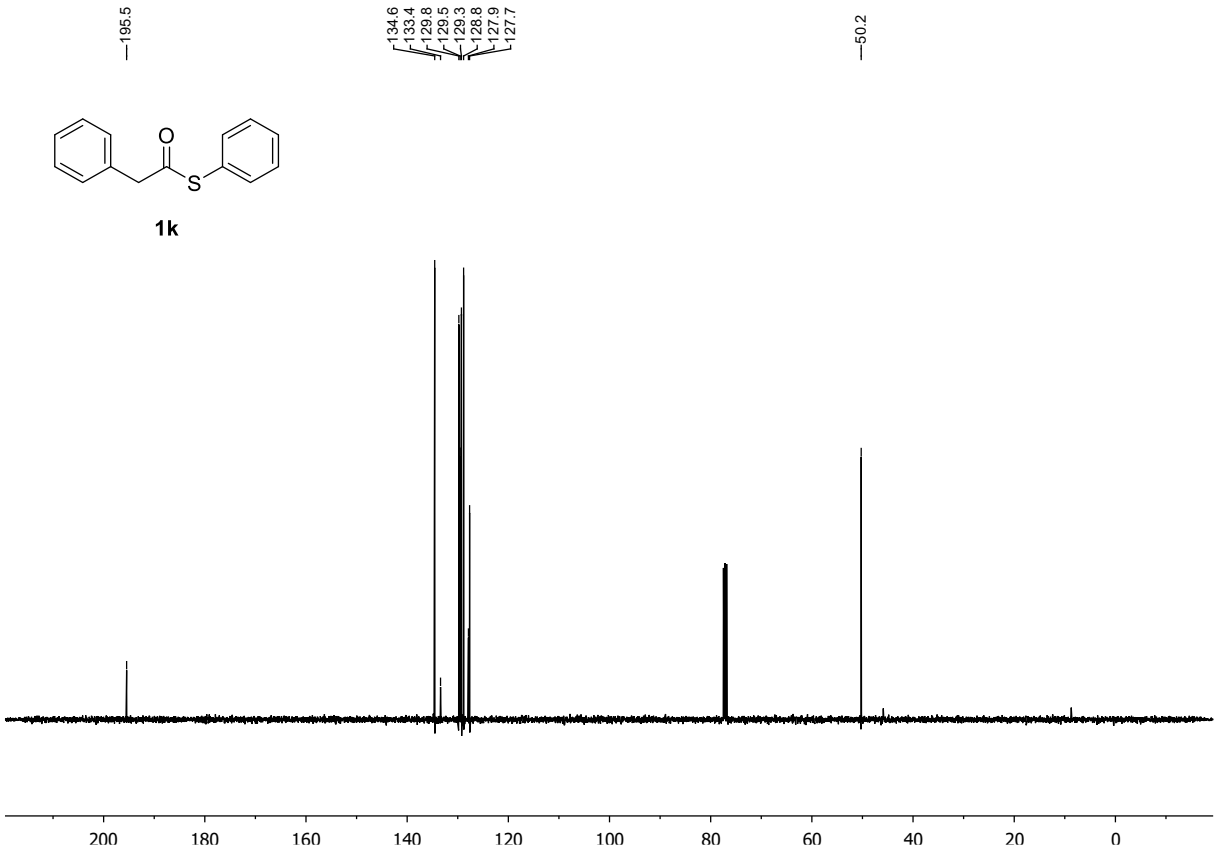

Figure S31. ^{13}C NMR spectrum (101 MHz, $CDCl_3$) of **1k**.

***S*-Phenyl hexanethioate (1l):**

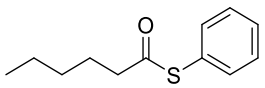

1l

$C_{12}H_{16}OS$ (208.32 g/mol)

Following **GP-A1**, **1l** was synthesized using hexanoyl chloride (1.39 g, 10.0 mmol, 1.0 equiv.), thiophenol (1.23 mL, 12.0 mmol, 1.2 equiv.) and triethylamine (1.39 mL, 10.0 mmol, 1.0 equiv.). Purification by column chromatography (*n*-hexane/EtOAc, gradient 100:0 to 95:5 over 10 CV) afforded **1l** (0.89 g, 4.27 mmol, 43%) as colorless oil. Conforms to reported analytical data.[15]

^{1}H NMR (400 MHz, $CDCl_3$, δ): 7.47 – 7.37 (m, 5H), 2.65 (t, *J* = 7.5 Hz, 2H), 1.78 – 1.66 (m, 2H), 1.42 – 1.27 (m, 4H), 0.96 – 0.86 (m, 3H).

^{13}C{^{1}H} NMR (101 MHz, $CDCl_3$, δ): 197.7, 134.6, 129.4, 129.3, 128.1, 43.8, 31.2, 25.4, 22.5, 14.0.

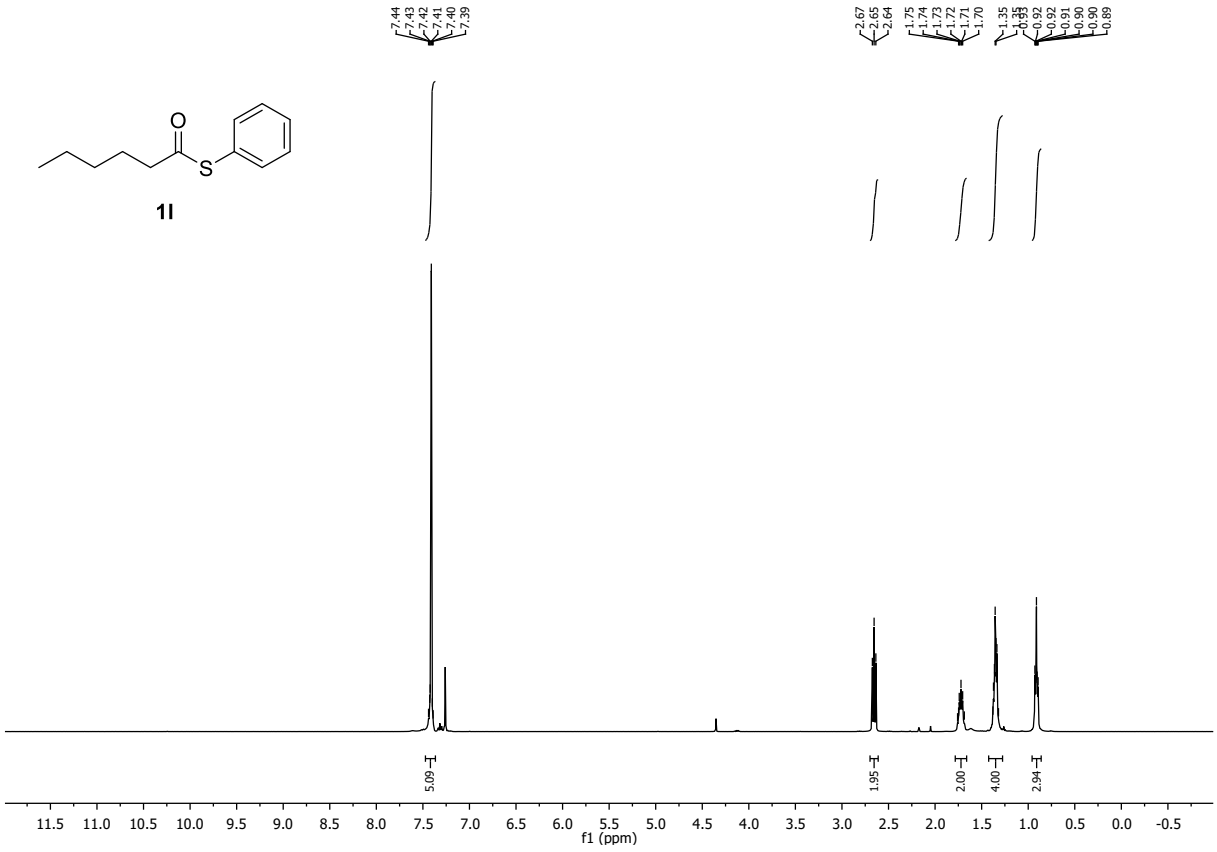

Figure S32. ^{1}H NMR spectrum (400 MHz, $CDCl_3$) of **1l**.

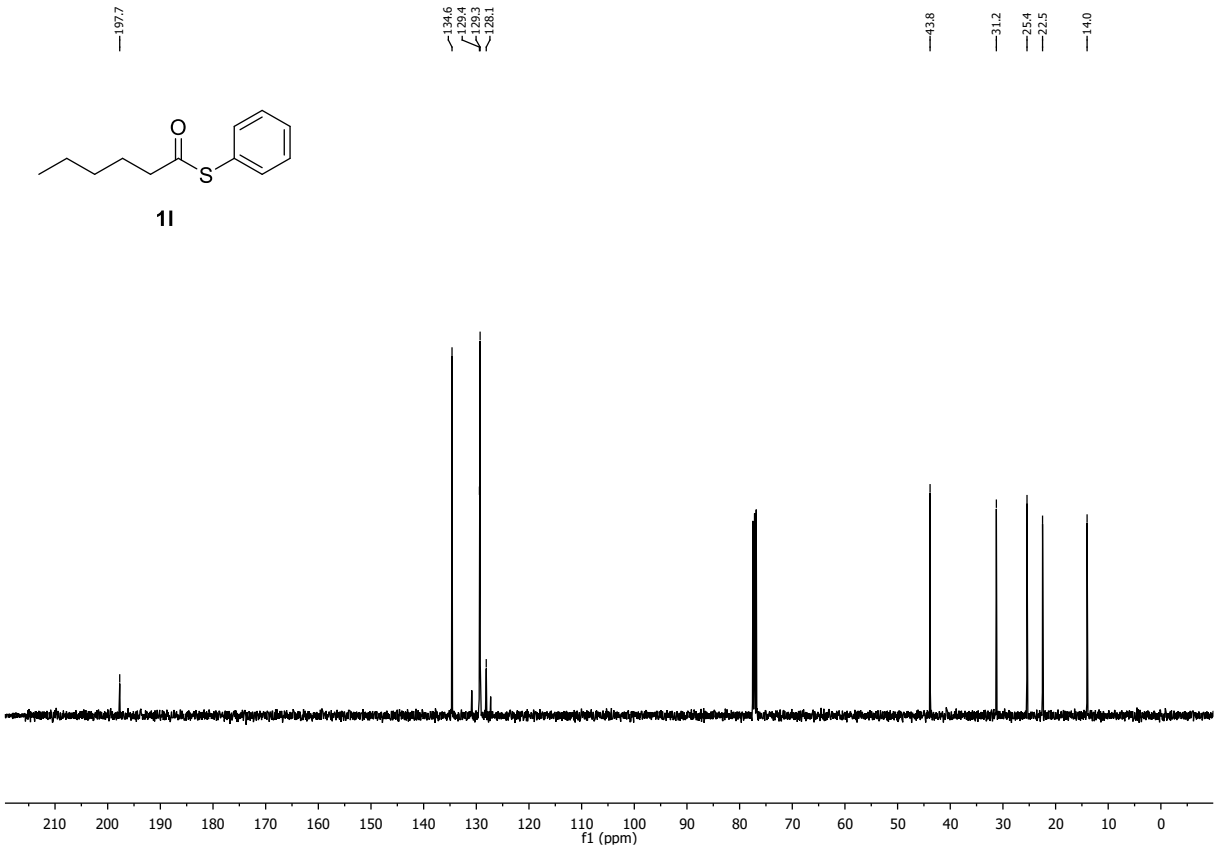

Figure S33. ^{13}C NMR spectrum (101 MHz, $CDCl_3$) of **1l**.

***S*-Phenyl pent-4-enethioate (1m):**

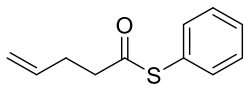

1m

$C_{11}H_{12}OS$ (192.28 g/mol)

Following **GP-A1**, **1m** was synthesized using 4-pentenoyl chloride (1.19 g, 10.0mmol, 1 equiv.), thiophenol (1.32 g, 12.0 mmol, 1.2 equiv.), and triethylamine (1.21 g, 12.0 mmol, 1.2 equiv.). Removal of the solvent afforded **1m** (1.04 g, 5.39 mmol, 54%) as yellow liquid, which was used as received. Conforms to reported analytical data.[16]

^{1}H NMR (400 MHz, $CDCl_3$, δ): δ 7.42 (s, 5H), 5.93 – 5.78 (m, 1H), 5.16 – 5.04 (m, 2H), 2.82 – 2.73 (m, 2H), 2.53 – 2.43 (m, 2H).

^{13}C{^{1}H} NMR (101 MHz, $CDCl_3$, δ): 196.8, 136.1, 134.6, 129.5, 129.3, 127.6, 116.1, 42.9, 29.4.

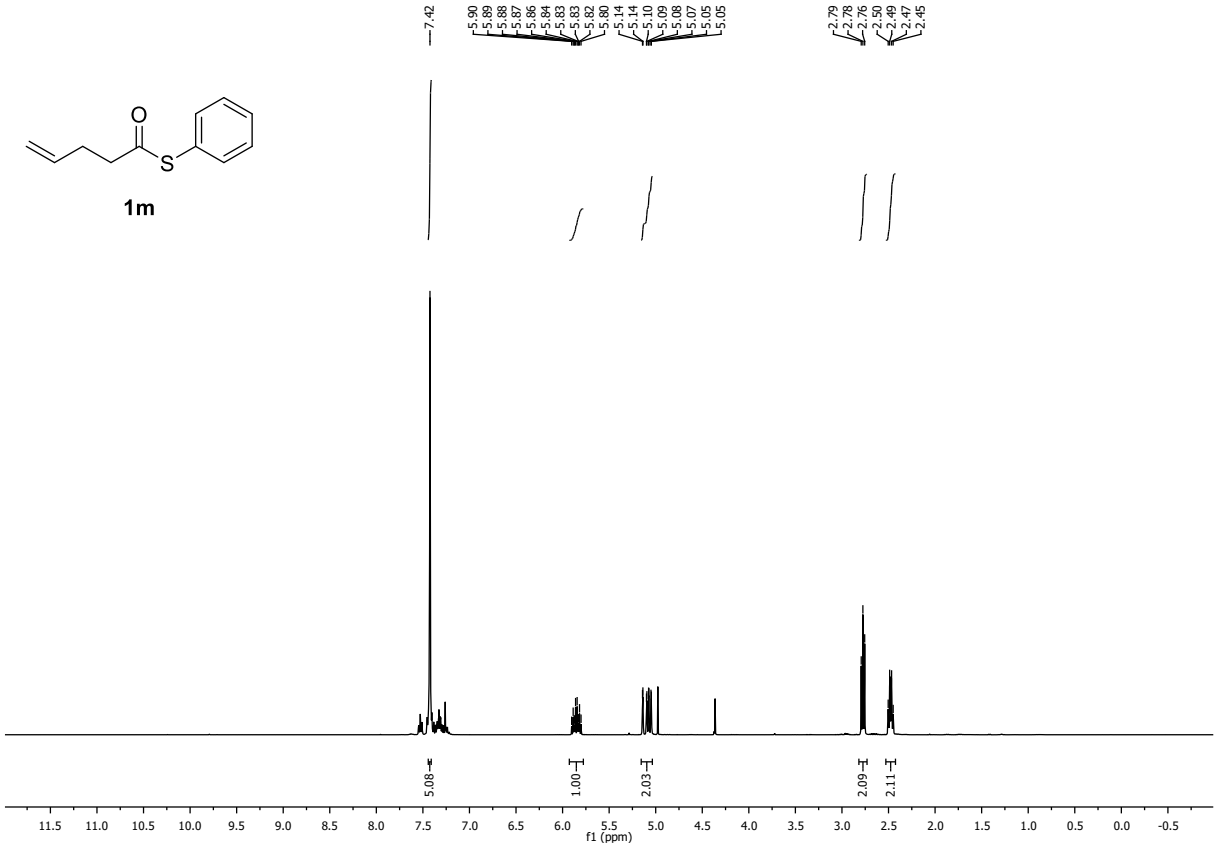

Figure S34. ^{1}H NMR spectrum (400 MHz, $CDCl_3$) of **1m**.

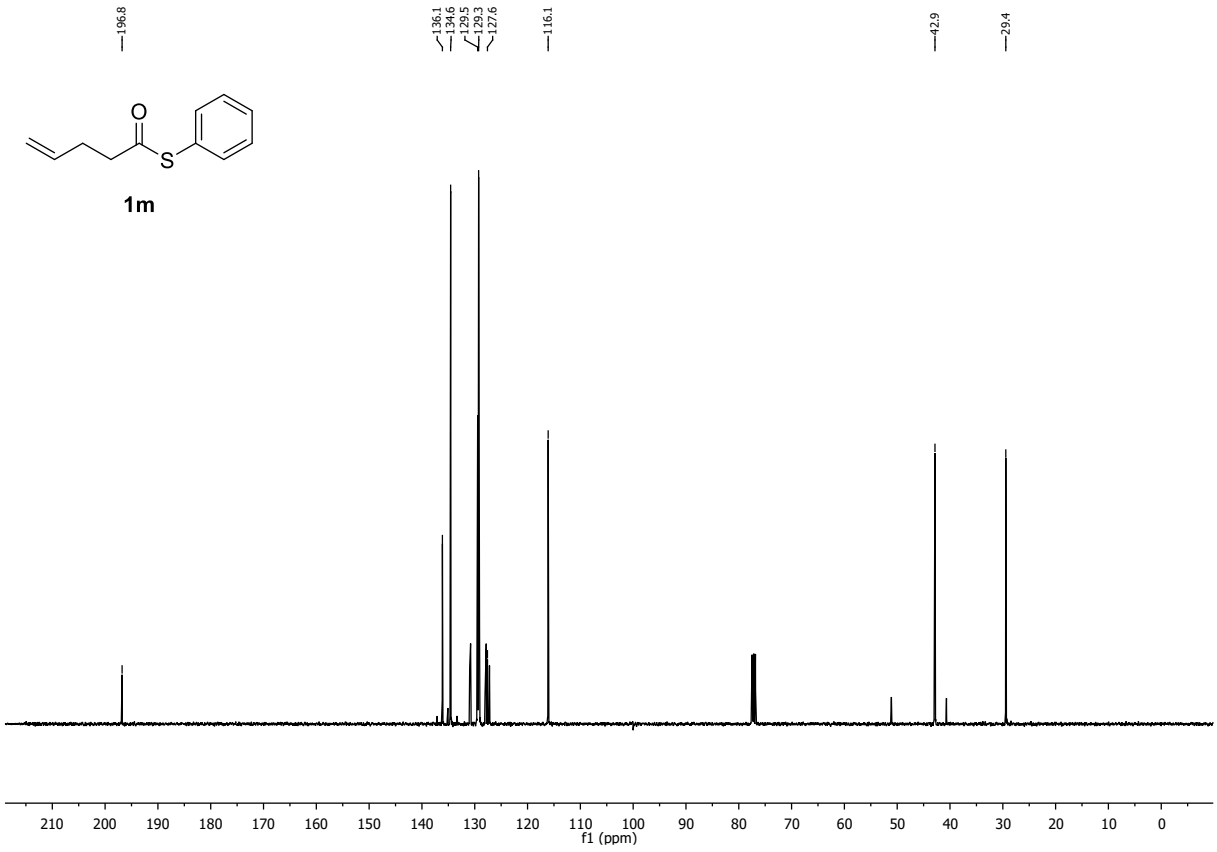

Figure S35. ^{13}C NMR spectrum (101 MHz, $CDCl_3$) of **1m**.

***S*-Phenyl cyclohexanecarbothioate (1n):**

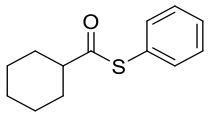

1n

$C_{13}H_{16}OS$ (220.33 g/mol)

Following **GP-A1**, **1n** was synthesized using cyclohexanecarbonyl chloride (2.75 mL, 20.0 mmol, 1.0 equiv.), thiophenol (2.45 mL, 24.0 mmol, 1.2 equiv.) and triethylamine (3.34 mL, 24.0 mmol, 1.2 equiv.). Purification by crystallization (DCM/*n*-hexane) afforded **1n** (2.64 g, 12.0 mmol, 60%) as colorless solid. Conforms to reported analytical data.[11]

^{1}H NMR (400 MHz, $CDCl_3$, δ): 7.40 (m, 5H), 2.61 (m, 1H), 2.07 – 1.95 (m, 2H), 1.88 – 1.76 (m, 2H), 1.73 – 1.62 (m, 1H), 1.53 (m, 2H), 1.40 – 1.16 (m, 3H).

^{13}C{^{1}H} NMR (101 MHz, $CDCl_3$, δ): 200.9, 134.7, 129.3, 129.2, 128.1, 52.7, 29.7, 25.7, 25.6.

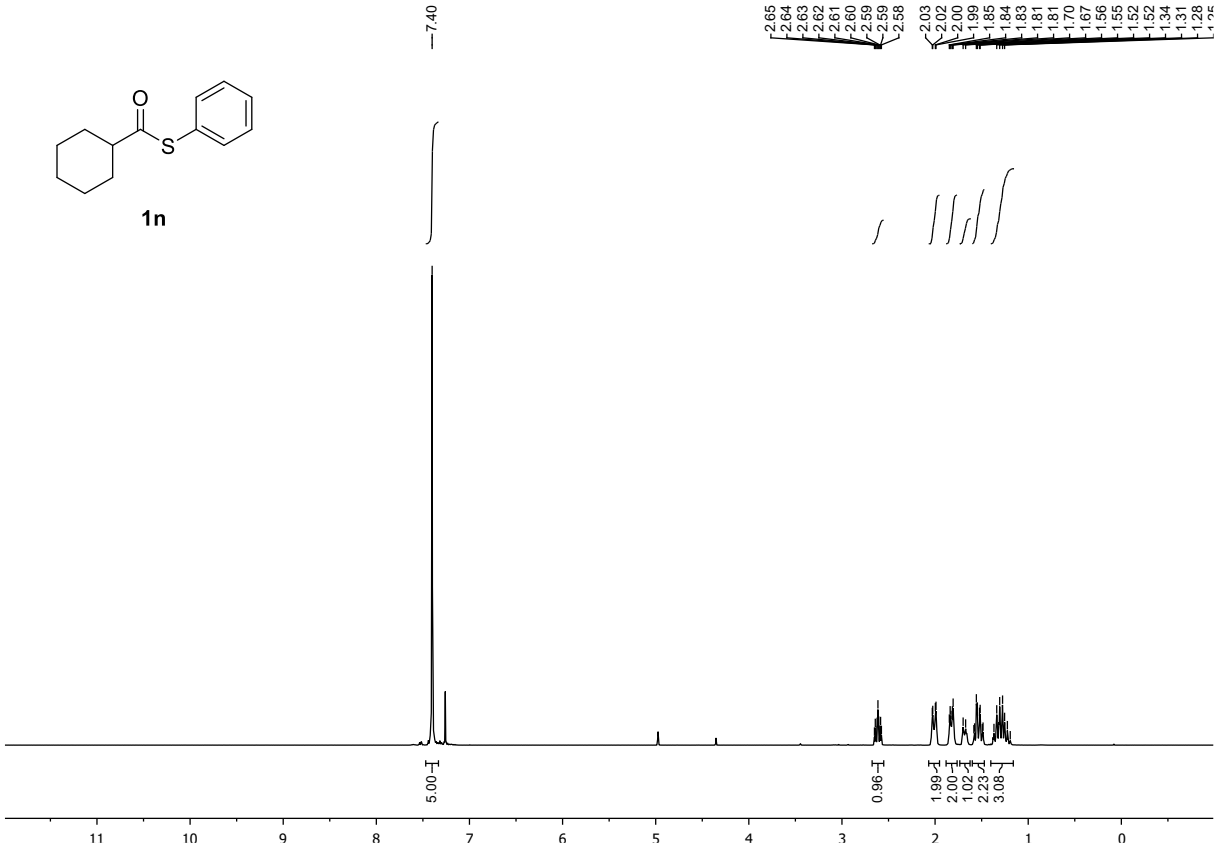

Figure S36. ^{1}H NMR spectrum (400 MHz, $CDCl_3$) of **1n**.

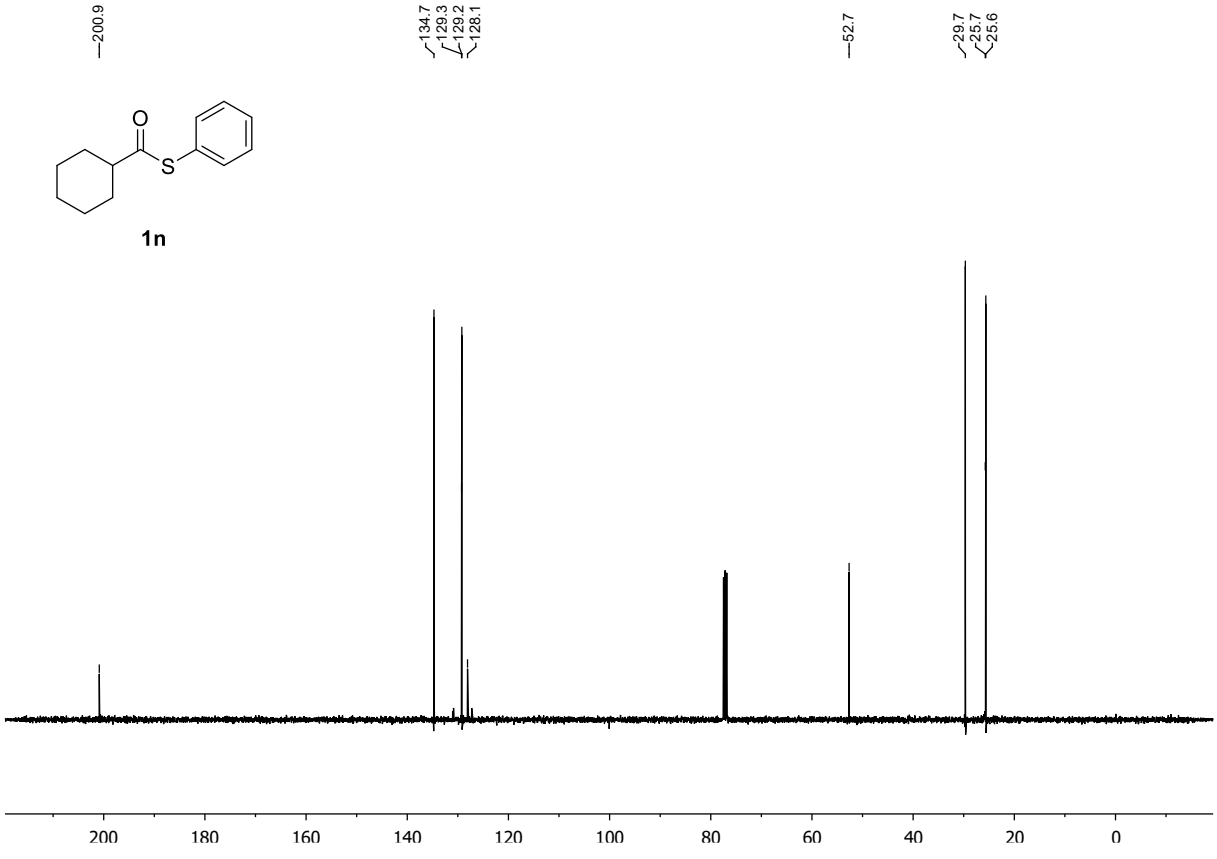

Figure S37. ^{13}C NMR spectrum (101 MHz, $CDCl_3$) of **1n**.

***S*-Phenyl 1-acetylpiperidine-4-carbothioate (1p):**

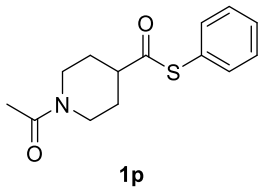

1p

$C_{14}H_{17}NO_2S$ (263.36 g/mol)

Following **GP-A1**, **1p** was synthesized using 1-acetylpiperidine-4-carbonyl chloride (3.79 g, 20.0 mmol, 1.0 equiv.), thiophenol (2.04 mL, 20.0 mmol, 1.0 equiv.) and triethylamine (2.78 mL, 20.0 mmol, 1.0 equiv.). Purification by crystallization (DCM/*n*-hexane) afforded **1p** (2.67 g, 10.2 mmol, 51%) as colorless solid.

m.p.: 128.7 °C.

^{1}H NMR (400 MHz, $CDCl_3$, δ): 7.44 – 7.36 (m, 5H), 4.53 (m, 1H), 3.85 (m, 1H), 3.27 – 2.99 (m, 1H), 2.84 (m, 2H), 2.10 (s, 3H), 2.01 (m, 2H), 1.87 – 1.58 (m, 2H).

^{13}C{^{1}H} NMR (101 MHz, $CDCl_3$, δ): 199.2, 169.0, 134.7, 129.6, 129.4, 127.2, 49.9, 45.7, 40.9, 28.8, 21.5.

HR-MS (ESI): m/z calc for $[M+H]^+$ 264.10528, found 264.10521 (err. -0.25 ppm).

IR (ATR, $\tilde{\nu}$ [cm^{-1}]): 3054 (w), 2950 (w), 2924 (w), 2898 (w), 2861 (w), 1694 (s), 1623 (s), 1471 (w), 1439 (s), 1365 (w), 1314 (m), 1270 (m), 1236 (m), 1191 (w), 1168 (w), 1120 (m), 1094 (w), 1064 (m), 1031 (w), 989 (w), 956 (s), 919 (m), 826 (w), 792 (s), 743 (s), 714 (w), 688 (s).

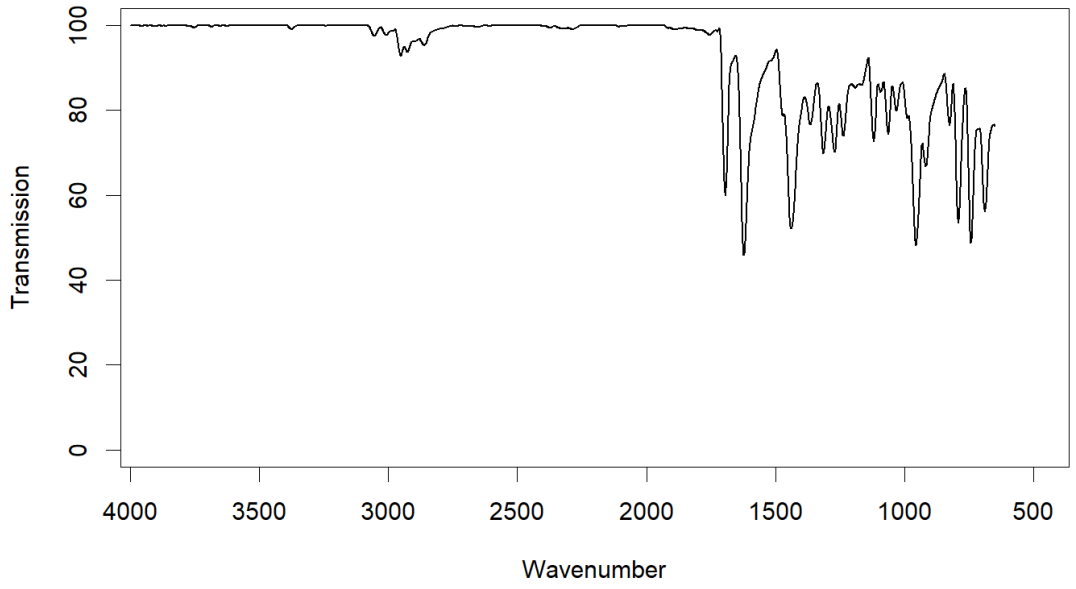

Figure S38. IR spectrum (neat, ATR) of **1p**.

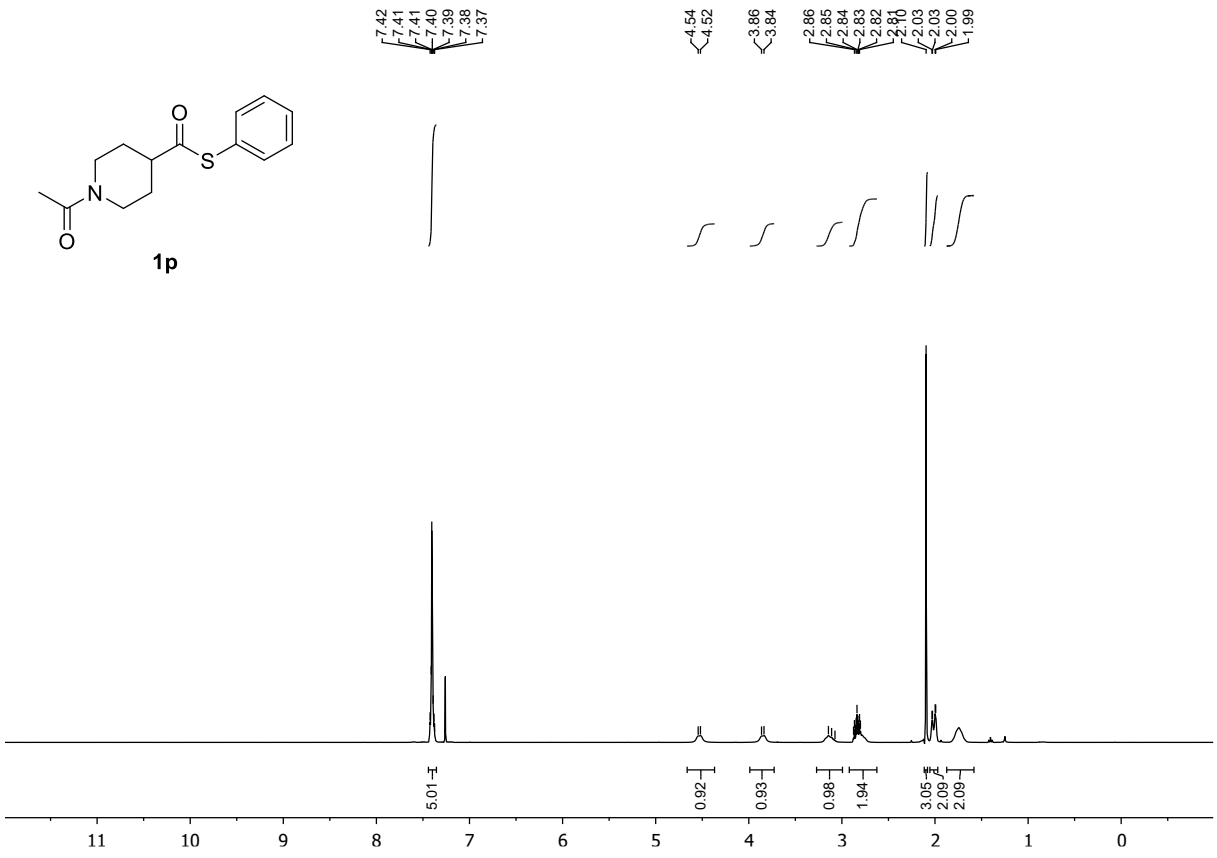

Figure S39. ^{1}H NMR spectrum (400 MHz, $CDCl_3$) of **1p**.

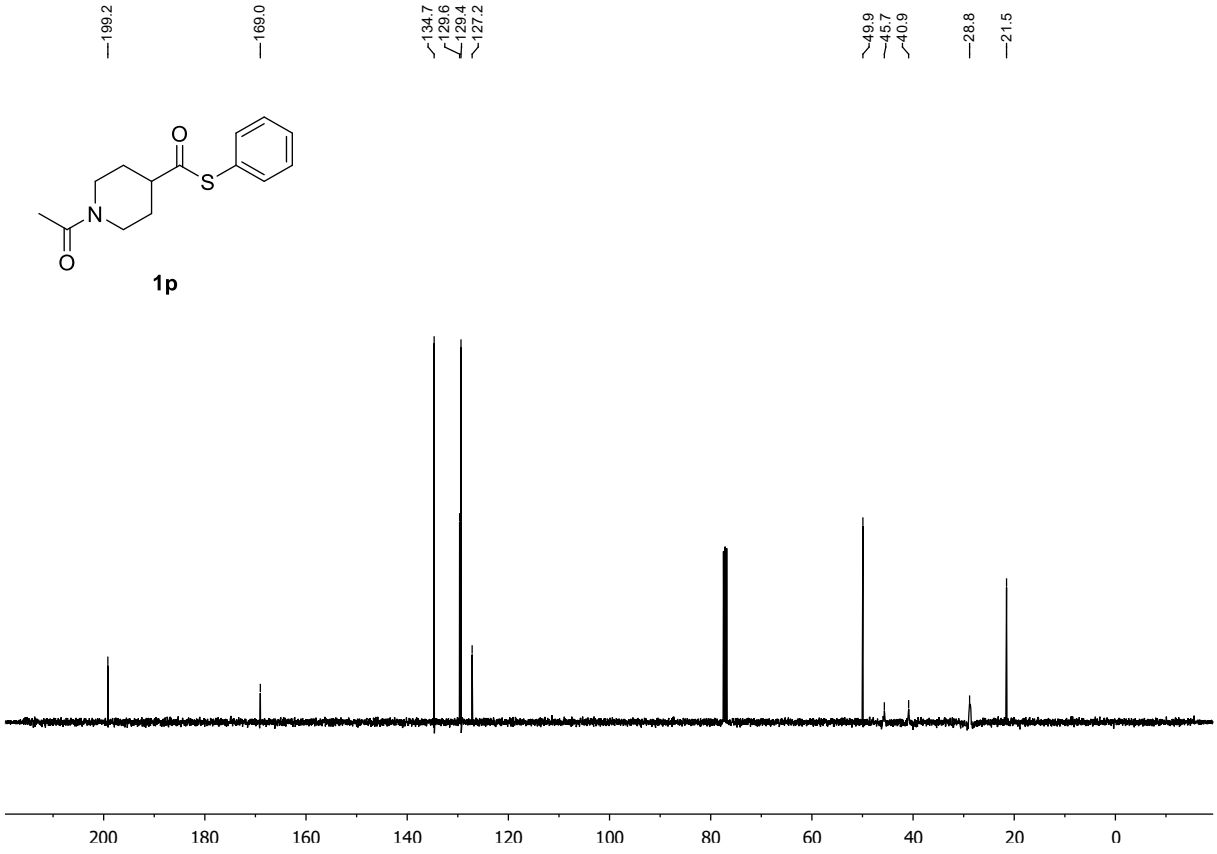

Figure S40. ^{13}C NMR spectrum (101 MHz, $CDCl_3$) of **1p**.

***S*-Phenyl cyclopropanecarbothioate (1q):**

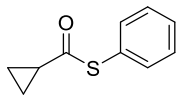

1q

$C_{10}H_{10}OS$ (178.25 g/mol)

Following **GP-A1**, **1q** was synthesized using cyclopropanecarbonyl chloride (1.81 mL, 20.0 mmol, 1.0 equiv.), thiophenol (2.04 mL, 20.0 mmol, 1.0 equiv.) and triethylamine (2.78 mL, 20.0 mmol, 1.0 equiv.). Purification by crystallization at low temperature (-20 °C, DCM/*n*-hexane) afforded **1q** (2.51 g, 14.1 mmol, 84%) as colorless oil. Conforms to reported analytical data.[12]

^{1}H NMR (400 MHz, $CDCl_3$, δ): 7.48 – 7.36 (m, 5H), 2.11 (m, 1H), 1.22 (m, 2H), 1.04 – 0.98 (m, 2H).

^{13}C{^{1}H} NMR (101 MHz, $CDCl_3$, δ): 197.6, 134.6, 129.4, 129.2, 128.0, 22.3, 11.3.

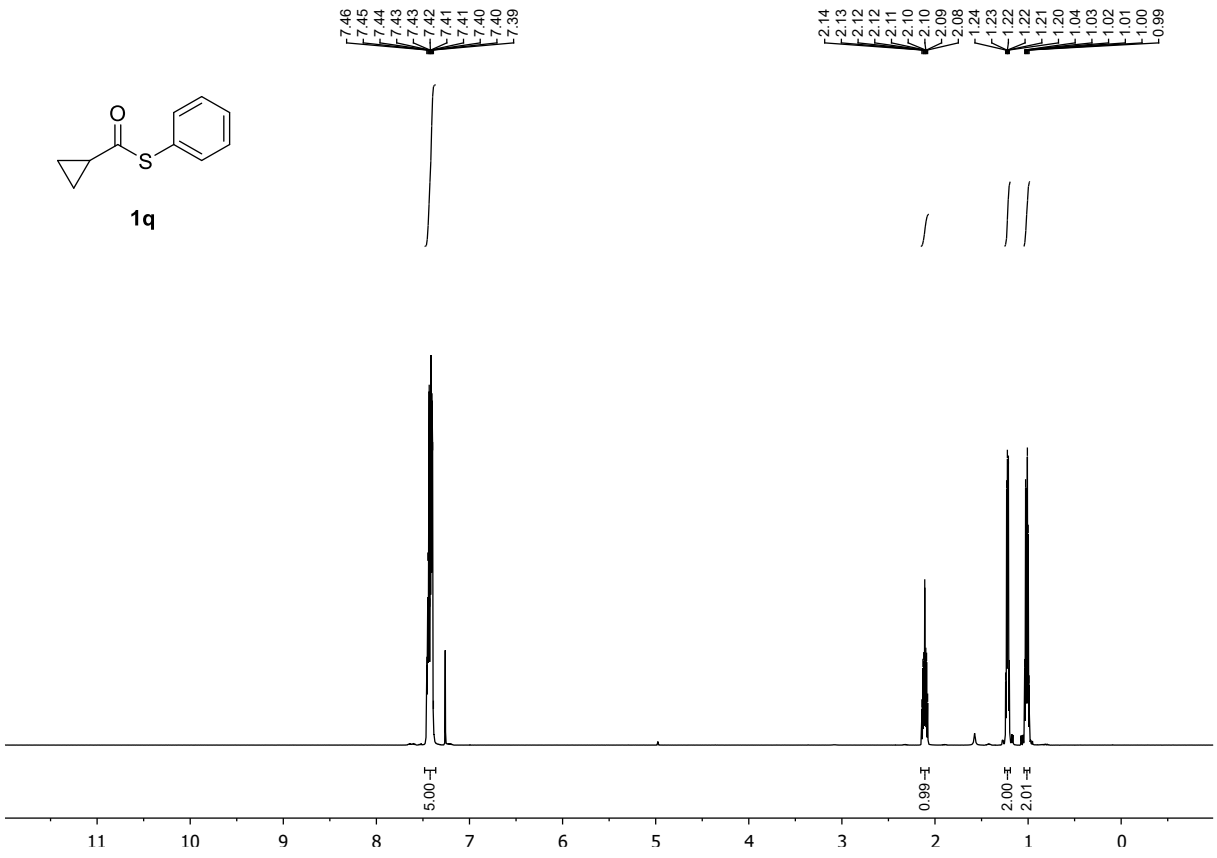

Figure S41. ^{1}H NMR spectrum (400 MHz, $CDCl_3$) of **1q**.

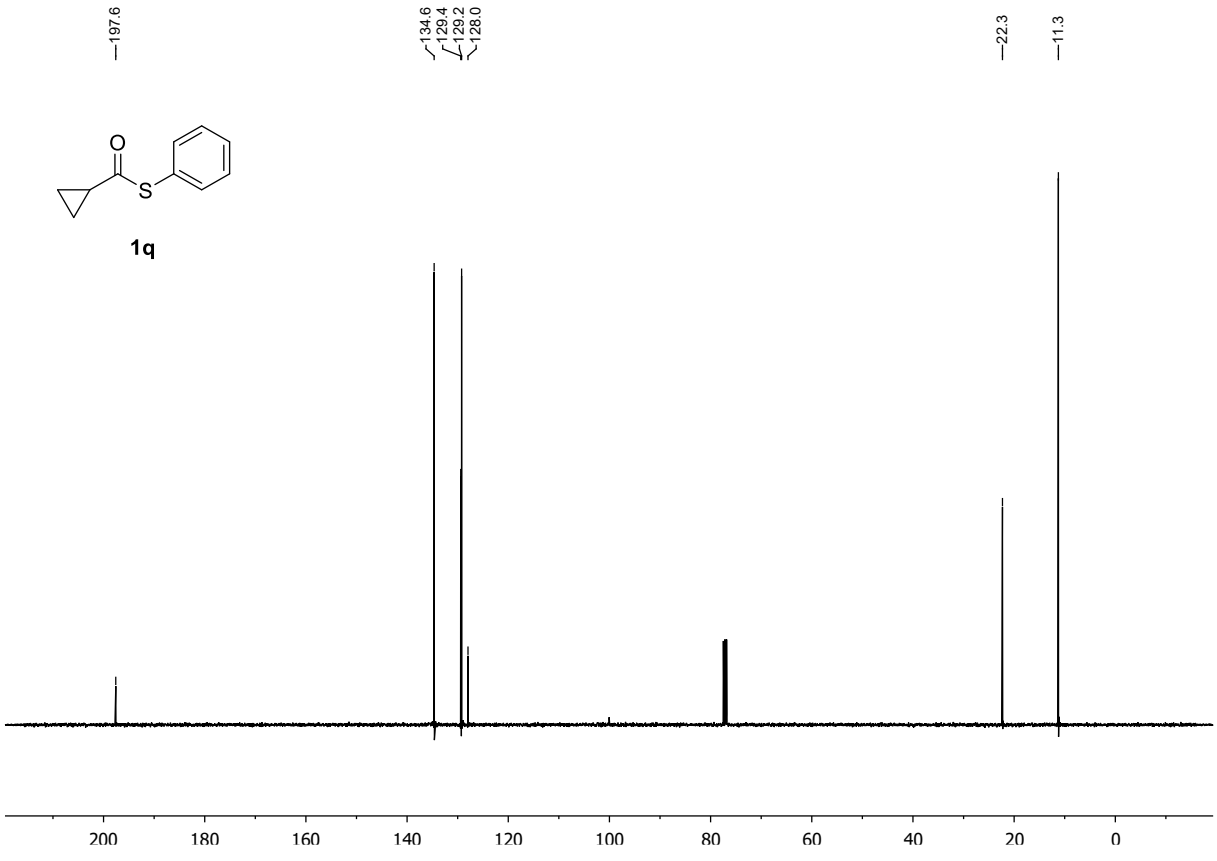

Figure S42. ^{13}C NMR spectrum (101 MHz, $CDCl_3$) of **1q**.

***S*-Phenyl adamantane-1-carbothioate (1r):**

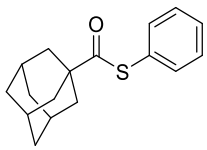

1r

$C_{17}H_{20}OS$ (272.41 g/mol)

Following **GP-A1**, **1r** was synthesized using adamantane-1-carbonyl chloride (3.97 g, 20.0 mmol, 1.0 equiv.), thiophenol (2.04 mL, 20.0 mmol, 1.0 equiv.) and triethylamine (2.78 mL, 20.0 mmol, 1.0 equiv.). Purification by crystallization at low temperature (-20 °C, DCM/*n*-hexane) afforded **1r** (3.63 g, 9.7 mmol, 49%) as colorless liquid (at ambient temperature). Conforms to reported analytical data.[12]

^{1}H NMR (400 MHz, $CDCl_3$, δ): 7.45 – 7.32 (m, 5H), 2.13 – 2.05 (m, 3H), 2.05 – 1.99 (m, 6H), 1.81 – 1.70 (m, 6H).

^{13}C{^{1}H} NMR (101 MHz, $CDCl_3$, δ): 204.3, 135.2, 129.2, 129.1, 128.2, 49.2, 39.4, 36.6, 28.4.

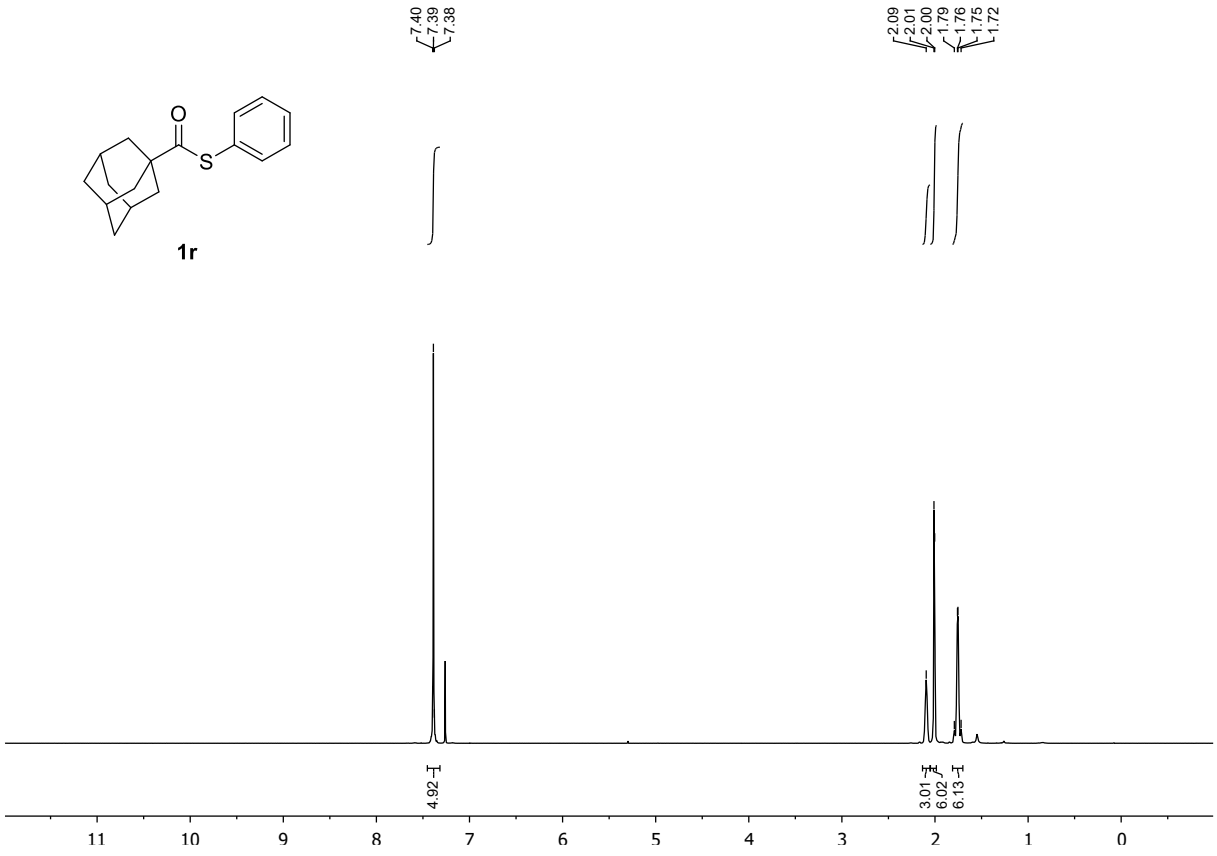

Figure S43. ^{1}H NMR spectrum (400 MHz, $CDCl_3$) of **1r**.

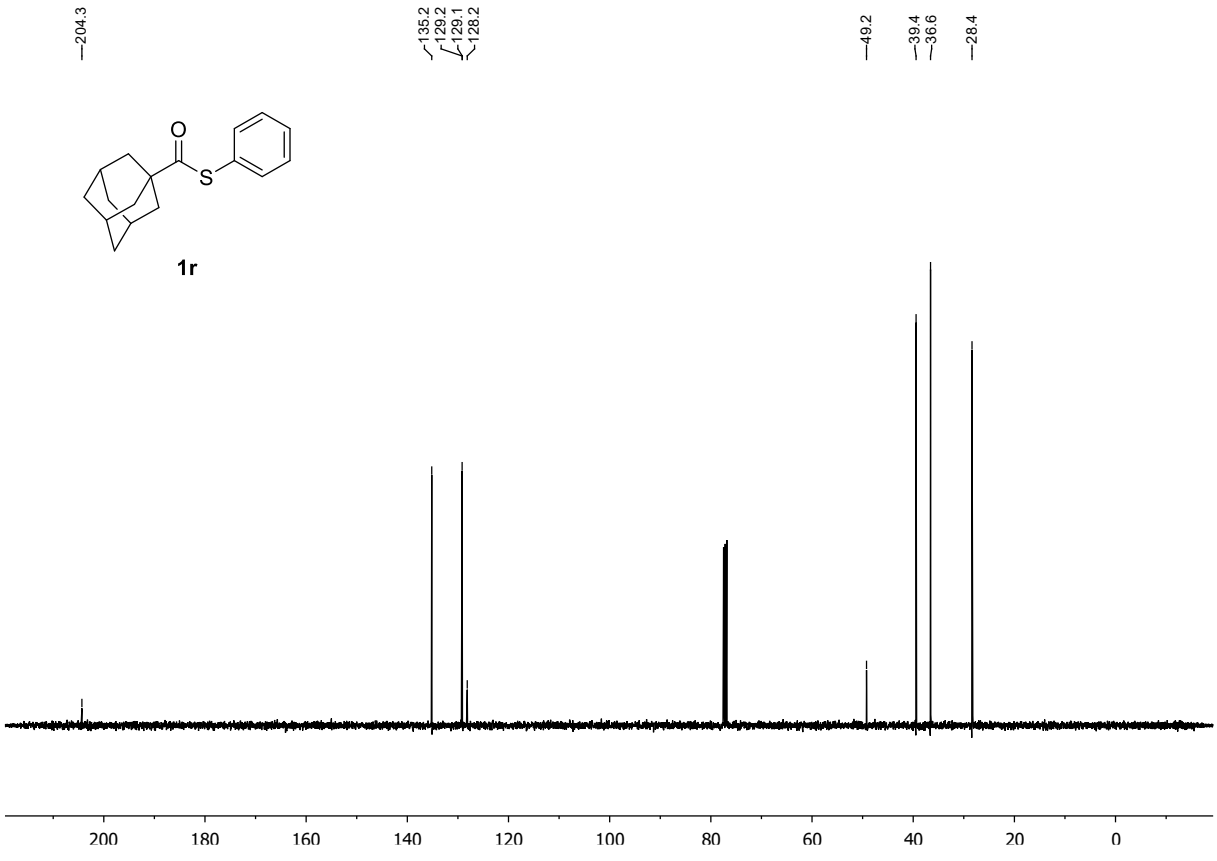

Figure S44. ^{13}C NMR spectrum (101 MHz, $CDCl_3$) of **1r**.

***S*-Phenyl 2-(4-isobutylphenyl)propanethioate (1s):**

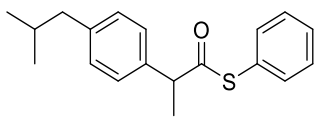

1s

$C_{19}H_{22}OS$ (298.44 g/mol)

Following **GP-A2**, **1s** was synthesized using Ibuprofen (2.06 g, 10.0 mmol, 1.0 equiv.), thiophenol (1.23 mL, 12.0 mmol, 1.2 equiv.), EDCI (2.88 g, 15.0 mmol, 1.5 equiv.) and DMAP (122 mg, 1.0 mmol, 0.1 equiv.). Purification by flash column chromatography (*n*-hexane/EtOAc, gradient 100:0 to 95:5 over 10 CV) afforded **1s** (2.14 g, 7.17 mmol, 72%) as colorless oil. Conforms to reported analytical data.[14]

R_f: 0.18 (*n*-hexane).

^{1}H NMR (400 MHz, $CDCl_3$, δ): 7.42 – 7.34 (m, 5H), 7.30 – 7.26 (m, 2H), 7.20 – 7.11 (m, 2H), 3.99 (q, *J* = 7.1 Hz, 1H), 2.50 (d, *J* = 7.2 Hz, 2H), 1.97 – 1.82 (m, 1H), 1.59 (d, *J* = 7.1 Hz, 3H), 0.94 (d, *J* = 6.6 Hz, 6H).

^{13}C{^{1}H} NMR (101 MHz, $CDCl_3$, δ): 199.4, 141.2, 136.8, 134.6, 129.6, 129.3, 129.2, 128.2, 127.9, 53.9, 45.2, 30.3, 22.5, 18.8.

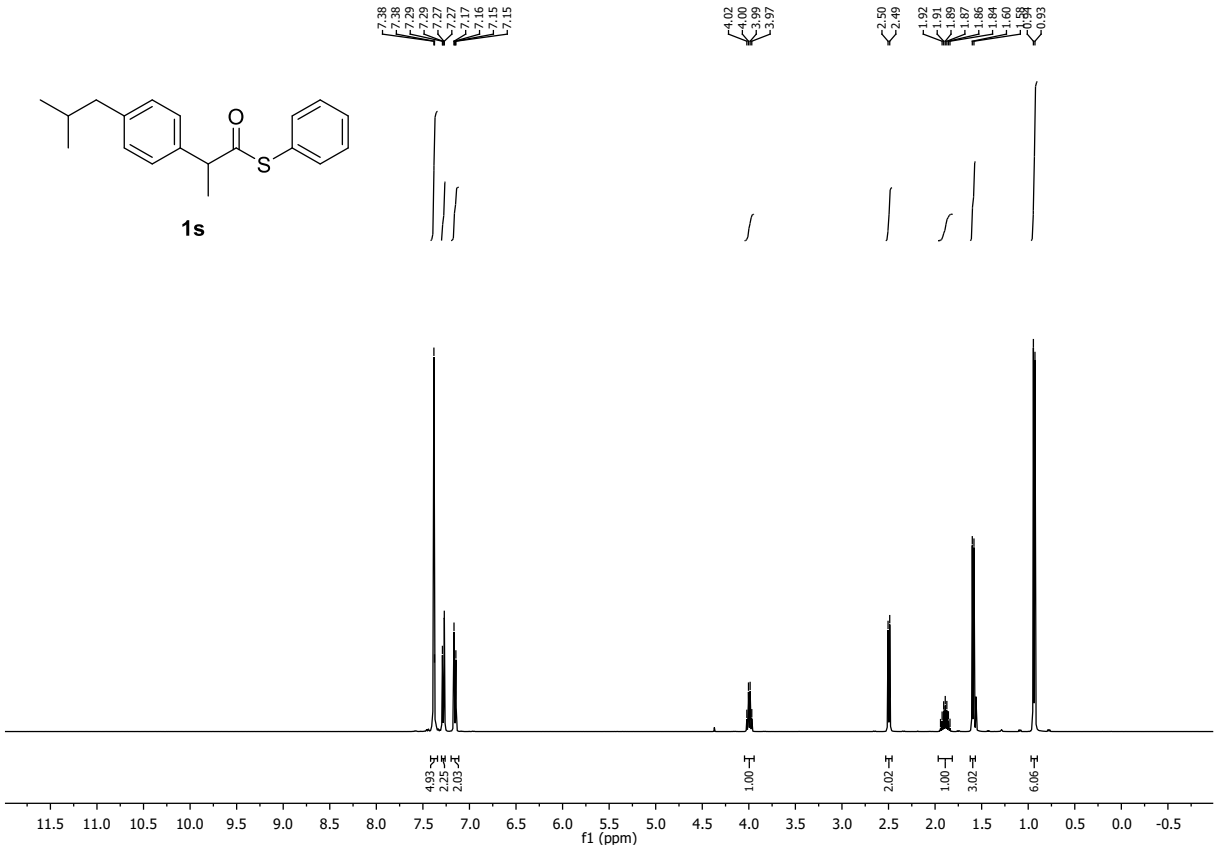

Figure S45. ^{1}H NMR (400 MHz, $CDCl_3$) spectrum of **1s**.

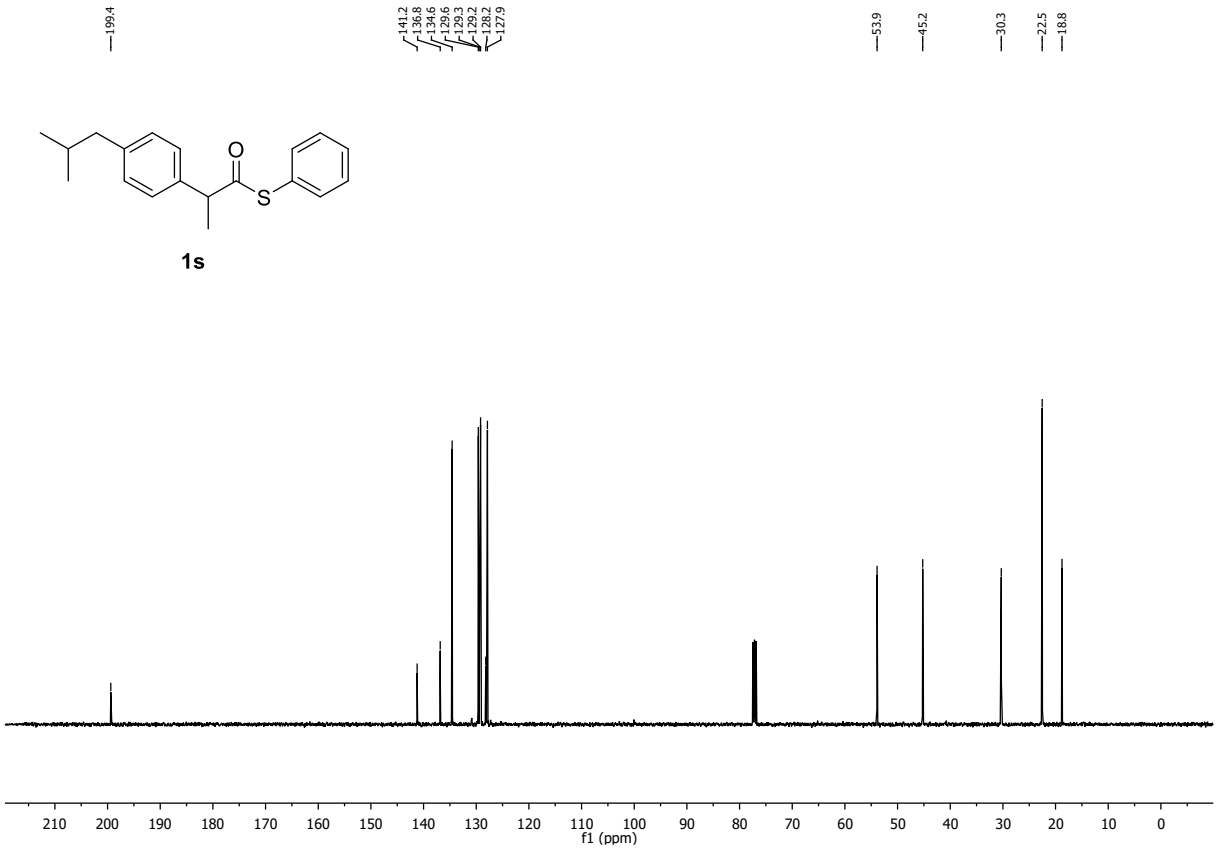

Figure S46. ^{13}C NMR (101 MHz, $CDCl_3$) spectrum of **1s**.

***S*-Phenyl 3-(4,5-diphenyloxazol-2-yl)propanethioate (1t):**

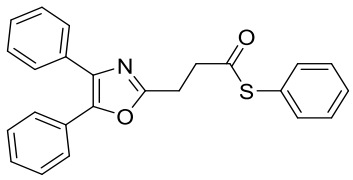

1t

$C_{24}H_{19}NO_2S$ (385.48 g/mol)

Following **GP-A2**, **1t** was synthesized using Oxaprozin (2.93 g, 10.0 mmol, 1.0 equiv.), thiophenol (1.23 mL, 12.0 mmol, 1.2 equiv.), EDCI (2.88 g, 15.0 mmol, 1.5 equiv.) and DMAP (122 mg, 1.0 mmol, 0.1 equiv.). Purification by flash column chromatography (*n*-hexane/EtOAc, gradient 100:0 to 90:10 over 10 CV) afforded **1t** (393 mg, 1.02 mmol, 10%) as yellow oil. Conforms to reported analytical data.[14]

R$_f$: 0.45 (*n*-hexane/EtOAc 80:20).

^{1}H NMR (400 MHz, $CDCl_3$, δ): 7.67 – 7.62 (m, 1H), 7.61 – 7.56 (m, 1H), 7.46 – 7.32 (m, 5H), 3.31 – 3.22 (m, 2H).

^{13}C{^{1}H} NMR (101 MHz, $CDCl_3$, δ): 196.0, 161.4, 145.7, 135.3, 134.7, 132.5, 129.7, 129.4, 129.0, 128.8, 128.7, 128.7, 128.3, 128.0, 127.4, 126.6, 40.2, 23.8.

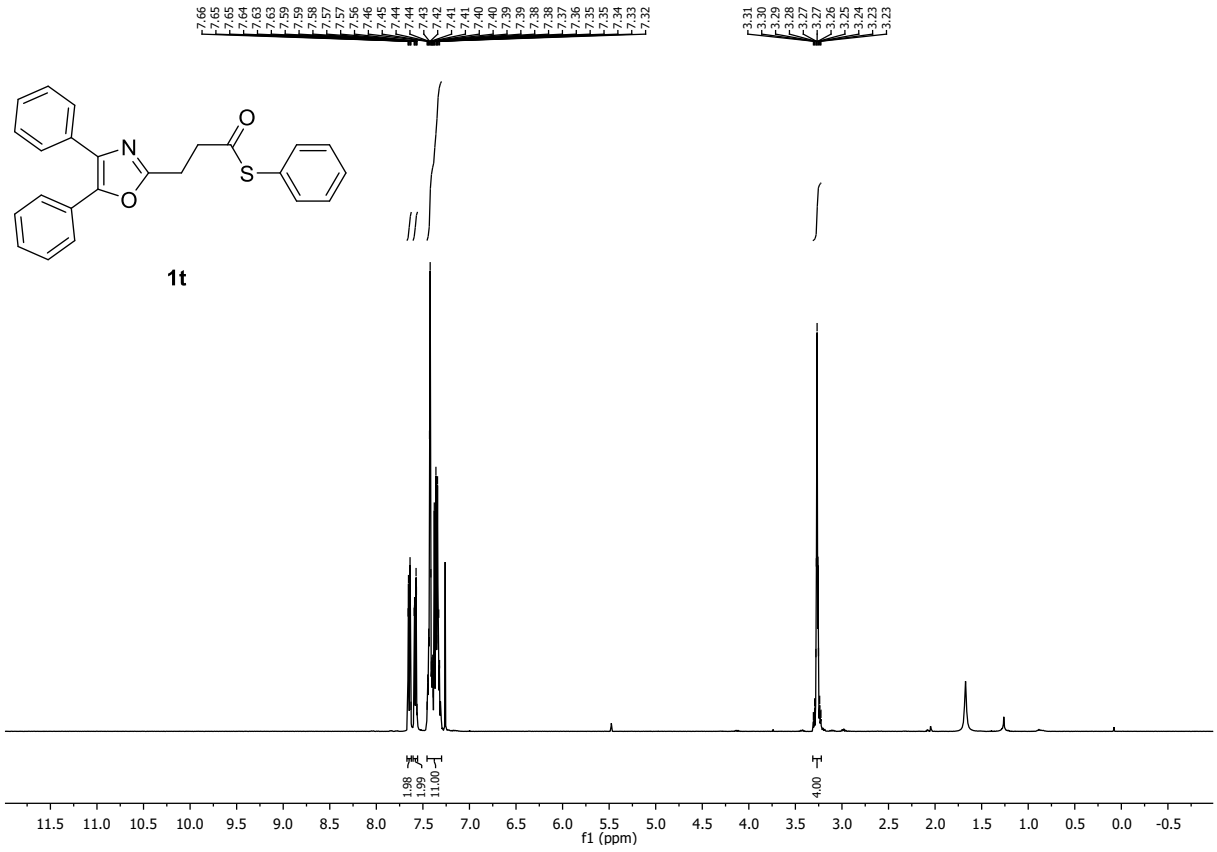

Figure S47. ^{1}H NMR (400 MHz, $CDCl_3$) spectrum of **1t**.

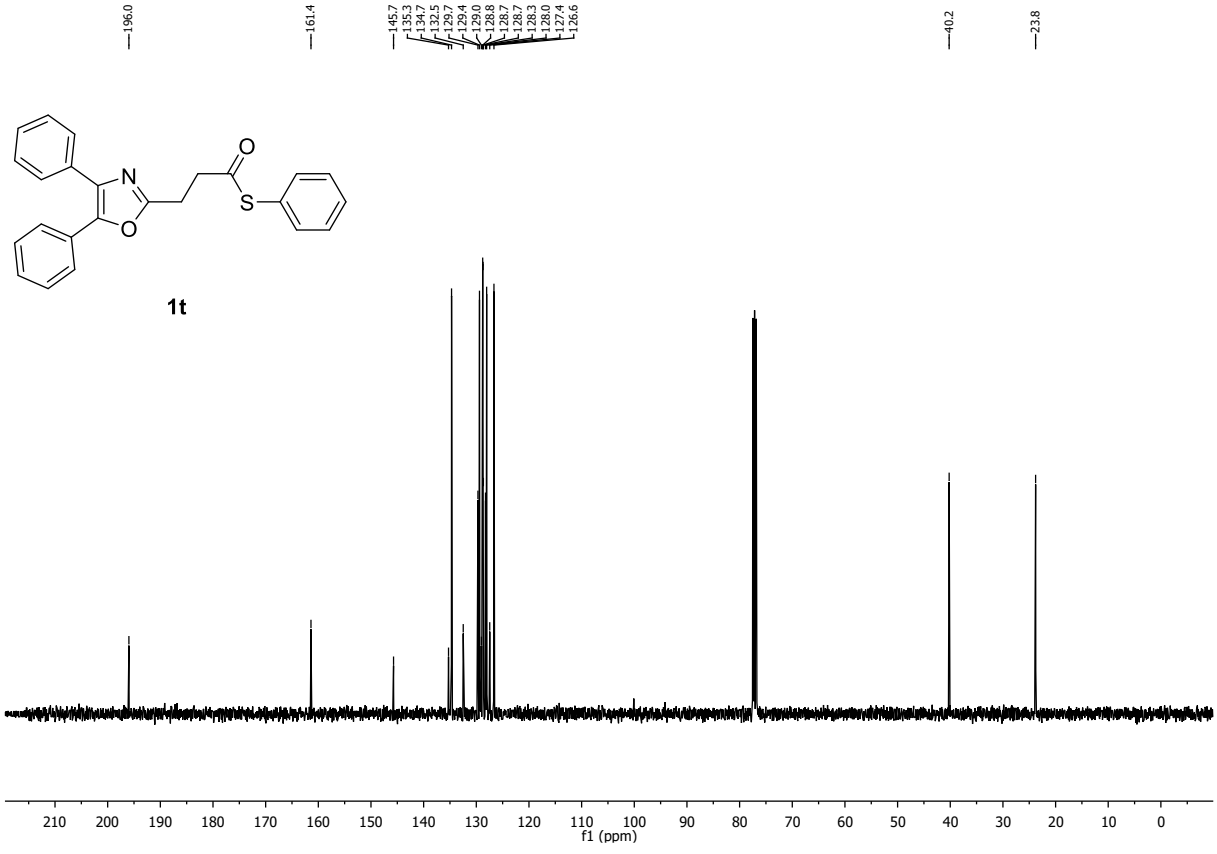

Figure S48. ^{13}C NMR (101 MHz, $CDCl_3$) spectrum of **1t**.

***S*-Phenyl 4-(*N*,*N*-dipropylsulfamoyl)benzothioate (1u):**

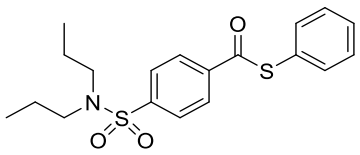

1u

$C_{19}H_{23}NO_3S_2$ (377.52 g/mol)

Following **GP-A2**, **1u** was synthesized using Probenecid (2.85 g, 10.0 mmol, 1.0 equiv.), thiophenol (1.23 mL, 12.0 mmol, 1.2 equiv.), EDCI (2.88 g, 15.0 mmol, 1.5 equiv.) and DMAP (122 mg, 1.0 mmol, 0.1 equiv.). Purification by flash column chromatography (*n*-hexane/EtOAc, gradient 100:0 to 30:70 over 10 CV) afforded **1u** (2.22 g, 5.87 mmol, 59%) as colorless solid. Conforms to reported analytical data.[14]

R_f: 0.61 (*n*-hexane/EtOAc 80:20).

^{1}H NMR (400 MHz, $CDCl_3$, δ): 8.17 – 8.09 (m, 2H), 7.96 – 7.88 (m, 2H), 7.56 – 7.44 (m, 5H), 3.16 – 3.07 (m, 4H), 1.64 – 1.49 (m, 4H, *residual water under compound peak*), 0.88 (t, *J* = 7.4 Hz, 6H).

^{13}C{^{1}H} NMR (101 MHz, $CDCl_3$, δ): 189.4, 144.9, 139.6, 135.1, 130.1, 129.6, 128.2, 127.5, 126.7, 50.1, 22.1, 11.3.

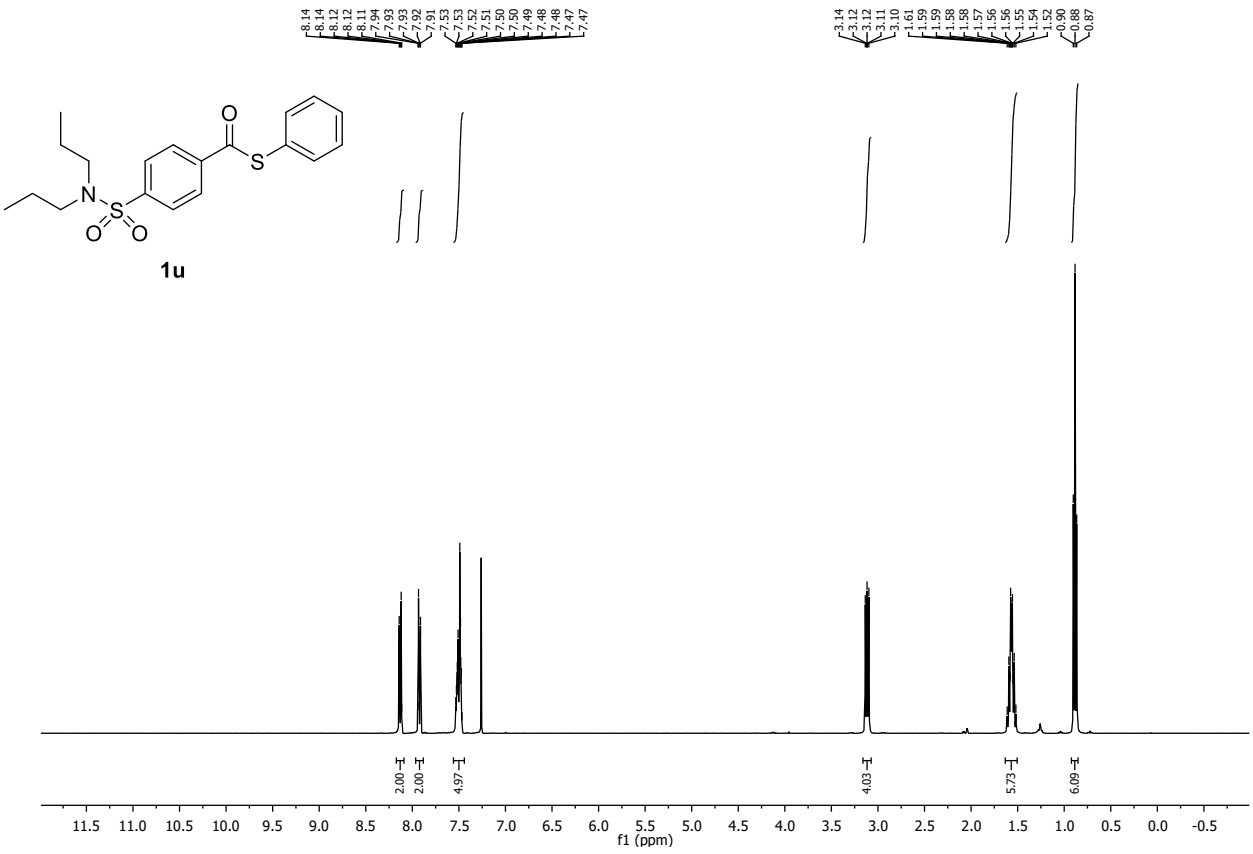

Figure S49. ^{1}H NMR (400 MHz, $CDCl_3$) spectrum of **1u**.

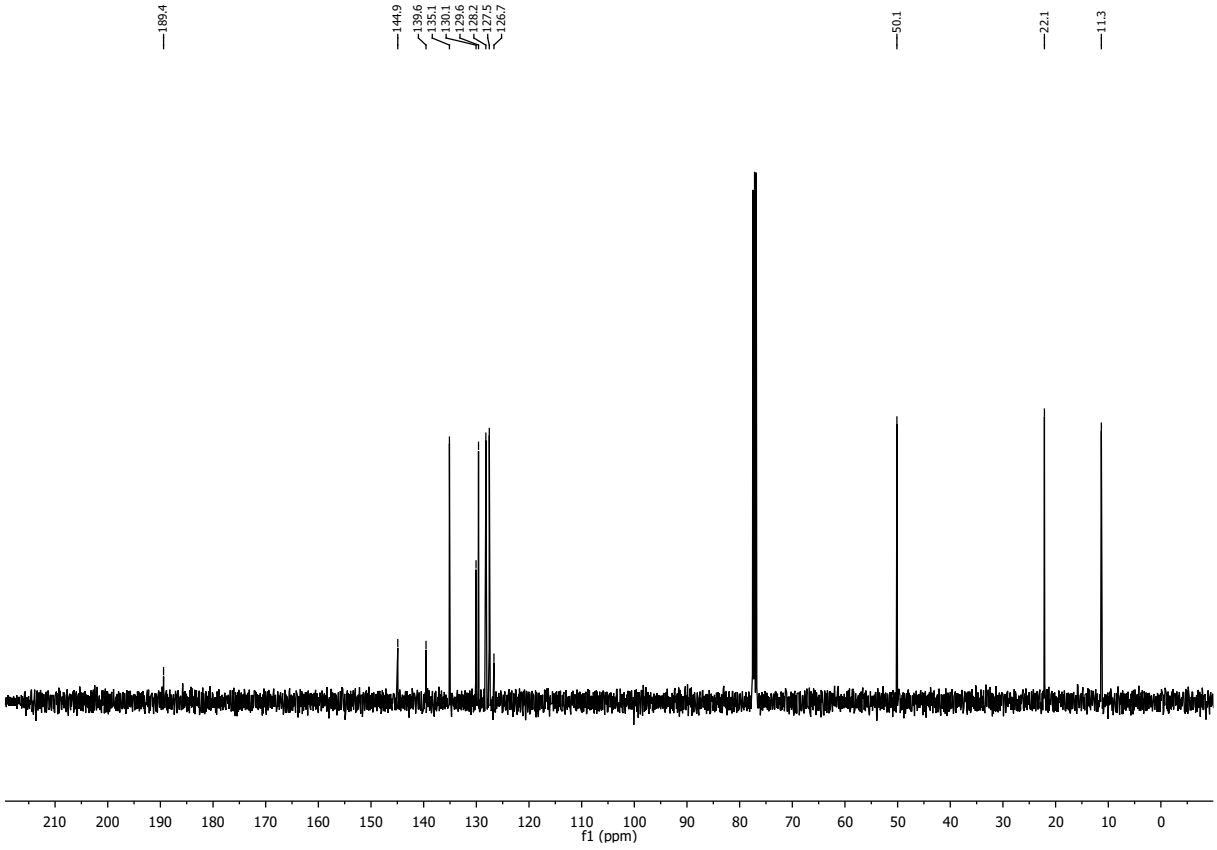

Figure S50. ^{13}C NMR (101 MHz, $CDCl_3$) spectrum of **1u**.

***S*-Phenyl 3-(cyclopropylmethoxy)-4-(difluoromethoxy)benzothioate (1v):**

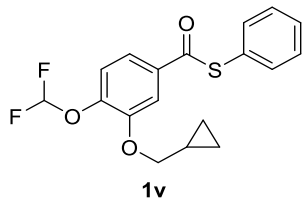

1v

$C_{18}H_{16}F_2O_3S$ (350.38 g/mol)

Following **GP-A2**, **1v** was synthesized using 3-(cyclopropylmethoxy)-4-(difluoromethoxy)benzoic acid (2.58 g, 10.0 mmol, 1.0 equiv.), thiophenol (1.23 mL, 12.0 mmol, 1.2 equiv.), EDCI (2.88 g, 15.0 mmol, 1.5 equiv.) and DMAP (122 mg, 1.0 mmol, 0.1 equiv.). Purification by flash column chromatography (*n*-hexane/EtOAc, gradient 100:0 to 80:20 over 10 CV) afforded **1v** (2.28 g, 6.78 mmol, 68%) as colorless solid.

R_f: 0.47 (*n*-hexane/EtOAc 90:10).

m.p.: 69.6 – 71.1 °C.

^{1}H NMR (400 MHz, $CDCl_3$, δ): 7.69 (dd, *J* = 8.4, 2.0 Hz, 1H), 7.58 (d, *J* = 2.0 Hz, 1H), 7.55 – 7.45 (m, 5H), 7.30 – 7.27 (m, 1H), 6.75 (t, *J* = 74.8 Hz, 1H), 3.96 (d, *J* = 6.9 Hz, 2H), 1.39 – 1.29 (m, 1H), 0.74 – 0.62 (m, 2H), 0.47 – 0.33 (m, 2H).

^{13}C{^{1}H} NMR (101 MHz, $CDCl_3$, δ): 189.2, 150.6, 144.7, 135.2, 134.8, 129.8, 129.4, 127.2, 122.1, 121.1, 115.8 (t, J = 261.6 Hz), 112.9, 74.3, 10.2, 3.5.

^{19}F NMR (376 MHz, $CDCl_3$, δ): -81.9 (d, *J* = 74.8 Hz).

HR-MS (ESI): m/z calc for $[M+K]^+$ 389.04198, found 389.04213 (err. -0.38 ppm).

IR (ATR, $\tilde{\nu}$ [cm^{-1}]): 3071 (w), 3014 (w), 2935 (w), 1679 (m), 1593 (w), 1500 (m), 1474 (w), 1403 (m), 1370 (w), 1318 (w), 1268 (s), 1213 (w), 1157 (w), 1109 (s), 1049 (s), 1020 (s), 979 (s), 908 (m), 878 (m), 855 (m), 833 (m), 785 (s), 744 (s), 681 (s).

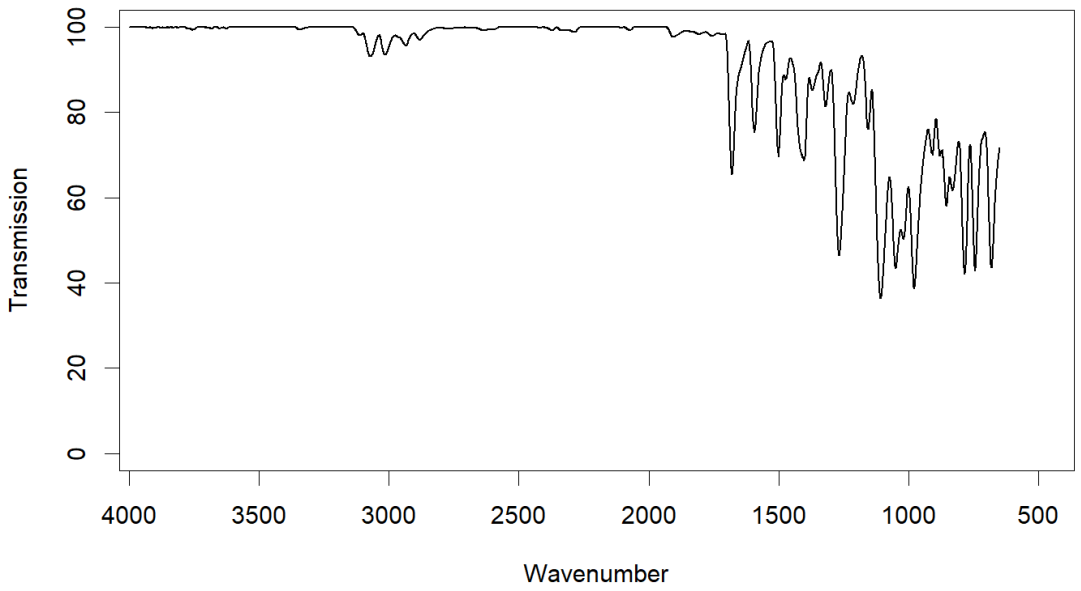

Figure S51. IR spectrum (ATR, neat) of **1v**.

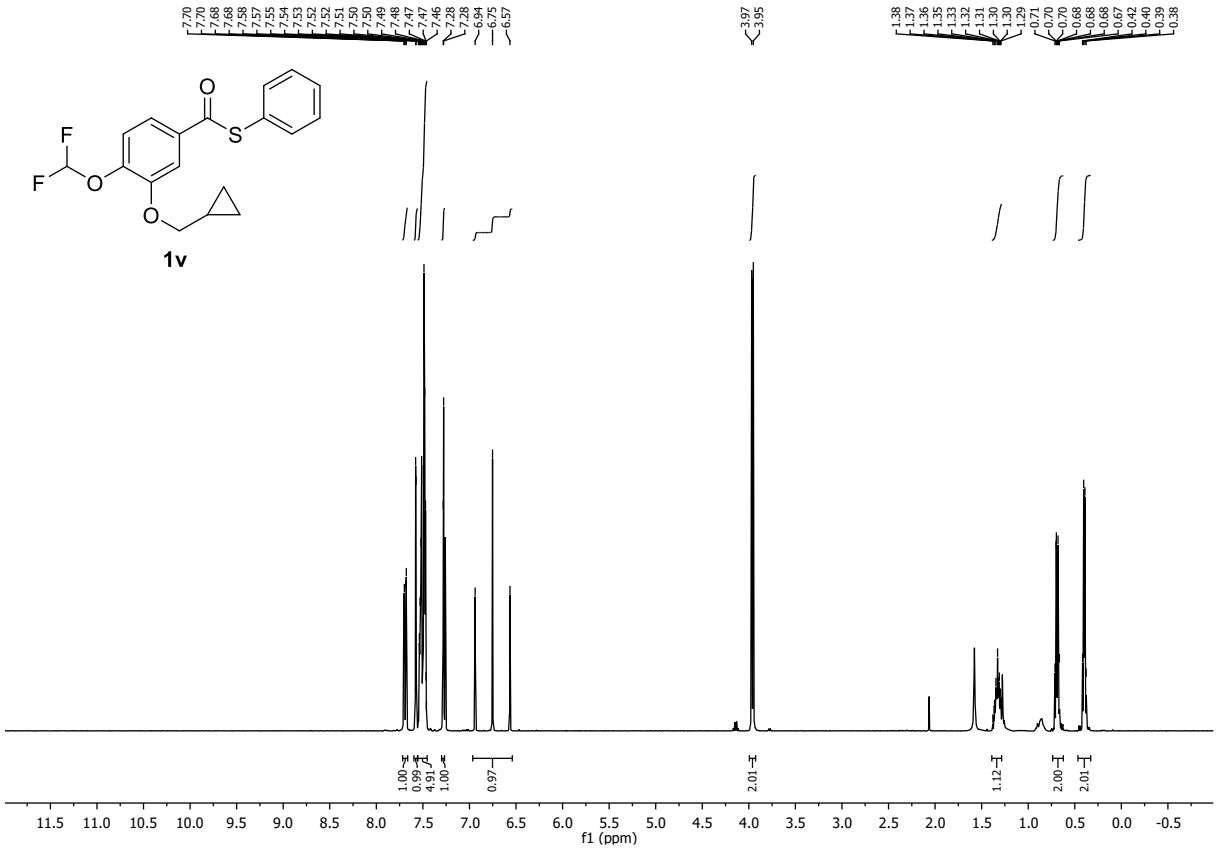

Figure S52. ^{1}H NMR (400 MHz, $CDCl_3$) spectrum of **1v**.

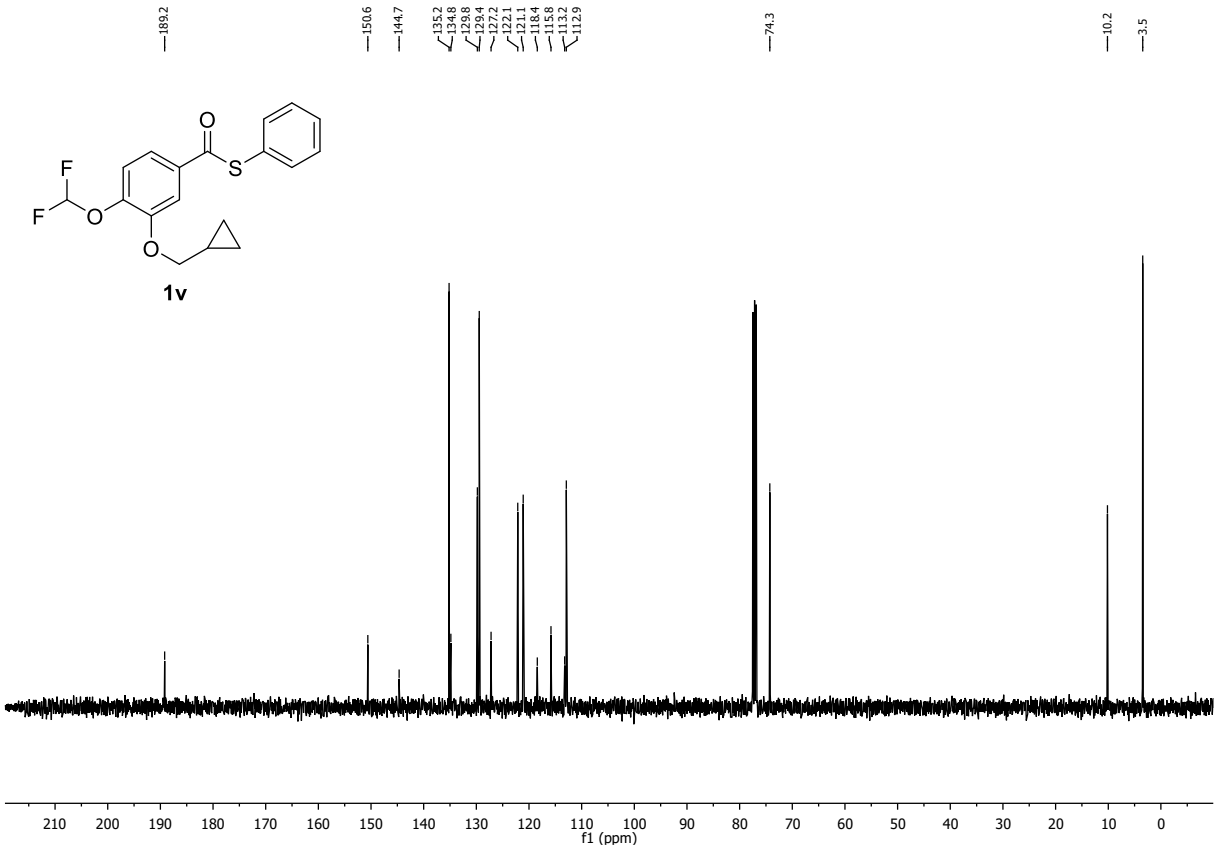

Figure S53. ^{13}C NMR (101 MHz, $CDCl_3$) spectrum of **1v**.

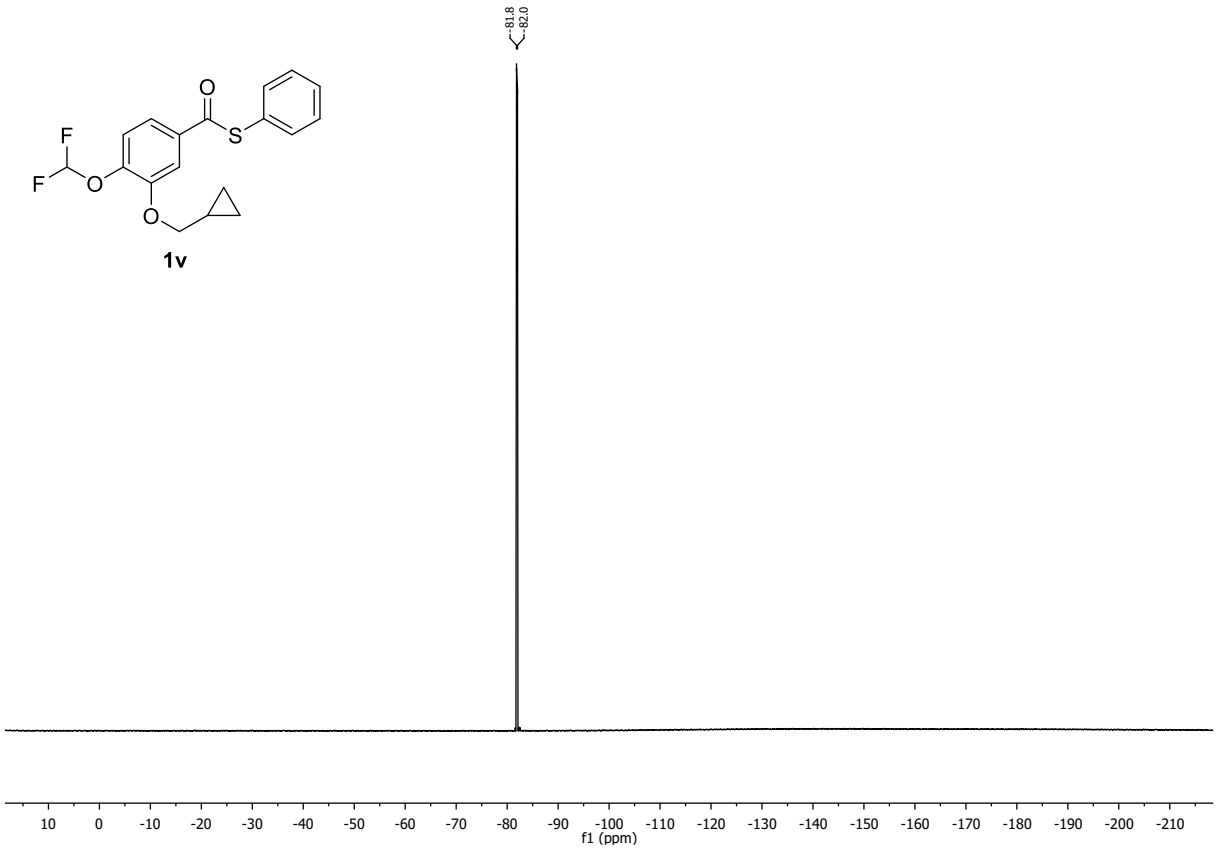

Figure S54. ^{19}F NMR (376 MHz, $CDCl_3$) spectrum of **1v**.

5.3 Synthesis of Ketones

1,4-Diphenylbutan-1-one (3aa):

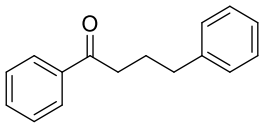

3aa

$C_{16}H_{16}O$ (224.30 g/mol)

Following **GP-B**, **3aa** was synthesized using *S*-phenyl benzothioate (**1a**) (214 mg, 1.0 mmol, 1.0 equiv.), (3-bromopropyl)benzene (398 mg, 2.0 mmol, 2.0 equiv.), $NiCl_2 \cdot (H_2O)_6$ (23.8 mg, 0.1 mmol, 10 mol%), 4,4'-di-*tert*-butyl-2,2'-bipyridine (53.7 mg, 0.2 mmol, 20 mol%), zinc powder (131 mg, 2.0 mmol, 2.0 equiv.), sodium chloride (117 mg, 2.0 mmol, 2.0 equiv.) and pyridine (158 mg, 2.0 mmol, 2 equiv.). Purification by flash column chromatography (*n*-hexane/EtOAc gradient 100:0 to 90:10 over 10 CV) afforded **3aa** (191 mg, 852 µmol, 85%) as colorless solid. Conforms to reported analytical data.[17]

An upscale reaction using *S*-phenyl benzothioate (**1a**) (4.29 g, 20.0 mmol, 1.0 equiv.), (3-bromopropyl)benzene (6.09 mL, 40.0 mmol, 2.0 equiv.), $NiCl_2 \cdot (H_2O)_6$ (0.48 g, 2.0 mmol, 10 mol%), 4,4'-di-*tert*-butyl-2,2'-bipyridine (1.07 g, 4.0 mmol, 20 mol%), zinc powder (2.62 g, 40.0 mmol, 2.0 equiv.), sodium chloride (2.34 g, 40.0 mmol, 2.0 equiv.) and pyridine (3.24 mL, 40.0 mmol, 2 equiv.) gave 1 in 89% yield (3.99 g, 17.8 mmol). This reaction was conducted in a 50 mL SS jar using 3 × 4 g SS balls.

Rf: 0.55 (*n*-hexane/EtOAc 90:10).

^{1}H NMR (400 MHz, $CDCl_3$, δ): 7.98 – 7.89 (m, 2H), 7.60 – 7.51 (m, 1H), 7.50 – 7.41 (m, 2H), 7.34 – 7.27 (m, 2H), 7.25 – 7.16 (m, 3H), 2.99 (t, *J* = 7.4 Hz, 2H), 2.74 (t, *J* = 7.4 Hz, 2H), 2.10 (tt, *J* = 7.4, 7.4 Hz, 2H).

^{13}C{^{1}H} NMR (101 MHz, $CDCl_3$, δ): 200.2, 141.8, 137.1, 133.1, 128.7, 128.6, 128.5, 128.1, 126.1, 37.8, 35.3, 25.8.

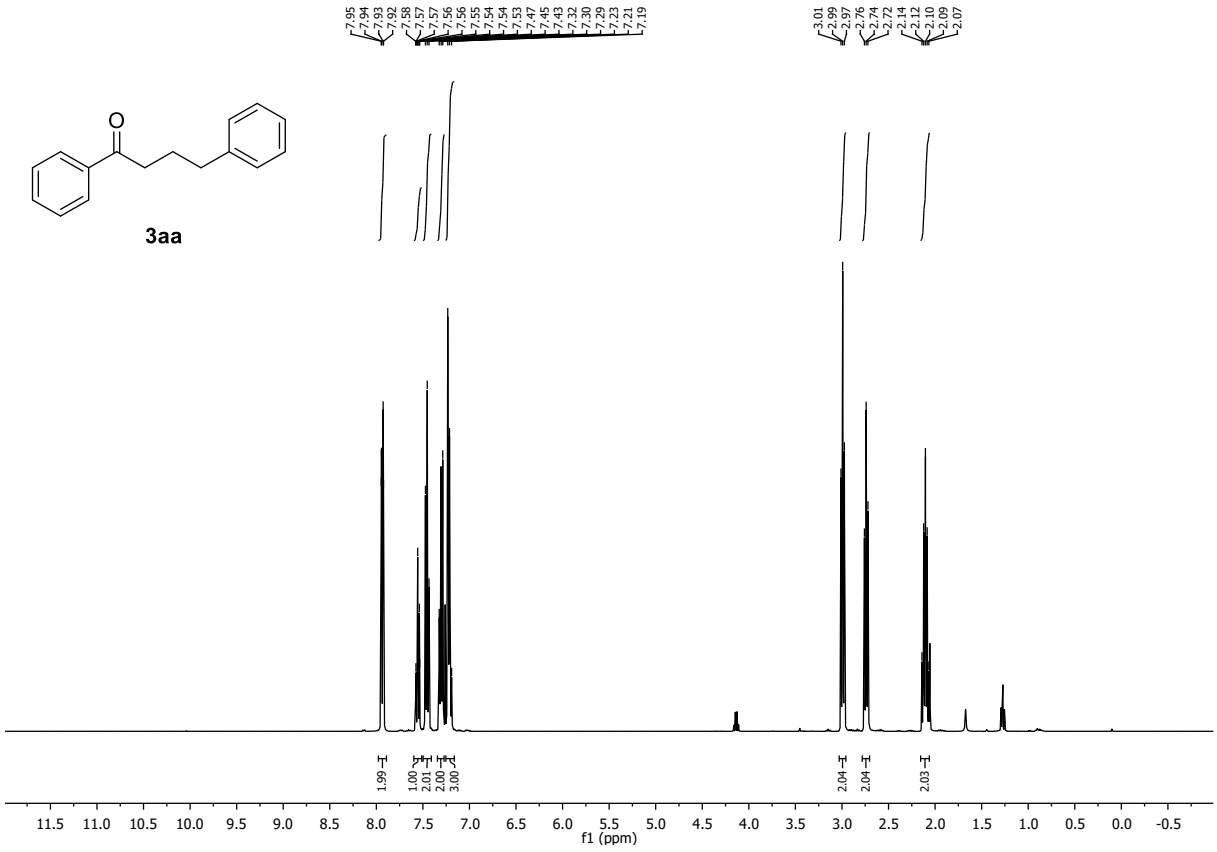

Figure S55. ^{1}H NMR spectrum (400 MHz, $CDCl_3$) of **3aa**.

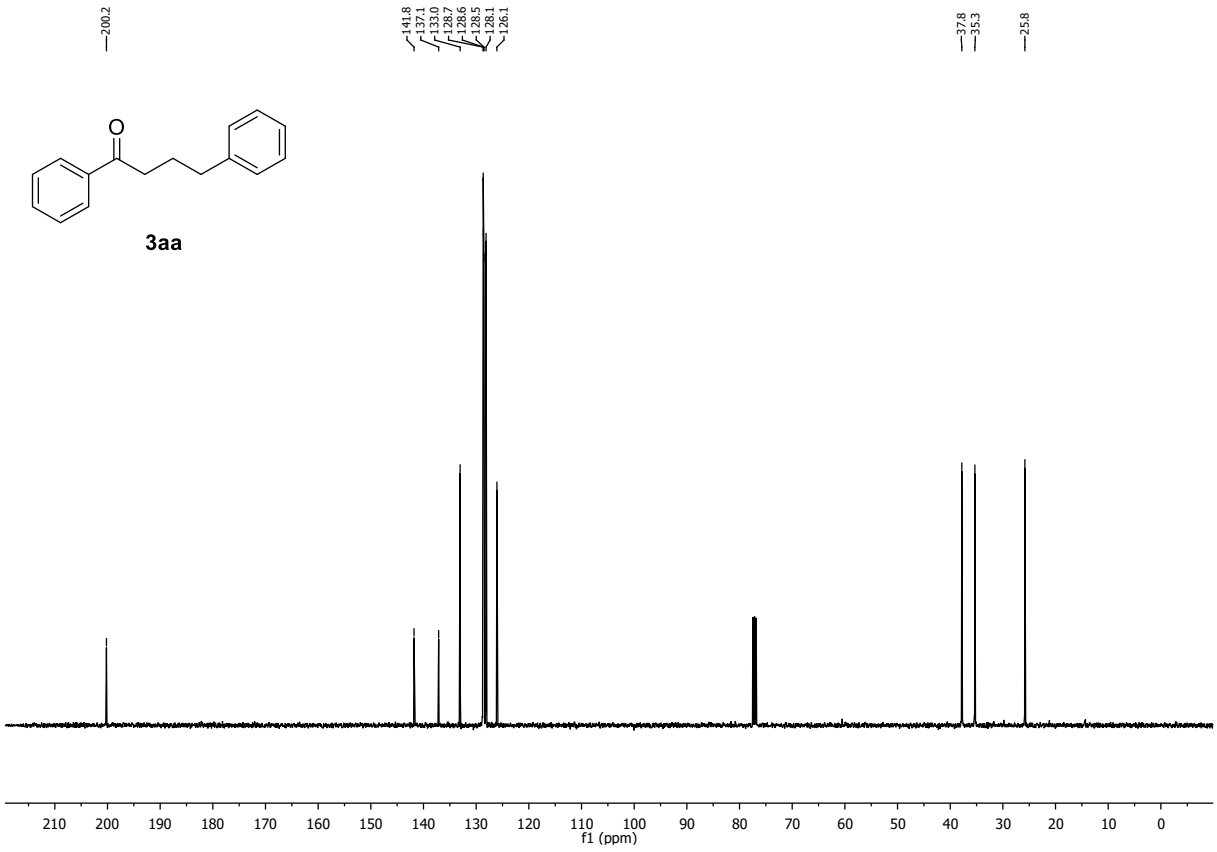

Figure S56. ^{13}C NMR spectrum (101 MHz, $CDCl_3$) of **3aa**.

4-Phenyl-1-(*o*-tolyl)butan-1-one (3ba):

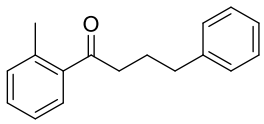

3ba

$C_{17}H_{18}O$ (238.33 g/mol)

Following **GP-B**, **3ba** was synthesized using *S*-phenyl 2-methylbenzothioate (**1b**) (228.0 mg, 1.0 mmol, 1.0 equiv.), (3-bromopropyl)benzene (398 mg, 2.0 mmol, 2.0 equiv.), $NiCl_2 \cdot (H_2O)_6$ (23.8 mg, 0.1 mmol, 10 mol%), 4,4'-di-*tert*-butyl-2,2'-bipyridine (57.3 mg, 0.2 mmol, 20 mol%), zinc powder (131.0 mg, 2.0 mmol, 2.0 equiv.), NaCl (117.0 mg, 2.0 mmol, 2.0 equiv.) and pyridine (158 mg, 2.0 mmol, 2.0 equiv.). Purification by flash column chromatography (*n*-hexane/EtOAc gradient 100:0 to 90:10 over 10 CV) afforded **3ba** (162 mg, 681 µmol, 68%) as colorless oil. Conforms to reported analytical data.[18]

R_f: 0.56 (*n*-hexane/EtOAc 90:10).

^{1}H NMR (400 MHz, $CDCl_3$, δ): 7.44 – 7.39 (m, 1H), 7.20 (m, 1H), 7.17 – 7.11 (m, 2H), 7.11 – 7.01 (m, 5H), 2.75 (t, *J* = 7.3 Hz, 2H), 2.56 (t, *J* = 7.5 Hz. 2H), 2.34 (s, 3H), 1.91 (tt, *J* = 7.5, 7.3 Hz, 2H).

^{13}C{^{1}H} NMR (101 MHz, $CDCl_3$, δ): 204.5, 141.8, 138.3, 137.9, 132.0, 131.2, 128.6, 128.5, 128.4, 126.1, 125.7, 40.9, 35.3, 26.0, 21.3.

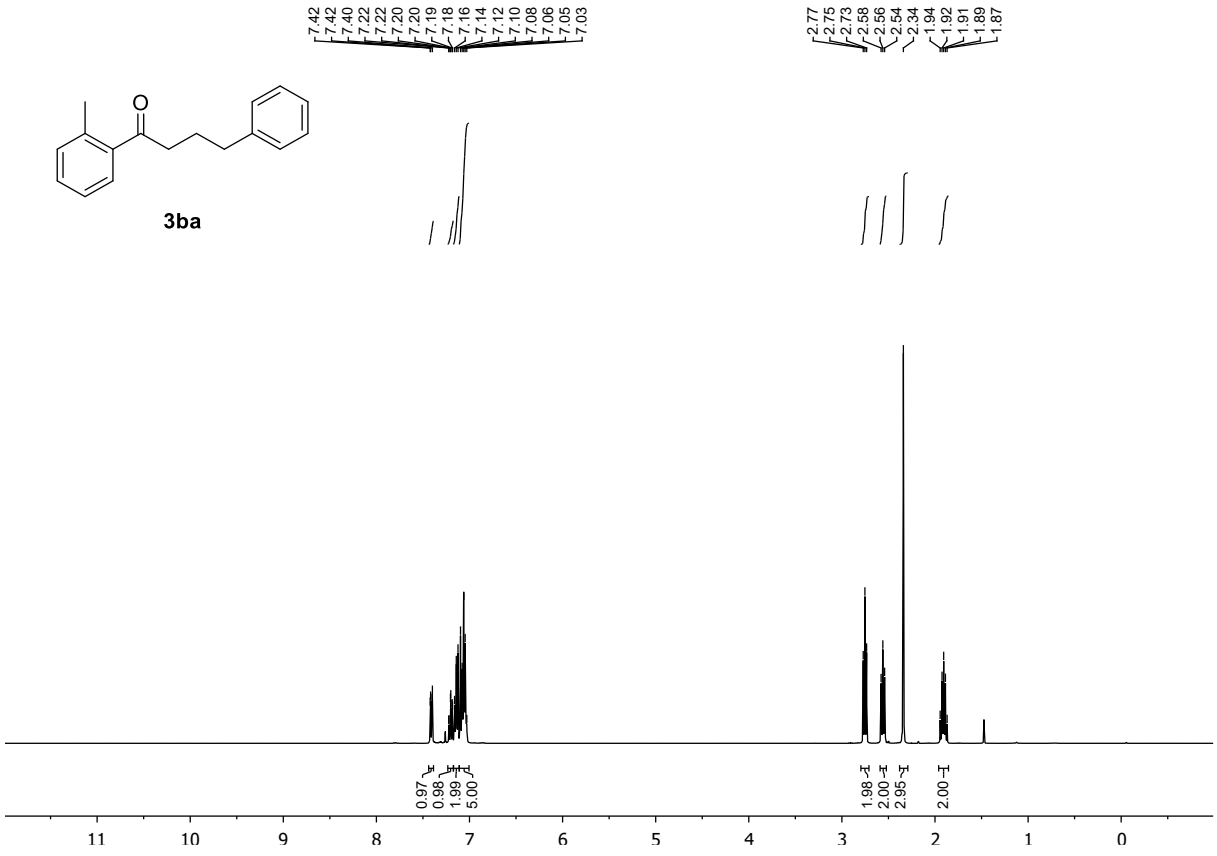

Figure S57. ^{1}H NMR spectrum (400 MHz, $CDCl_3$) of **3ba**.

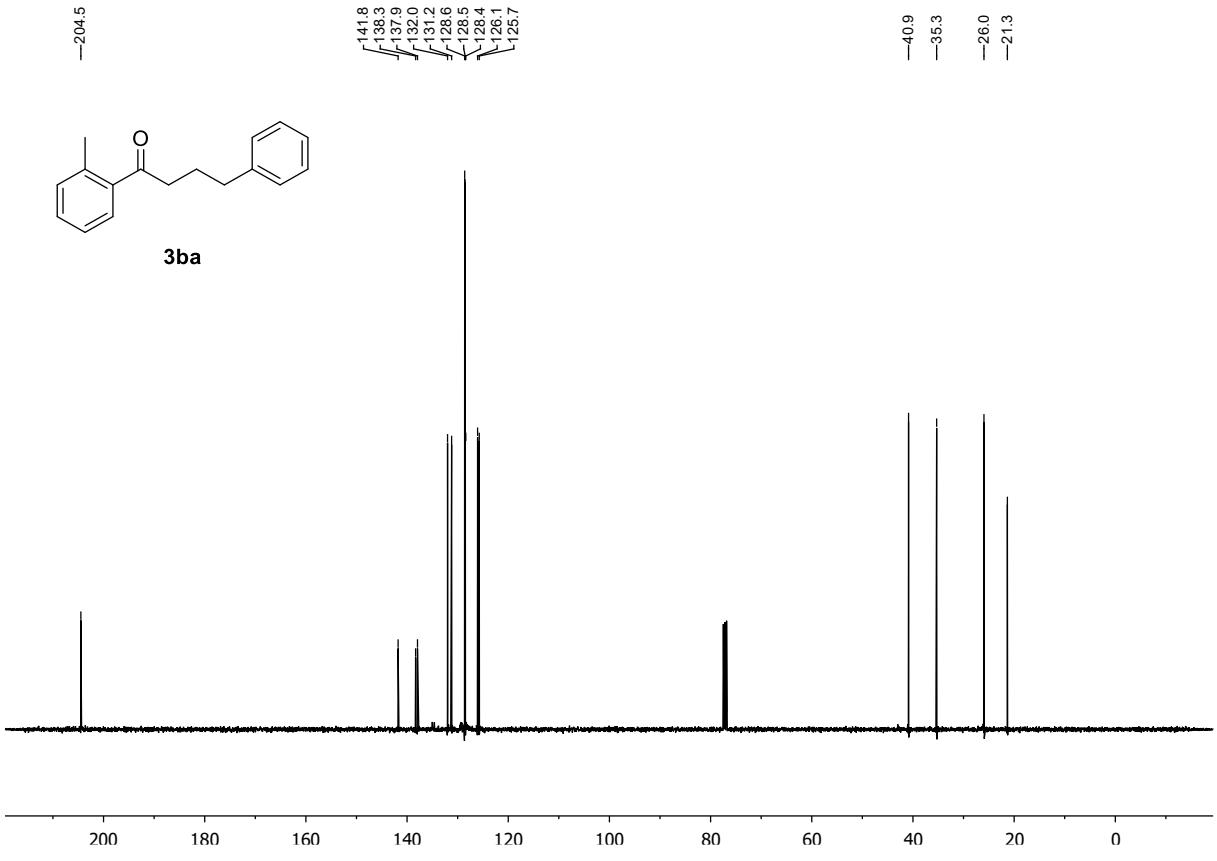

Figure S58. ^{13}C NMR spectrum (101 MHz, $CDCl_3$) of **3ba**.

1-(Naphthalen-1-yl)-4-phenylbutan-1-one (3ca):

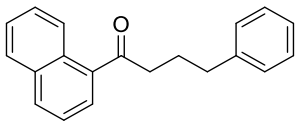

3ca

$C_{20}H_{18}O$ (274.36 g/mol)

Following **GP-B**, **3ca** was synthesized using *S*-phenyl naphthalene-1-carbothioate (**1c**) (264.0 mg, 1.0 mmol, 1.0 equiv.), (3-bromopropyl)benzene (398 mg, 2.0 mmol, 2.0 equiv.), $NiCl_2 \cdot (H_2O)_6$ (23.8 mg, 0.1 mmol, 10 mol%), 4,4'-di-*tert*-butyl-2,2'-bipyridine (53.7 mg, 0.2 mmol, 20 mol%), zinc powder (131 mg, 2.0 mmol, 2.0 equiv.), sodium chloride (117 mg, 2.0 mmol, 2.0 equiv.) and pyridine (158 mg, 2.0 mmol, 2 equiv.). Purification by flash column chromatography (*n*-hexane/EtOAc gradient 100:0 to 90:10 over 10 CV) afforded **3ca** (144 mg, 525 µmol, 53%) as yellow oil. Conforms to reported analytical data.[18]

R_f: 0.45 (*n*-hexane/EtOAc 90:10).

^{1}H NMR (400 MHz, $CDCl_3$, δ): 8.56 (m, 1H), 7.98 (m, 1H), 7.88 (m, 1H), 7.79 (dd, *J* = 7.2, 1.2 Hz, 1H), 7.64 – 7.44 (m, 3H), 7.34 – 7.27 (m, 2H), 7.25 – 7.16 (m, 3H), 3.08 (t, *J* = 7.3 Hz, 2H), 2.77 (t, *J* = 7.5 Hz, 2H), 2.15 (tt, *J* = 7.5, 7.3 Hz, 2H).

^{13}C{^{1}H} NMR (101 MHz, $CDCl_3$, δ): 204.7, 141.7, 136.4, 134.1, 132.5, 130.2, 128.6, 128.5, 128.0, 127.3, 126.5, 126.1, 125.9, 124.5, 100.1, 41.5, 35.4, 26.3.

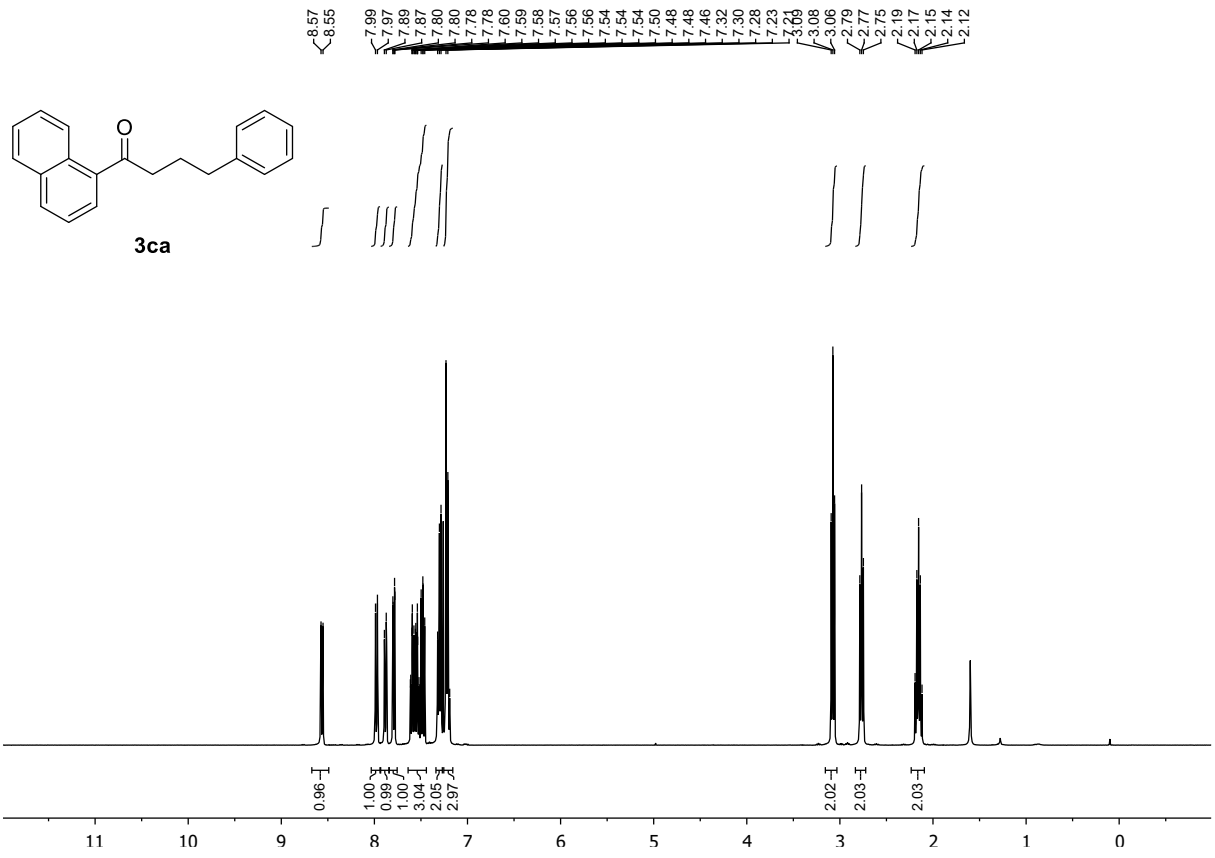

Figure S59. ^{1}H NMR spectrum (400 MHz, $CDCl_3$) of **3ca**.

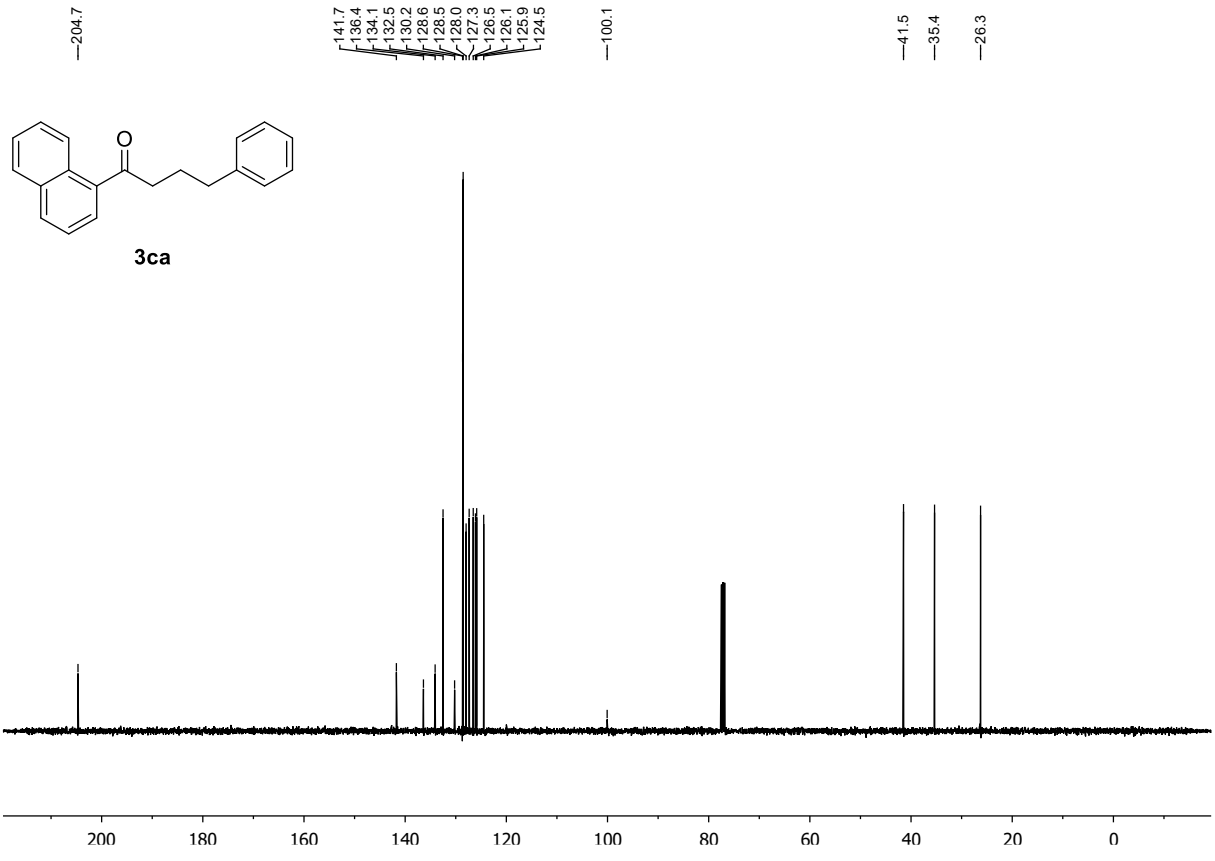

Figure S60. ^{13}C NMR spectrum (101 MHz, $CDCl_3$) of **3ca**.

1-(3-Chlorophenyl)-4-phenylbutan-1-one (3da):

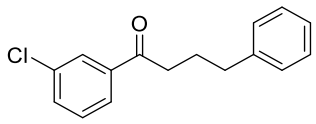

3da

$C_{16}H_{15}ClO$ (258.75 g/mol)

Following **GP-B**, **3da** was synthesized using *S*-phenyl 3-chlorobenzothioate (**1d**) (249.0 mg, 1.0 mmol, 1.0 equiv.), (3-bromopropyl)benzene (398 mg, 2.0 mmol, 2.0 equiv.), $NiCl_2 \cdot (H_2O)_6$ (23.8 mg, 0.1 mmol, 10 mol%), 4,4'-di-*tert*-butyl-2,2'-bipyridine (53.7 mg, 0.2 mmol, 20 mol%), zinc powder (131 mg, 2.0 mmol, 2.0 equiv.), sodium chloride (117 mg, 2.0 mmol, 2.0 equiv.) and pyridine (158 mg, 2.0 mmol, 2 equiv.). Purification by flash column chromatography (*n*-hexane/EtOAc gradient 100:0 to 90:10 over 10 CV) afforded **3da** (174 mg, 672 µmol, 67%) as colorless solid. Conforms to reported analytical data.[14]

R_f: 0.48 (*n*-hexane/EtOAc 90:10).

^{1}H NMR (400 MHz, $CDCl_3$, δ): 7.89 (dd, *J* = 1.9, 1.9 Hz, 1H), 7.79 (m, 1H), 7.56 – 7.48 (m, 1H), 7.39 (m, 1H), 7.34 – 7.27 (m, 2H), 7.25 – 7.17 (m, 3H), 2.95 (t, *J* = 7.3 Hz, 2H), 2.73 (t, *J* = 7.5 Hz, 2H), 2.09 (tt, *J* = 7.5, 7.3 Hz, 2H).

^{13}C{^{1}H} NMR (101 MHz, $CDCl_3$, δ): 198.8, 141.6, 138.6, 135.0, 133.0, 130.0, 128.6, 128.6, 128.3, 126.2, 126.2, 37.9, 35.2, 25.6.

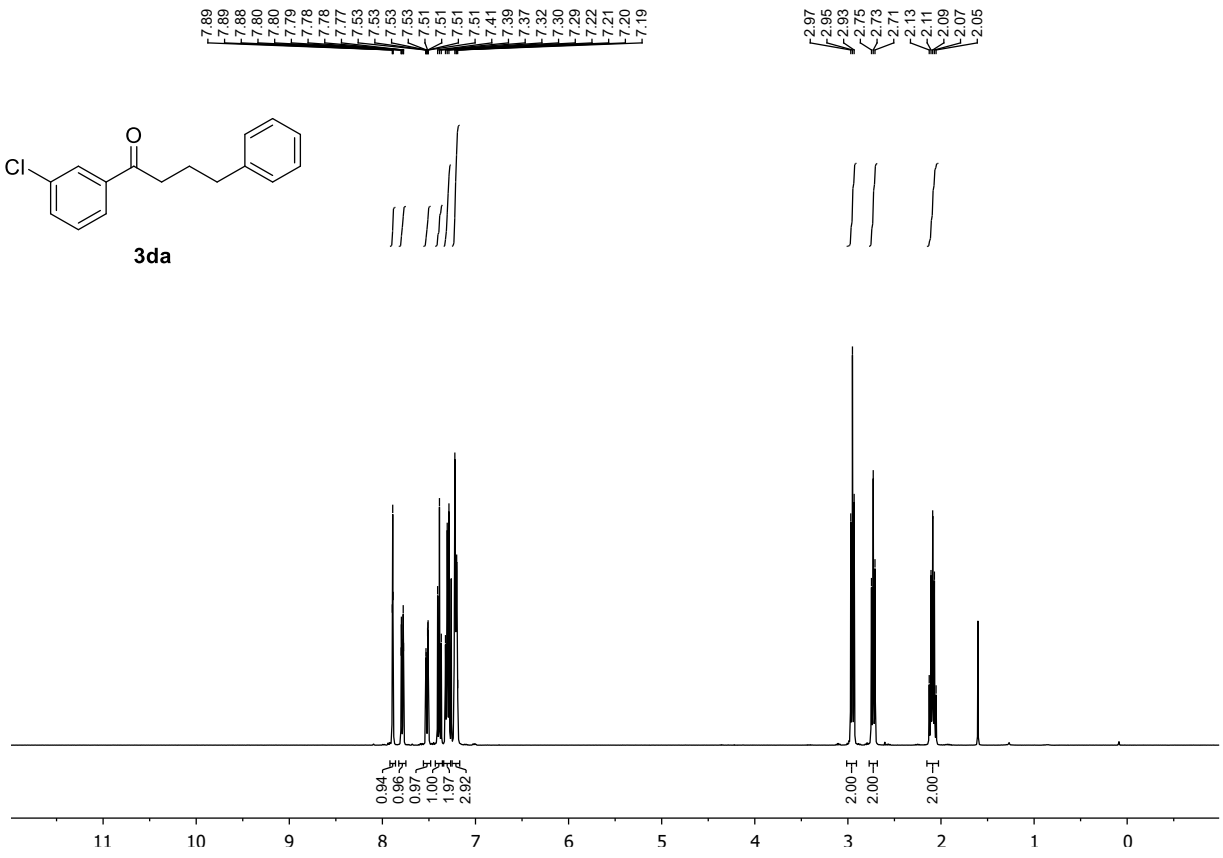

Figure S61. ^{1}H NMR spectrum (400 MHz, $CDCl_3$) of **3da**.

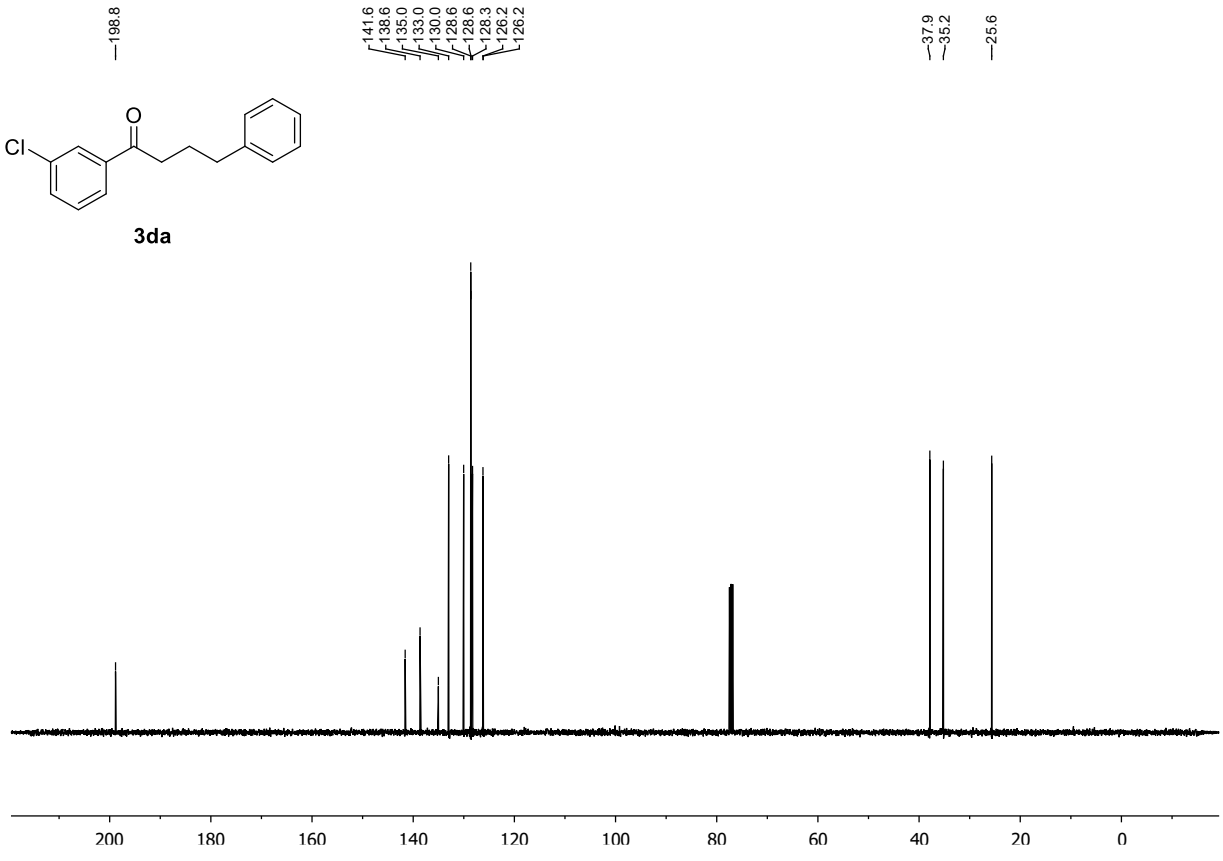

Figure S62. ^{13}C NMR spectrum (101 MHz, $CDCl_3$) of **3da**.

1-(3-Bromophenyl)-4-phenylbutan-1-one (3ea):

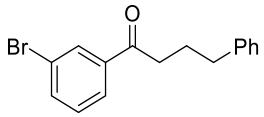

3ea

$C_{16}H_{15}BrO$ (303.20 g/mol)

Following **GP-B**, **3ea** was synthesized using *S*-phenyl 3-bromobenzothioate (**1e**) (293 mg, 1.0 mmol, 1.0 equiv.), (3-bromopropyl)benzene (398 mg, 2.0 mmol, 2.0 equiv.), $NiCl_2 \cdot (H_2O)_6$ (23.8 mg, 0.1 mmol, 10 mol%), 4,4'-di-*tert*-butyl-2,2'-bipyridine (53.7 mg, 0.2 mmol, 20 mol%), zinc powder (131 mg, 2.0 mmol, 2.0 equiv.), sodium chloride (117 mg, 2.0 mmol, 2.0 equiv.) and pyridine (158 mg, 2.0 mmol, 2 equiv.). Purification by flash column chromatography (*n*-hexane/EtOAc gradient 100:0 to 90:10 over 10 CV) afforded **3ea** (156 mg, 514 µmol, 51%) as colorless oil. Conforms to reported analytical data.[19]

R_f: 0.56 (*n*-hexane/EtOAc 90:10).

^{1}H NMR (400 MHz, $CDCl_3$, δ): δ 8.08 – 8.01 (m, 1H), 7.87 – 7.80 (m, 1H), 7.72 – 7.62 (m, 1H), 7.37 – 7.27 (m, 3H), 7.25 – 7.15 (m, 3H), 2.94 (t, *J* = 7.3 Hz, 2H), 2.72 (t, *J* = 7.5 Hz, 2H), 2.15 – 2.02 (m, 2H).

^{13}C{^{1}H} NMR (101 MHz, $CDCl_3$, δ): 198.8, 141.6, 138.9, 135.9, 131.2, 130.3, 128.6, 128.6, 126.7, 126.2, 123.1, 37.9, 35.2, 25.7.

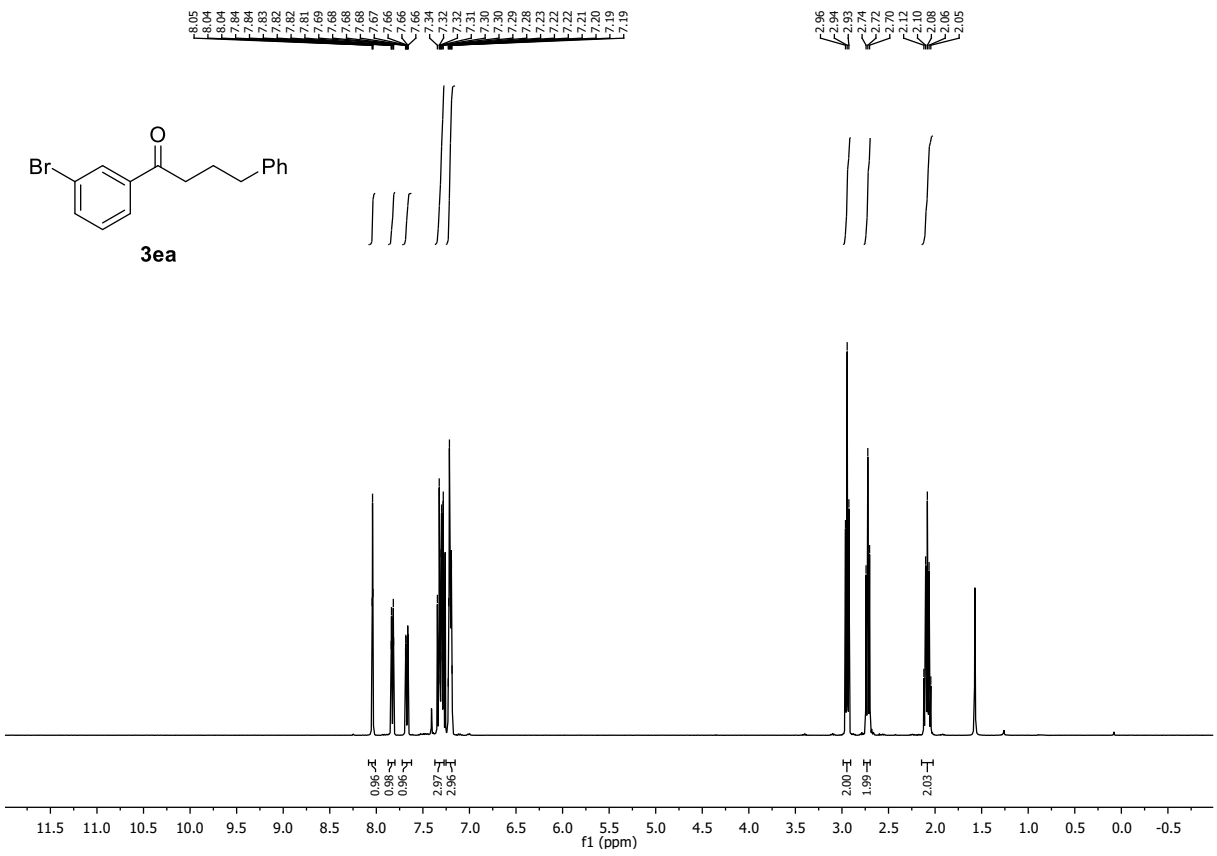

Figure S63. ^{1}H NMR spectrum (400 MHz, $CDCl_3$) of **3ea**.

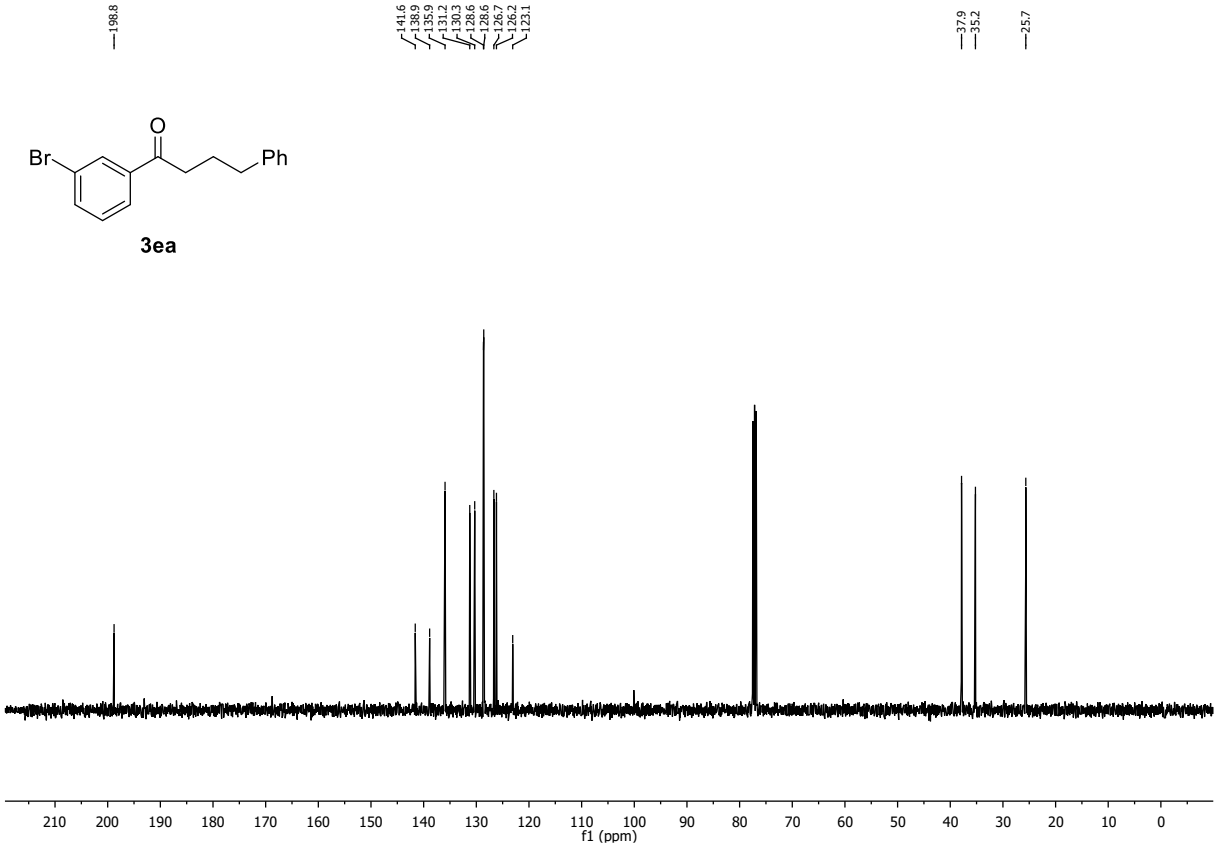

Figure S64. ^{13}C NMR spectrum (101 MHz, $CDCl_3$) of **3ea**.

4-Phenyl-1-(4-(trifluoromethyl)phenyl)butan-1-one (3fa):

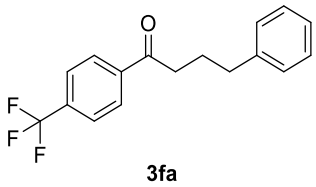

3fa

$C_{17}H_{15}F_3O$ (292.30 g/mol)

Following **GP-B**, **3fa** was synthesized using *S*-phenyl 4-(trifluoromethyl)benzothioate (**1f**) (282 mg, 1.0 mmol, 1.0 equiv.), (3-bromopropyl)benzene (398 mg, 2.0 mmol, 2.0 equiv.), $NiCl_2 \cdot (H_2O)_6$ (23.8 mg, 0.1 mmol, 10 mol%), 4,4'-di-*tert*-butyl-2,2'-bipyridine (53.7 mg, 0.2 mmol, 20 mol%), zinc powder (131 mg, 2.0 mmol, 2.0 equiv.), sodium chloride (117 mg, 2.0 mmol, 2.0 equiv.) and pyridine (158 mg, 2.0 mmol, 2 equiv.). Purification by flash column chromatography (*n*-hexane/EtOAc gradient 100:0 to 90:10 over 10 CV) afforded **3fa** (139 mg, 476 µmol, 48%) as colorless solid. Conforms to reported analytical data.[17]

R_f: 0.58 (*n*-hexane/EtOAc 90:10).

^{1}H NMR (400 MHz, $CDCl_3$, δ): 8.02 – 7.95 (m, 2H), 7.72 – 7.65 (m, 2H), 7.32 – 7.24 (m, 2H), 7.22 – 7.16 (m, 3H), 2.97 (t, *J* = 7.3 Hz, 2H), 2.72 (t, *J* = 7.5 Hz, 2H), 2.14 – 2.03 (m, 2H).

^{13}C{1H} NMR (101 MHz, CDCl3, δ): 199.1, 141.5, 139.7, 134.4 (q, *J* = 32.7 Hz), 128.62, 128.58, 128.4, 126.2, 125.7 (q, *J* = 3.6 Hz), 123.8 (q, *J* = 272.8 Hz), 38.0, 35.2, 25.6.

^{19}F NMR (376 MHz, $CDCl_3$, δ): -63.1.

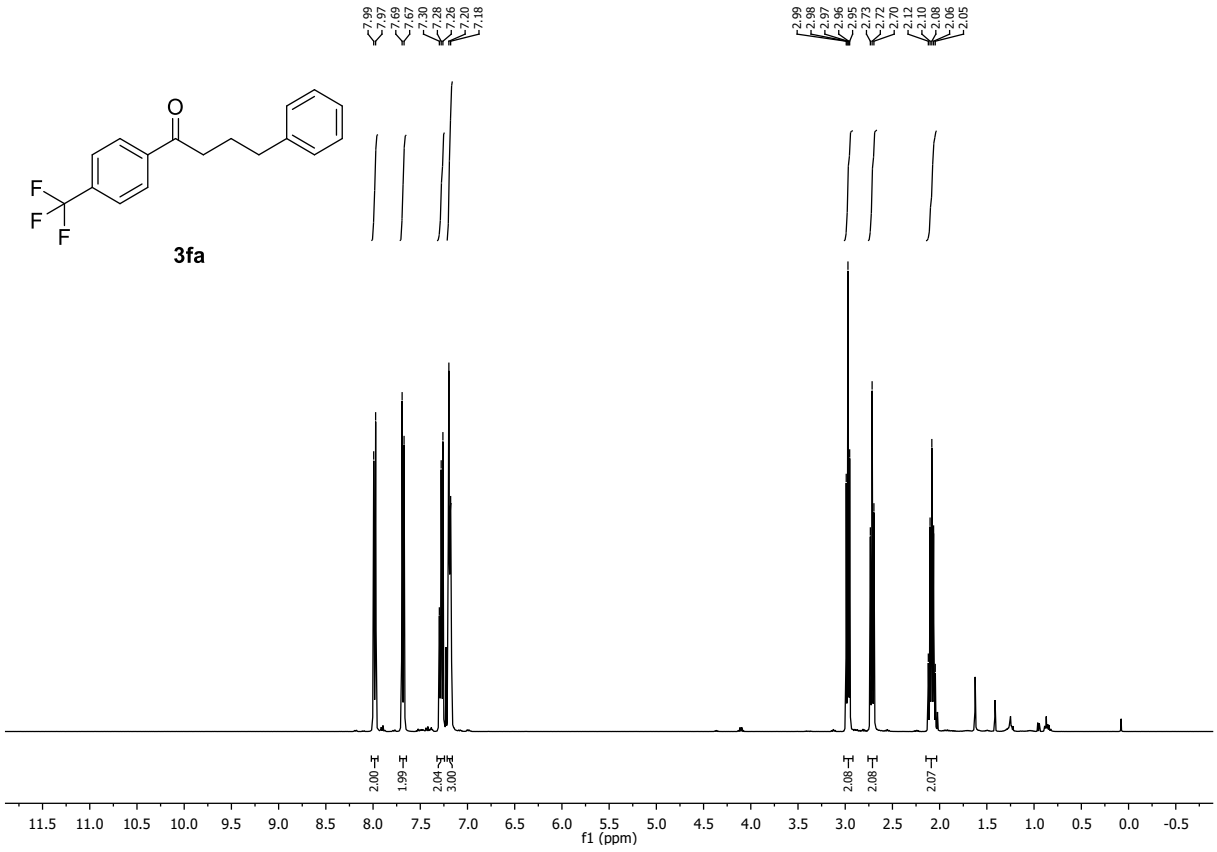

Figure S65. ^{1}H NMR spectrum (400 MHz, $CDCl_3$) of **3fa**.

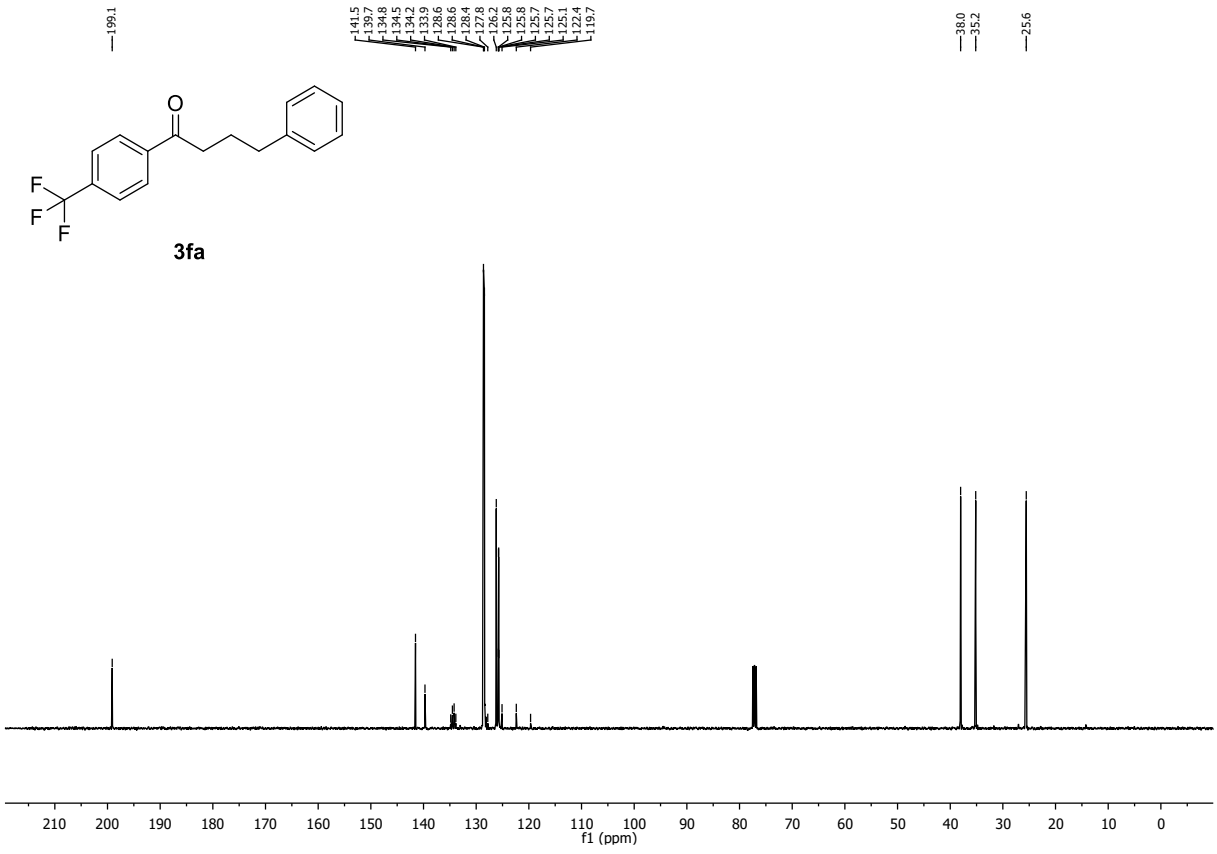

Figure S66. ^{13}C NMR spectrum (101 MHz, $CDCl_3$) of **3fa**.

Figure S67. ^{19}F NMR spectrum (376 MHz, $CDCl_3$) of **3fa**.

Methyl 4-(4-phenylbutanoyl)benzoate (3ga):

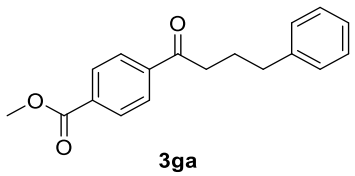

3ga

$C_{18}H_{18}O_3$ (282.34 g/mol)

Following **GP-B**, **3ga** was synthesized using methyl 4-((phenylthio)carbonyl)benzoate (**1g**) (272.0 mg, 1.0 mmol, 1.0 equiv.), (3-bromopropyl)benzene (398 mg, 2.0 mmol, 2.0 equiv.), $NiCl_2 \cdot (H_2O)_6$ (23.8 mg, 0.1 mmol, 10 mol%), 4,4'-di-*tert*-butyl-2,2'-bipyridine (53.7 mg, 0.2 mmol, 20 mol%), zinc powder (131 mg, 2.0 mmol, 2.0 equiv.), sodium chloride (117 mg, 2.0 mmol, 2.0 equiv.) and pyridine (158 mg, 2.0 mmol, 2 equiv.). Purification by flash column chromatography (*n*-hexane/EtOAc gradient 100:0 to 80:20 over 10 CV) afforded **3ga** (149 mg, 526 µmol, 53%) as colorless solid. Conforms to reported analytical data.[20]

R_f: 0.61 (*n*-hexane/EtOAc 80:20).

^{1}H NMR (400 MHz, $CDCl_3$, δ): 8.14 – 8.06 (m, 2H), 8.00 – 7.92 (m, 2H), 7.33 – 7.27 (m, 2H), 7.23 – 7.17 (m, 3H), 3.95 (s, 3H), 3.00 (t, *J* = 7.3 Hz, 2H), 2.73 (t, *J* = 7.5 Hz, 2H), 2.10 (tt, *J* = 7.5, 7.3 Hz, 2H).

^{13}C{^{1}H} NMR (101 MHz, $CDCl_3$, δ): 199.7, 166.4, 141.6, 140.3, 133.9, 129.9, 128.6, 128.6, 128.0, 126.2, 52.6, 38.2, 35.2, 25.6.

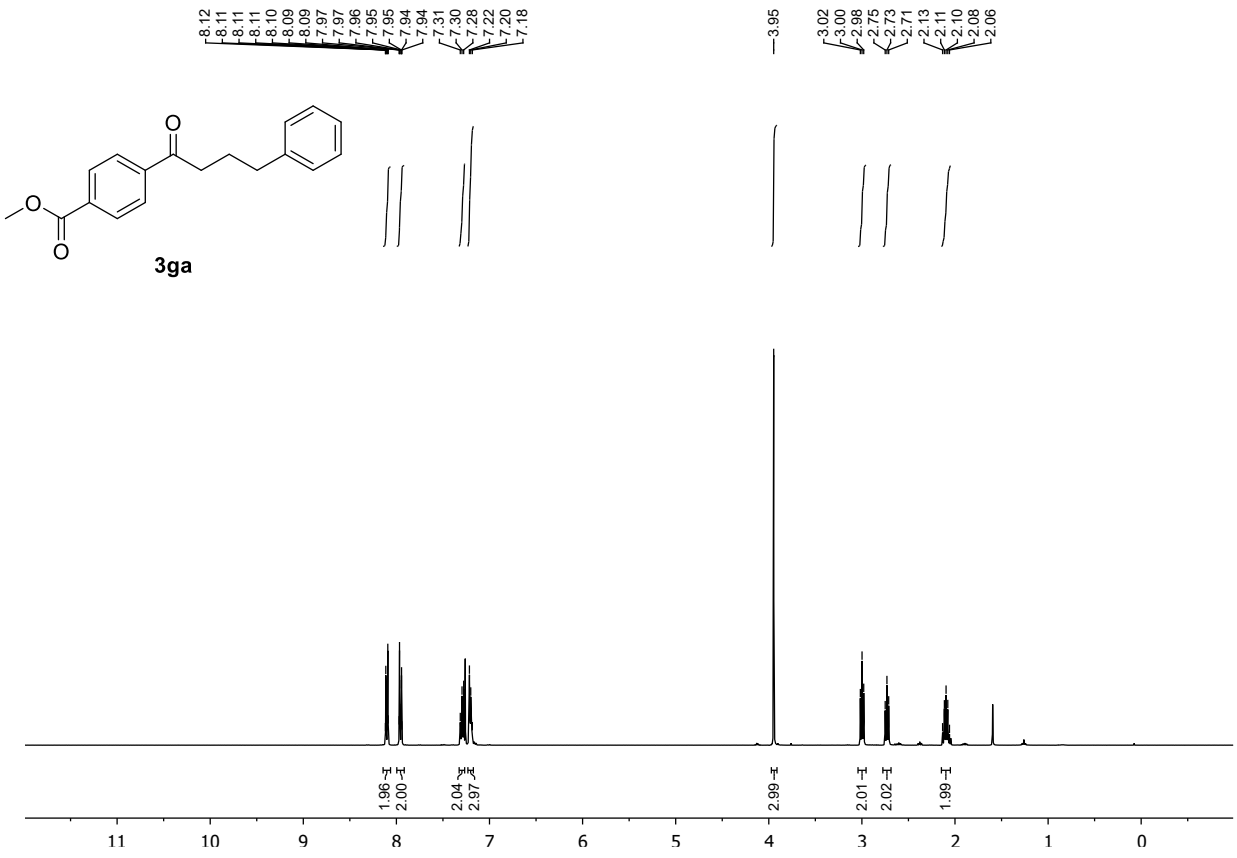

Figure S68. ^{1}H NMR spectrum (400 MHz, $CDCl_3$) of **3ga**.

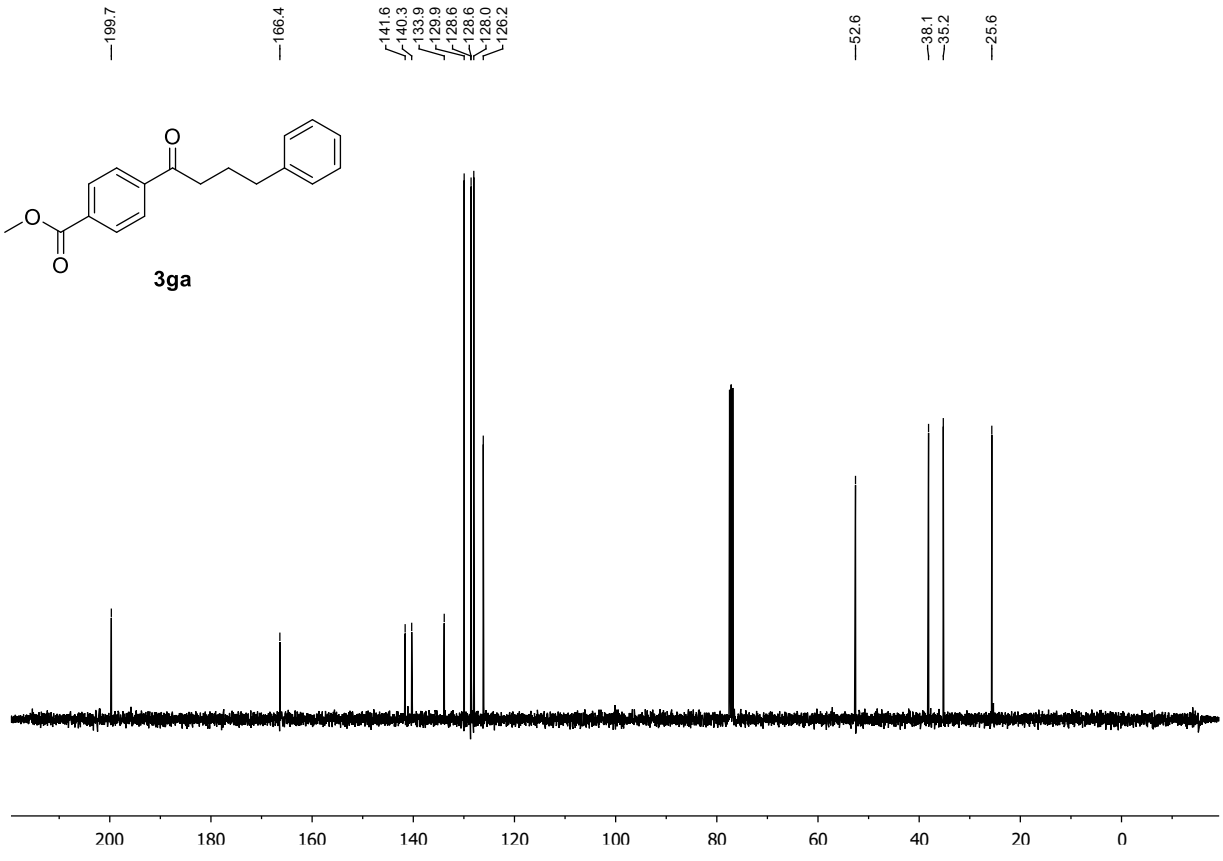

Figure S69. ^{13}C NMR spectrum (101 MHz, $CDCl_3$) of **3ga**.

1-(4-Methoxyphenyl)-4-phenylbutan-1-one (3ha):

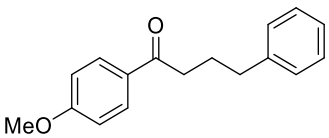

3ha

$C_{17}H_{18}O_2$ (254.33 g/mol)

Following **GP-B**, **3ha** was synthesized using *S*-phenyl 4-methoxybenzothioate (**1h**) (244.0 mg, 1.0 mmol, 1.0 equiv.), (3-bromopropyl)benzene (398 mg, 2.0 mmol, 2.0 equiv.), $NiCl_2 \cdot (H_2O)_6$ (23.8 mg, 0.1 mmol, 10 mol%), 4,4'-di-*tert*-butyl-2,2'-bipyridine (53.7 mg, 0.2 mmol, 20 mol%), zinc powder (131 mg, 2.0 mmol, 2.0 equiv.), sodium chloride (117 mg, 2.0 mmol, 2.0 equiv.) and pyridine (158 mg, 2.0 mmol, 2 equiv.). Purification by flash column chromatography (*n*-hexane/EtOAc gradient 100:0 to 85:15 over 10 CV) afforded **3ha** (166 mg, 652 µmol, 65%) as colorless solid. Conforms to reported analytical data.[17]

R_f: 0.35 (*n*-hexane/EtOAc 90:10).

^{1}H NMR (400 MHz, $CDCl_3$, δ): 7.95 – 7.86 (m, 2H), 7.35 – 7.26 (m, 2H), 7.24 – 7.16 (m, 3H), 6.96 – 6.87 (m, 2H), 3.86 (s, 3H), 2.93 (t, *J* = 7.3 Hz, 2H), 2.72 (t, *J* = 7.5 Hz, 2H), 2.08 (tt, *J* = 7.5, 7.3 Hz, 2H).

^{13}C{^{1}H} NMR (101 MHz, $CDCl_3$, δ): 198.9, 163.5, 141.9, 130.4, 130.3, 128.7, 128.5, 126.0, 113.8, 55.6, 37.5, 35.4, 26.1.

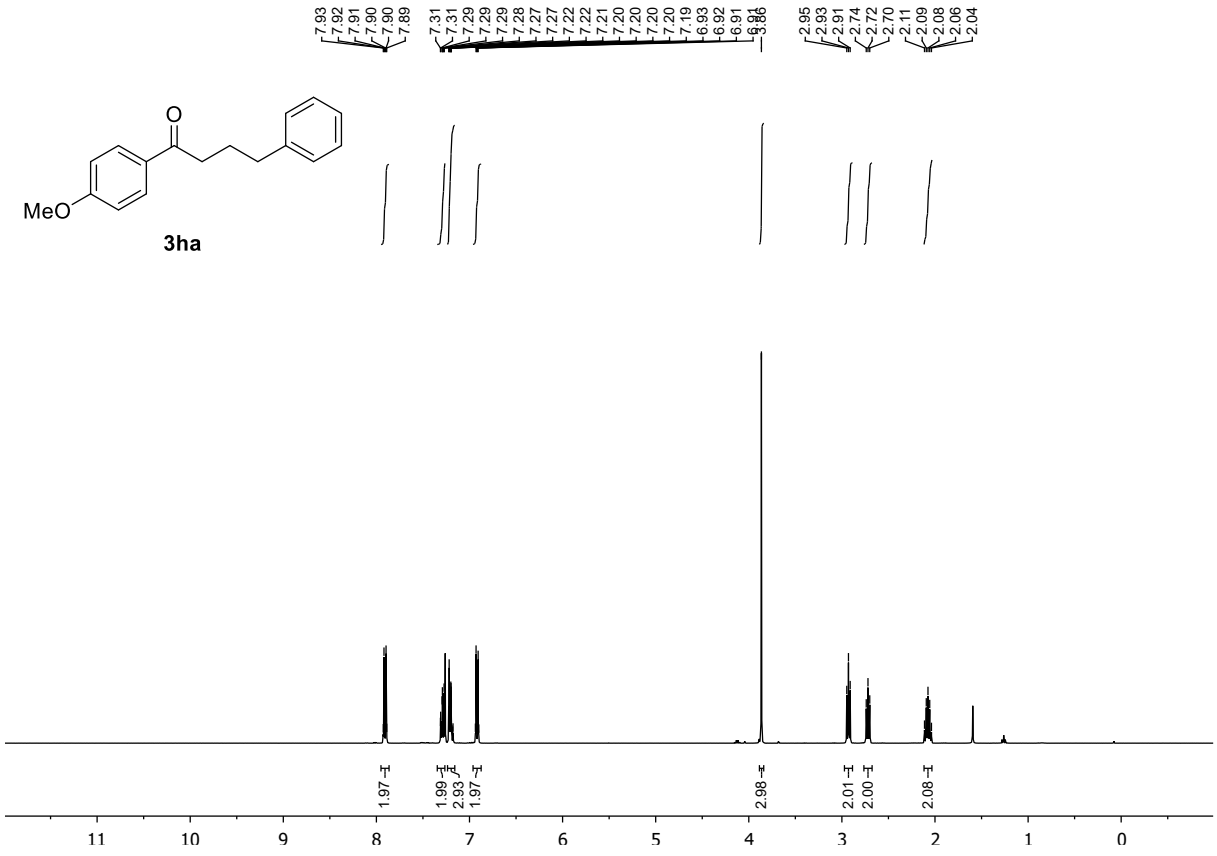

Figure S70. ^{1}H NMR spectrum (400 MHz, $CDCl_3$) of **3ha**.

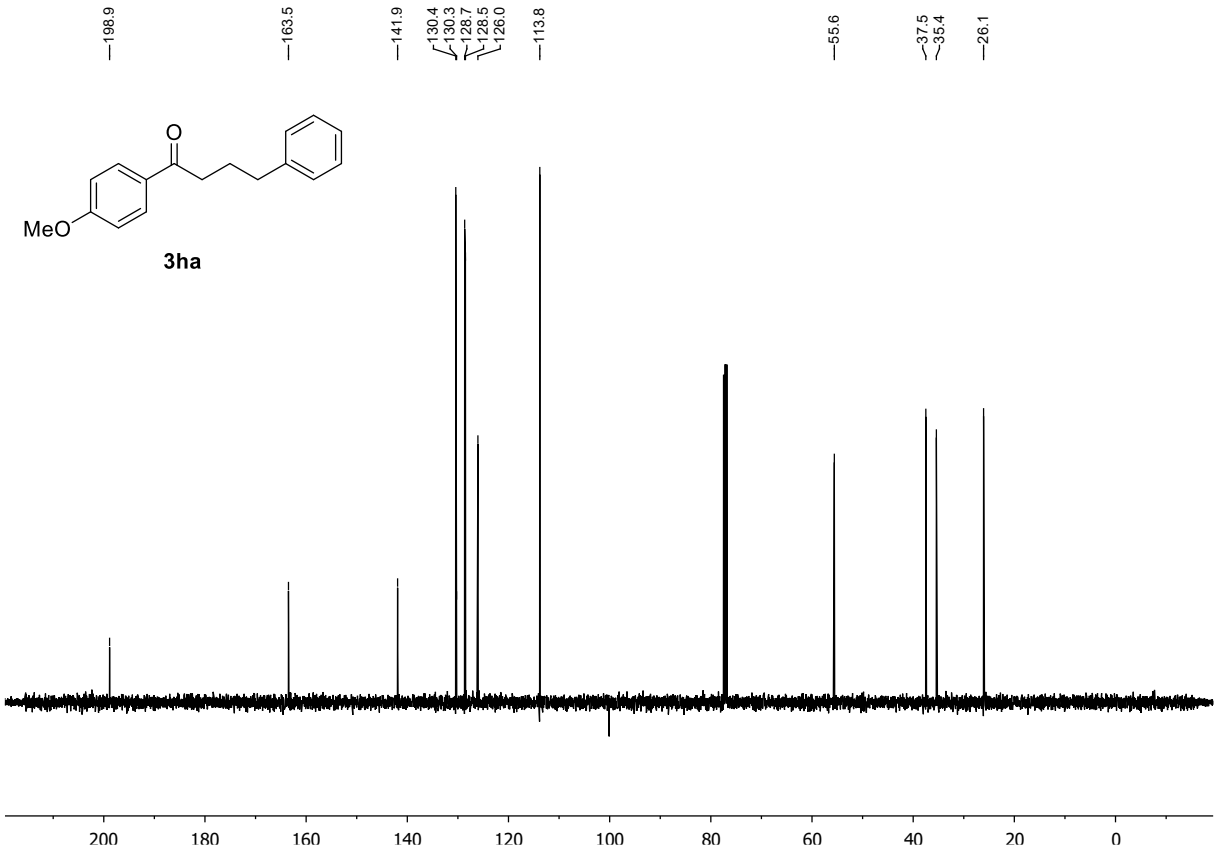

Figure S71. ^{13}C NMR spectrum (101 MHz, $CDCl_3$) of **3ha**.

1-(Benzo[*d*][1,3]dioxol-5-yl)-4-phenylbutan-1-one (3ia):

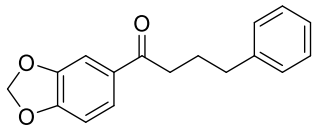

3ia

$C_{17}H_{16}O_3$ (268.31 g/mol)

Following **GP-B**, **3ia** was synthesized using *S*-phenyl benzo[*d*][1,3]dioxole-5-carbothioate (**1i**) (258 mg, 1.0 mmol, 1.0 equiv.), (3-bromopropyl)benzene (398 mg, 2.0 mmol, 2.0 equiv.), $NiCl_2 \cdot (H_2O)_6$ (23.8 mg, 0.1 mmol, 10 mol%), 4,4'-di-*tert*-butyl-2,2'-bipyridine (53.7 mg, 0.2 mmol, 20 mol%), zinc powder (131 mg, 2.0 mmol, 2.0 equiv.), sodium chloride (117 mg, 2.0 mmol, 2.0 equiv.) and pyridine (158 mg, 2.0 mmol, 2 equiv.). Purification by flash column chromatography (*n*-hexane/EtOAc gradient 100:0 to 75:25 over 10 CV) afforded **3ia** (88 mg, 328 µmol, 33%) as colorless oil. Conforms to reported analytical data.[17]

R_f: 0.61 (*n*-hexane/EtOAc 80:20).

^{1}H NMR (400 MHz, $CDCl_3$, δ): 7.51 (dd, *J* = 8.2, 1.7 Hz, 1H), 7.41 (d, *J* = 1.7 Hz, 1H), 7.32 – 7.27 (m, 2H), 7.23 – 7.17 (m, 3H), 6.83 (d, *J* = 8.1 Hz, 1H), 6.03 (s, 2H), 2.90 (t, *J* = 7.3 Hz, 2H), 2.71 (t, *J* = 7.6 Hz, 2H), 2.13 – 2.00 (m, 2H).

^{13}C{1H} NMR (101 MHz, $CDCl_3$, δ): 198.3, 151.7, 148.3, 141.8, 135.3, 132.0, 128.6, 128.5, 126.1, 124.3, 107.9, 101.9, 37.6, 35.3, 26.1.

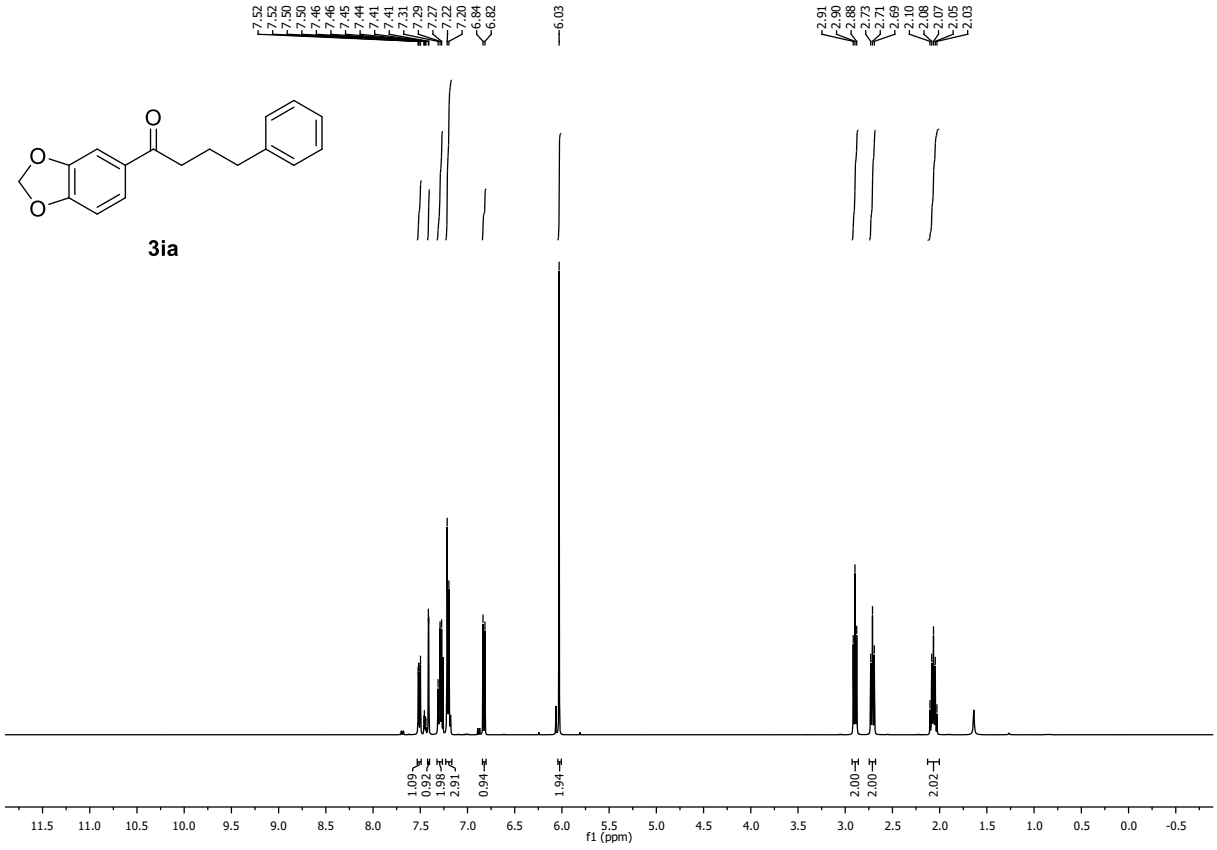

Figure S72. ^{1}H NMR spectrum (400 MHz, $CDCl_3$) of **3ia**.

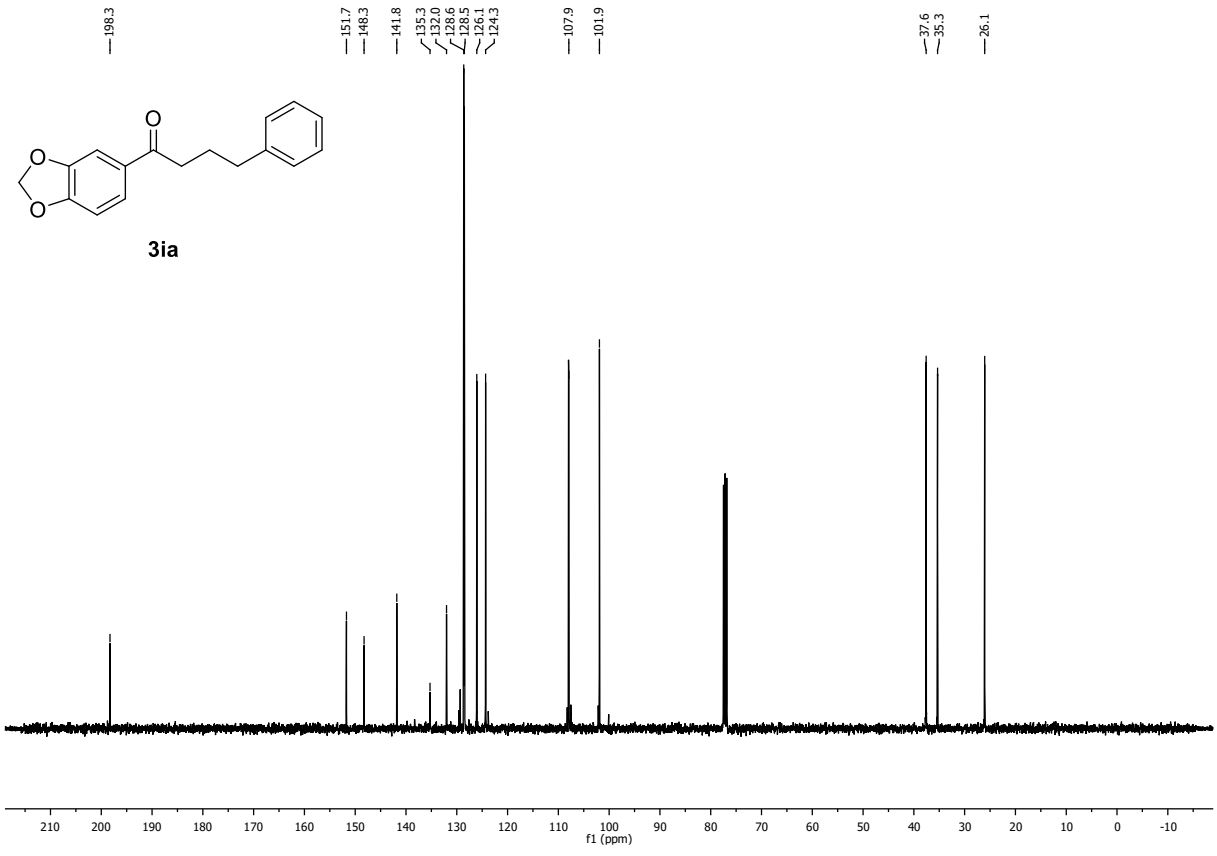

Figure S73. ^{13}C NMR spectrum (101 MHz, $CDCl_3$) of **3ia**.

1,6-Diphenylhexan-3-one (3ja):

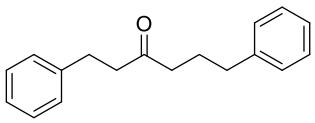

3ja

$C_{18}H_{20}O$ (252.15 g/mol)

Following **GP-B**, **3ja** was synthesized using *S*-phenyl 3-phenylpropanethioate (**1j**) (242 mg, 1.0 mmol, 1.0 equiv.), (3-bromopropyl)benzene (398 mg, 2.0 mmol, 2.0 equiv.), $NiCl_2 \cdot (H_2O)_6$ (23.8 mg, 0.1 mmol, 10 mol%), 4,4'-di-*tert*-butyl-2,2'-bipyridine (53.7 mg, 0.2 mmol, 20 mol%), zinc powder (131 mg, 2.0 mmol, 2.0 equiv.), sodium chloride (117 mg, 2.0 mmol, 2.0 equiv.) and pyridine (158 mg, 2.0 mmol, 2 equiv.). Purification by flash column chromatography (*n*-hexane/EtOAc gradient 100:0 to 90:10 over 10 CV) afforded **3ja** (194 mg, 769 µmol, 77%) as colorless solid. Conforms to reported analytical data.[21]

R_f: 0.41 (*n*-hexane/EtOAc 90:10).

^{1}H NMR (400 MHz, $CDCl_3$, δ): 7.35 – 7.27 (m, 4H), 7.24 – 7.13 (m, 6H), 2.91 (t, *J* = 7.6 Hz, 2H), 2.72 (t, *J* = 7.6 Hz, 2H), 2.62 (t, *J* = 7.6 Hz, 2H), 2.41 (t, *J* = 7.3 Hz, 2H), 1.97 – 1.89 (m, 2H).

^{13}C{^{1}H} NMR (101 MHz, $CDCl_3$, δ): 209.9, 141.6, 141.2, 128.6, 128.5, 128.4, 126.2, 126.0, 44.4, 42.2, 35.2, 29.9, 25.3.

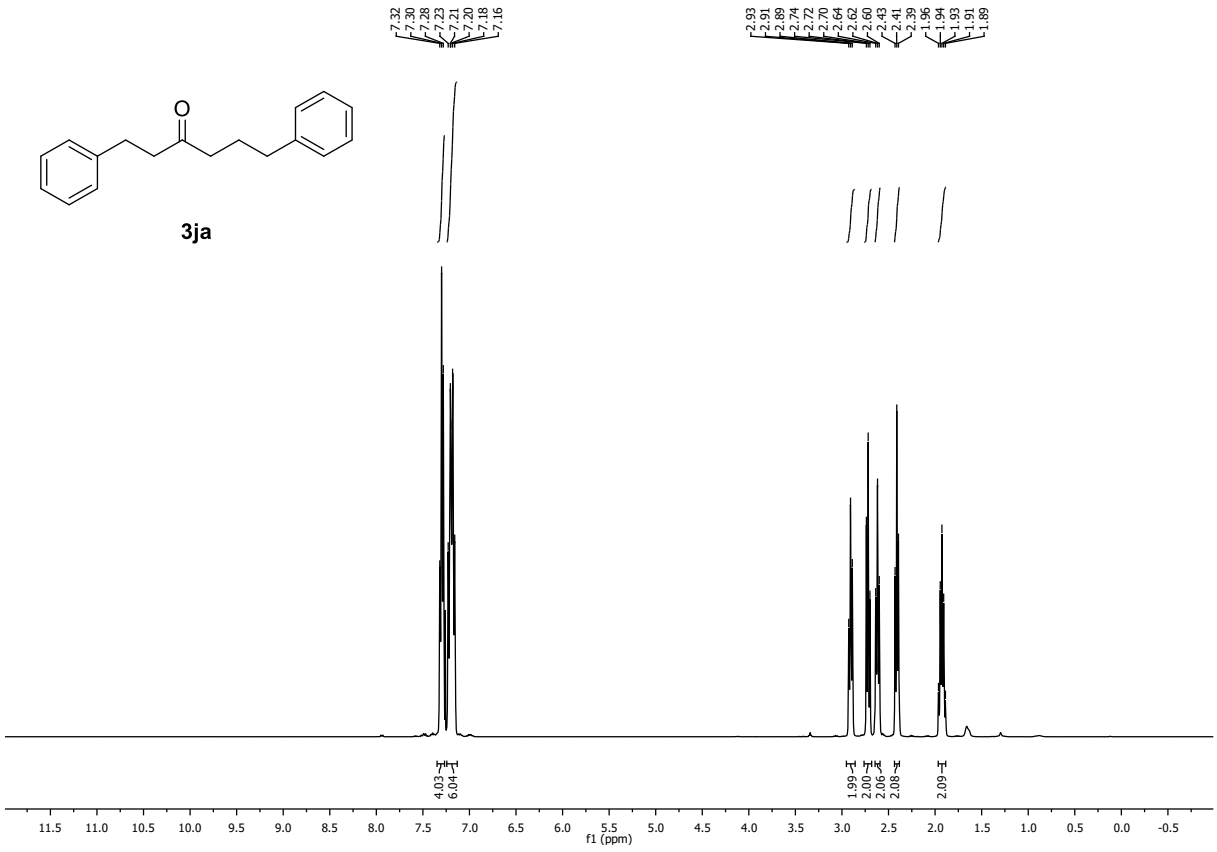

Figure S74. ^{1}H NMR spectrum (400 MHz, $CDCl_3$) of **3ja**.

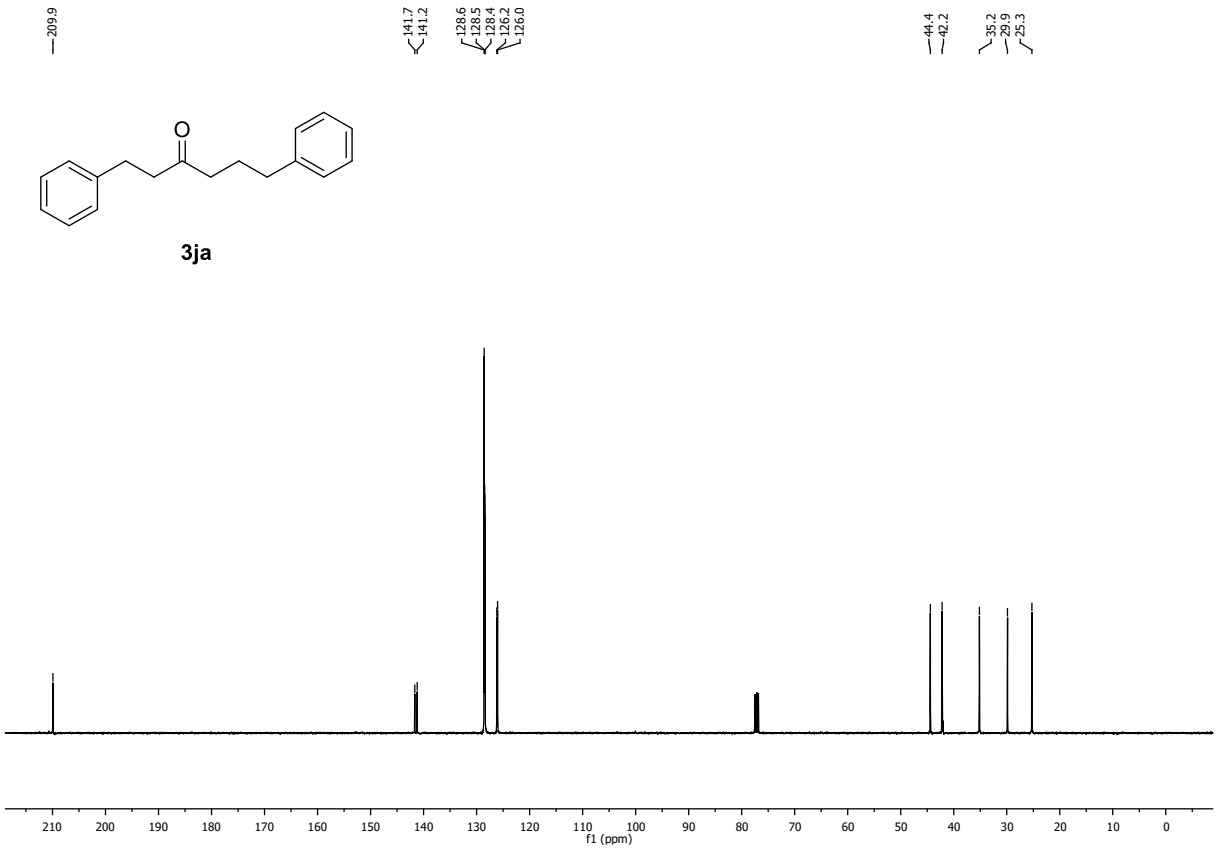

Figure S75. ^{13}C NMR spectrum (101 MHz, $CDCl_3$) of **3ja**.

1,5-Diphenylpentan-2-one (3ka):

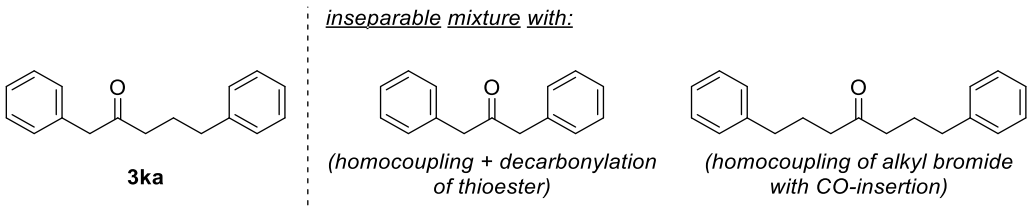

$C_{17}H_{18}O$ (238.33 g/mol)

Following **GP-B**, **3ka** was synthesized using *S*-phenyl 2-phenylethanethioate (**1k**) (228 mg, 1.0 mmol, 1.0 equiv.), (3-bromopropyl)benzene (398 mg, 2.0 mmol, 2.0 equiv.), $NiCl_2 \cdot (H_2O)_6$ (23.8 mg, 0.1 mmol, 10 mol%), 4,4'-di-*tert*-butyl-2,2'-bipyridine (53.7 mg, 0.2 mmol, 20 mol%), zinc powder (131 mg, 2.0 mmol, 2.0 equiv.), sodium chloride (117 mg, 2.0 mmol, 2.0 equiv.) and pyridine (158 mg, 2.0 mmol, 2 equiv.). Purification by flash column chromatography (*n*-hexane/EtOAc gradient 100:0 to 90:10 over 10 CV) afforded **3ka** (90 mg, 376 µmol, 38%) as colorless oil. Conforms to reported analytical data.[22]

Note: The product was isolated as an inseparable mixture with side-products (see above). The yield was calculated by determining the purity of the crude sample (160 mg, 56 w% purity) by ^{1}H NMR spectroscopy. NMR-signals were assigned by 2D-NMR spectroscopy.

R$_f$: 0.41 (*n*-hexane/EtOAc 90:10).

^{1}H NMR (400 MHz, $CDCl_3$, δ): 7.26 – 7.13 (m, 5H), 7.12 – 6.98 (m, 5H), 3.55 (s, 2H), 2.36 (t, *J* = 7.2 Hz, 2H), 2.28 (t, *J* = 7.3 Hz, 2H), 1.79 (tt, *J* = 7.3, 7.2 Hz, 2H).

^{13}C{^{1}H} NMR (101 MHz, $CDCl_3$, δ): 208.2, 141.7, 134.4, 129.5, 128.8, 128.6, 128.5, 127.1, 126.0, 50.3, 42.0, 41.2, 25.3.

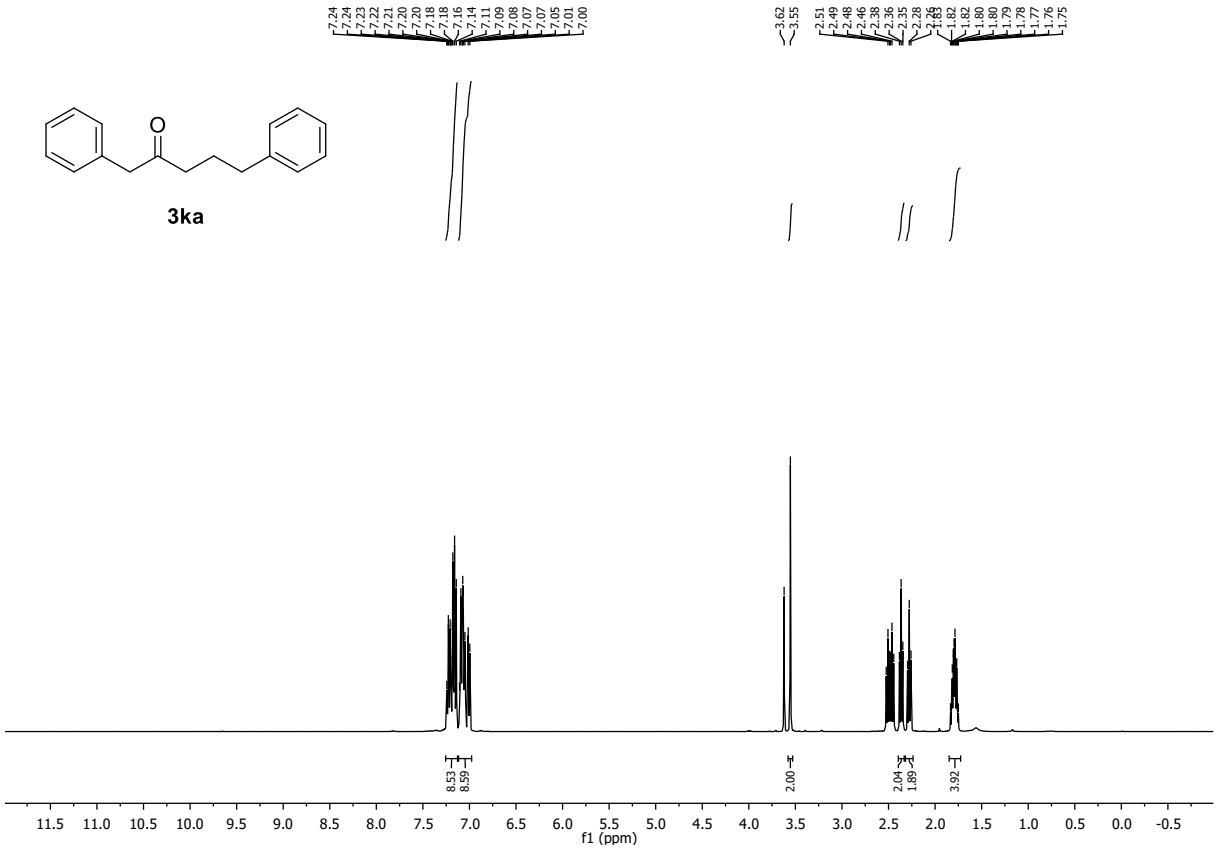

Figure S76. ^{1}H NMR spectrum (400 MHz, $CDCl_3$) of **3ka**.

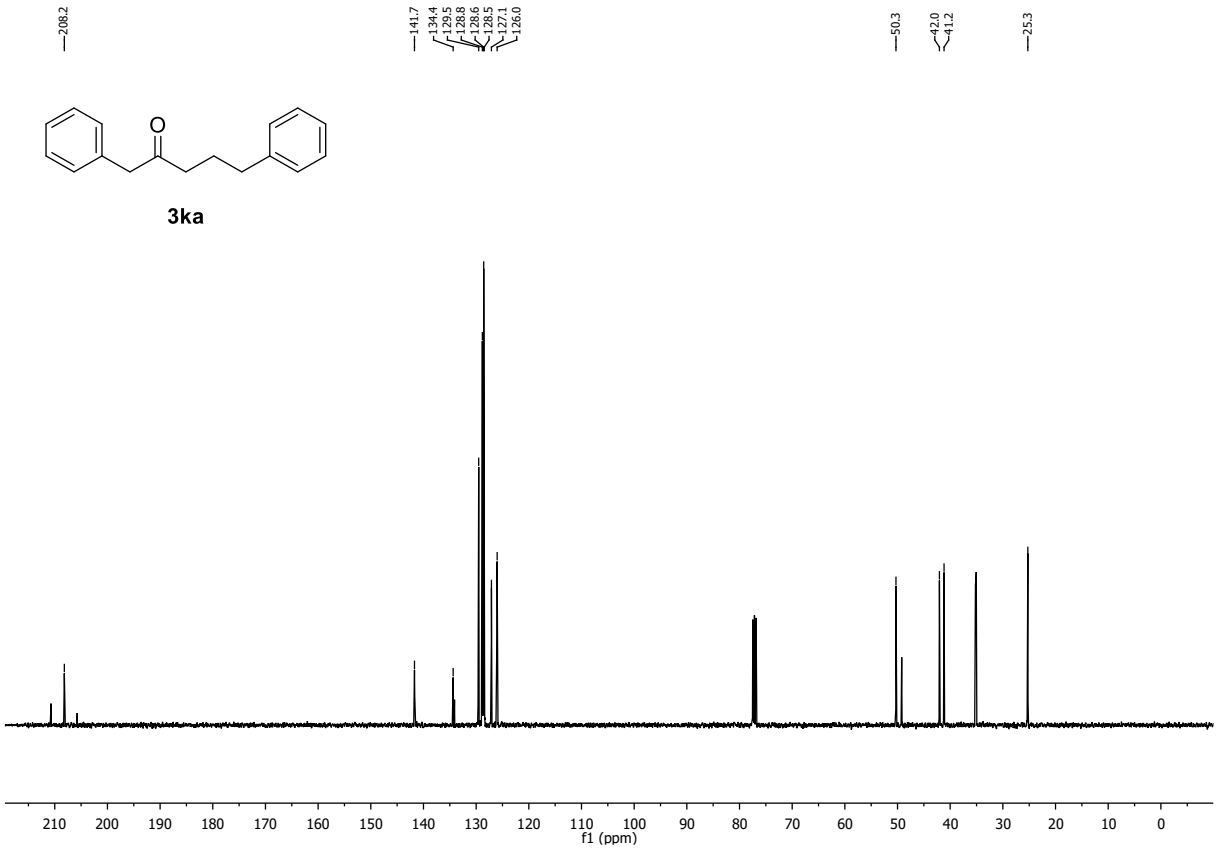

Figure S77. ^{13}C NMR spectrum (101 MHz, $CDCl_3$) of **3ka**.

1-Phenylnonan-4-one (3la):

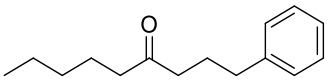

3la

$C_{15}H_{22}O$ (218.34 g/mol)

Following **GP-B**, **3la** was synthesized using *S*-phenyl hexanethioate (**1l**) (208 mg, 1.0 mmol, 1.0 equiv.), (3-bromopropyl)benzene (398 mg, 2.0 mmol, 2.0 equiv.), $NiCl_2 \cdot (H_2O)_6$ (23.8 mg, 0.1 mmol, 10 mol%), 4,4'-di-*tert*-butyl-2,2'-bipyridine (53.7 mg, 0.2 mmol, 20 mol%), zinc powder (131 mg, 2.0 mmol, 2.0 equiv.), sodium chloride (117 mg, 2.0 mmol, 2.0 equiv.) and pyridine (158 mg, 2.0 mmol, 2 equiv.). Purification by flash column chromatography (*n*-hexane/EtOAc gradient 100:0 to 90:10 over 10 CV) afforded **3la** (181 mg, 830 µmol, 83%) as colorless liquid.[18]

R_f: 0.57 (*n*-hexane/EtOAc 90:10).

^{1}H NMR (400 MHz, $CDCl_3$, δ): 7.32 – 7.26 (m, 2H), 7.24 – 7.13 (m, 3H), 2.62 (t, *J* = 7.6 Hz, 2H), 2.41 (t, *J* = 7.4 Hz, 2H), 2.36 (t, *J* = 7.4 Hz, 2H), 1.91 (tt, *J* = 7.6, 7.4 Hz, 2H), 1.56 (tt, *J* = 7.5, 7.4 Hz, 2H), 1.37 – 1.19 (m, 4H), 0.89 (t, *J* = 7.1 Hz, 3H).

^{13}C{^{1}H} NMR (101 MHz, $CDCl_3$, δ): 211.3, 141.8, 128.6, 128.5, 126.0, 43.0, 42.0, 35.3, 31.5, 25.4, 23.7, 22.6, 14.0.

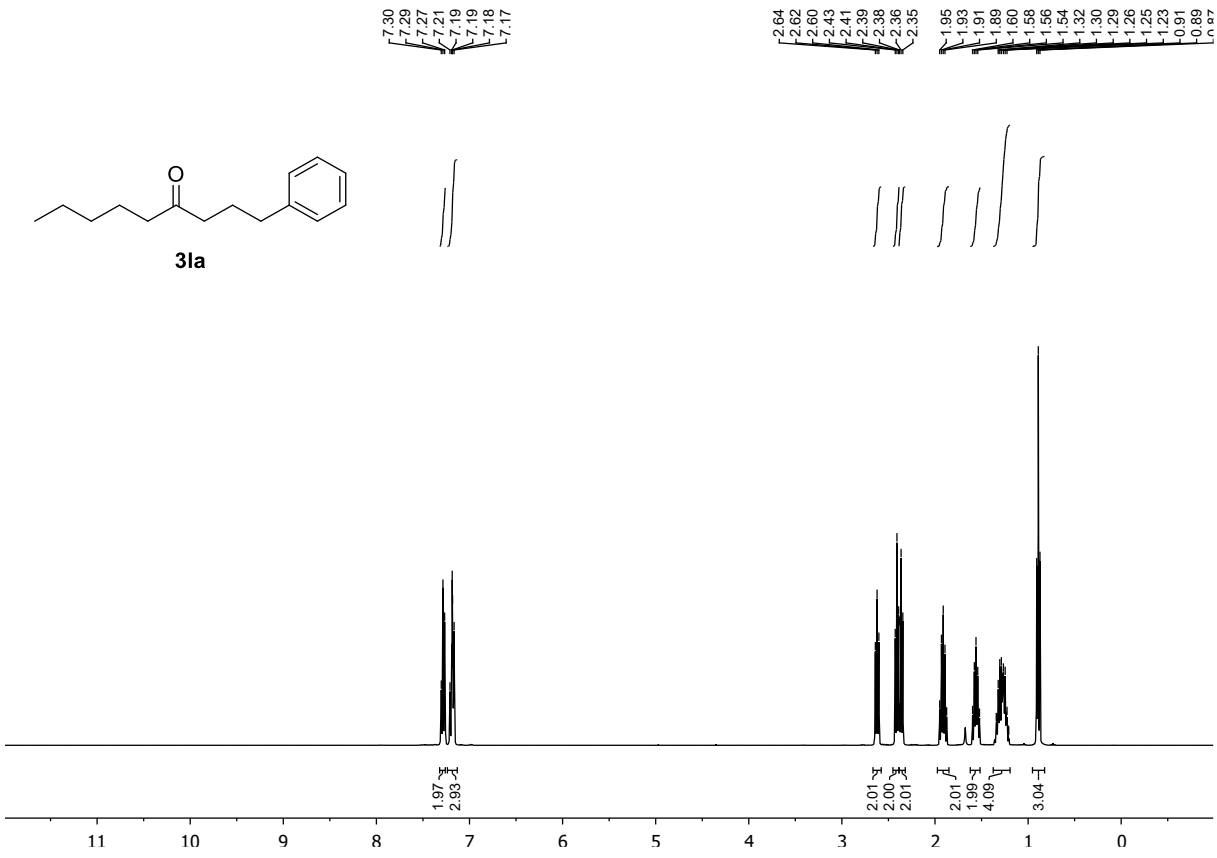

Figure S78. ^{1}H NMR spectrum (400 MHz, $CDCl_3$) of **3la**.

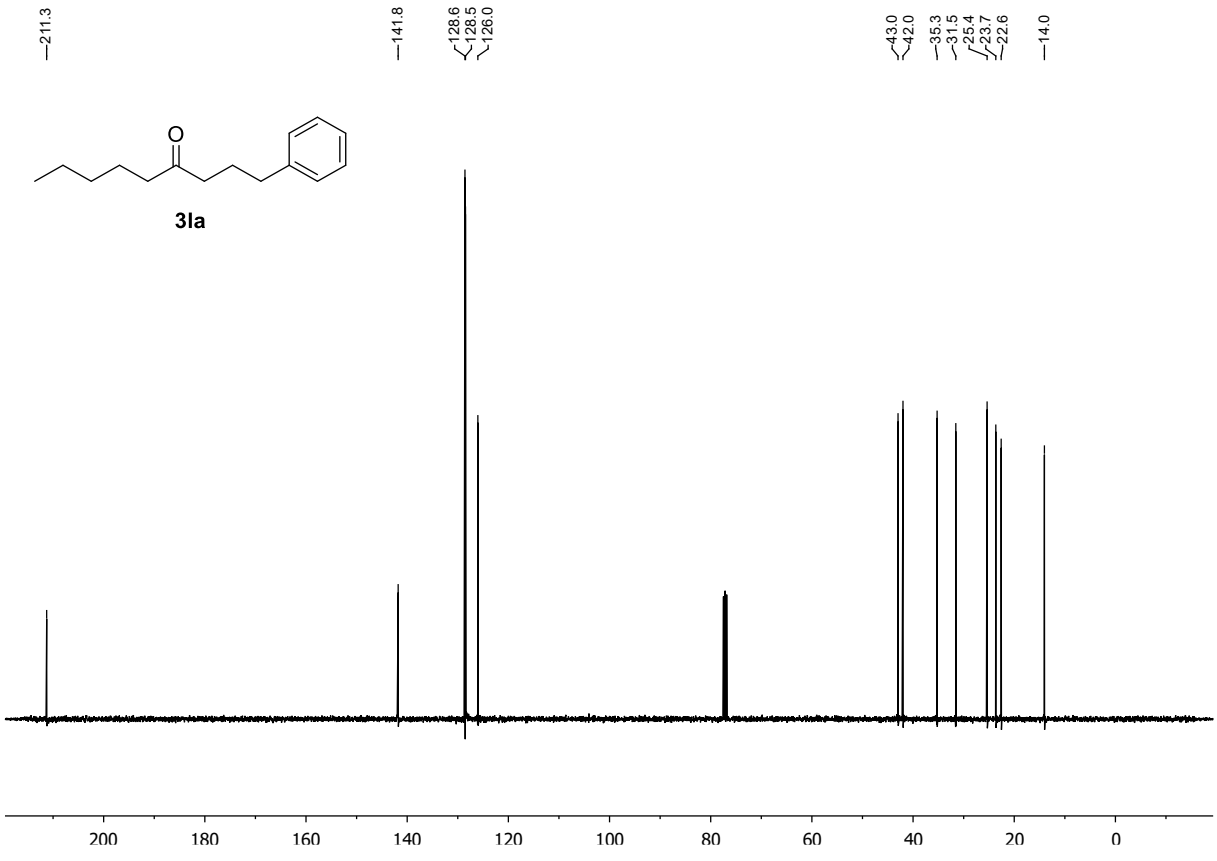

Figure S79. ^{13}C NMR spectrum (101 MHz, $CDCl_3$) of **3la**.

1-Phenyloct-7-en-4-one (3ma):

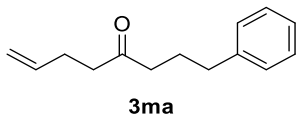

3ma

$C_{14}H_{18}O$ (202.30 g/mol)

Following **GP-B**, **3ma** was synthesized using *S*-phenyl pent-4-enethioate (**1m**) (192 mg, 1.0 mmol, 1.0 equiv.), (3-bromopropyl)benzene (398 mg, 2.0 mmol, 2.0 equiv.), $NiCl_2 \cdot (H_2O)_6$ (23.8 mg, 0.1 mmol, 10 mol%), 4,4'-di-*tert*-butyl-2,2'-bipyridine (53.7 mg, 0.2 mmol, 20 mol%), zinc powder (131 mg, 2.0 mmol, 2.0 equiv.), sodium chloride (117 mg, 2.0 mmol, 2.0 equiv.) and pyridine (158 mg, 2.0 mmol, 2 equiv.). Purification by flash column chromatography (*n*-hexane/EtOAc gradient 100:0 to 85:15 over 10 CV) afforded **3ma** (112 mg, 554 µmol, 55%) as colorless oil. Conforms to reported analytical data.[21]

R$_f$: 0.51 (*n*-hexane/EtOAc 90:10).

^{1}H NMR (400 MHz, $CDCl_3$, δ): 7.32 – 7.26 (m, 2H), 7.23 – 7.15 (m, 3H), 5.95 – 5.68 (m, 1H), 5.08 – 4.93 (m, 2H), 2.63 (t, *J* = 7.6 Hz, 2H), 2.52 – 2.40 (m, 4H), 2.36 – 2.26 (m, 2H), 1.99 – 1.86 (m, 2H).

^{13}C{^{1}H} NMR (101 MHz, $CDCl_3$, δ): 210.1, 141.7, 137.2, 128.6, 128.5, 126.0, 115.3, 42.1, 41.9, 35.2, 27.9, 25.3.

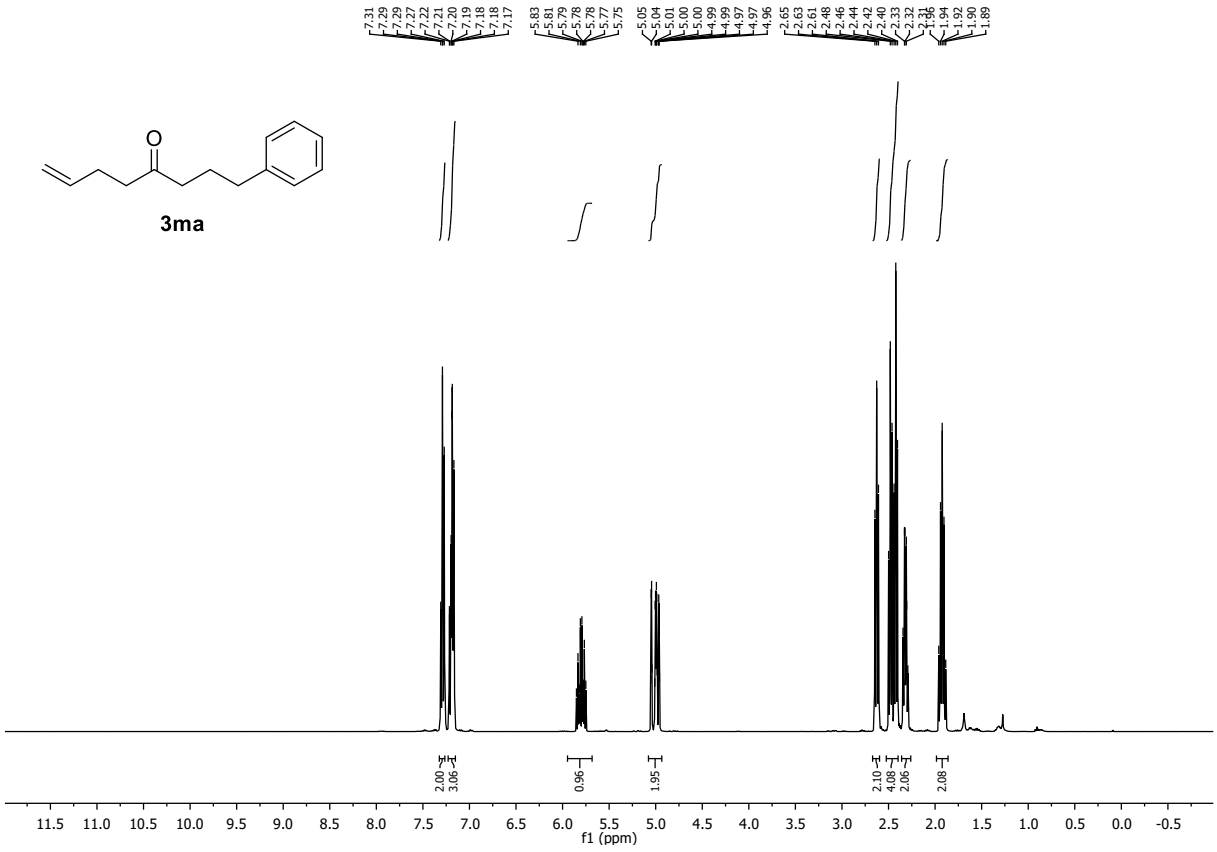

Figure S80. ^{1}H NMR spectrum (400 MHz, $CDCl_3$) of **3ma**.

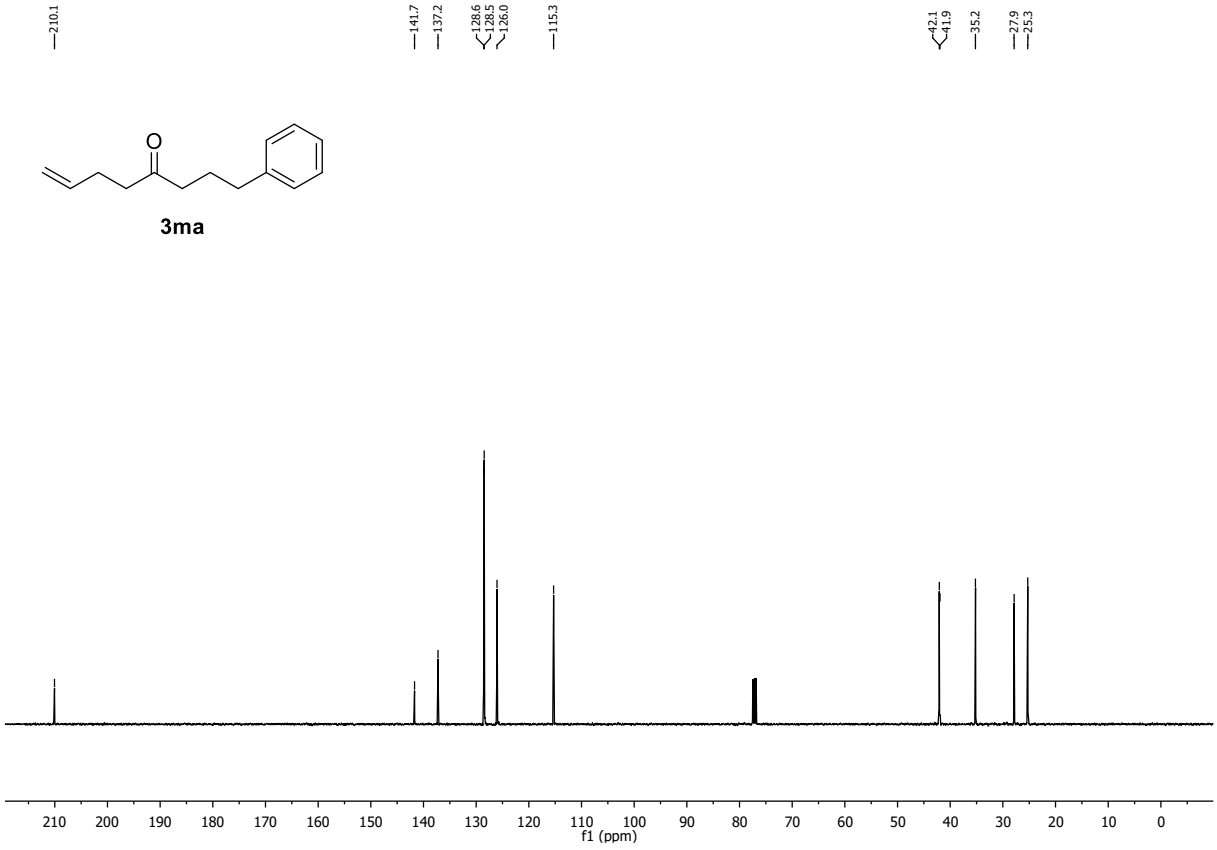

Figure S81. ^{13}C NMR spectrum (101 MHz, $CDCl_3$) of **3ma**.

1-Cyclohexyl-4-phenylbutan-1-one (3na):

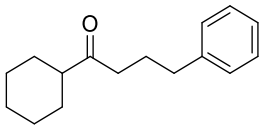

3na

$C_{16}H_{22}O$ (230.35 g/mol)

Following **GP-B**, **3na** was synthesized using *S*-phenyl cyclohexanecarbothioate (**1n**) (220.0 mg, 1.0 mmol, 1.0 equiv.), (3-bromopropyl)benzene (398 mg, 2.0 mmol, 2.0 equiv.), $NiCl_2 \cdot (H_2O)_6$ (23.8 mg, 0.1 mmol, 10 mol%), 4,4'-di-*tert*-butyl-2,2'-bipyridine (53.7 mg, 0.2 mmol, 20 mol%), zinc powder (131 mg, 2.0 mmol, 2.0 equiv.), sodium chloride (117 mg, 2.0 mmol, 2.0 equiv.) and pyridine (158 mg, 2.0 mmol, 2 equiv.). Purification by flash column chromatography (*n*-hexane/EtOAc gradient 100:0 to 90:10 over 10 CV) afforded **3na** (153 mg, 662 µmol, 66%) as colorless oil. Conforms to reported analytical data.[17]

R_f: 0.64 (*n*-hexane/EtOAc 90:10).

^{1}H NMR (400 MHz, $CDCl_3$, δ): 7.33 – 7.26 (m, 2H), 7.24 – 7.11 (m, 3H), 2.61 (t, *J* = 7.6 Hz, 2H), 2.44 (t, *J* = 7.3 Hz, 2H), 2.31 (m, 1H), 1.90 (tt, *J* = 7.6, 7.3 Hz, 2H), 1.84 – 1.71 (m, 4H), 1.71 – 1.63 (m, 1H), 1.39 – 1.11 (m, 5H).

^{13}C{^{1}H} NMR (101 MHz, $CDCl_3$, δ): 214.1, 141.9, 128.6, 128.5, 126.0, 51.0, 39.9, 35.3, 28.6, 26.0, 25.8, 25.2.

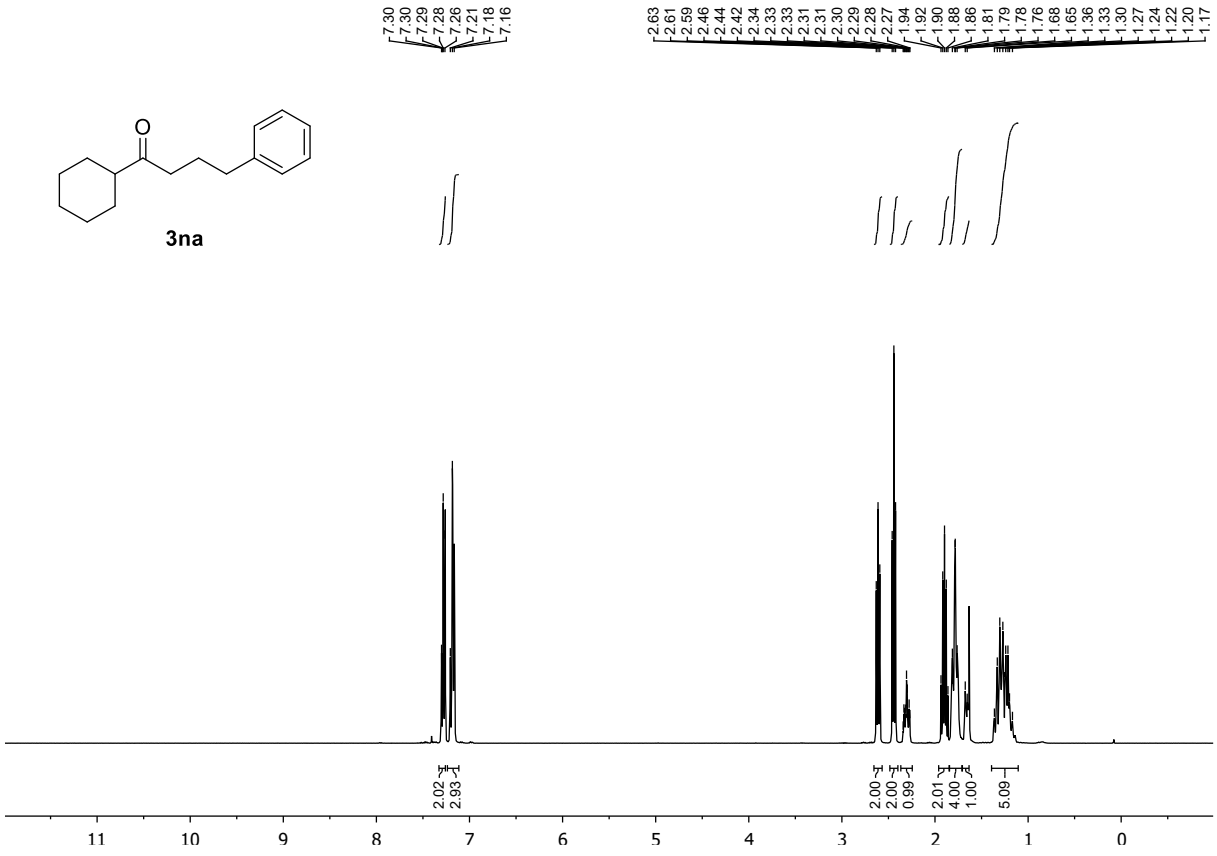

Figure S82. ^{1}H NMR spectrum (400 MHz, $CDCl_3$) of **3na**.

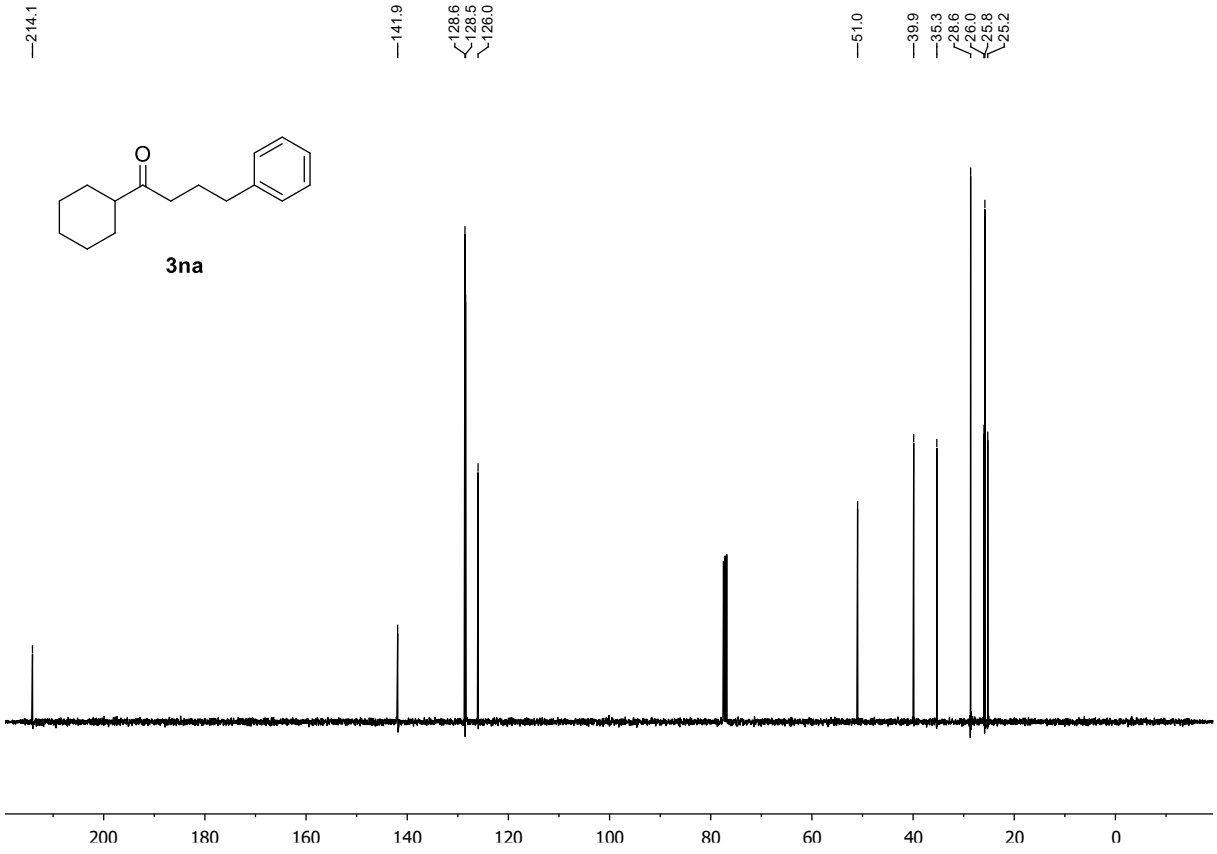

Figure S83. ^{13}C NMR spectrum (101 MHz, $CDCl_3$) of **3na**.

4-Phenyl-1-(tetrahydro-2*H*-pyran-4-yl)butan-1-one (3oa):

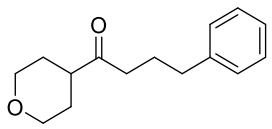

3oa

$C_{15}H_{20}O_2$ (232.32 g/mol)

Following **GP-B**, **3oa** was synthesized using *S*-phenyl tetrahydro-2H-pyran-4-carbothioate (**1o**) (222 mg, 1.0 mmol, 1.0 equiv.), (3-bromopropyl)benzene (398 mg, 2.0 mmol, 2.0 equiv.), $NiCl_2 \cdot (H_2O)_6$ (23.8 mg, 0.1 mmol, 10 mol%), 4,4'-di-*tert*-butyl-2,2'-bipyridine (53.7 mg, 0.2 mmol, 20 mol%), zinc powder (131 mg, 2.0 mmol, 2.0 equiv.), sodium chloride (117 mg, 2.0 mmol, 2.0 equiv.) and pyridine (158 mg, 2.0 mmol, 2 equiv.). Purification by flash column chromatography (*n*-hexane/EtOAc gradient 100:0 to 80:20 over 10 CV) afforded **3oa** (128 mg, 551 µmol, 55%) as colorless oil. Conforms to reported analytical data.[17]

R$_f$: 0.12 (*n*-hexane/EtOAc 90:10).

^{1}H NMR (400 MHz, $CDCl_3$, δ): 7.31 – 7.25 (m, 2H), 7.21 – 7.14 (m, 3H), 3.98 (m, 2H), 3.45 – 3.35 (m, 2H), 2.62 (t, *J* = 7.5 Hz, 2H), 2.54 – 2.47 (m, 1H), 2.45 (t, *J* = 7.2 Hz, 2H), 1.98 – 1.87 (m, 2H), 1.74 – 1.63 (m, 4H).

^{13}C{^{1}H} NMR (101 MHz, $CDCl_3$, δ): 211.8, 141.6, 128.5, 128.5, 126.1, 67.3, 47.6, 39.4, 35.1, 28.2, 25.0.

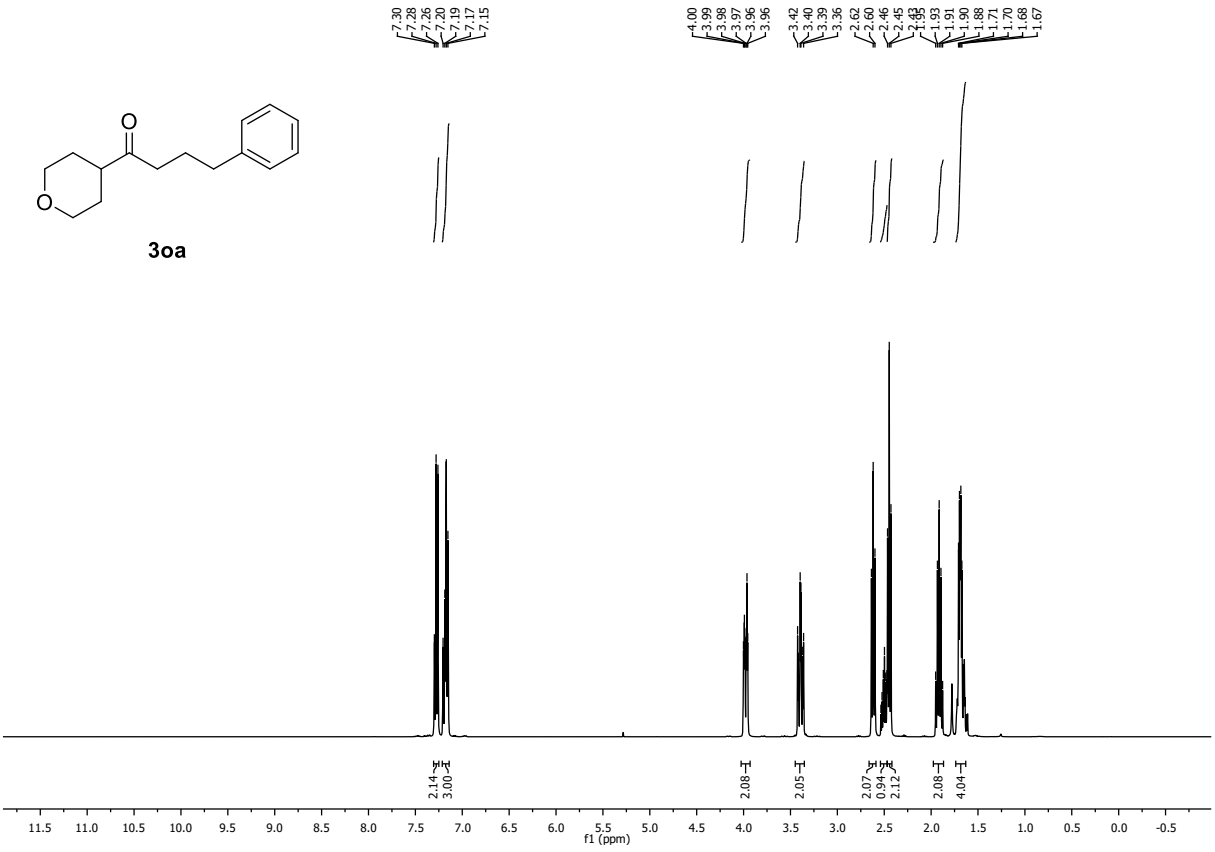

Figure S84. ^{1}H NMR spectrum (400 MHz, $CDCl_3$) of **3oa**.

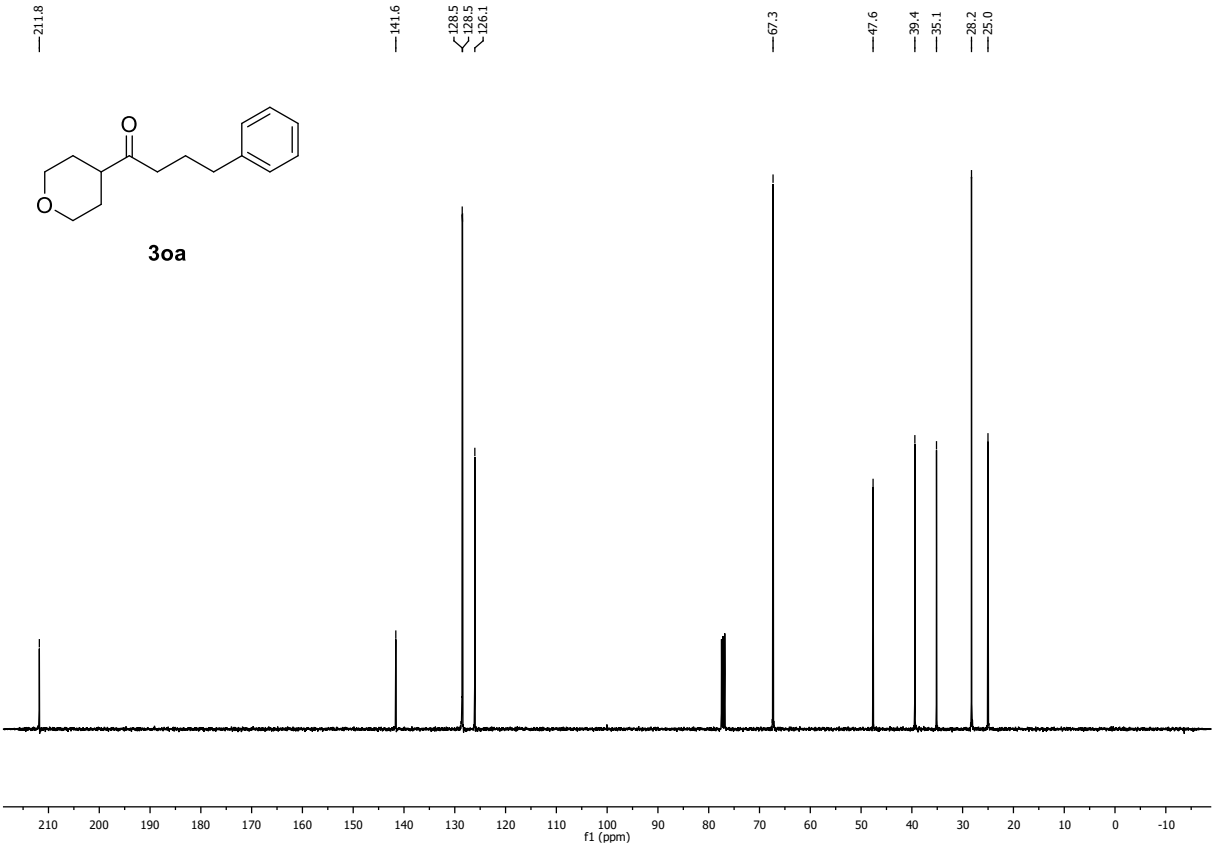

Figure S85. ^{13}C NMR spectrum (101 MHz, $CDCl_3$) of **3oa**.

1-(1-Acetylpiperidin-4-yl)-4-phenylbutan-1-one (3pa):

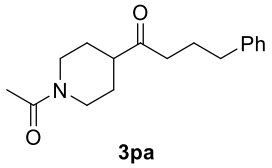

3pa

$C_{17}H_{23}NO_2$ (273.38 g/mol)

Following **GP-B**, **3pa** was synthesized using *S*-phenyl 1-acetylpiperidine-4-carbothioate (**1p**) (263 mg, 1.0 mmol, 1.0 equiv.), (3-bromopropyl)benzene (398 mg, 2.0 mmol, 2.0 equiv.), $NiCl_2 \cdot (H_2O)_6$ (23.8 mg, 0.1 mmol, 10 mol%), 4,4'-di-*tert*-butyl-2,2'-bipyridine (53.7 mg, 0.2 mmol, 20 mol%), zinc powder (131 mg, 2.0 mmol, 2.0 equiv.), sodium chloride (117 mg, 2.0 mmol, 2.0 equiv.) and pyridine (158 mg, 2.0 mmol, 2 equiv.). Purification by flash column chromatography (Al_2O_3, DCM/MeOH gradient 100:0 to 0:100 over 10 CV) afforded **3pa** (145 mg, 531 µmol, 53%) as pale red oil.

^{1}H NMR (400 MHz, $CDCl_3$, δ): 7.43 – 7.35 (m, 3H), 7.33 – 7.28 (m, 2H), 4.69 – 4.58 (m, 1H), 3.97 – 3.89 (m, 1H), 3.24 – 3.12 (m, 1H), 2.83 – 2.70 (m, 3H), 2.66 – 2.54 (m, 3H), 2.19 (s, 3H), 2.07 – 1.99 (m, 2H), 1.97 – 1.89 (m, 2H), 1.73 – 1.54 (m, 2H).

^{13}C{^{1}H} NMR (101 MHz, $CDCl_3$, δ): 211.6, 169.0, 141.5, 128.5, 128.5, 126.1, 48.4, 45.9, 41.1, 39.8, 35.1, 27.8, 27.6, 25.0, 21.5.

HR-MS (ESI): m/z calc for $[M+Na]^+$ 296.16210, found 296.16245 (err. -1.17 ppm).

IR (ATR, $\tilde{\nu}$ [cm^{-1}]): 3058 (w), 3021 (w), 2930 (w), 2857 (w), 1702 (m), 1633 (s), 1549 (w), 1439 (s), 1367 (m), 1306 (w), 1273 (m), 1228 (m), 1202 (w), 1124 (w), 1094 (w), 1068 (w), 1023 (w), 978 (m), 915 (m), 848 (w), 796 (w), 728 (vs), 699 (s).

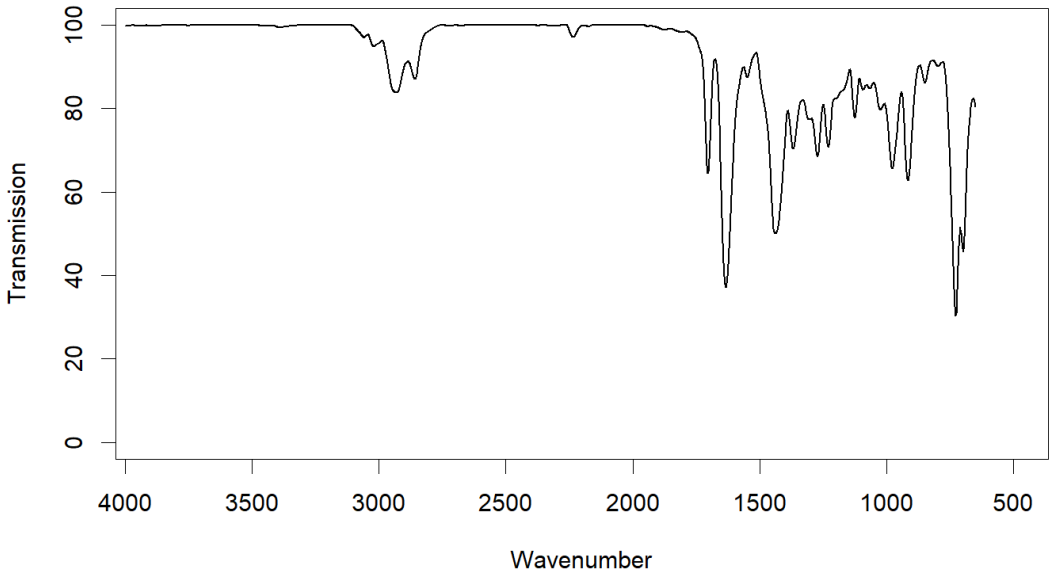

Figure S86. IR spectrum (ATR, neat) of **3pa**.

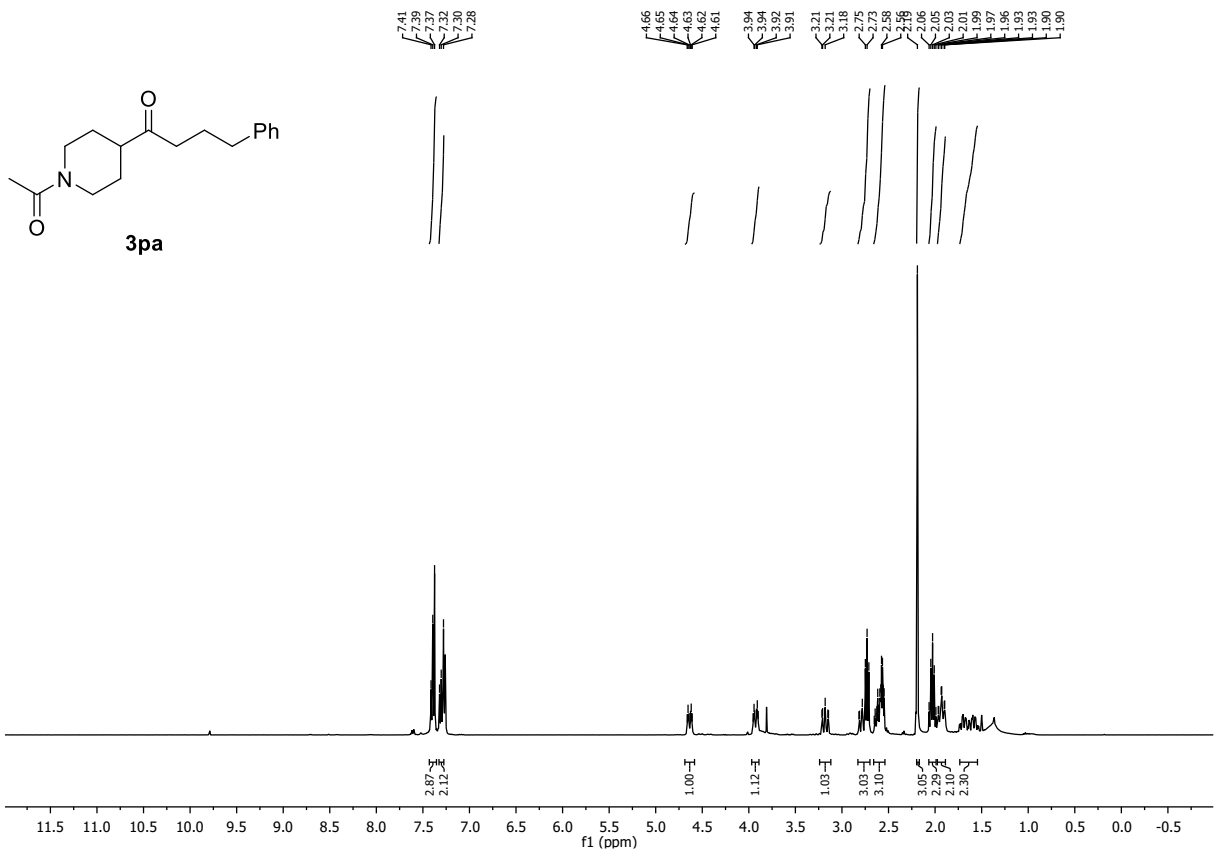

Figure S87. ^{1}H NMR spectrum (400 MHz, $CDCl_3$) of **3pa**.

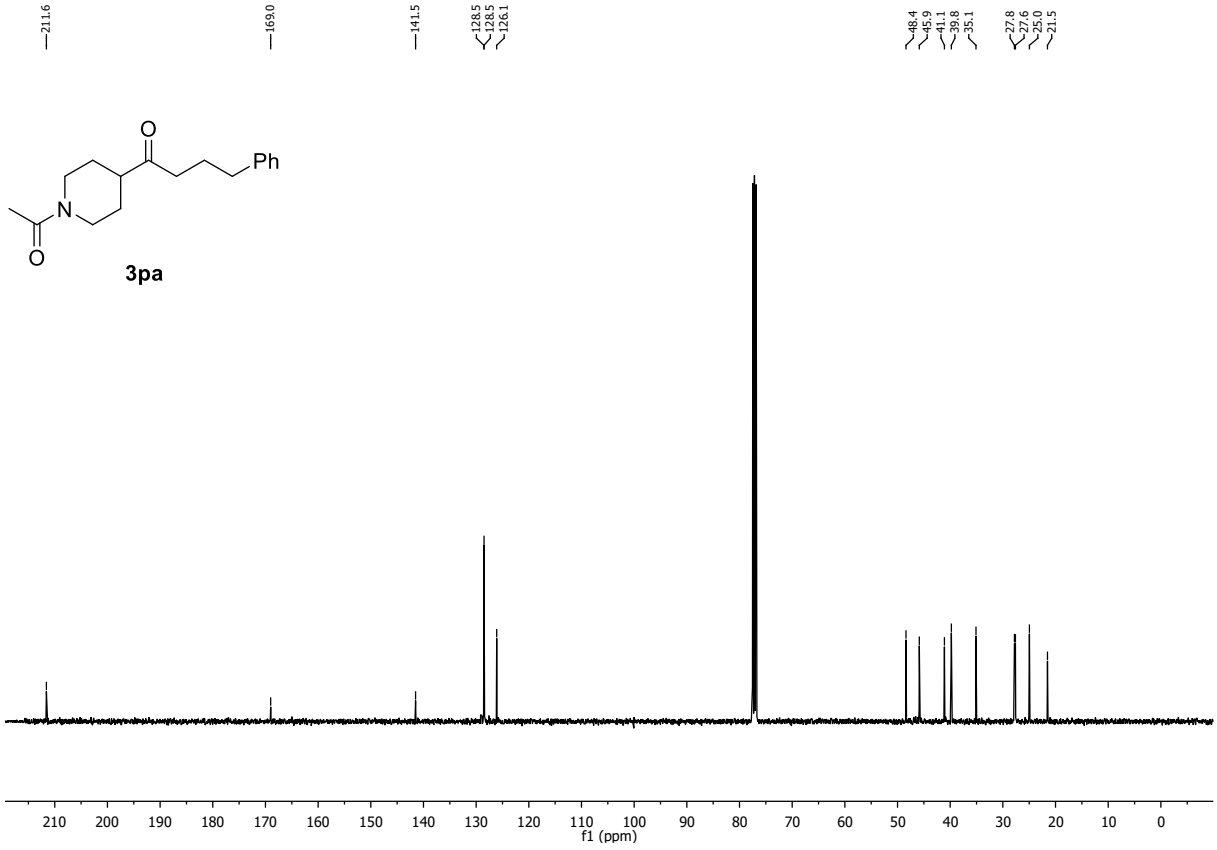

Figure S88. ^{13}C NMR spectrum (101 MHz, $CDCl_3$) of **3pa**.

1-Cyclopropyl-4-phenylbutan-1-one (3qa):

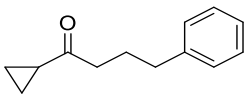

3qa

$C_{13}H_{16}O$ (188.27 g/mol)

Following **GP-B**, **3qa** was synthesized using *S*-phenyl cyclopropanecarbothioate (**1q**) (178.0 mg, 1.0 mmol, 1.0 equiv.), (3-bromopropyl)benzene (398 mg, 2.0 mmol, 2.0 equiv.), $NiCl_2 \cdot (H_2O)_6$ (23.8 mg, 0.1 mmol, 10 mol%), 4,4'-di-*tert*-butyl-2,2'-bipyridine (53.7 mg, 0.2 mmol, 20 mol%), zinc powder (131 mg, 2.0 mmol, 2.0 equiv.), sodium chloride (117 mg, 2.0 mmol, 2.0 equiv.) and pyridine (158 mg, 2.0 mmol, 2 equiv.). Purification by flash column chromatography (*n*-hexane/EtOAc gradient 100:0 to 90:10 over 10 CV) afforded **3qa** (150.5 mg, 0.799 mmol, 80%) as colorless oil. Conforms to reported analytical data.[17]

Rf: 0.49 (*n*-hexane/EtOAc 90:10).

^{1}H NMR (400 MHz, $CDCl_3$, δ): 7.34 – 7.26 (m, 2H), 7.23 – 7.16 (m, 3H), 2.64 (t, *J* = 7.6 Hz, 2H), 2.57 (t, *J* = 7.4 Hz, 2H), 1.95 (tt, *J* = 7.6, 7.4 Hz, 2H), 1.92 – 1.86 (m, 1H), 1.04 – 0.97 (m, 2H), 0.88 – 0.81 (m, 2H).

^{13}C{^{1}H} NMR (101 MHz, $CDCl_3$, δ): 210.9, 141.8, 128.6, 128.5, 126.0, 42.8, 35.3, 25.6, 20.5, 10.7.

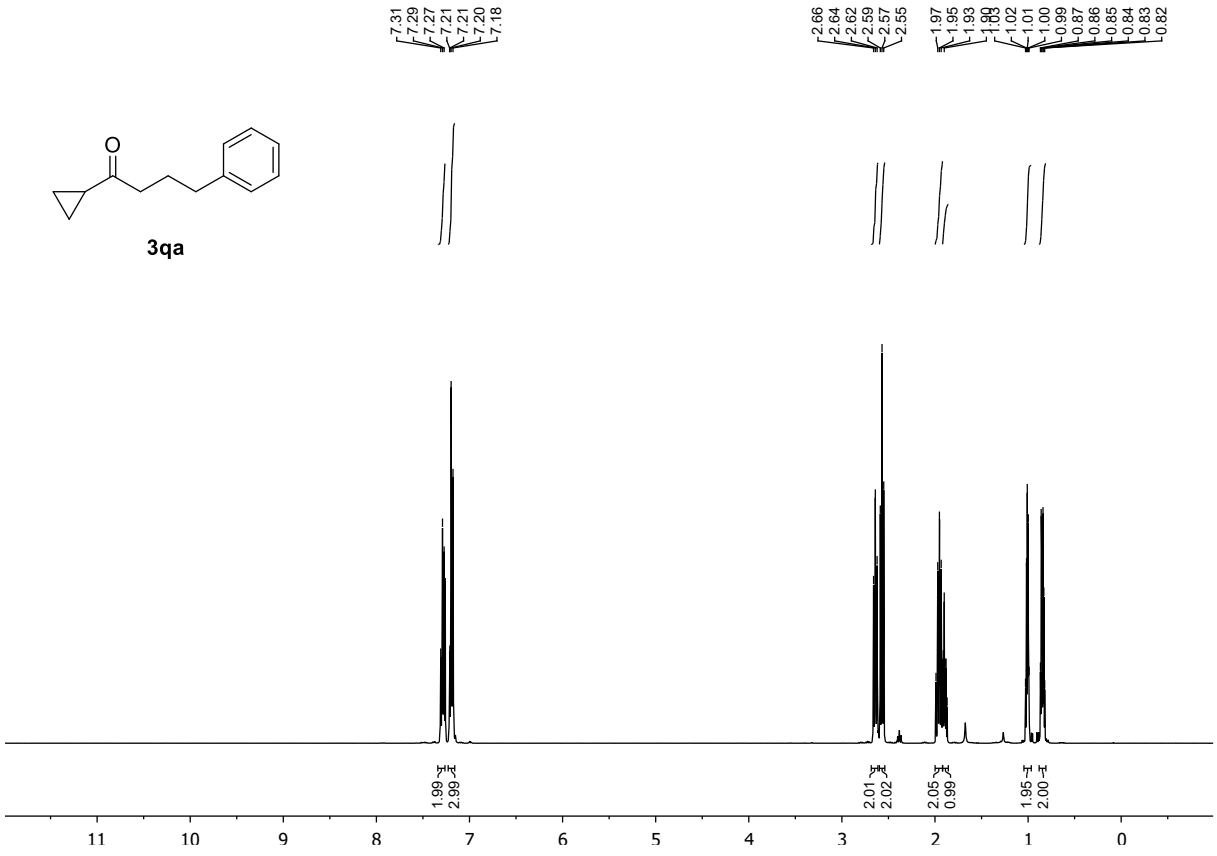

Figure S89. ^{1}H NMR spectrum (400 MHz, $CDCl_3$) of **3qa**.

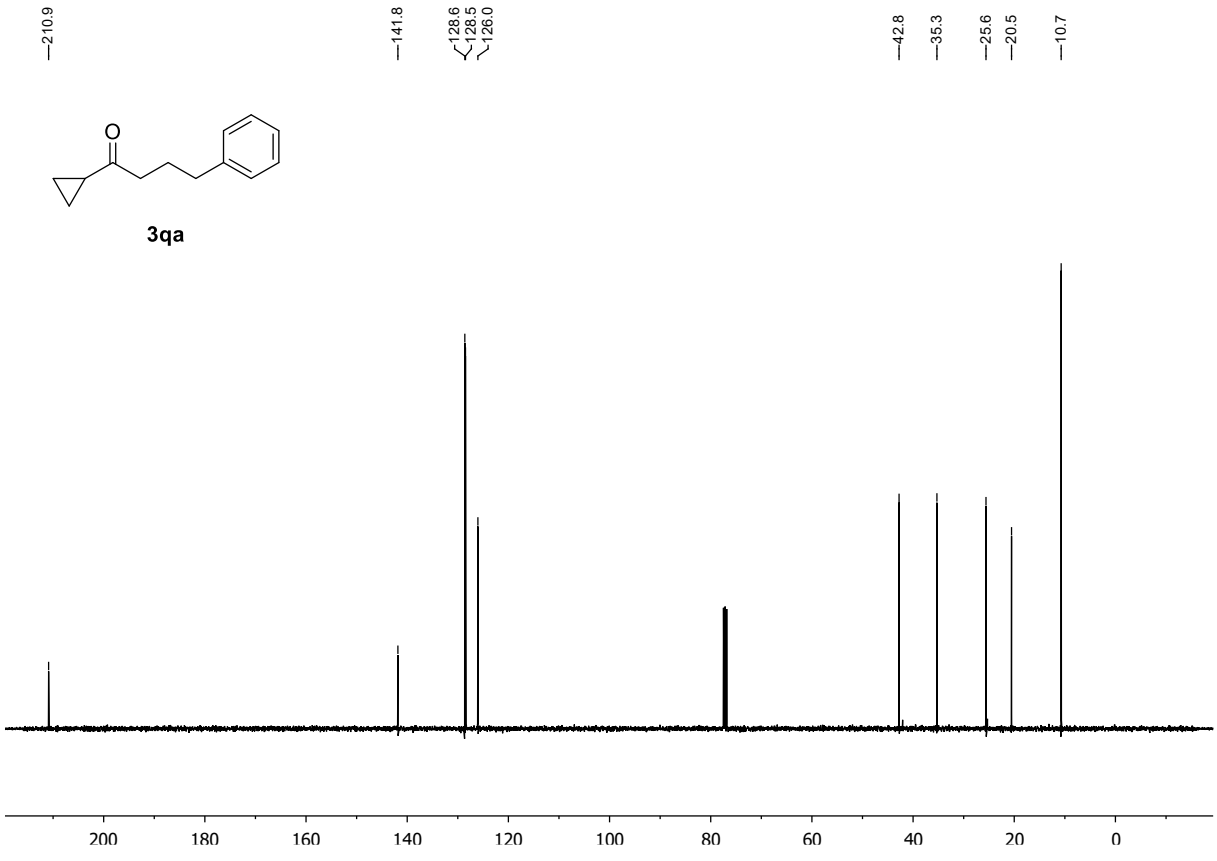

Figure S90. ^{13}C NMR spectrum (101 MHz, $CDCl_3$) of **3qa**.

1-(Adamantan-1-yl)-4-phenylbutan-1-one (3ra):

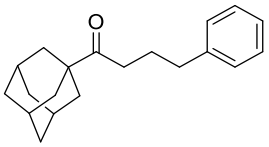

3ra

$C_{20}H_{26}O$ (282.43 g/mol)

Following **GP-B**, **3ra** was synthesized using *S*-phenyl adamantane-1-carbothioate (**1r**) (272.0 mg, 1.0 mmol, 1.0 equiv.), (3-bromopropyl)benzene (398 mg, 2.0 mmol, 2.0 equiv.), $NiCl_2 \cdot (H_2O)_6$ (23.8 mg, 0.1 mmol, 10 mol%), 4,4'-di-*tert*-butyl-2,2'-bipyridine (53.7 mg, 0.2 mmol, 20 mol%), zinc powder (131 mg, 2.0 mmol, 2.0 equiv.), sodium chloride (117 mg, 2.0 mmol, 2.0 equiv.) and pyridine (158 mg, 2.0 mmol, 2 equiv.). Purification by flash column chromatography (*n*-hexane/EtOAc gradient 100:0 to 90:10 over 10 CV) afforded **3ra** (58 mg, 205 µmol, 21%) as colorless oil. Conforms to reported analytical data.[17]

R$_f$: 0.67 (*n*-hexane/EtOAc 90:10).

^{1}H NMR (400 MHz, $CDCl_3$, δ): 7.33 – 7.26 (m, 2H), 7.24 – 7.11 (m, 3H), 2.60 (t, *J* = 7.5 Hz, 2H), 2.46 (t, *J* = 7.3 Hz, 2H), 2.06 – 1.99 (m, 3H), 1.88 (tt, *J* = 7.5, 7.3 Hz, 2H), 1.80 – 1.64 (m, 12H).

^{13}C{^{1}H} NMR (101 MHz, $CDCl_3$, δ): 215.5, 142.1, 128.6, 128.4, 125.9, 46.4, 38.4, 36.7, 35.4, 35.3, 28.1, 25.3.

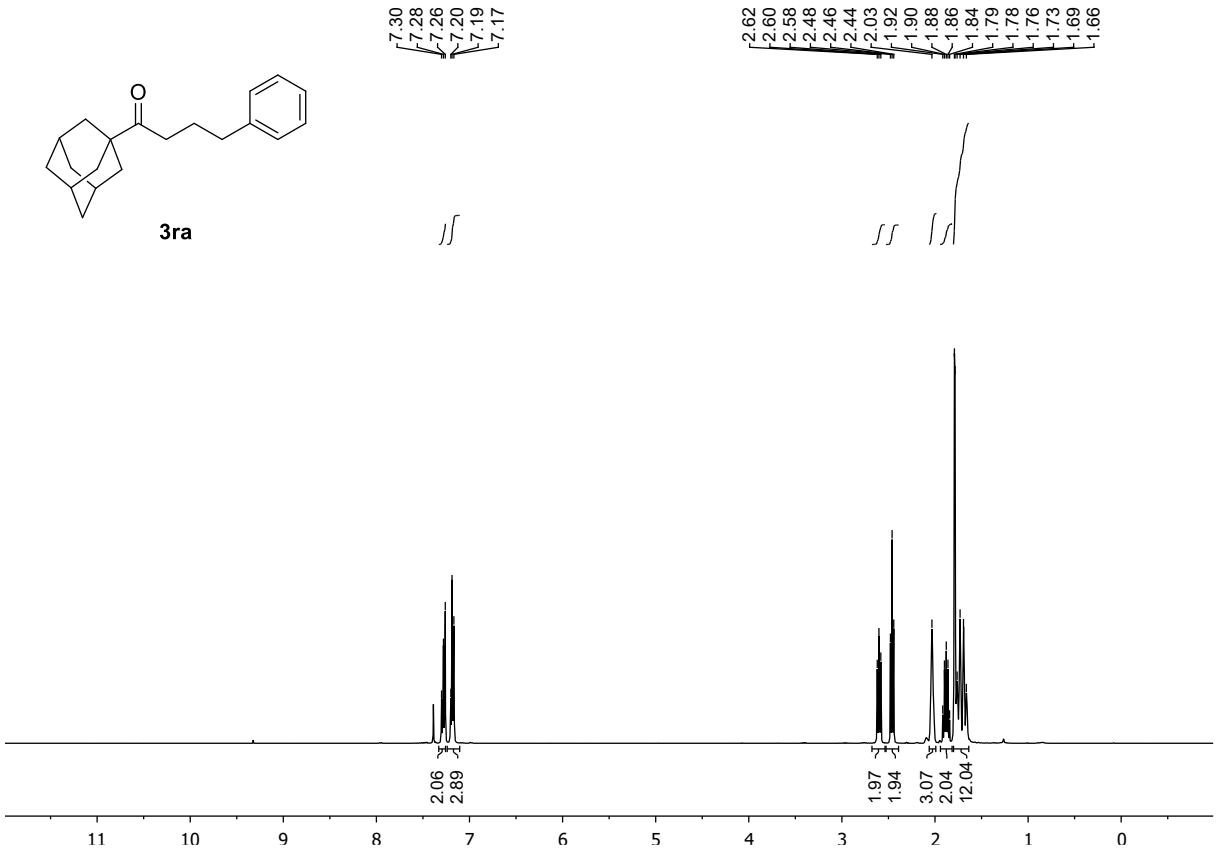

Figure S91. ^{1}H NMR spectrum (400 MHz, $CDCl_3$) of **3ra**.

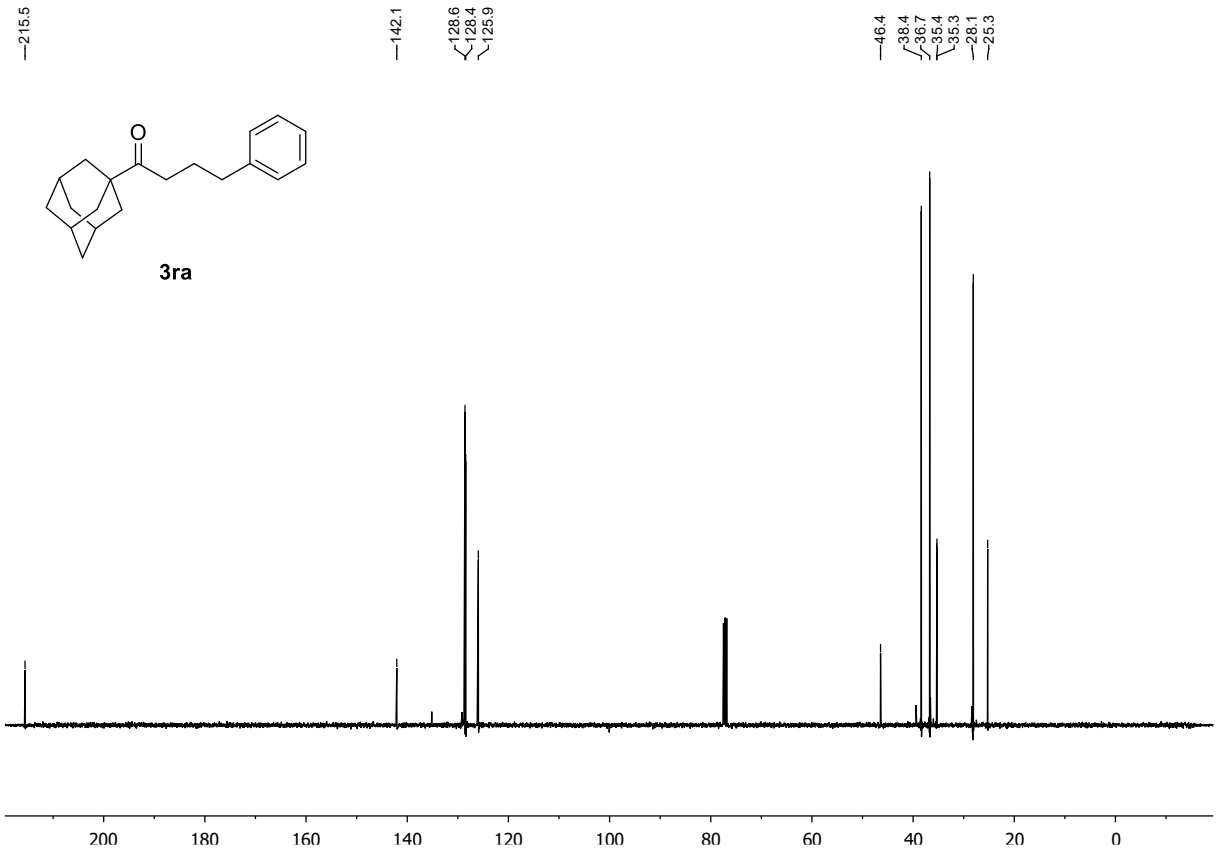

Figure S92. ^{13}C NMR spectrum (101 MHz, $CDCl_3$) of **3ra**.

2-(4-Isobutylphenyl)-6-phenylhexan-3-one (3sa):

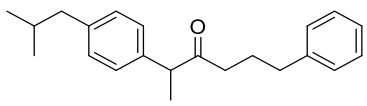

3sa

$C_{22}H_{28}O$ (308.47 g/mol)

Following **GP-B**, **3sa** was synthesized using *S*-phenyl 2-(4-isobutylphenyl)propanethioate (**1s**) (298 mg, 1.0 mmol, 1.0 equiv.), (3-bromopropyl)benzene (398 mg, 2.0 mmol, 2.0 equiv.), $NiCl_2{\cdot}(H_2O)_6$ (23.8 mg, 0.1 mmol, 10 mol%), 4,4'-di-*tert*-butyl-2,2'-bipyridine (53.7 mg, 0.2 mmol, 20 mol%), zinc powder (131 mg, 2.0 mmol, 2.0 equiv.), sodium chloride (117 mg, 2.0 mmol, 2.0 equiv.) and pyridine (158 mg, 2.0 mmol, 2 equiv.). Deviating from **GP-B**, the reaction time was set to 2 h. Purification by flash column chromatography (*n*-hexane/EtOAc gradient 100:0 to 90:10 over 10 CV) afforded **3sa** (167 mg, 541 µmol, 54%) as colorless oil. Conforms to reported analytical data.[23]

Rf: 0.52 (*n*-hexane/EtOAc 90:10).

^{1}H NMR (400 MHz, $CDCl_3$, δ): 7.25 – 7.20 (m, 2H), 7.18 – 7.13 (m, 1H), 7.13 – 7.08 (m, 4H), 7.07 – 7.02 (m, 2H), 3.70 (q, *J* = 6.9 Hz), 2.57 – 2.29 (m, 6H), 1.90 – 1.77 (m, 3H), 1.37 (d, *J* = 6.9 Hz, 3H), 0.91 (d, *J* = 6.6 Hz, 6H).

^{13}C{^{1}H} NMR (101 MHz, $CDCl_3$, δ): 211.0, 141.8, 140.7, 137.9, 129.7, 128.5, 128.4, 127.7, 125.9, 52.8, 45.2, 40.2, 35.1, 30.3, 25.5, 22.5, 17.5.

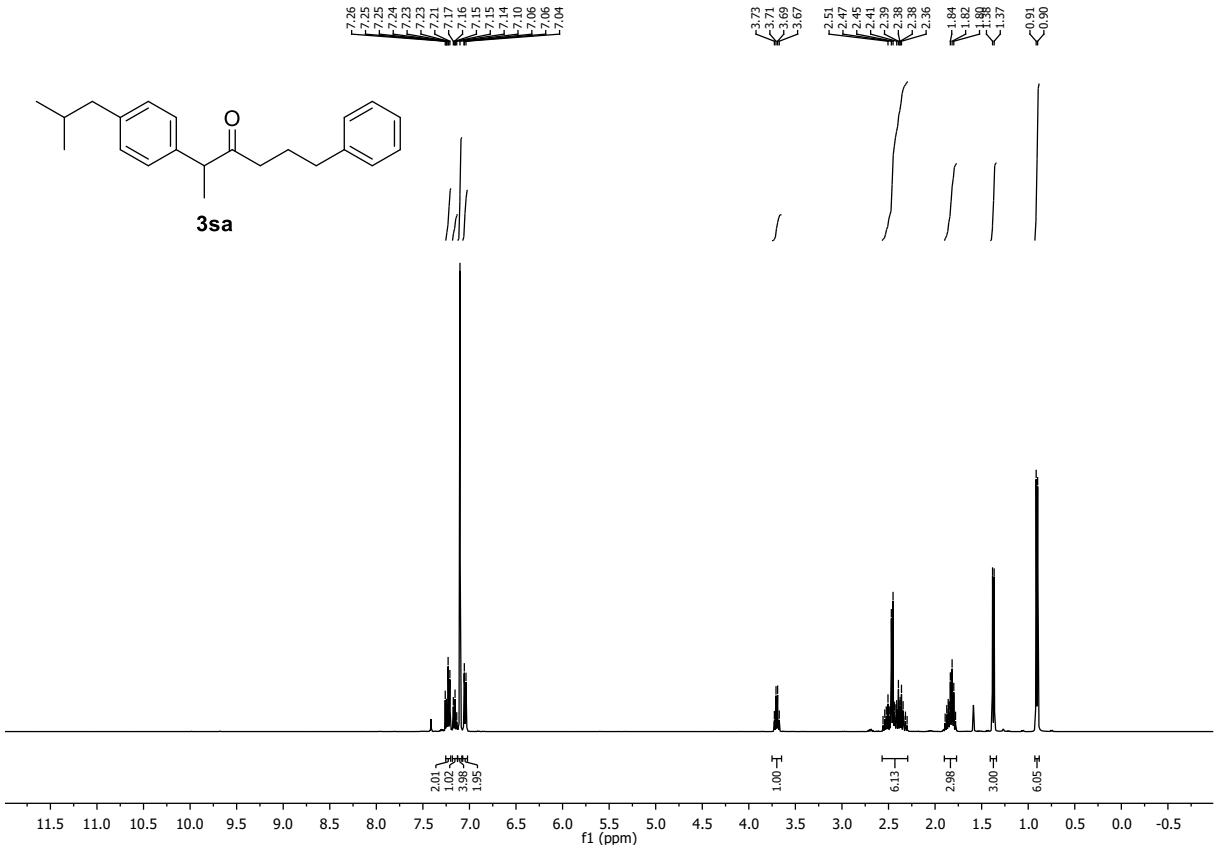

Figure S93. ^{1}H NMR spectrum (400 MHz, $CDCl_3$) of **3sa**.

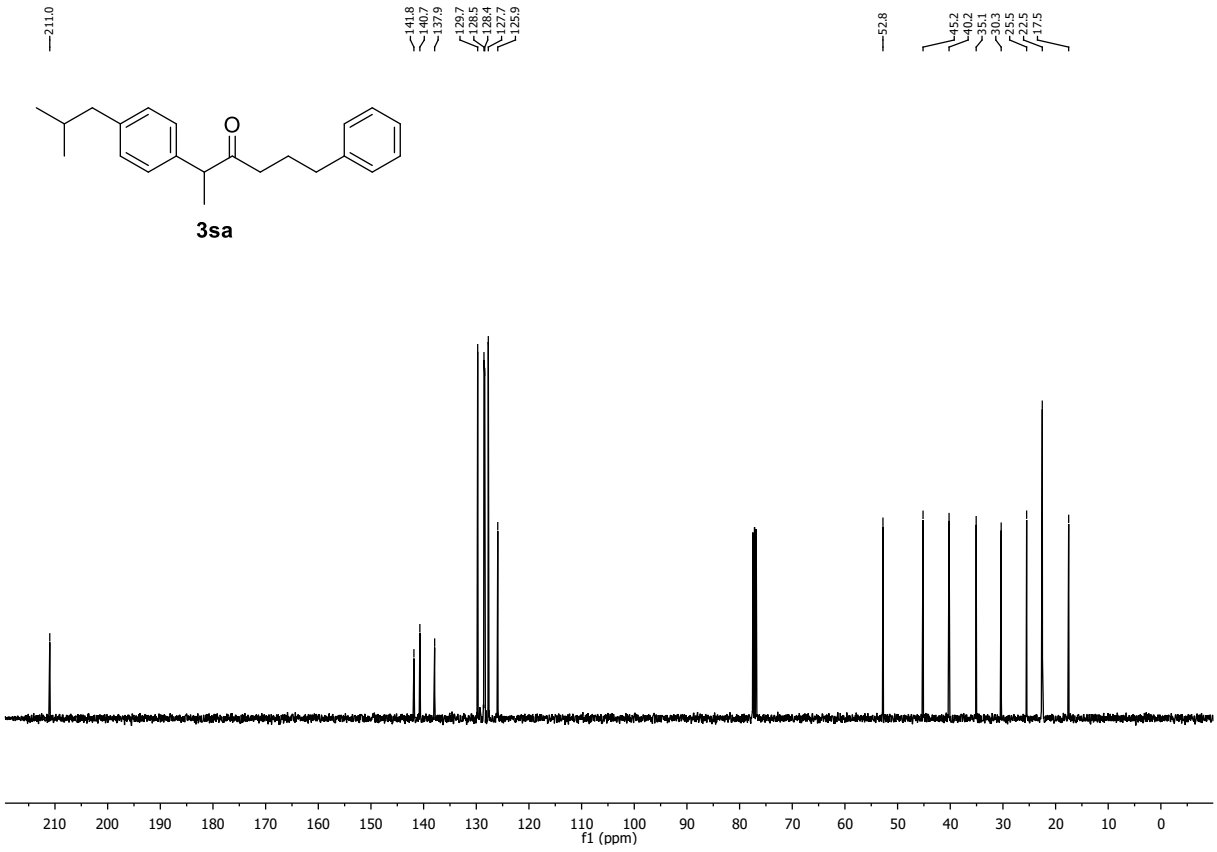

Figure S94. ^{13}C NMR spectrum (101 MHz, $CDCl_3$) of **3sa**.

1-(4,5-Diphenyloxazol-2-yl)-6-phenylhexan-3-one (3ta):

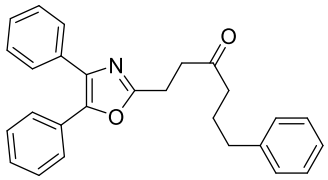

3ta

$C_{27}H_{25}NO_2$ (395.50 g/mol)

Following **GP-B**, **3ta** was synthesized using *S*-phenyl 3-(4,5-diphenyloxazol-2-yl)propanethioate (**1t**) (385 mg, 1.0 mmol, 1.0 equiv.), (3-bromopropyl)benzene (398 mg, 2.0 mmol, 2.0 equiv.), $NiCl_2 \cdot (H_2O)_6$ (23.8 mg, 0.1 mmol, 10 mol%), 4,4'-di-*tert*-butyl-2,2'-bipyridine (53.7 mg, 0.2 mmol, 20 mol%), zinc powder (131 mg, 2.0 mmol, 2.0 equiv.), sodium chloride (117 mg, 2.0 mmol, 2.0 equiv.) and pyridine (158 mg, 2.0 mmol, 2 equiv.). Purification by flash column chromatography (*n*-hexane/EtOAc gradient 100:0 to 90:10 over 10 CV) afforded (78 mg 197 µmol, 20%) as colorless oil.

R_f: 0.19 (*n*-hexane/EtOAc 90:10).

^{1}H NMR (400 MHz, $CDCl_3$, δ): 7.47 – 7.36 (m, 4H), 7.21 – 6.97 (m, 11H), 2.95 (t, *J* = 7.6 Hz, 2H), 2.82 (t, *J* = 7.3 Hz, 2H), 2.47 (t, *J* = 7.6 Hz, 2H), 2.35 (t, *J* = 7.3 Hz, 2H), 1.85 – 1.74 (m, 2H).

^{13}C{^{1}H} NMR (101 MHz, $CDCl_3$, δ): 208.6, 162.5, 145.5, 141.6, 135.1, 132.5, 129.1, 128.8, 128.7, 128.60, 128.56, 128.5, 128.2, 128.0, 126.6, 126.1, 42.1, 39.2, 35.2, 25.4, 22.3.

HR-MS (ESI): m/z calc for $[M+H]^+$ 396.19581, found 396.19602 (err. -0.54 ppm).

IR (ATR, $\tilde{\nu}$ [cm^{-1}]): 3055 (w), 3025 (w), 2924 (w), 2857 (w), 1712 (s), 1572 (m), 1496 (w), 1444 (m), 1410 (w), 1361 (m), 1320 (w), 1284 (w), 1217 (m), 1176 (w), 1147 (w), 1097 (w), 1060 (m), 1023 (m), 990 (w), 960 (m), 912 (w), 848 (w), 758 (s), 692 (vs).

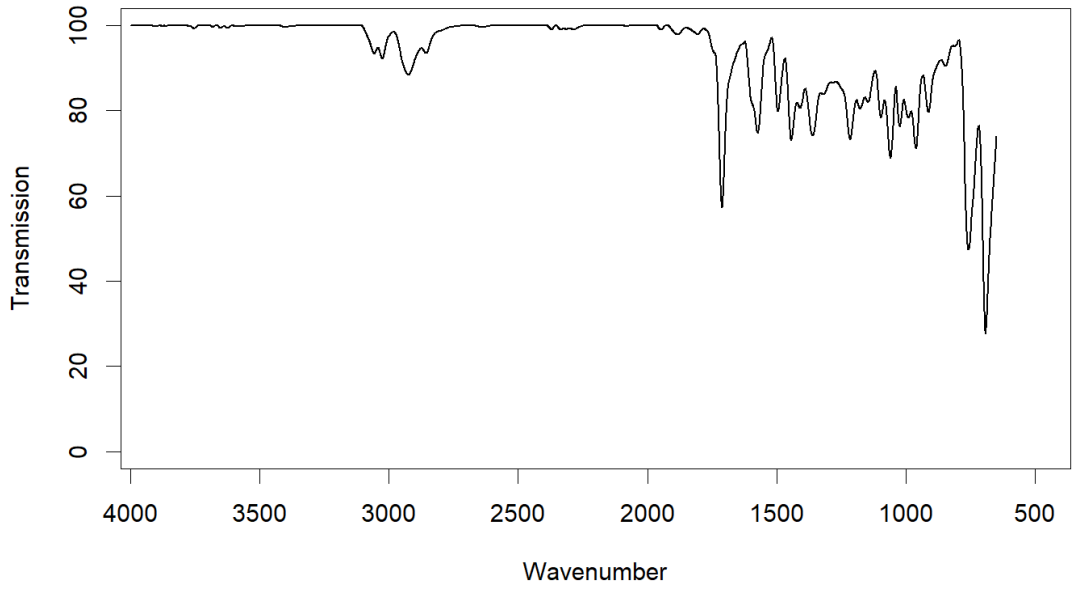

Figure S95. IR spectrum (ATR, neat) of **3ta**.

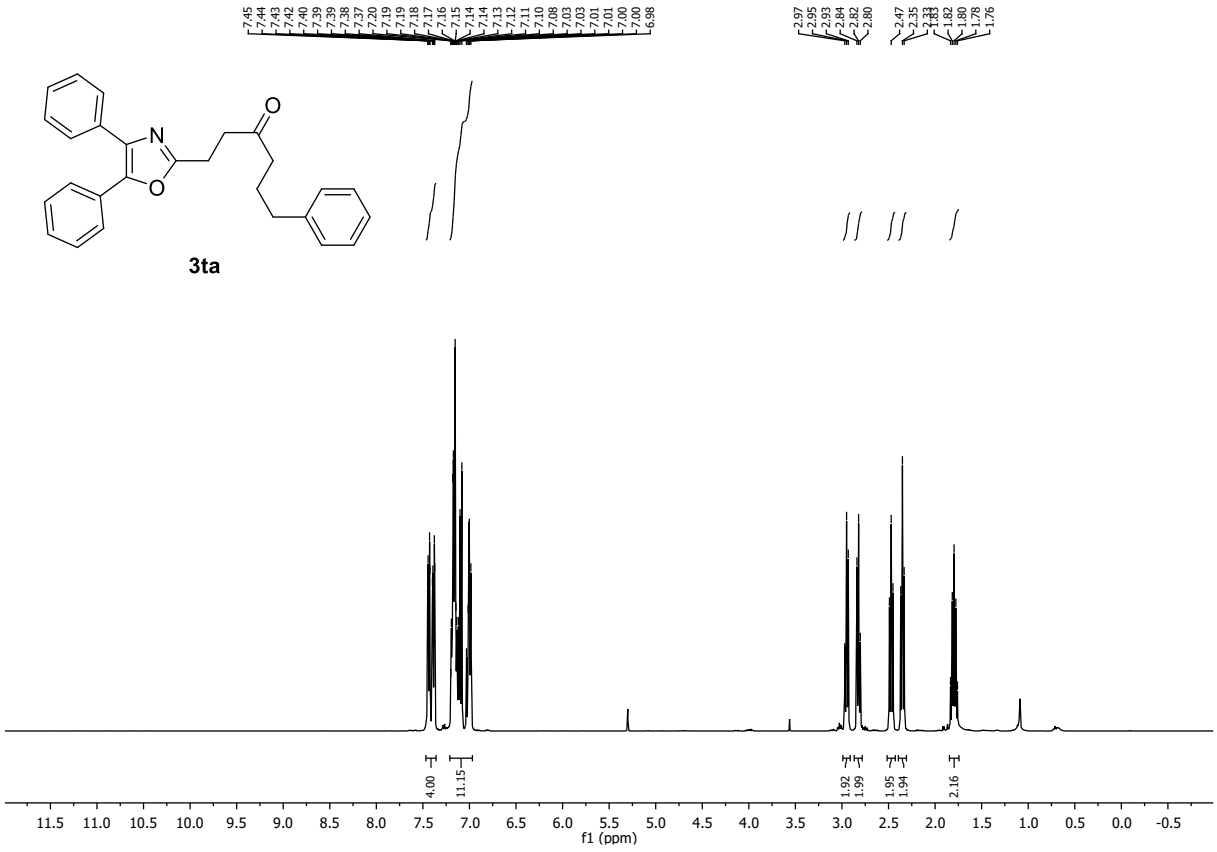

Figure S96. ^{1}H NMR spectrum (400 MHz, $CDCl_3$) of **3ta**.

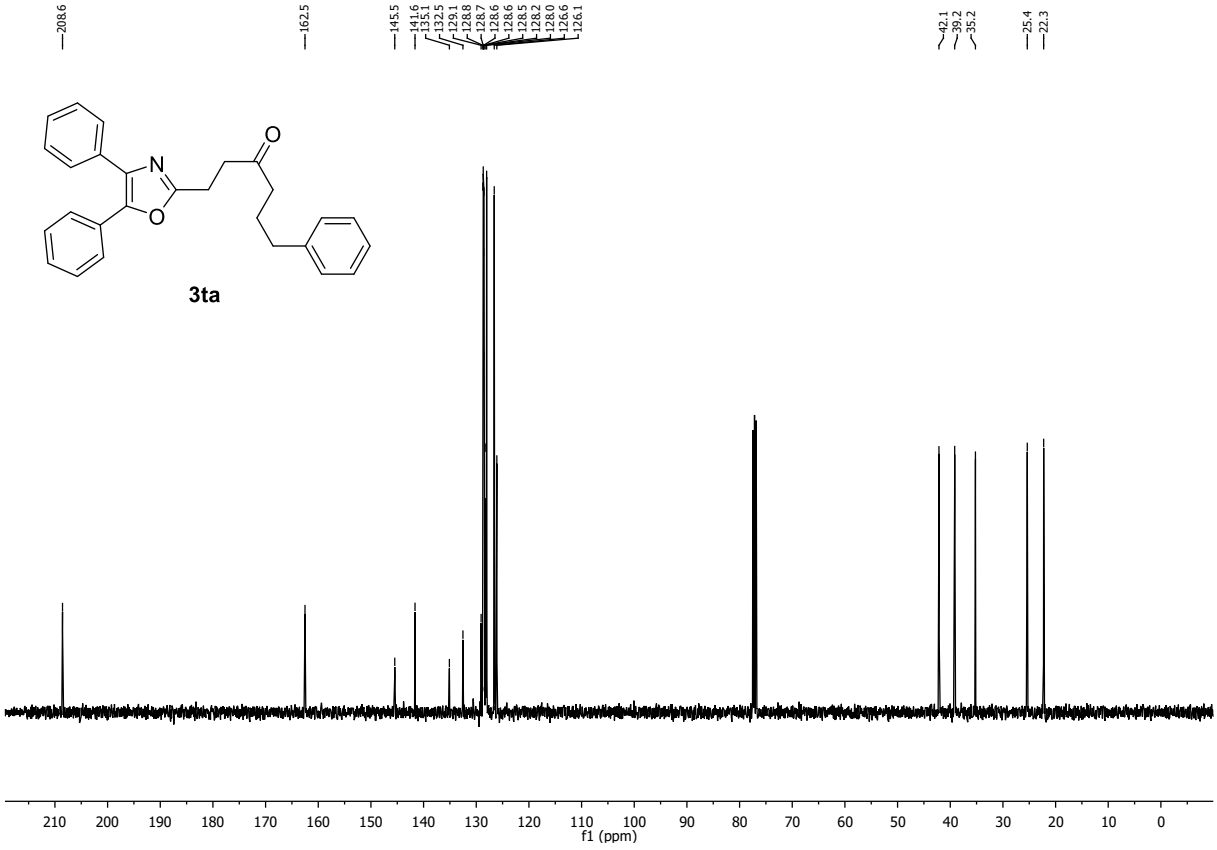

Figure S97. ^{13}C NMR spectrum (101 MHz, $CDCl_3$) of **3ta**.

4-(4-Phenylbutanoyl)-*N*,*N*-dipropylbenzenesulfonamide (3ua):

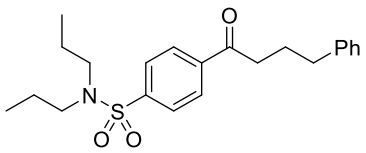

3ua

$C_{22}H_{29}NO_3S$ (387.54 g/mol)

Following **GP-B**, **3ua** was synthesized using *S*-phenyl 4-(*N*,*N*-dipropylsulfamoyl)benzothioate (**1u**) (377 mg, 1.0 mmol, 1.0 equiv.), (3-bromopropyl)benzene (398 mg, 2.0 mmol, 2.0 equiv.), $NiCl_2 \cdot (H_2O)_6$ (23.8 mg, 0.1 mmol, 10 mol%), 4,4'-di-*tert*-butyl-2,2'-bipyridine (53.7 mg, 0.2 mmol, 20 mol%), zinc powder (131 mg, 2.0 mmol, 2.0 equiv.), sodium chloride (117 mg, 2.0 mmol, 2.0 equiv.) and pyridine (158 mg, 2.0 mmol, 2 equiv.). Purification by flash column chromatography (*n*-hexane/EtOAc gradient 100:0 to 50:50 over 10 CV) afforded (190 mg 490 µmol, 49%) as colorless solid. Conforms to reported analytical data.[23]

R_f: 0.85 (*n*-hexane/EtOAc 50:50).

^{1}H NMR (400 MHz, $CDCl_3$, δ): 8.00 (d, *J* = 8.4 Hz, 2H), 7.87 (d, *J* = 8.4 Hz, 2H), 7.33 – 7.27 (m, 2H), 7.24 – 7.17 (m, 3H), 3.14 – 3.05 (m, 4H), 2.99 (t, *J* = 7.2 Hz, 2H), 2.73 (t, *J* = 7.5 Hz, 2H), 2.15 – 2.04 (m, 2H), 1.60 – 1.49 (m, 4H, *residual water under compound peak*), 0.87 (t, *J* = 7.4 Hz, 6H).

^{13}C{^{1}H} NMR (101 MHz, $CDCl_3$, δ): 199.1, 144.2, 141.5, 139.7, 128.7, 128.65, 128.61, 127.4, 126.2, 50.1, 38.1, 35.2, 25.6, 22.1, 11.3.

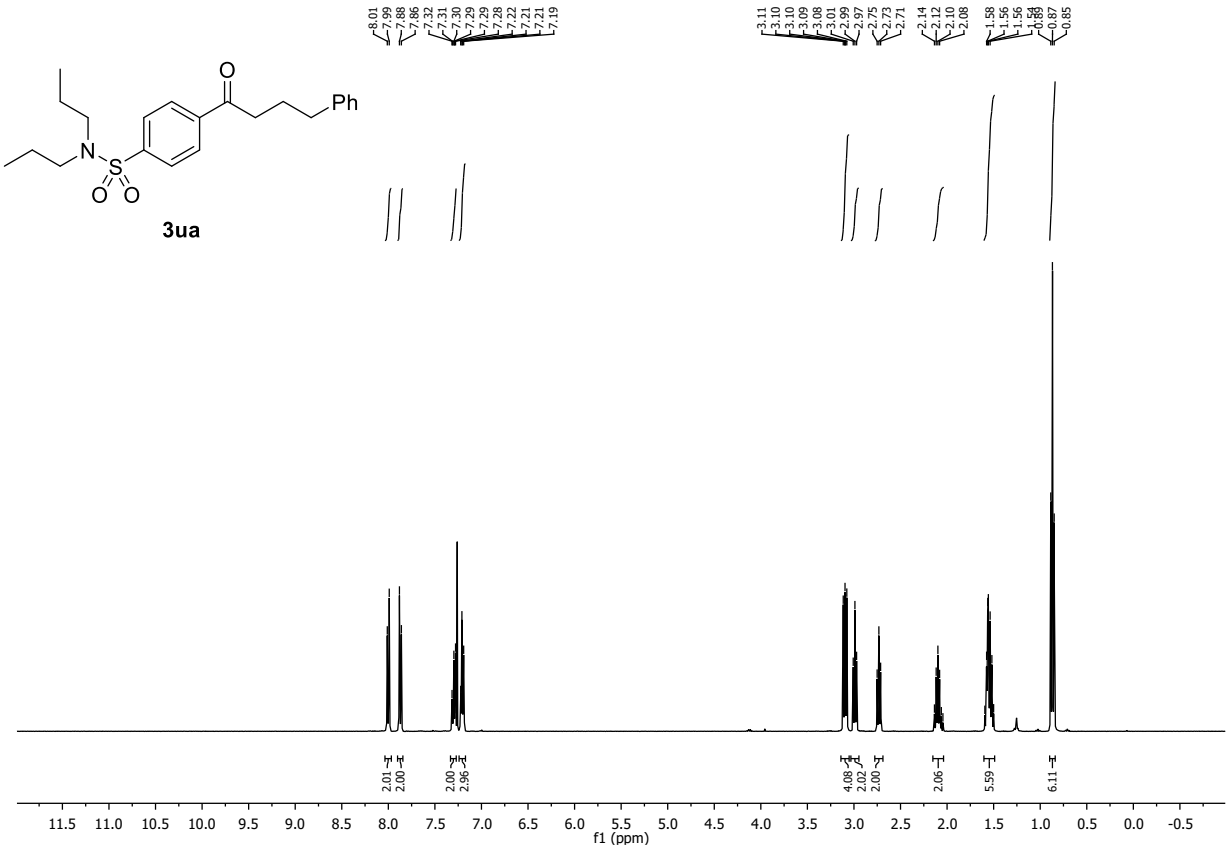

Figure S98. ^{1}H NMR spectrum (400 MHz, $CDCl_3$) of **3ua**.

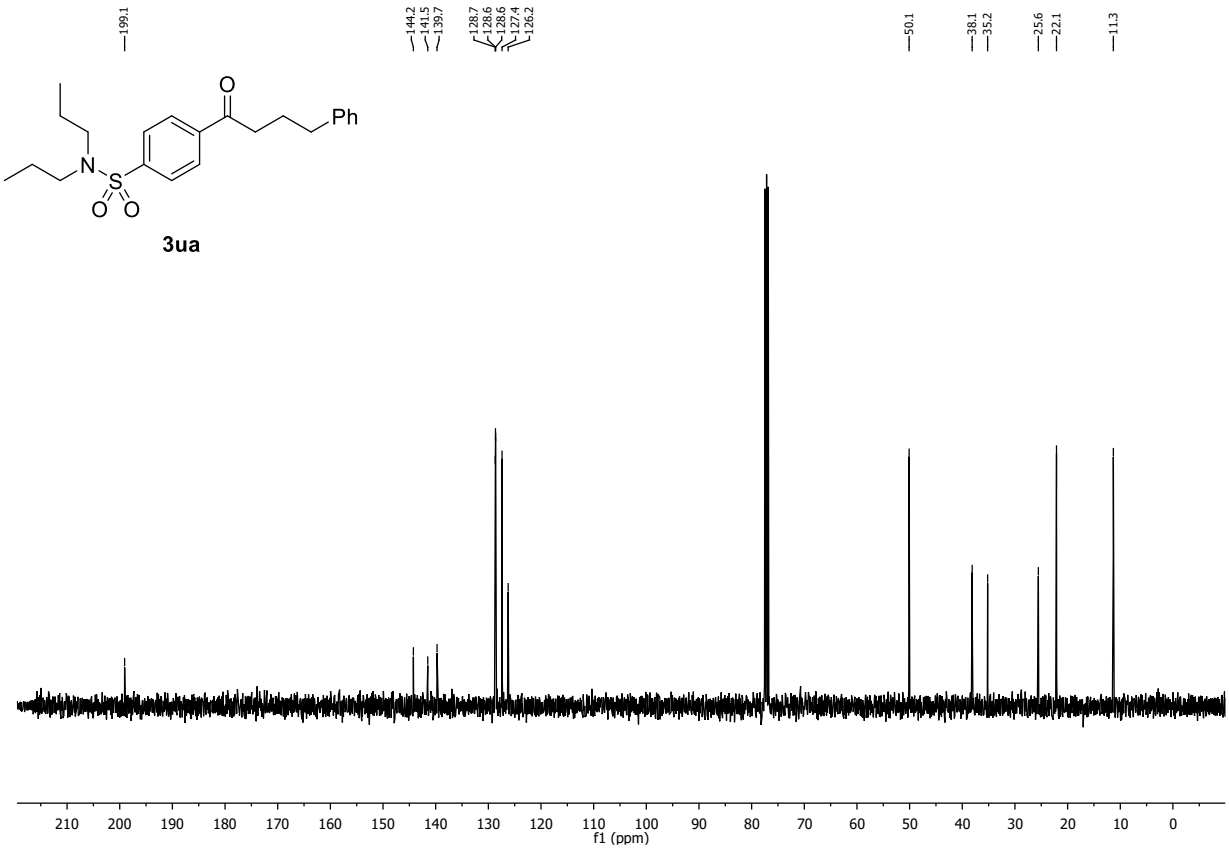

Figure S99. ^{13}C NMR spectrum (101 MHz, $CDCl_3$) of **3ua**.

1-(3-(Cyclopropylmethoxy)-4-(difluoromethoxy)phenyl)-4-phenylbutan-1-one (3va):

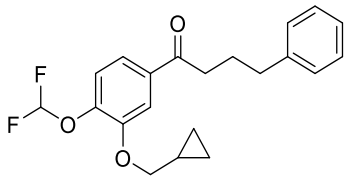

3va

$C_{21}H_{22}F_2O_3$ (360.40 g/mol)

Following **GP-B**, **3va** was synthesized using *S*-phenyl 3-(cyclopropylmethoxy)-4-(difluoromethoxy)benzothioate (**1v**) (350 mg, 1.0 mmol, 1.0 equiv.), (3-bromopropyl)benzene (398 mg, 2.0 mmol, 2.0 equiv.), $NiCl_2 \cdot (H_2O)_6$ (23.8 mg, 0.1 mmol, 10 mol%), 4,4'-di-*tert*-butyl-2,2'-bipyridine (53.7 mg, 0.2 mmol, 20 mol%), zinc powder (131 mg, 2.0 mmol, 2.0 equiv.), sodium chloride (117 mg, 2.0 mmol, 2.0 equiv.) and pyridine (158 mg, 2.0 mmol, 2 equiv.). Purification by flash column chromatography (*n*-hexane/EtOAc gradient 100:0 to 85:15 over 10 CV) afforded (285 mg, 791 µmol, 79%) as colorless oil.

Rf: 0.39 (*n*-hexane/EtOAc 90:10).

^{1}H NMR (400 MHz, $CDCl_3$, δ): 7.54 (d, *J* = 1.9 Hz, 1H), 7.46 (dd, *J* = 8.3, 1.9 Hz, 1H), 7.33 – 7.27 (m, 2H), 7.24 – 7.16 (m, 4H), 6.72 (t, *J* = 75.1 Hz, 1H), 3.92 (d, *J* = 6.9 Hz, 2H), 2.94 (t, *J* = 7.3 Hz, 2H), 2.72 (t, *J* = 7.5 Hz, 2H), 2.14 – 2.01 (m, 2H), 1.38 – 1.23 (m, 1H), 0.71 – 0.62 (m, 2H), 0.44 – 0.30 (m, 2H).

^{13}C{^{1}H} NMR (101 MHz, $CDCl_3$, δ): 198.9, 150.6, 144.2, 141.7, 135.3, 128.63, 128.56, 126.1, 121.9, 121.7, 115.9 (t, *J* = 260.7 Hz), 113.4, 74.2, 37.7, 35.3, 25.9, 10.2, 3.4.

^{19}F NMR (376 MHz, $CDCl_3$, δ): -81.9 (d, *J* = 75.1 Hz).

HR-MS (ESI): m/z calc for $[M+Na]^+$ 383.14292, found 383.14298 (err. -0.14 ppm).

IR (ATR, $\tilde{\nu}$ [cm^{-1}]): 3078 (w), 3021 (w), 2931 (w), 2869 (w), 1680 (m), 1594 (w), 1504 (m), 1452 (w), 1413 (m), 1403 (m), 1359 (w), 1314 (w), 1265 (s), 1192 (w), 1108 (vs), 1049 (s), 1023 (s), 997 (s), 915 (w), 885 (w), 811 (w), 740 (s), 699 (s).

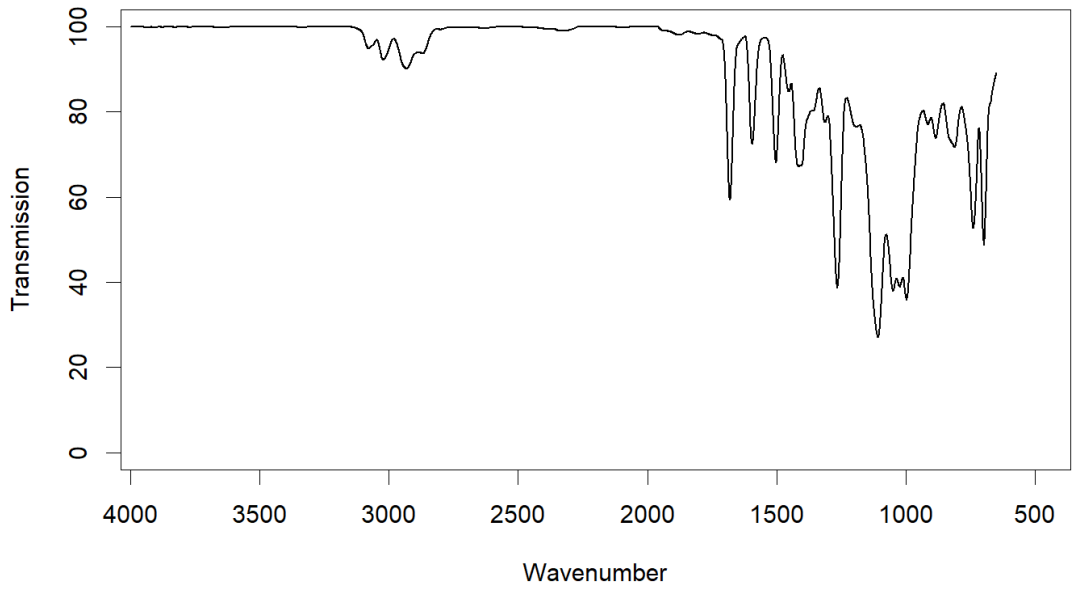

Figure S100. IR spectrum (ATR, neat) of **3va**.

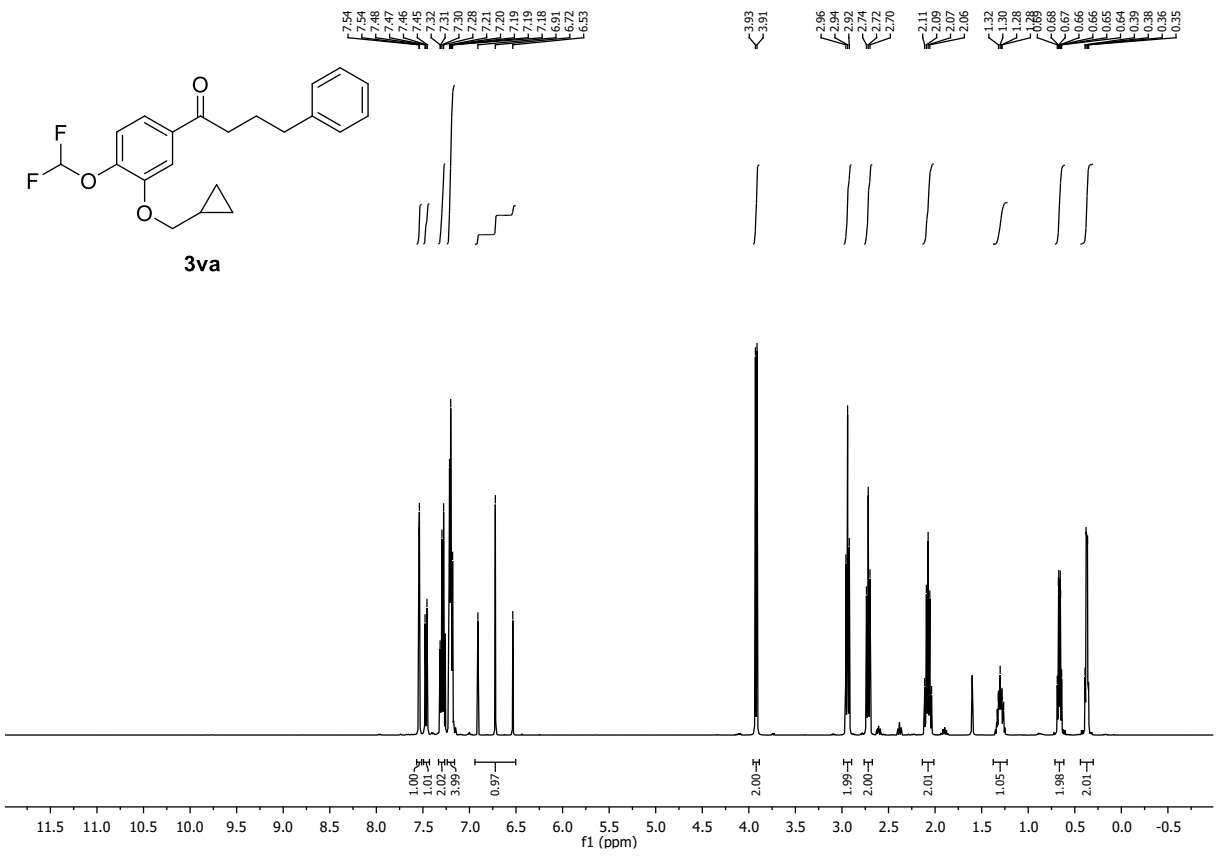

Figure S101. ^{1}H NMR spectrum (400 MHz, $CDCl_3$) of **3va**.

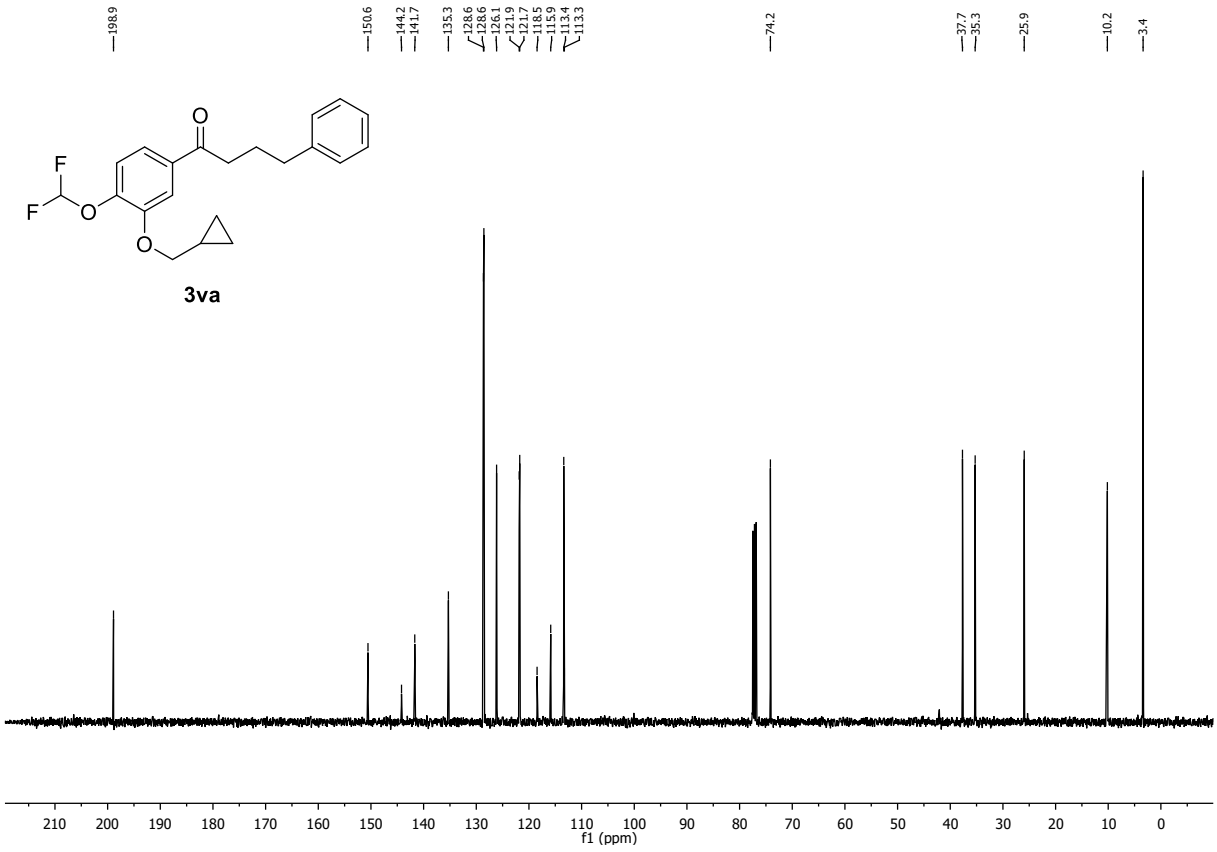

Figure S102. ^{13}C NMR spectrum (101 MHz, $CDCl_3$) of **3va**.

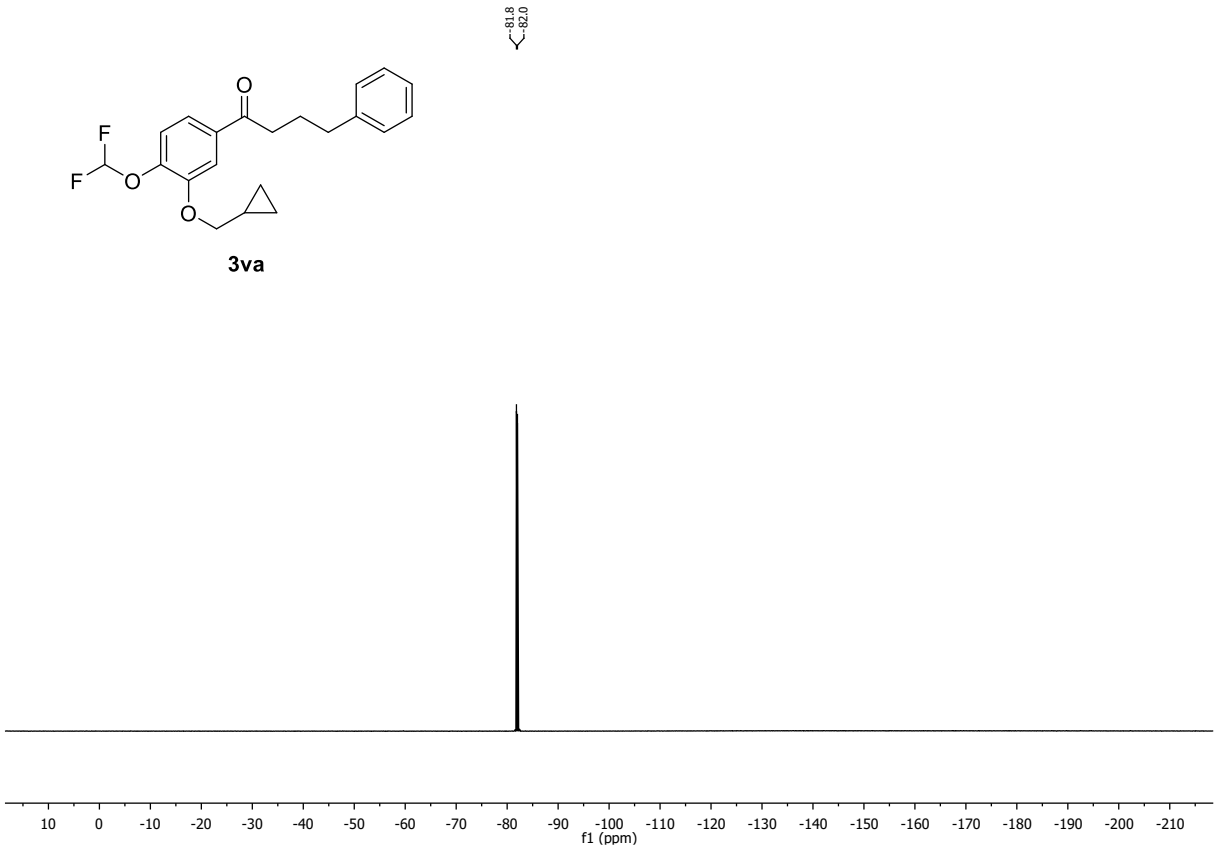

Figure S103. ^{19}F NMR spectrum (376 MHz, $CDCl_3$) of **3va**.

1-Phenylhexan-3-one (3jb):

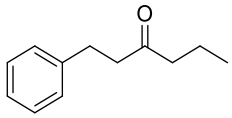

3jb

$C_{12}H_{16}O$ (176.26 g/mol)

Following **GP-B**, **3jb** was synthesized using *S*-phenyl 3-phenylpropanethioate (**1j**) (242.0 mg, 1.0 mmol, 1.0 equiv.), 1-bromopropane (256 mg, 2.0 mmol, 2.0 equiv.), $NiCl_2 \cdot (H_2O)_6$ (23.8 mg, 0.1 mmol, 10 mol), 4,4'-di-*tert*-butyl-2,2'-bipyridine (53.7 mg, 0.2 mmol, 20 mol%), zinc powder (131 mg, 2.0 mmol, 2.0 equiv.), sodium chloride (117 mg, 2.0 mmol, 2.0 equiv.) and pyridine (158 mg, 2.0 mmol, 2 equiv.). Purification by flash column chromatography (*n*-hexane/EtOAc gradient 100:0 to 90:10 over 10 CV) afforded **3jb** (122 mg, 691 µmol, 69%) as colorless oil. Conforms to reported analytical data.[24]

R_f: 0.54 (*n*-hexane/EtOAc 90:10).

^{1}H NMR (400 MHz, $CDCl_3$, δ): 7.32 – 7.26 (m, 2H), 7.24 – 7.13 (m, 3H), 2.90 (t, *J* = 7.6 Hz, 2H), 2.73 (t, *J* = 7.6 Hz, 2H), 2.37 (t, *J* = 7.3 Hz, 2H), 1.60 (tt, *J* = 7.6, 7.4 Hz, 2H), 0.90 (t, *J* = 7.4 Hz, 3H).

^{13}C{^{1}H} NMR (101 MHz, $CDCl_3$, δ): 210.3, 141.3, 128.6, 128.4, 126.2, 45.1, 44.4, 29.9, 17.4, 13.9.

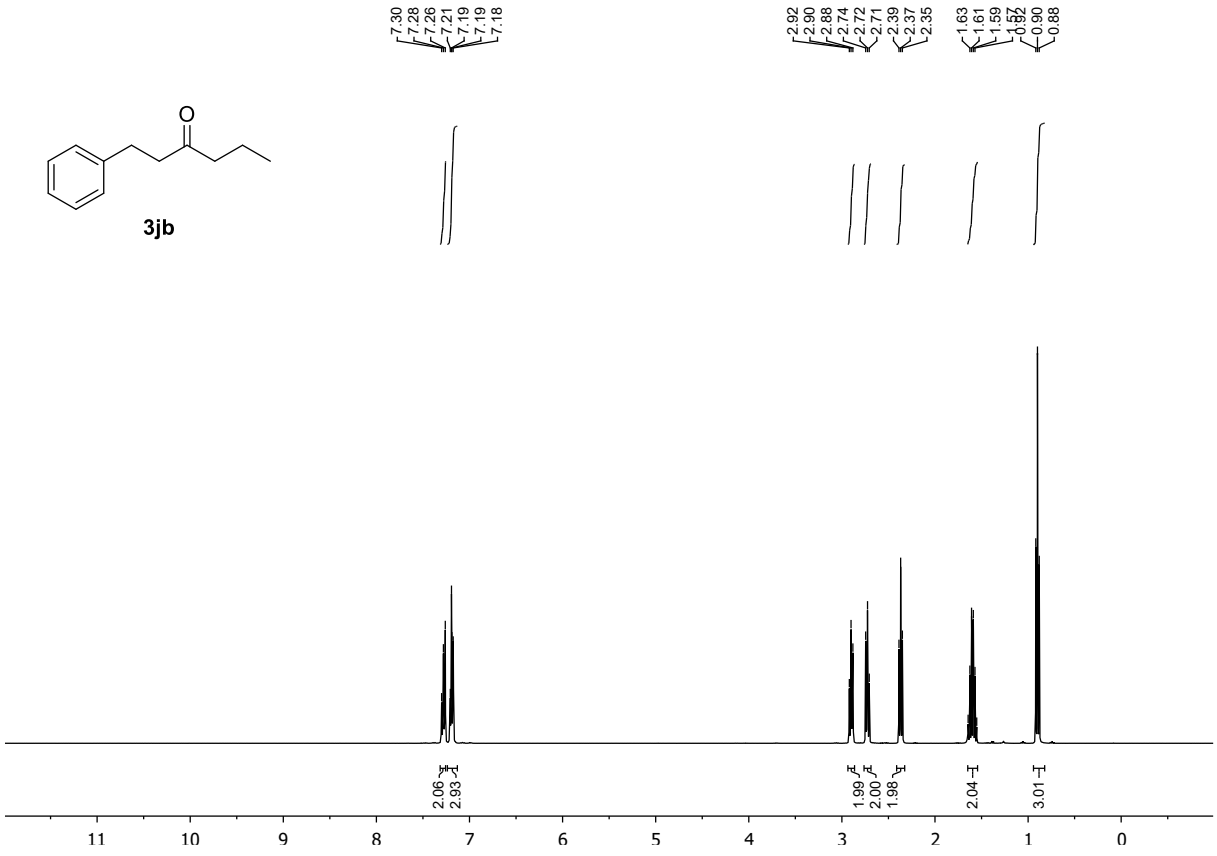

Figure S104. ^{1}H NMR spectrum (400 MHz, $CDCl_3$) of **3jb**.

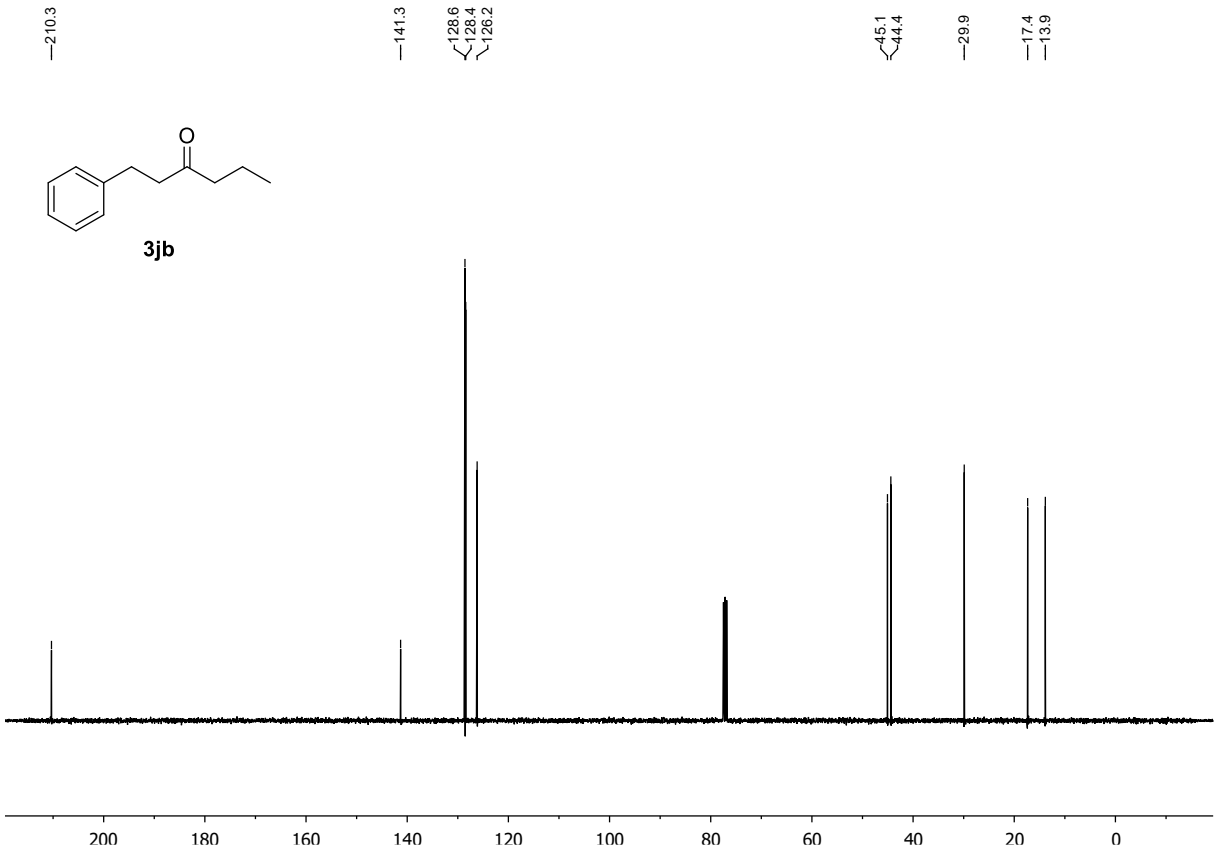

Figure S105. ^{13}C NMR spectrum (101 MHz, $CDCl_3$) of **3jb**.

6-Chloro-1-phenylhexan-3-one (3jc):

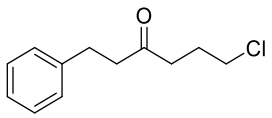

3jc

$C_{12}H_{15}ClO$ (210.70 g/mol)

Following **GP-B**, **3jc** was synthesized using *S*-phenyl 3-phenylpropanethioate (**1j**) (242.0 mg, 1.0 mmol, 1.0 equiv.), 1-bromo-3-chloropropane (315 mg, 2.0 mmol, 2.0 equiv.), $NiCl_2 \cdot (H_2O)_6$ (23.8 mg, 0.1 mmol, 10 mol%), 4,4'-di-*tert*-butyl-2,2'-bipyridine (53.7 mg, 0.2 mmol, 20 mol%), zinc powder (131 mg, 2.0 mmol, 2.0 equiv.), sodium chloride (117 mg, 2.0 mmol, 2.0 equiv.) and pyridine (158 mg, 2.0 mmol, 2 equiv.). Purification by flash column chromatography (*n*-hexane/EtOAc gradient 100:0 to 90:10 over 10 CV) afforded **3jc** (99 mg, 468 µmol, 47%) as colorless oil. Conforms to reported analytical data.[25]

R_f: 0.44 (*n*-hexane/EtOAc 90:10).

^{1}H NMR (400 MHz, $CDCl_3$, δ): 7.34 – 7.26 (m, 2H), 7.24 – 7.14 (m, 3H), 3.55 (t, *J* = 6.5 Hz, 2H), 2.92 (t, *J* = 7.6 Hz, 2H), 2.75 (t, *J* = 7.6 Hz, 2H), 2.59 (t, *J* = 7.0 Hz, 2H), 2.04 (tt, *J* = 7.6, 6.5 Hz, 2H).

^{13}C{^{1}H} NMR (101 MHz, $CDCl_3$, δ): 208.9, 141.0, 128.6, 128.4, 126.3, 44.54, 44.51, 39.6, 29.9, 26.3.

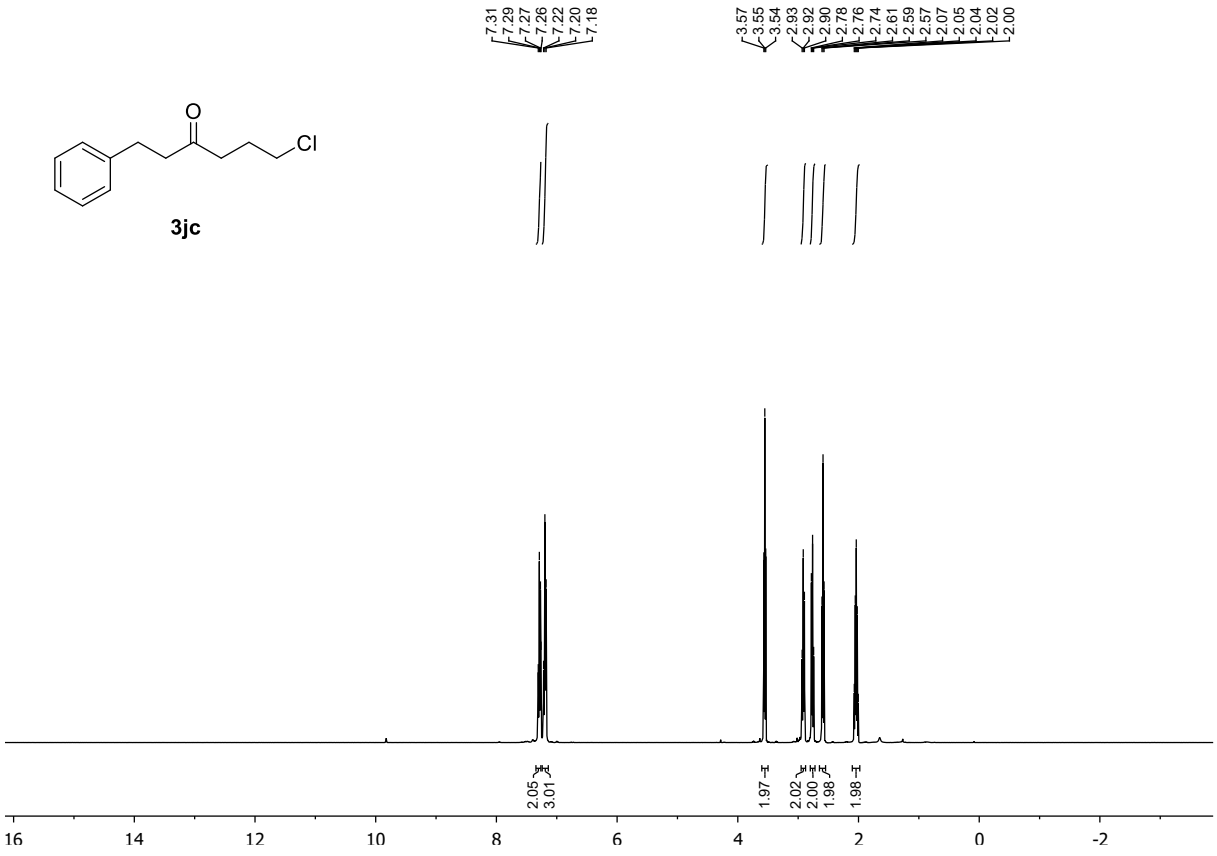

Figure S106. ^{1}H NMR spectrum (400 MHz, $CDCl_3$) of **3jc**.

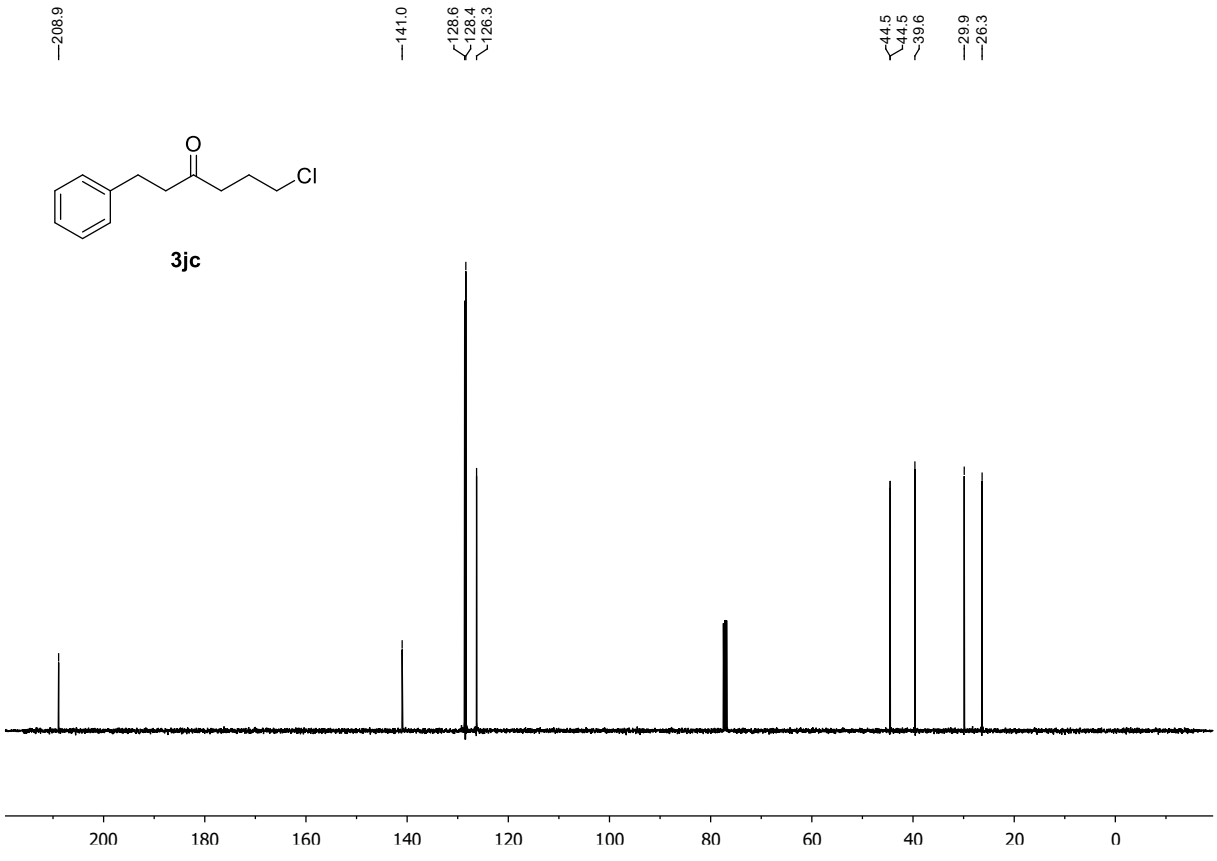

Figure S107. ^{13}C NMR spectrum (101 MHz, $CDCl_3$) of **3jc**.

1-(2-Chlorophenyl)-5-phenylpentan-3-one (3jd):

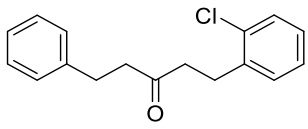

3jd

$C_{17}H_{17}ClO$ (272.77 g/mol)

Following **GP-B**, **3jd** was synthesized using *S*-Phenyl benzenepropanethioate (**1j**) (242 mg, 1.0 mmol, 1.0 equiv.), 1-(2-bromoethyl)-2-chlorobenzene (439 mg, 2.0 mmol, 2.0 equiv.), $NiCl_2 \cdot (H_2O)_6$ (23.8 mg, 0.1 mmol, 10 mol%), 4,4'-di-*tert*-butyl-2,2'-bipyridine (53.7 mg, 0.2 mmol, 20 mol%), zinc powder (131 mg, 2.0 mmol, 2.0 equiv.), sodium chloride (117 mg, 2.0 mmol, 2.0 equiv.) and pyridine (158 mg, 2.0 mmol, 2 equiv.). Purification by flash column chromatography (*n*-hexane/EtOAc gradient 100:0 to 80:20 over 10 CV) afforded **3jd** (79 mg 290 µmol, 29%) as colorless oil.

R_f: 0.49 (*n*-hexane/EtOAc 90:10).

^{1}H NMR (400 MHz, $CDCl_3$, δ): 7.36 – 7.25 (m, 3H, *residual solvent signal under peak*), 7.22 – 7.11 (m, 6H), 3.00 (t, *J* = 7.6 Hz, 2H), 2.90 (t, *J* = 7.6 Hz, 2H), 2.76 – 2.70 (m, 4H).

^{13}C{^{1}H} NMR (101 MHz, $CDCl_3$, δ): 209.0, 141.1, 138.7, 134.0, 130.8, 129.7, 128.6, 128.4, 127.8, 127.0, 126.3, 44.5, 42.6, 29.9, 27.9.

HR-MS (ESI): m/z calc for $[M+H]^+$ 273.10407, found 273.10435 (err. 1.04 ppm).

IR (ATR, $\tilde{\nu}$ [cm^{-1}]): 3059 (w), 3025 (w), 2928 (w), 2898 (w), 1709 (s), 1598 (w), 1571 (w), 1474 (m), 1444 (m), 1407 (m), 1366 (m), 1291 (w), 1183 (w), 1116 (w), 1086 (m), 1043 (m), 978 (w), 945 (w), 911 (w), 747 (vs), 695 (s).

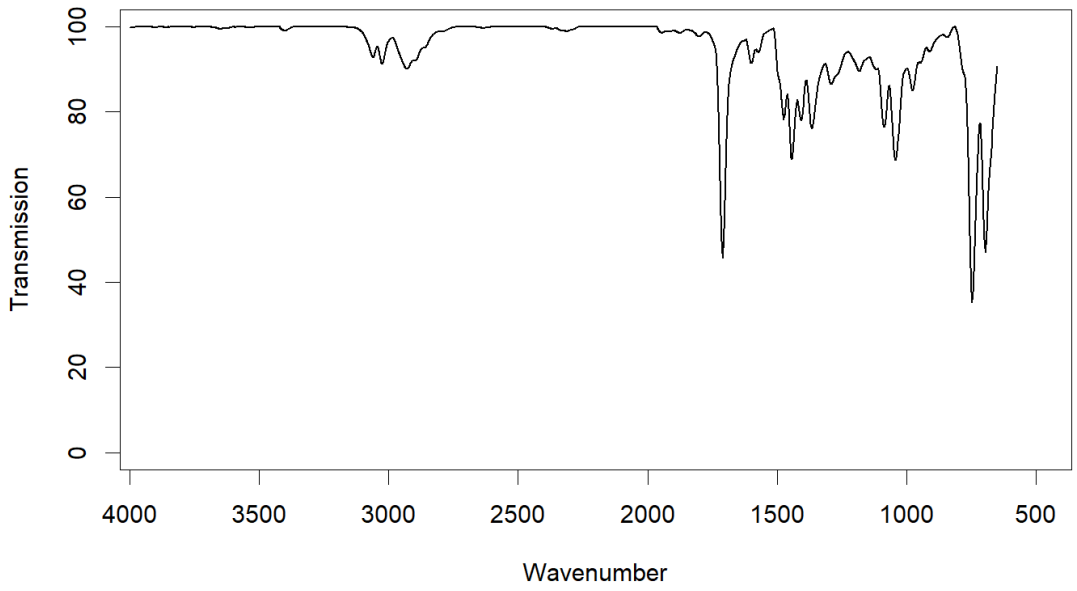

Figure S108. IR spectrum (ATR, neat) of **3jd**.

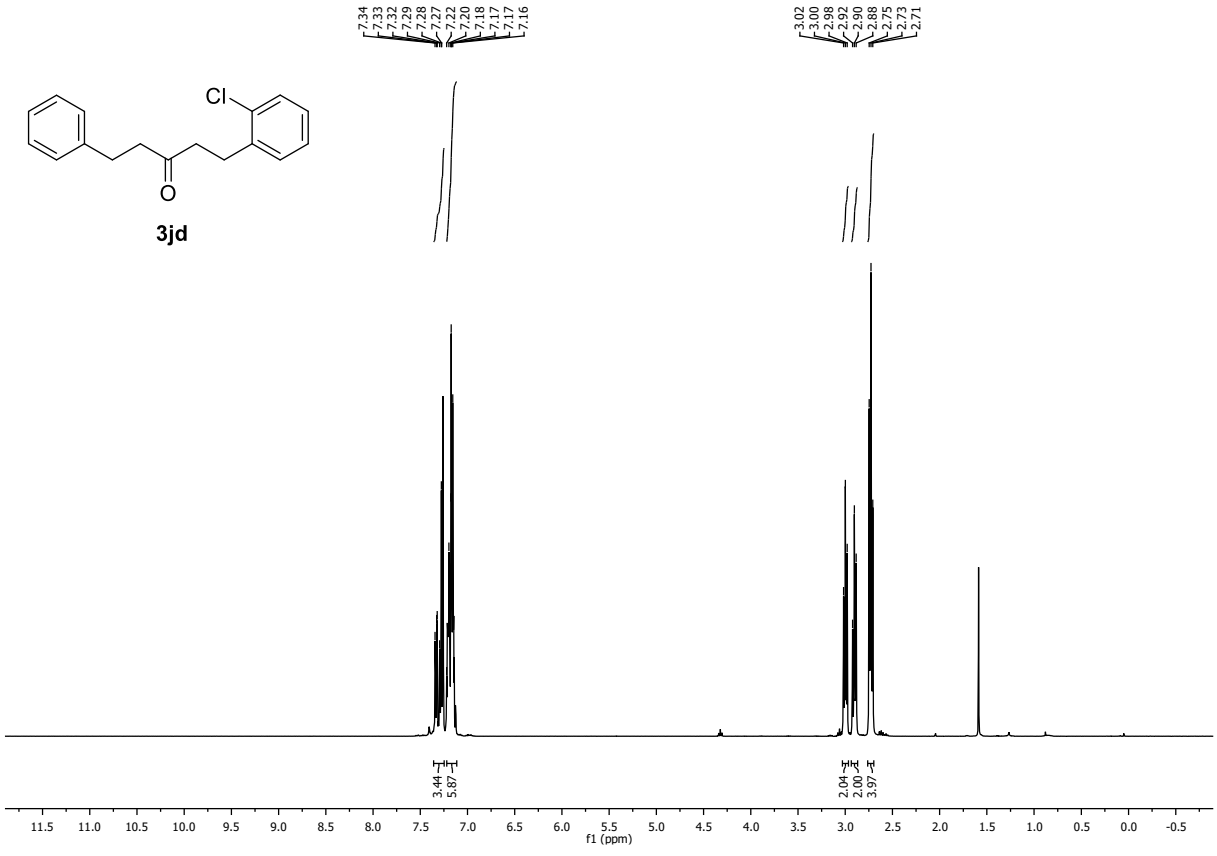

Figure S109. ^{1}H NMR spectrum (400 MHz, $CDCl_3$) of **3jd**.

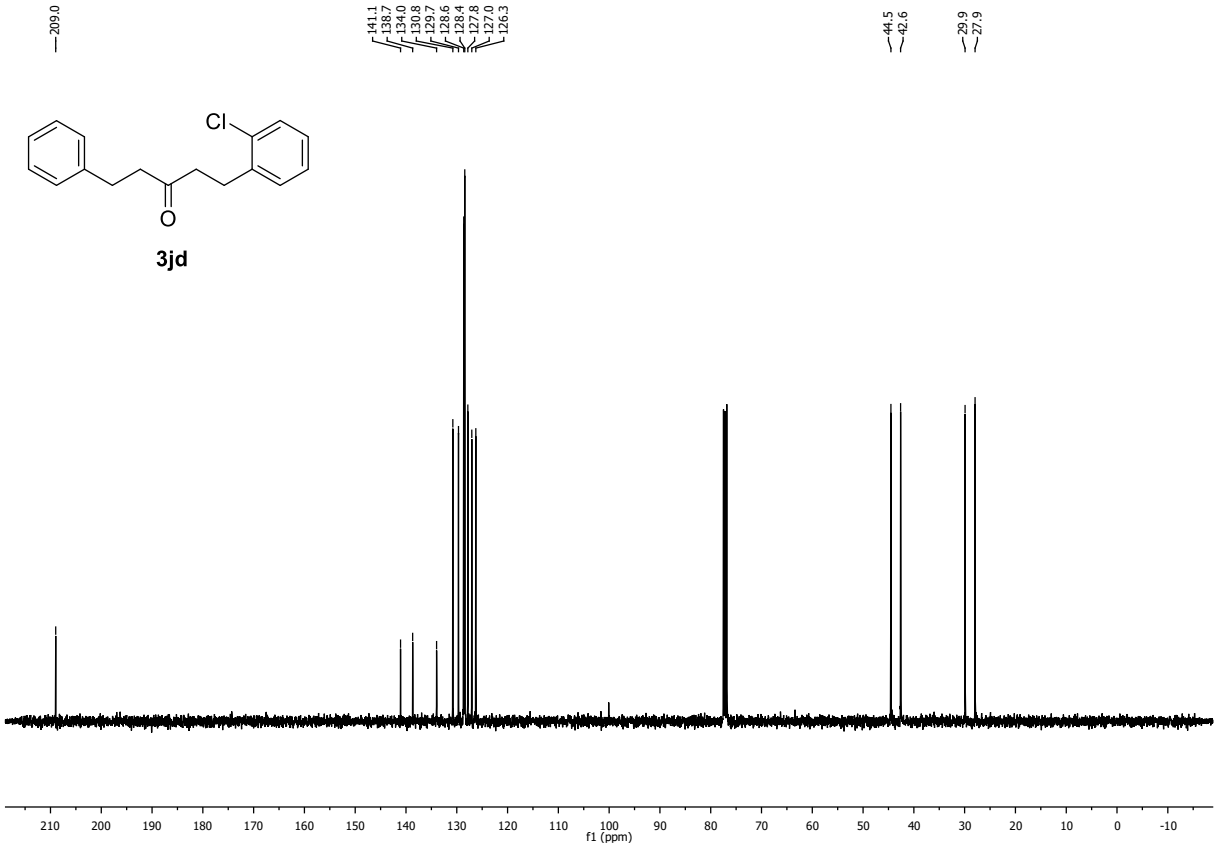

Figure S110. ^{13}C NMR spectrum (101 MHz, $CDCl_3$) of **3jd**.

6-(4-Bromophenyl)-1-phenylhexan-3-one (3je):

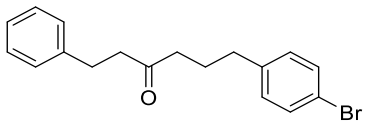

3je

$C_{18}H_{19}BrO$ (331.25 g/mol)

Following **GP-B**, **3je** was synthesized using *S*-Phenyl benzenepropanethioate (**1j**) (242 mg, 1.0 mmol, 1.0 equiv.), 1-Bromo-4-(3-bromopropyl)benzene (556 mg, 2.0 mmol, 2.0 equiv.), $NiCl_2 \cdot (H_2O)_6$ (23.8 mg, 0.1 mmol, 10 mol%), 4,4'-di-*tert*-butyl-2,2'-bipyridine (53.7 mg, 0.2 mmol, 20 mol%), zinc powder (131 mg, 2.0 mmol, 2.0 equiv.), sodium chloride (117 mg, 2.0 mmol, 2.0 equiv.) and pyridine (158 mg, 2.0 mmol, 2 equiv.). Purification by flash column chromatography (*n*-hexane/EtOAc gradient 100:0 to 90:10 over 10 CV) afforded (95 mg 287 µmol, 29%) as colorless oil.

R$_f$: 0.46 (*n*-hexane/EtOAc 90:10).

^{1}H NMR (400 MHz, $CDCl_3$, δ): 7.41 – 7.36 (m, 2H), 7.31 – 7.24 (m, 2H, *residual solvent signal under peak*), 7.23 – 7.14 (m, 3H), 7.03 – 6.97 (m, 2H), 2.89 (t, *J* = 7.6 Hz, 2H), 2.70 (t, *J* = 7.6 Hz, 2H), 2.54 (t, *J* = 7.6 Hz, 2H), 2.37 (t, *J* = 7.3 Hz, 2H), 1.93 – 1.80 (m, 2H).

^{13}C{^{1}H} NMR (101 MHz, $CDCl_3$, δ): 209.7, 141.1, 140.6, 131.6, 130.3, 128.6, 128.4, 126.3, 119.8, 44.5, 42.0, 34.5, 29.9, 25.0.

HR-MS (ESI): m/z calc for $[M+H]^+$ 331.06920, found 331.06972 (err. 1.55 ppm).

IR (ATR, $\tilde{\nu}$ [cm^{-1}]): 3058 (w), 3025 (w), 2929 (w), 2860 (w), 1709 (s), 1597 (w), 1485 (m), 1448 (m), 1403 (m), 1366 (m), 1276 (w), 1180 (w), 1094 (w), 1072 (m), 1034 (w), 1008 (m), 821 (m), 789 (m), 744 (s), 699 (s).

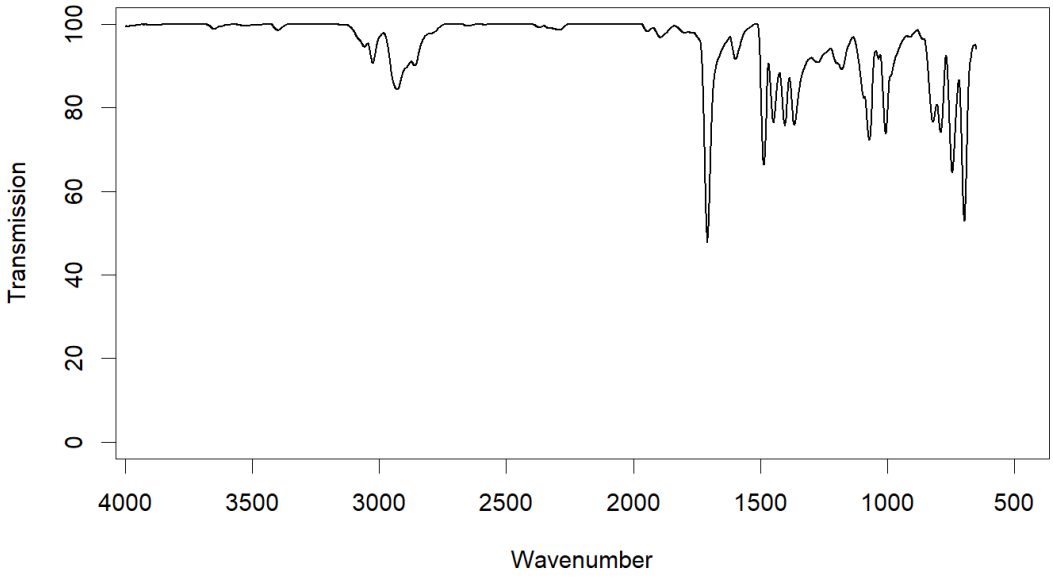

Figure S111. IR spectrum (ATR, neat) of **3je**.

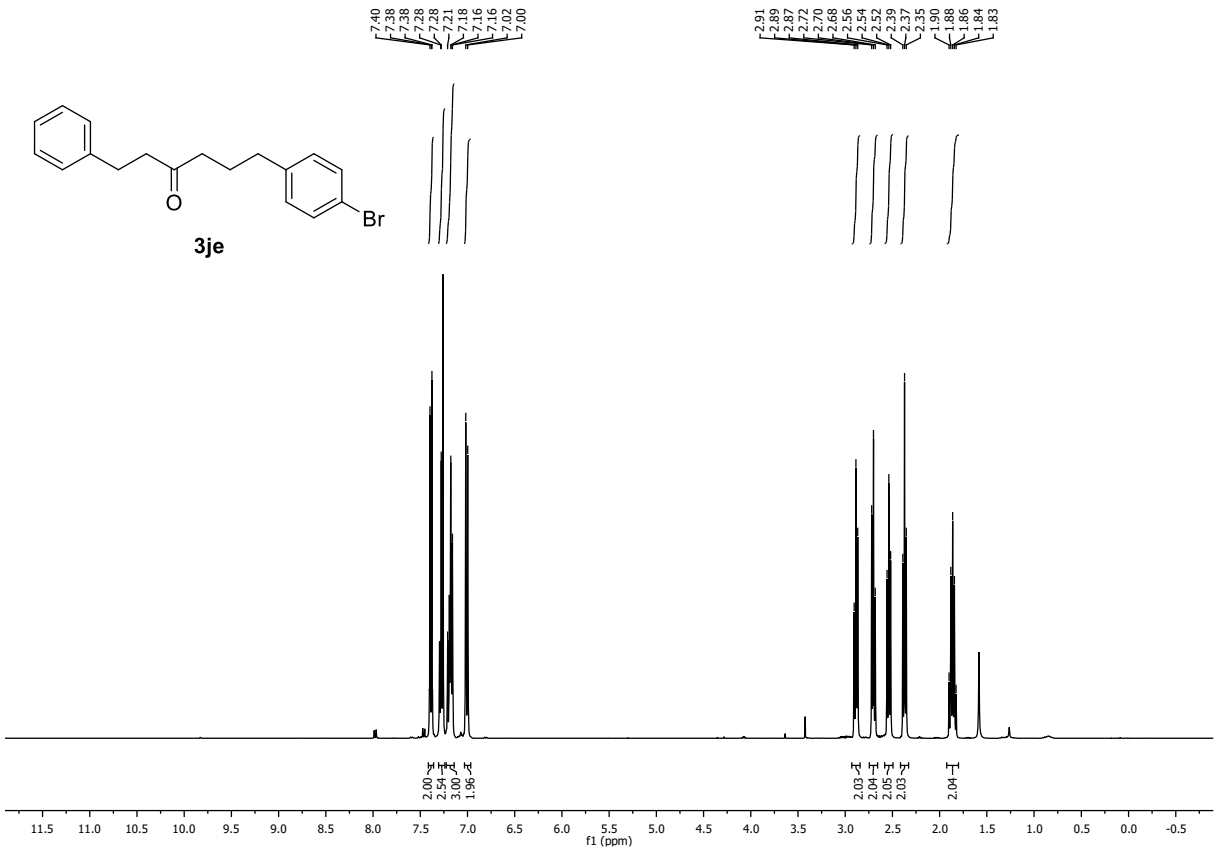

Figure S112. ^{1}H NMR spectrum (400 MHz, $CDCl_3$) of **3je**.

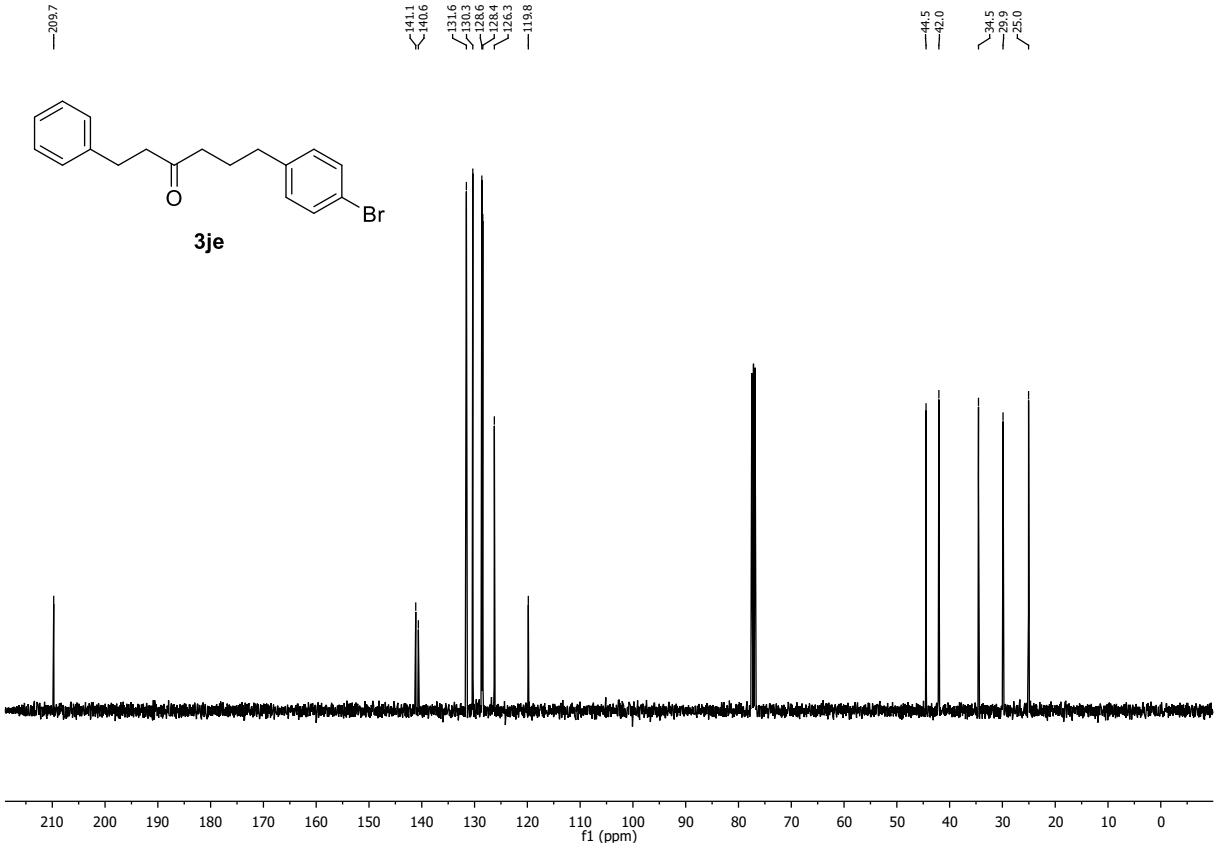

Figure S113. ^{13}C NMR spectrum (101 MHz, $CDCl_3$) of **3je**.

1-Phenyl-5-(4-(trifluoromethyl)phenyl)pentan-3-one (3jf):

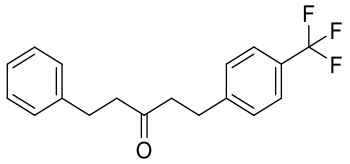

3jf

$C_{18}H_{17}F_3O$ (306.33 g/mol)

Following **GP-B**, **3jf** was synthesized using *S*-Phenyl benzenepropanethioate (**1j**) (242 mg, 1.0 mmol, 1.0 equiv.), 1-(2-bromoethyl)-4-trifluoromethyl)-benzene (505 mg, 2.0 mmol, 2.0 equiv.), $NiCl_2 \cdot (H_2O)_6$ (23.8 mg, 0.1 mmol, 10 mol%), 4,4'-di-*tert*-butyl-2,2'-bipyridine (53.7 mg, 0.2 mmol, 20 mol%), zinc powder (131 mg, 2.0 mmol, 2.0 equiv.), sodium chloride (117 mg, 2.0 mmol, 2.0 equiv.) and pyridine (158 mg, 2.0 mmol, 2 equiv.). Purification by flash column chromatography (*n*-hexane/EtOAc gradient 100:0 to 75:25 over 10 CV) afforded (142 mg 464 µmol, 46%) as yellow oil. Conforms to reported analytical data.[26]

R_f: 0.64 (*n*-hexane/EtOAc 80:20).

^{1}H NMR (400 MHz, $CDCl_3$, δ): 7.60 – 7.53 (m, 2H), 7.35 – 7.28 (m, 4H), 7.27 – 7.16 (m, 3H), 3.03 – 2.90 (m, 4H), 2.77 (m, 4H).

^{13}C{^{1}H} NMR (101 MHz, $CDCl_3$, δ): 208.5, 145.3, 140.9, 128.8, 128.6, 128.4, 126.3, 125.5 (q, J = 3.7 Hz), 124.4 (q, J = 271.9 Hz), 44.6, 44.1, 29.8, 29.5.

^{19}F NMR (376 MHz, $CDCl_3$, δ): -62.3.

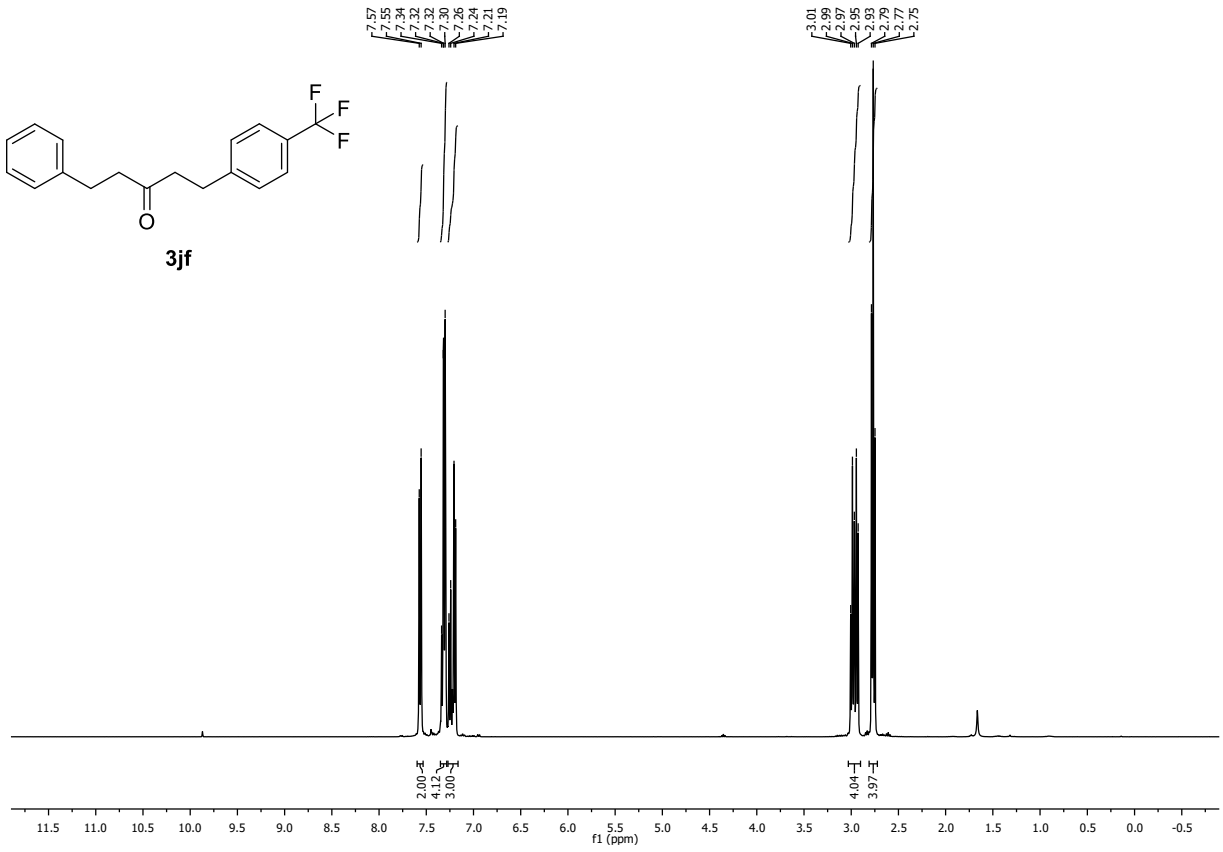

Figure S114. ^{1}H NMR spectrum (400 MHz, $CDCl_3$) of **3jf**.

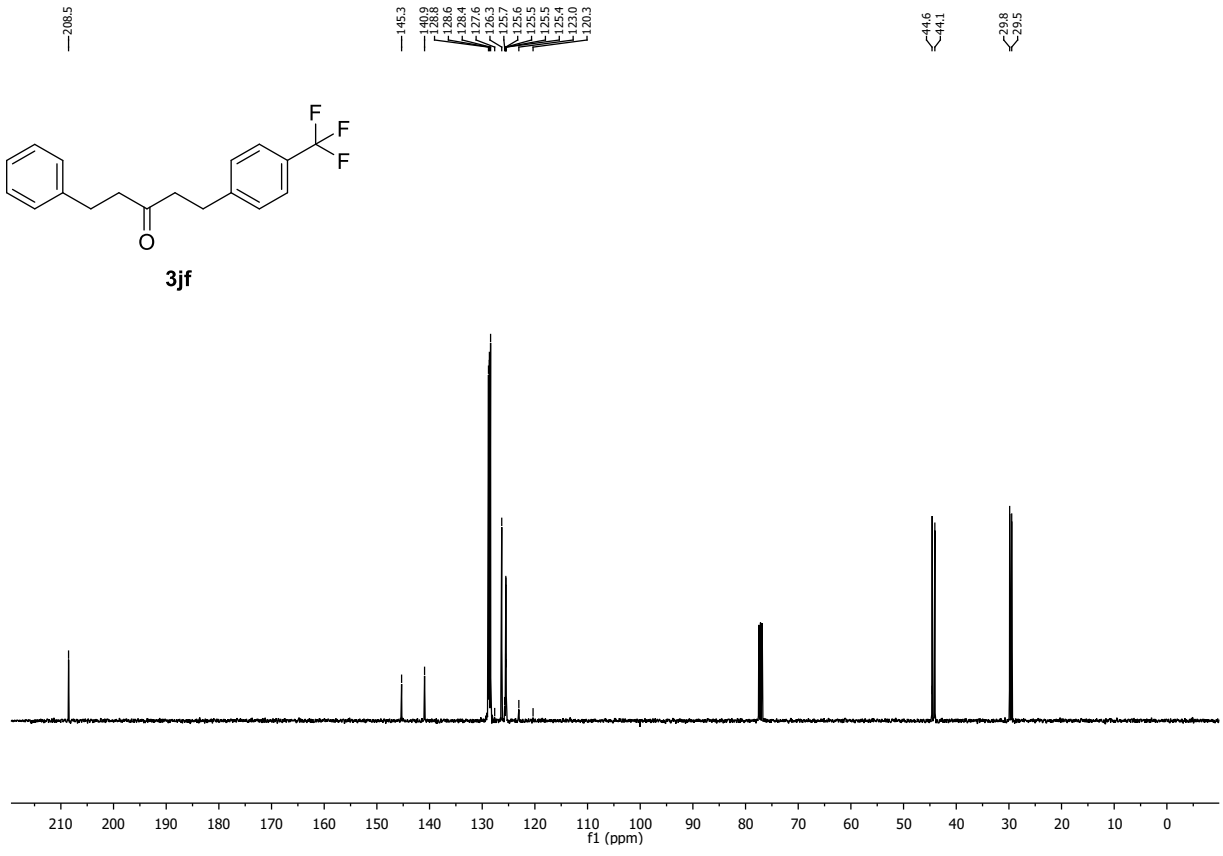

Figure S115. ^{13}C NMR spectrum (101 MHz, $CDCl_3$) of **3jf**.

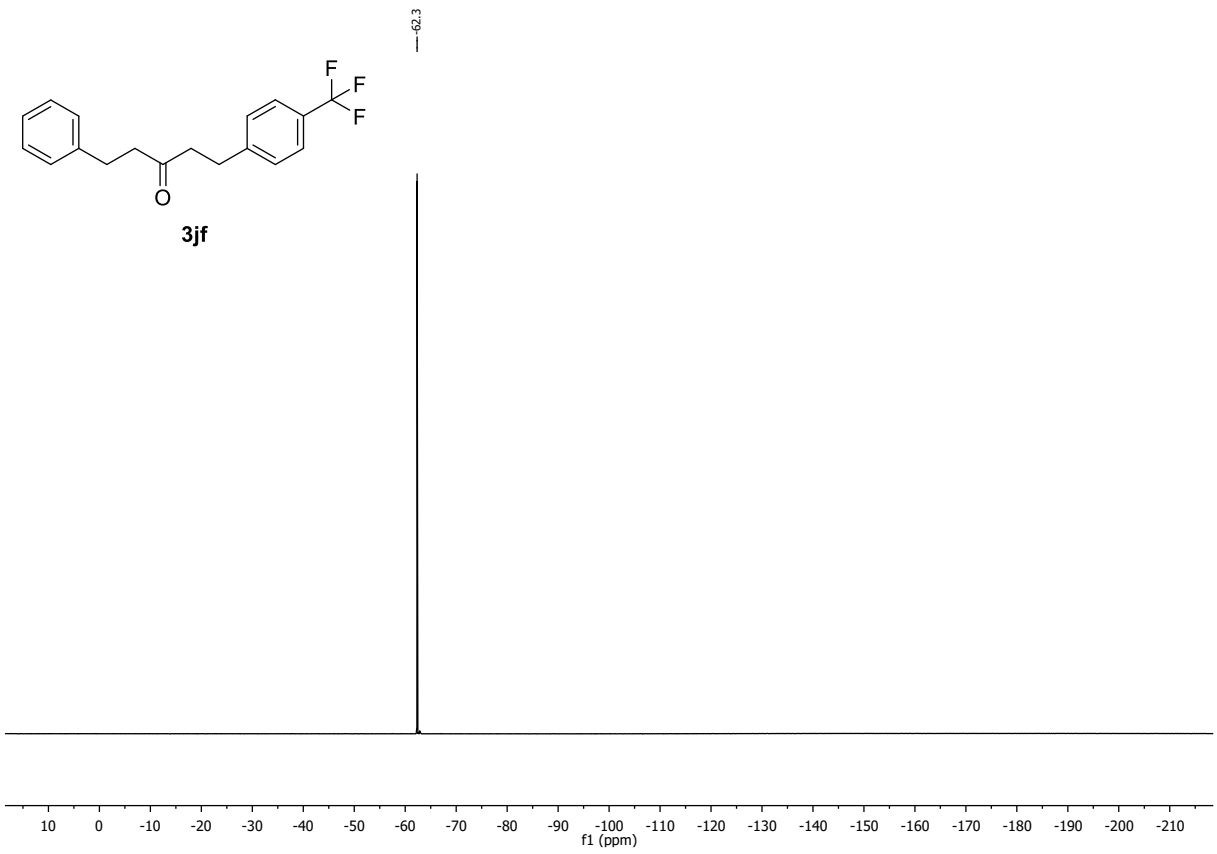

Figure S116. ^{19}F NMR spectrum (376 MHz, $CDCl_3$) of **3jf**.

1-((*tert*-Butyldimethylsilyl)oxy)-5-phenylpentan-3-one (3jg):

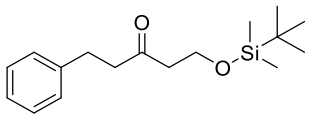

3jg

$C_{17}H_{28}O_2Si$ (292.49 g/mol)

Following **GP-B**, **3jg** was synthesized using *S*-Phenyl benzenepropanethioate (**1j**) (242 mg, 1.0 mmol, 1.0 equiv.), (2-bromoethoxy))(*tert*-butyl)dimethylsilane (478 mg, 2.0 mmol, 2.0 equiv.), $NiCl_2 \cdot (H_2O)_6$ (23.8 mg, 0.1 mmol, 10 mol%), 4,4'-di-*tert*-butyl-2,2'-bipyridine (53.7 mg, 0.2 mmol, 20 mol%), zinc powder (131 mg, 2.0 mmol, 2.0 equiv.), sodium chloride (117 mg, 2.0 mmol, 2.0 equiv.) and pyridine (158 mg, 2.0 mmol, 2 equiv.). Purification by flash column chromatography (*n*-hexane/EtOAc gradient 100:0 to 80:20 over 10 CV) afforded (113 mg 386 µmol, 39%) as colorless oil. Conforms to reported analytical data.[27]

R$_f$: 0.51 (*n*-hexane/EtOAc 80:20).

^{1}H NMR (400 MHz, $CDCl_3$, δ): 7.31 – 7.25 (m, 2H), 7.22 – 7.16 (m, 3H), 3.89 (t, *J* = 6.2 Hz, 2H), 2.90 (m, 2H), 2.79 (m, 2H), 2.60 (t, *J* = 6.2 Hz, 2H), 0.88 (s, 9H), 0.05 (s, 6H).

^{13}C{^{1}H} NMR (101 MHz, $CDCl_3$, δ): 209.1, 141.2, 128.6, 128.4, 126.1, 59.0, 45.9, 45.5, 29.6, 26.0, 18.3, -5.3.

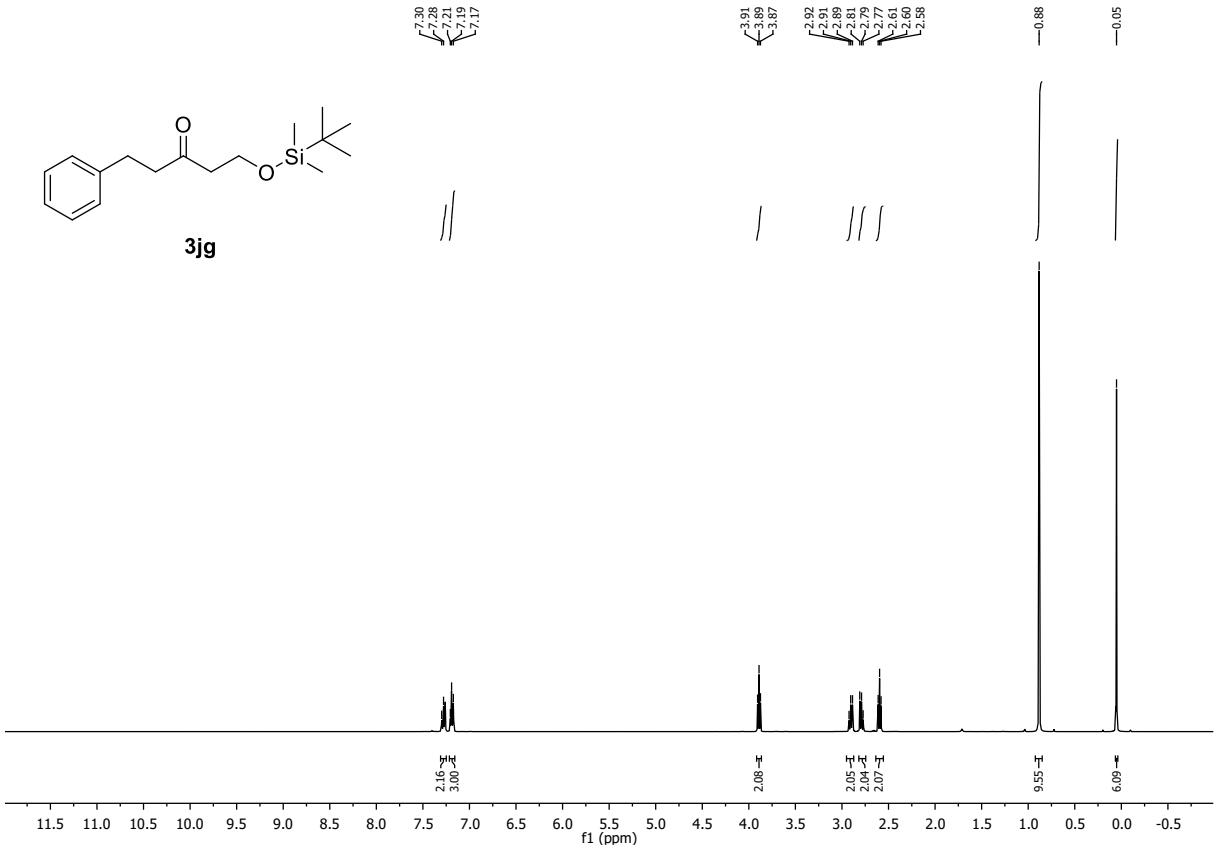

Figure S117. ^{1}H NMR spectrum (400 MHz, $CDCl_3$) of **3jg**.

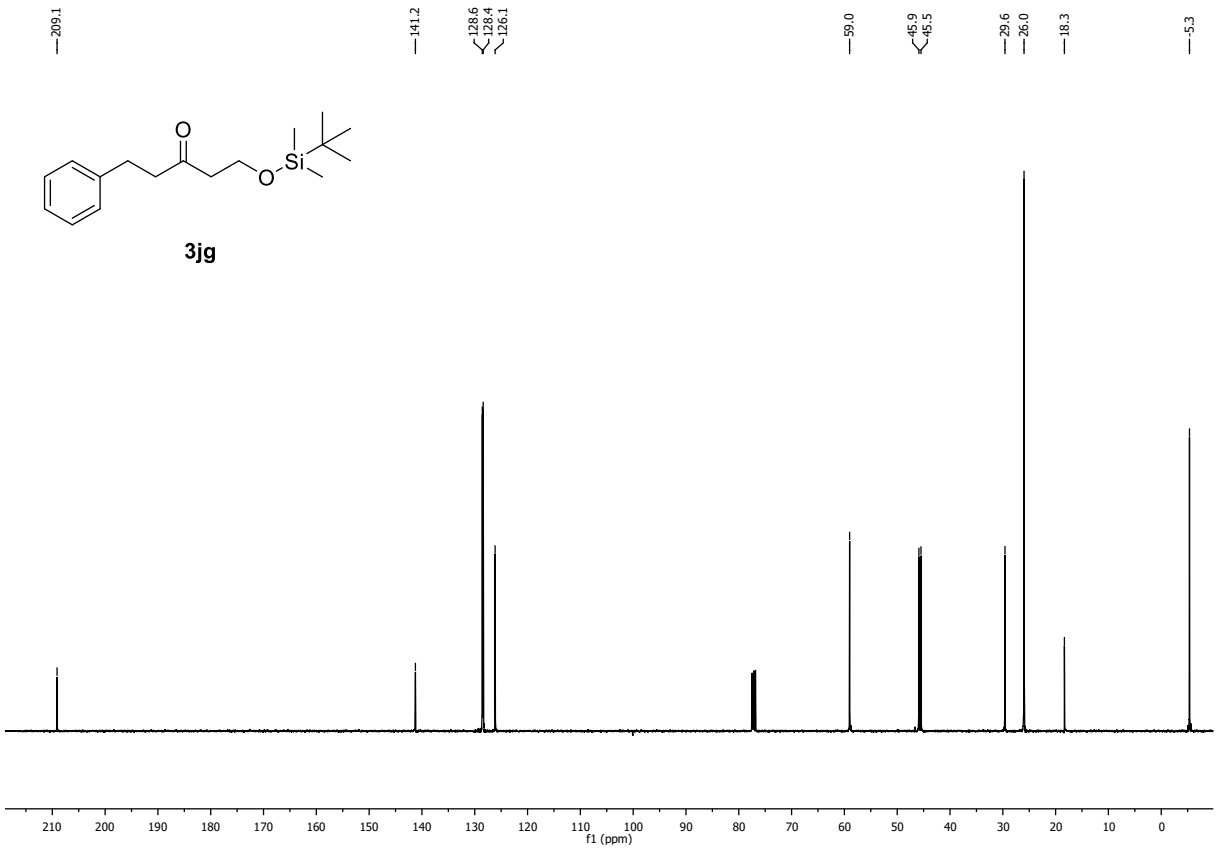

Figure S118. ^{13}C NMR spectrum (101 MHz, $CDCl_3$) of **3jg**.

7-Methoxy-1-phenylheptan-3-one (3jh):

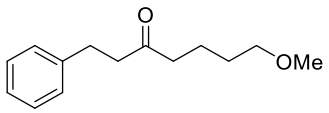

3jh

$C_{14}H_{20}O_2$ (220.31 g/mol)

Following **GP-B**, **3jh** was synthesized using *S*-phenyl 3-phenylpropanethioate (**1j**) (242 mg, 1.0 mmol, 1.0 equiv.), 1-bromo-4-methoxybutane (334 mg, 2.0 mmol, 2.0 equiv.), $NiCl_2 \cdot (H_2O)_6$ (23.8 mg, 0.1 mmol, 10 mol%), 4,4'-di-*tert*-butyl-2,2'-bipyridine (53.7 mg, 0.2 mmol, 20 mol%), zinc powder (131 mg, 2.0 mmol, 2.0 equiv.), sodium chloride (117 mg, 2.0 mmol, 2.0 equiv.) and pyridine (158 mg, 2.0 mmol, 2 equiv.). Purification by flash column chromatography (*n*-hexane/EtOAc gradient 100:0 to 50:50 over 10 CV) afforded (146 mg 662 µmol, 66%) as colorless oil.

R_f: 0.44 (*n*-hexane/EtOAc 80:20).

^{1}H NMR (400 MHz, $CDCl_3$, δ): 7.30 – 7.24 (m, 2H), 7.23 – 7.13 (m, 3H), 3.35 (t, *J* = 6.2 Hz, 2H), 3.31 (s, 3H), 2.89 (t, *J* = 7.6 Hz, 2H), 2.72 (t, *J* = 7.6 Hz, 2H), 2.41 (t, *J* = 7.2 Hz, 2H), 1.68 – 1.49 (m, 4H).

^{13}C{^{1}H} NMR (101 MHz, $CDCl_3$, δ): 210.0, 141.2, 128.6, 128.4, 126.2, 72.5, 58.6, 44.3, 42.8, 29.9, 29.2, 20.6.

HR-MS (ESI): m/z calc for $[M+Na]^+$ 243.13555, found 243.13583 (err. -1.15 ppm).

IR (ATR, $\tilde{\nu}$ [cm^{-1}]): 3059 (w), 3025 (w), 2927 (m), 2864 (w), 2827 (w), 1709 (s), 1601 (w), 1493 (w), 1449 (m), 1407 (w), 1369 (w), 1276 (w), 1184 (w), 1150 (w), 1113 (s), 1027 (w), 986 (w), 945 (w), 912 (w), 747 (m), 699 (s).

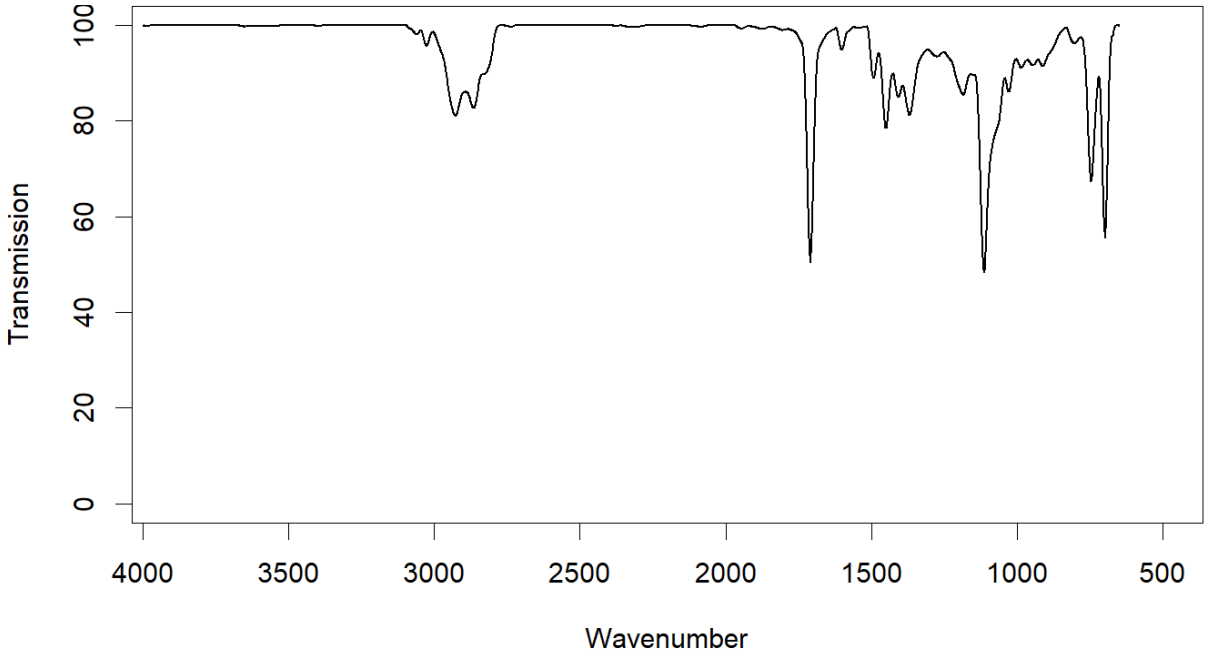

Figure S119. IR spectrum (ATR, neat) of **3jh**.

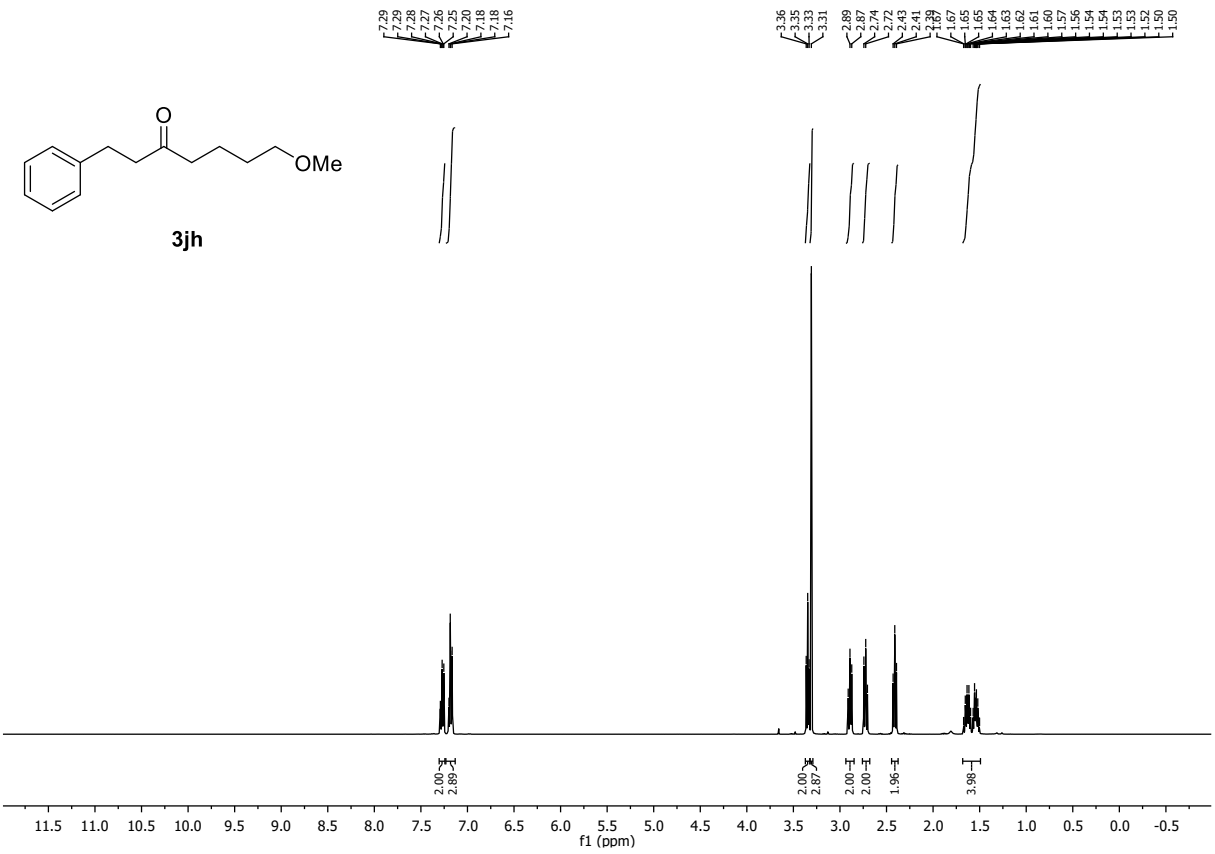

Figure S120. ^{1}H NMR spectrum (400 MHz, $CDCl_3$) of **3jh**.

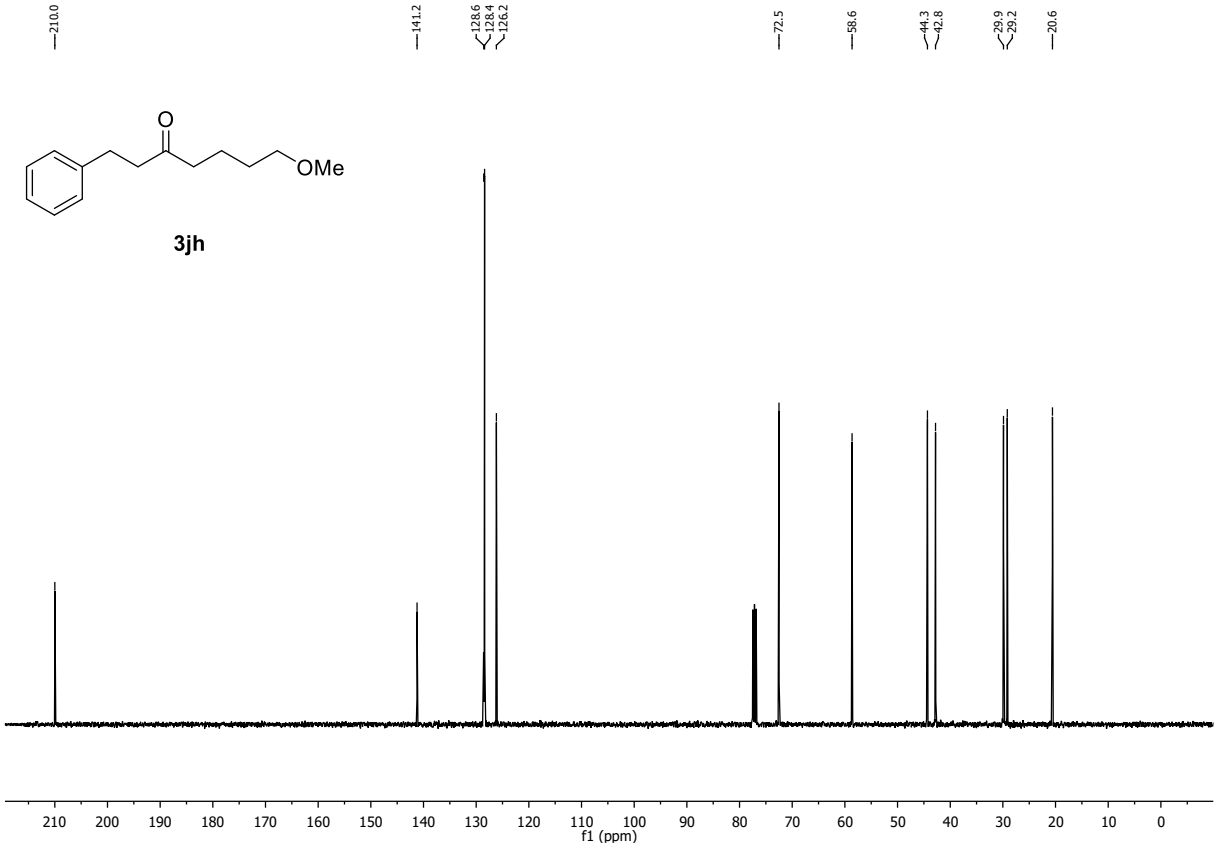

Figure S121. ^{13}C NMR spectrum (101 MHz, $CDCl_3$) of **3jh**.

Methyl 6-oxo-8-phenyloctanoate (3ji):

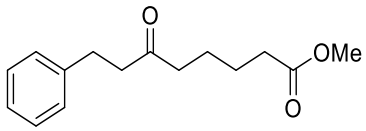

3ji

$C_{15}H_{20}O_3$ (248.32 g/mol)

Following **GP-B**, **3ji** was synthesized using *S*-phenyl 3-phenylpropanethioate (**1j**) (242.0 mg, 1.0 mmol, 1.0 equiv.), methyl 5-bromopentanoate (390 mg, 2.0 mmol, 2.0 equiv.), $NiCl_2 \cdot (H_2O)_6$ (23.8 mg, 0.1 mmol, 10 mol%), 4,4'-di-*tert*-butyl-2,2'-bipyridine (53.7 mg, 0.2 mmol, 20 mol%), zinc powder (131 mg, 2.0 mmol, 2.0 equiv.), sodium chloride (117 mg, 2.0 mmol, 2.0 equiv.) and pyridine (158 mg, 2.0 mmol, 2 equiv.). Purification by flash column chromatography (*n*-hexane/EtOAc gradient 100:0 to 80:20 over 10 CV) afforded **3ji** (164 mg, 661 µmol, 66%) as colorless oil. Conforms to reported analytical data.[28]

R_f: 0.21 (*n*-hexane/EtOAc 90:10).

^{1}H NMR (400 MHz, $CDCl_3$, δ): 7.30 – 7.25 (m, 2H), 7.22 – 7.13 (m, 3H), 3.66 (s, 3H), 2.89 (t, *J* = 7.6 Hz, 2H), 2.72 (t, *J* = 7.7 Hz, 2H), 2.44 – 2.35 (m, 2H), 2.33 – 2.26 (m, 2H), 1.63 – 1.54 (m, 4H).

^{13}C{^{1}H} NMR (101 MHz, $CDCl_3$, δ): 209.7, 173.9, 141.2, 128.6, 128.4, 126.2, 51.7, 44.4, 42.7, 33.9, 29.9, 24.5, 23.2.

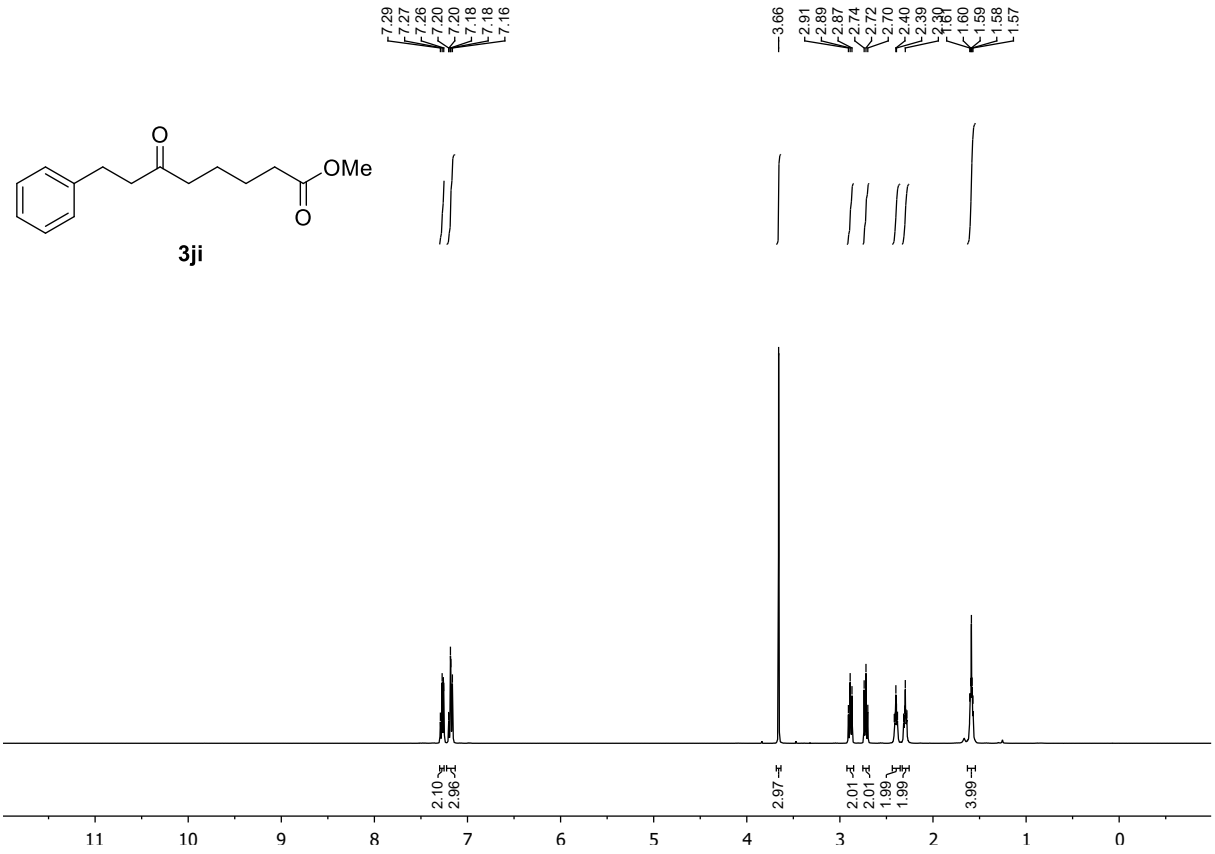

Figure S122. ^{1}H NMR spectrum (400 MHz, $CDCl_3$) of **3ji**.

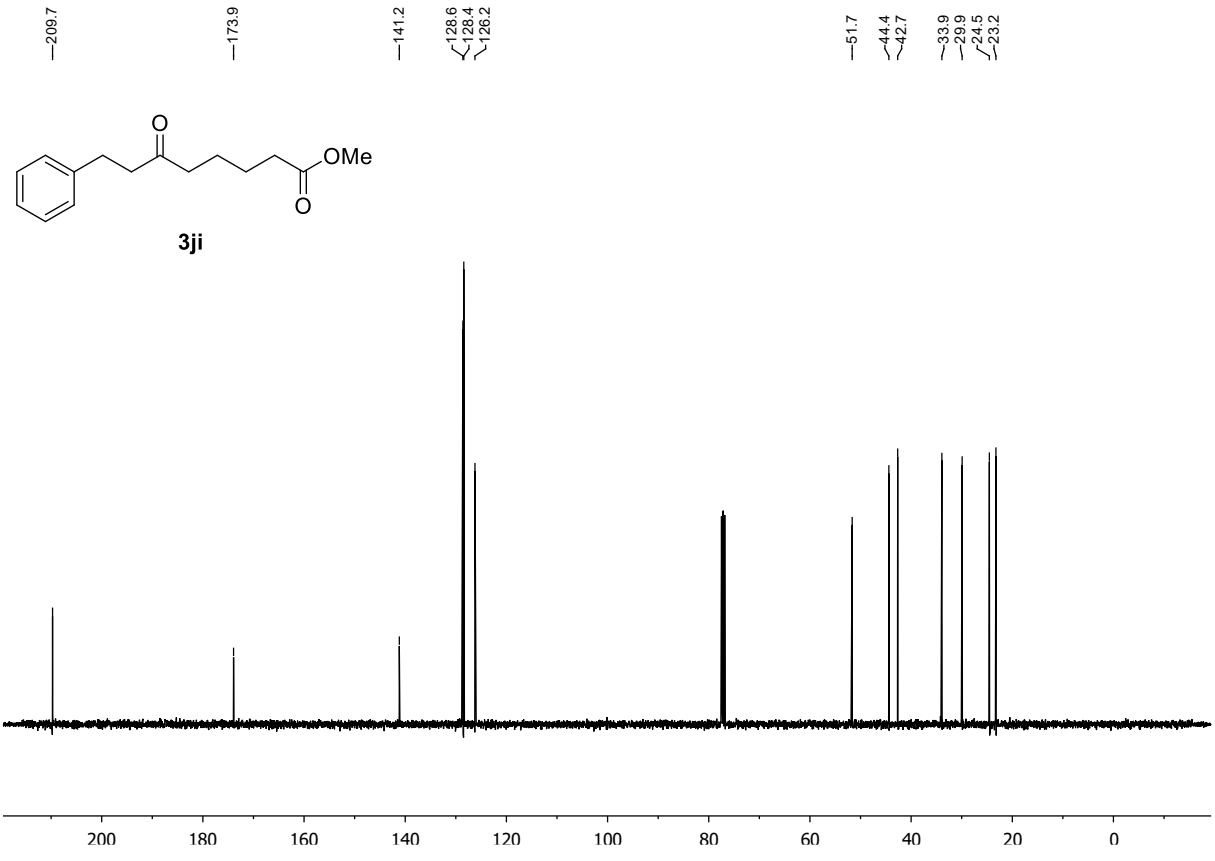

Figure S123. ^{13}C NMR spectrum (101 MHz, $CDCl_3$) of **3ji**.

Ethyl 6-oxo-6-phenylhexanoate (3ai):

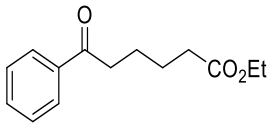

3ai

$C_{14}H_{18}O_3$ (234.30 g/mol)

Following **GP-B**, **3ai** was synthesized using *S*-phenyl benzothioate (**1a**) (214 mg, 1.0 mmol, 1.0 equiv.), ethyl 5-bromovalerate (418 mg, 2.0 mmol, 2.0 equiv.), $NiCl_2 \cdot (H_2O)_6$ (23.8 mg, 0.1 mmol, 10 mol%), 4,4'-di-*tert*-butyl-2,2'-bipyridine (53.7 mg, 0.2 mmol, 20 mol%), zinc powder (131 mg, 2.0 mmol, 2.0 equiv.), sodium chloride (117 mg, 2.0 mmol, 2.0 equiv.) and pyridine (158 mg, 2.0 mmol, 2 equiv.). Purification by flash column chromatography (*n*-hexane/EtOAc gradient 100:0 to 80:20 over 10 CV) afforded **3ai** (170 mg, 726 µmol, 73%) as colorless oil. Conforms to reported analytical data.[29]

R$_f$: 0.20 (*n*-hexane/EtOAc 90:10).

^{1}H NMR (400 MHz, $CDCl_3$, δ): 7.98 – 7.91 (m, 2H), 7.59 – 7.50 (m, 1H), 7.49 – 7.40 (m, 2H), 4.12 (q, *J* = 7.1 Hz, 2H), 2.99 (t, *J* = 6.9 Hz, 2H), 2.35 (t, *J* = 7.1 Hz, 2H), 1.75 (m, 4H), 1.24 (t, *J* = 7.1 Hz, 3H).

^{13}C{^{1}H} NMR (101 MHz, $CDCl_3$, δ): 199.9, 173.6, 137.1, 133.1, 128.7, 128.1, 60.4, 38.3, 34.3, 24.7, 23.8, 14.4.

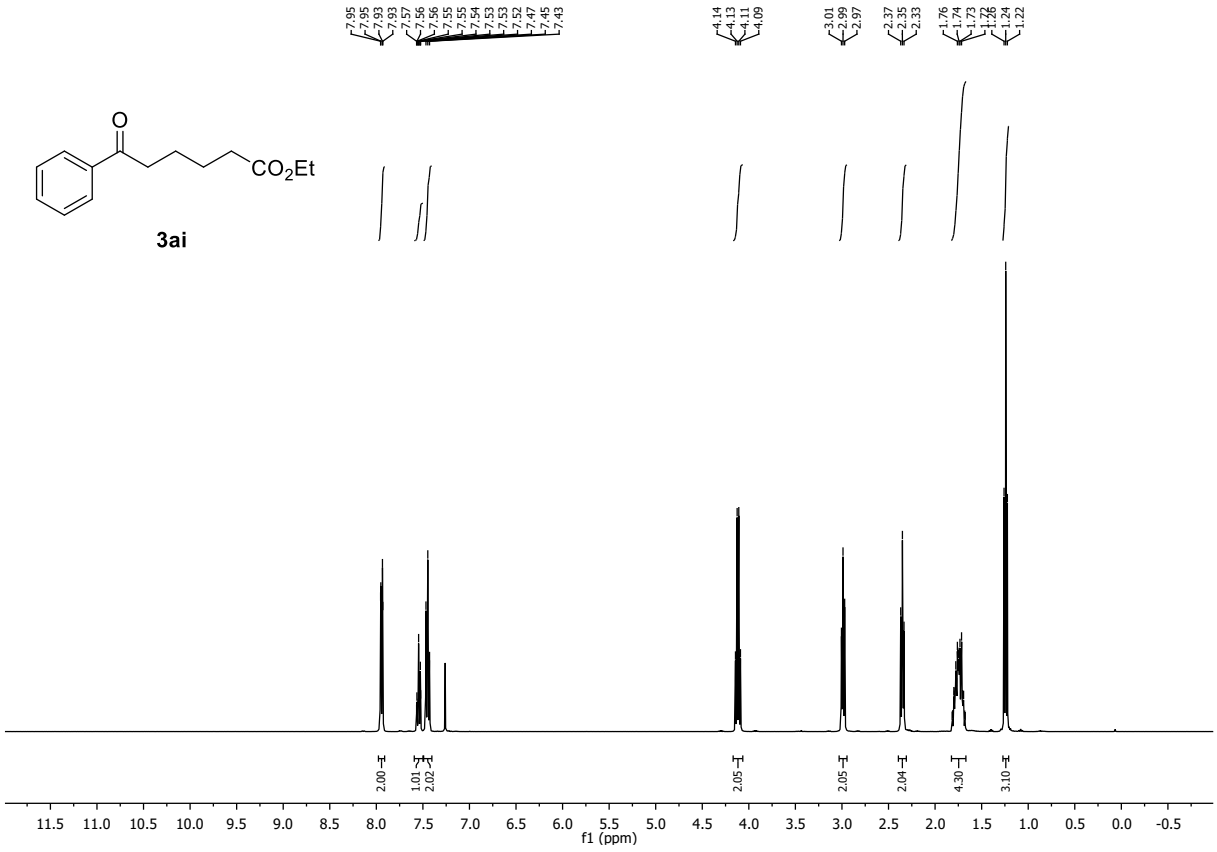

Figure S124. ^{1}H NMR spectrum (400 MHz, $CDCl_3$) of **3ai**.

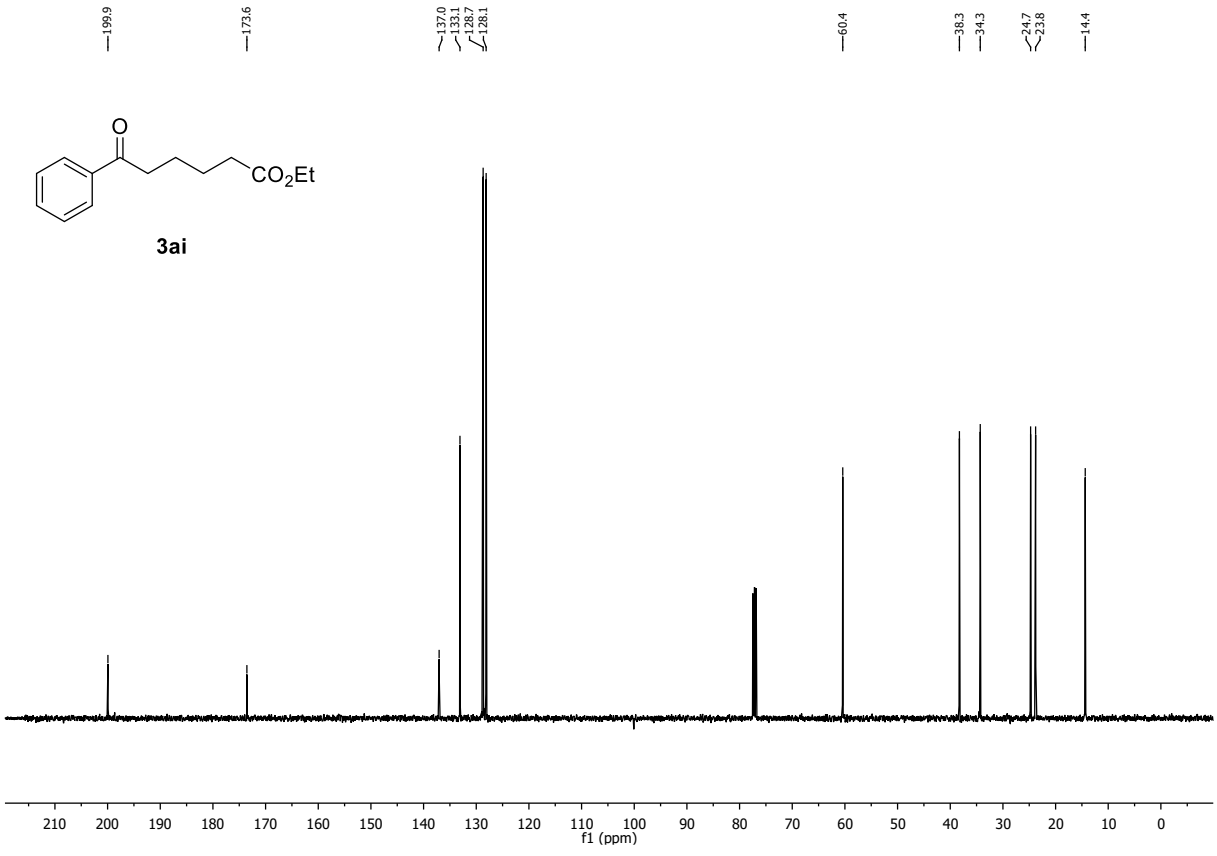

Figure S125. ^{13}C NMR spectrum (101 MHz, $CDCl_3$) of **3ai**.

4-Methyl-1-phenylheptan-3-one (3jj):

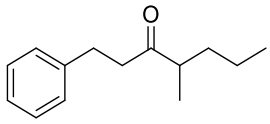

3jj

$C_{14}H_{20}O$ (204.31 g/mol)

Following **GP-B**, **3jj** was synthesized using *S*-phenyl 3-phenylpropanethioate (**1j**) (242 mg, 1.0 mmol, 1.0 equiv.), 2-bromopentane (302 mg, 2.0 mmol, 2.0 equiv.), $NiCl_2 \cdot (H_2O)_6$ (23.8 mg, 0.1 mmol, 10 mol%), 4,4'-di-*tert*-butyl-2,2'-bipyridine (53.7 mg, 0.2 mmol, 20 mol%), zinc powder (131 mg, 2.0 mmol, 2.0 equiv.), sodium chloride (117 mg, 2.0 mmol, 2.0 equiv.) and pyridine (158 mg, 2.0 mmol, 2 equiv.). Purification by flash column chromatography (*n*-hexane/EtOAc gradient 100:0 to 85:15 over 10 CV) afforded **3jj** (106 mg, 519 µmol, 52%) as colorless oil. Conforms to reported analytical data.[30]

R$_f$: 0.61 (*n*-hexane/EtOAc 90:10).

^{1}H NMR (400 MHz, $CDCl_3$, δ): 7.30 – 7.24 (m, 2H), 7.23 – 7.13 (m, 3H), 2.93 – 2.85 (m, 2H), 2.79 – 2.70 (m, 2H), 2.56 – 2.43 (m, 1H), 1.65 – 1.55 (m, 1H), 1.34 – 1.17 (m, 3H), 1.03 (d, *J* = 6.9 Hz, 3H), 0.87 (t, *J* = 7.1 Hz, 3H).

^{13}C{^{1}H} NMR (101 MHz, $CDCl_3$, δ): 214.0, 141.5, 128.6, 128.5, 126.2, 46.4, 42.8, 35.2, 29.9, 20.5, 16.3, 14.2.

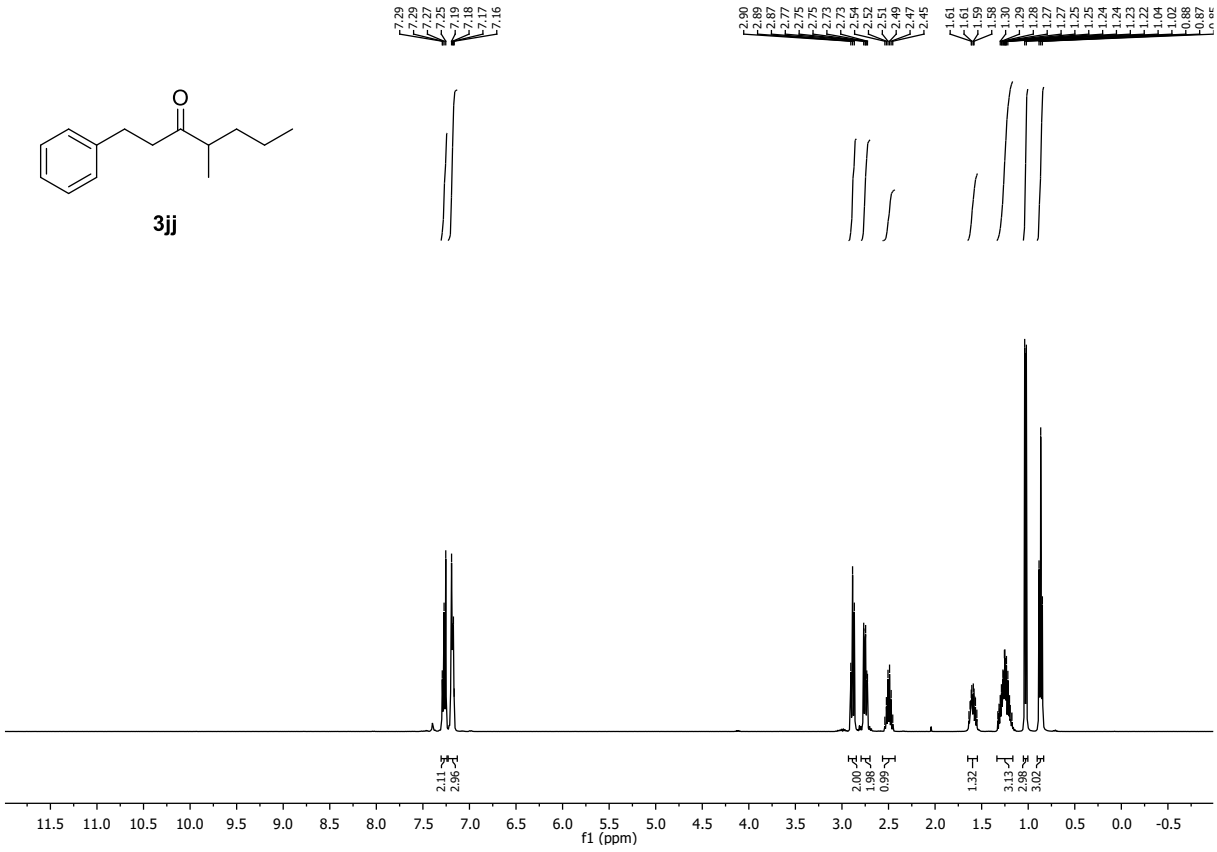

Figure S126. ^{1}H NMR spectrum (400 MHz, $CDCl_3$) of **3jj**.

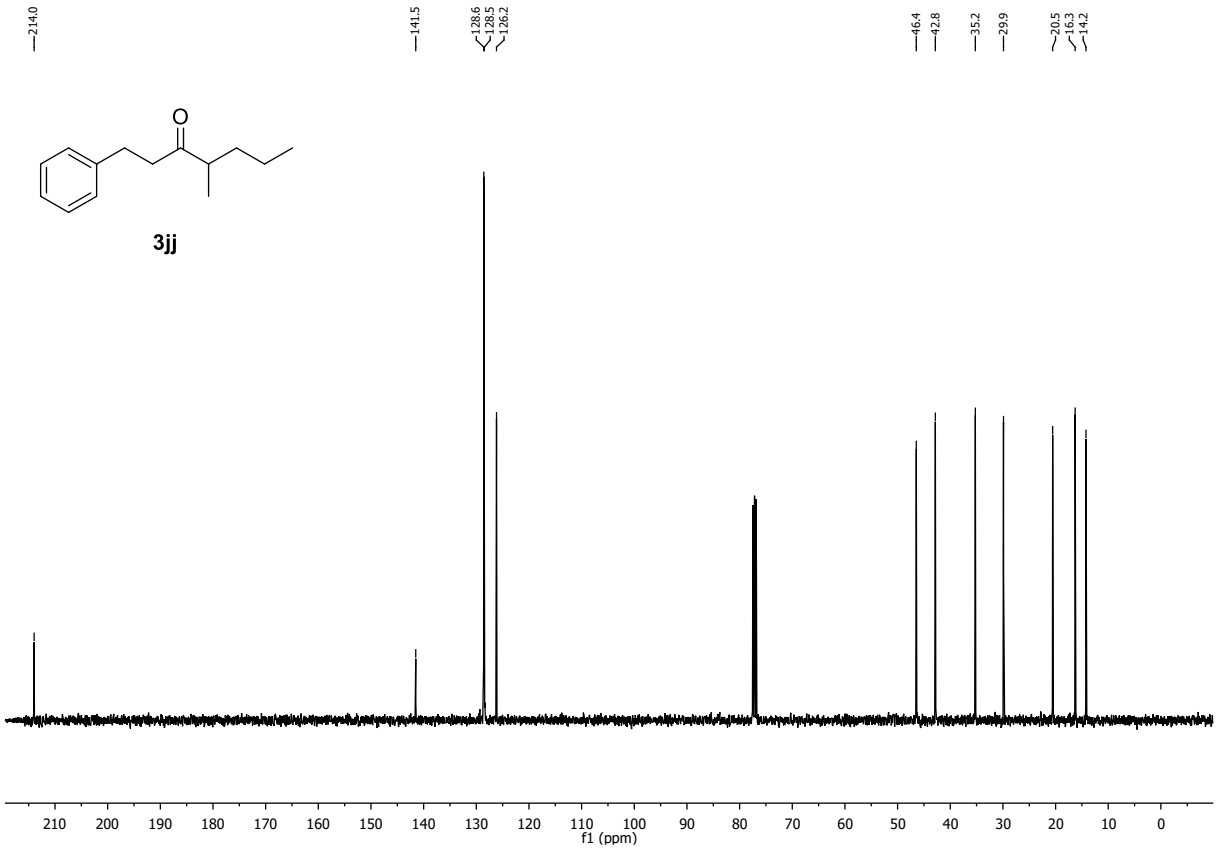

Figure S127. ^{13}C NMR spectrum (101 MHz, $CDCl_3$) of **3jj**.

1-Cyclohexyl-3-phenylpropan-1-one (3jk):

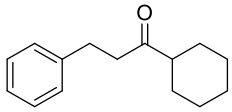

3jk

$C_{15}H_{20}O$ (216.32 g/mol)

Following **GP-B**, **3jk** was synthesized using *S*-Phenyl benzenepropanethioate (**1j**) (242 mg, 1.0 mmol, 1.0 equiv.), bromocyclohexane (326 mg, 2.0 mmol, 2.0 equiv.), $NiCl_2 \cdot (H_2O)_6$ (23.8 mg, 0.1 mmol, 10 mol%), 4,4'-di-*tert*-butyl-2,2'-bipyridine (53.7 mg, 0.2 mmol, 20 mol%), zinc powder (131 mg, 2.0 mmol, 2.0 equiv.), sodium chloride (117 mg, 2.0 mmol, 2.0 equiv.) and pyridine (158 mg, 2.0 mmol, 2 equiv.). Purification by flash column chromatography (*n*-hexane/EtOAc gradient 100:0 to 90:10 over 10 CV) afforded (175 mg, 809 µmol, 81%) as colorless solid. Conforms to reported analytical data.[17]

R_f: 0.60 (*n*-hexane/EtOAc 90:10).

^{1}H NMR (400 MHz, $CDCl_3$, δ): 7.34 – 7.26 (m, 2H), 7.21 – 7.15 (m, 3H), 2.89 (m, 2H), 2.76 (m, 2H), 2.38 – 2.25 (m, 1H), 1.85 – 1.63 (m, 5H), 1.38 – 1.16 (m, 5H).

^{13}C{^{1}H} NMR (101 MHz, $CDCl_3$, δ): 213.2, 141.5, 128.5, 128.4, 126.1, 51.0, 42.3, 29.8, 28.5, 25.9, 25.7.

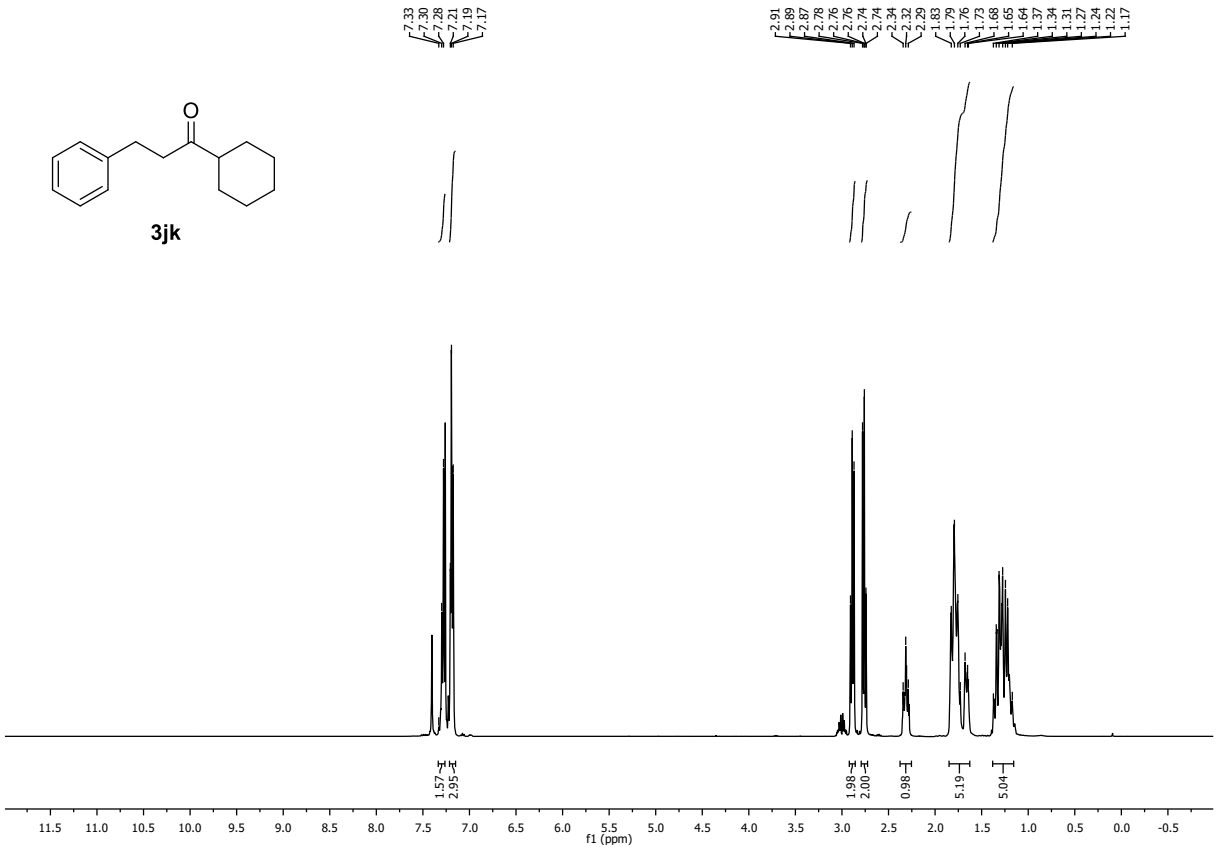

Figure S128. ^{1}H NMR spectrum (400 MHz, $CDCl_3$) of **3jk**.

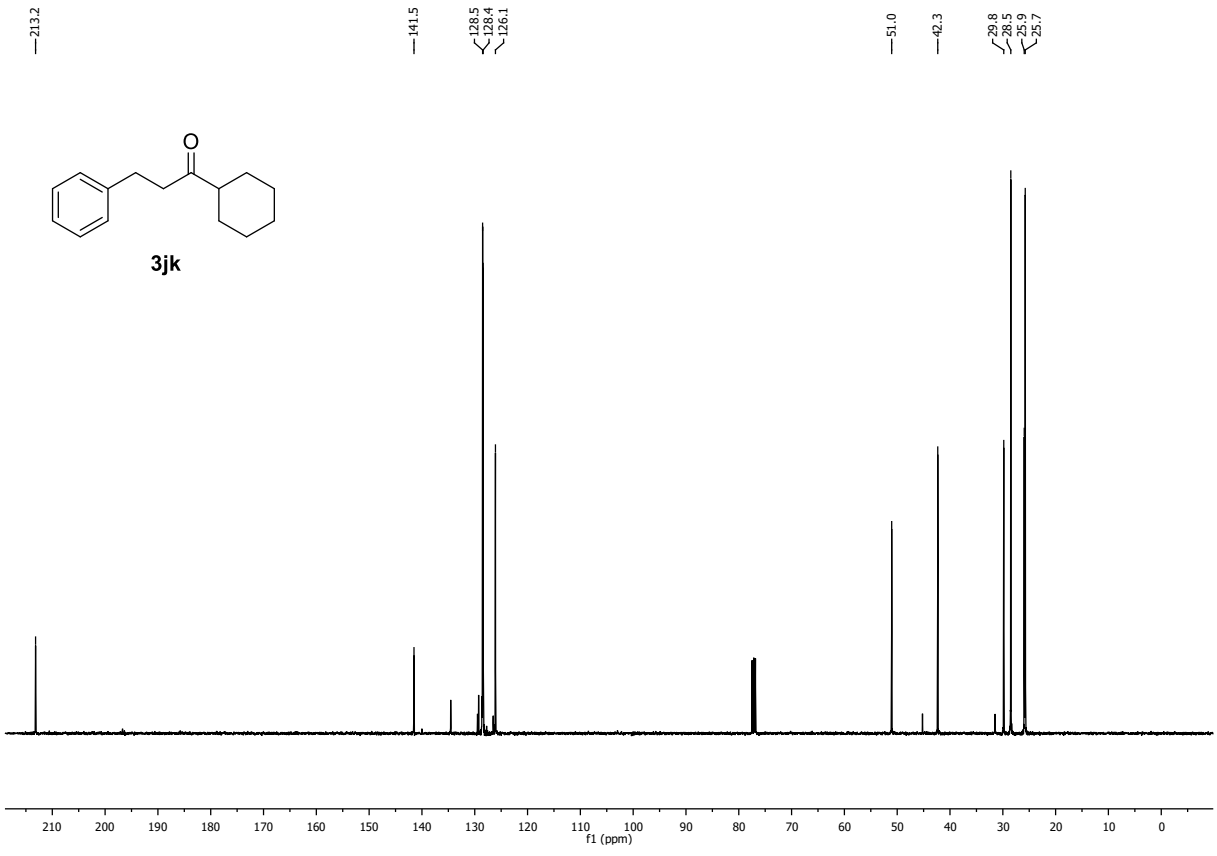

Figure S129. ^{13}C NMR spectrum (101 MHz, $CDCl_3$) of **3jk**.

1-(Oxetan-3-yl)-3-phenylpropan-1-one (3jl):

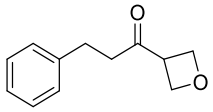

3jl

$C_{12}H_{14}O_2$ (190.24 g/mol)

Following **GP-B**, **3jl** was synthesized using *S*-Phenyl benzenepropanethioate (**1j**) (242 mg, 1.0 mmol, 1.0 equiv.), 3-bromooxethane (274 mg, 2.0 mmol, 2.0 equiv.), $NiCl_2 \cdot (H_2O)_6$ (23.8 mg, 0.1 mmol, 10 mol%), 4,4'-di-*tert*-butyl-2,2'-bipyridine (53.7 mg, 0.2 mmol, 20 mol%), zinc powder (131 mg, 2.0 mmol, 2.0 equiv.), sodium chloride (117 mg, 2.0 mmol, 2.0 equiv.) and pyridine (158 mg, 2.0 mmol, 2 equiv.). Purification by flash column chromatography (*n*-hexane/EtOAc gradient 100:0 to 80:20 over 10 CV) afforded **3jl** (79.1 mg, 416 µmol, 42%) as yellow oil.

R_f: 0.1 (*n*-hexane/EtOAc 90:10).

^{1}H NMR (400 MHz, $CDCl_3$, δ): 7.38 – 7.33 (m, 2H), 7.30 – 7.23 (m, 3H), 4.84 – 4.77 (m, 4H), 3.99 – 3.90 (m, 1H), 3.01 (t, *J* = 7.5 Hz, 2H), 2.80 (t, *J* = 7.5 Hz, 2H).

^{13}C{^{1}H} NMR (101 MHz, $CDCl_3$, δ): 207.0, 140.7, 128.6, 128.3, 126.4, 72.3, 45.4, 42.5, 29.5.

HR-MS (APCI): m/z calc for $[M+H]^+$ 191.10666, found 191.10650 (err. -0.8 ppm).

IR (ATR, $\tilde{\nu}$ [cm^{-1}]): 3058 (w), 3025 (w), 2951 (w), 2879 (w), 1706 (s), 1601 (w), 1493 (w), 1448 (w), 1403 (w), 1370 (m), 1276 (w), 1199 (w), 1154 (w), 1109 (m), 1079 (w), 1027 (w), 978 (s), 908 (m), 859 (w), 815 (w), 744 (s), 699 (s).

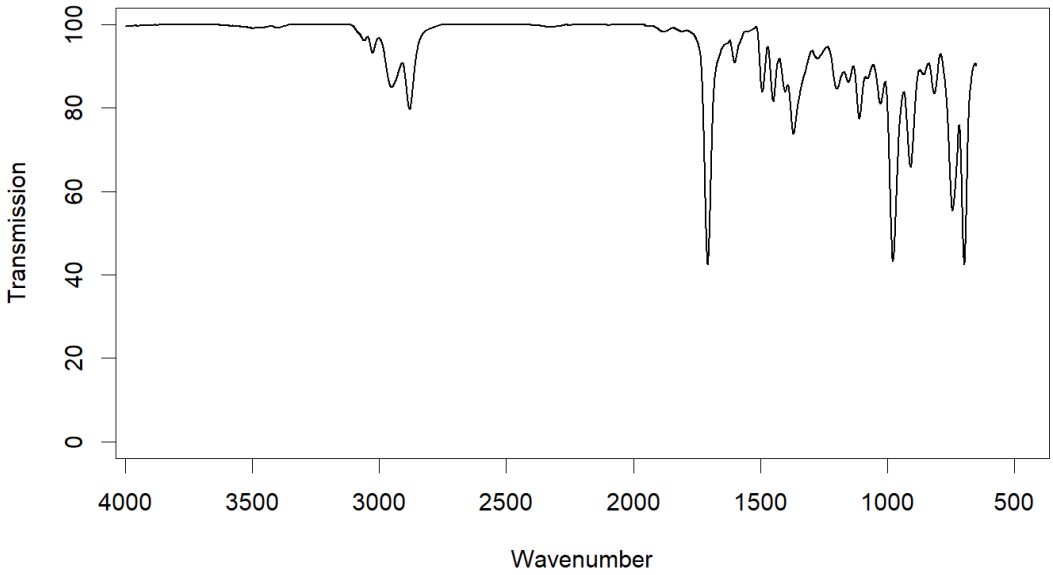

Figure S130. IR spectrum (ATR, neat) of **3jl**.

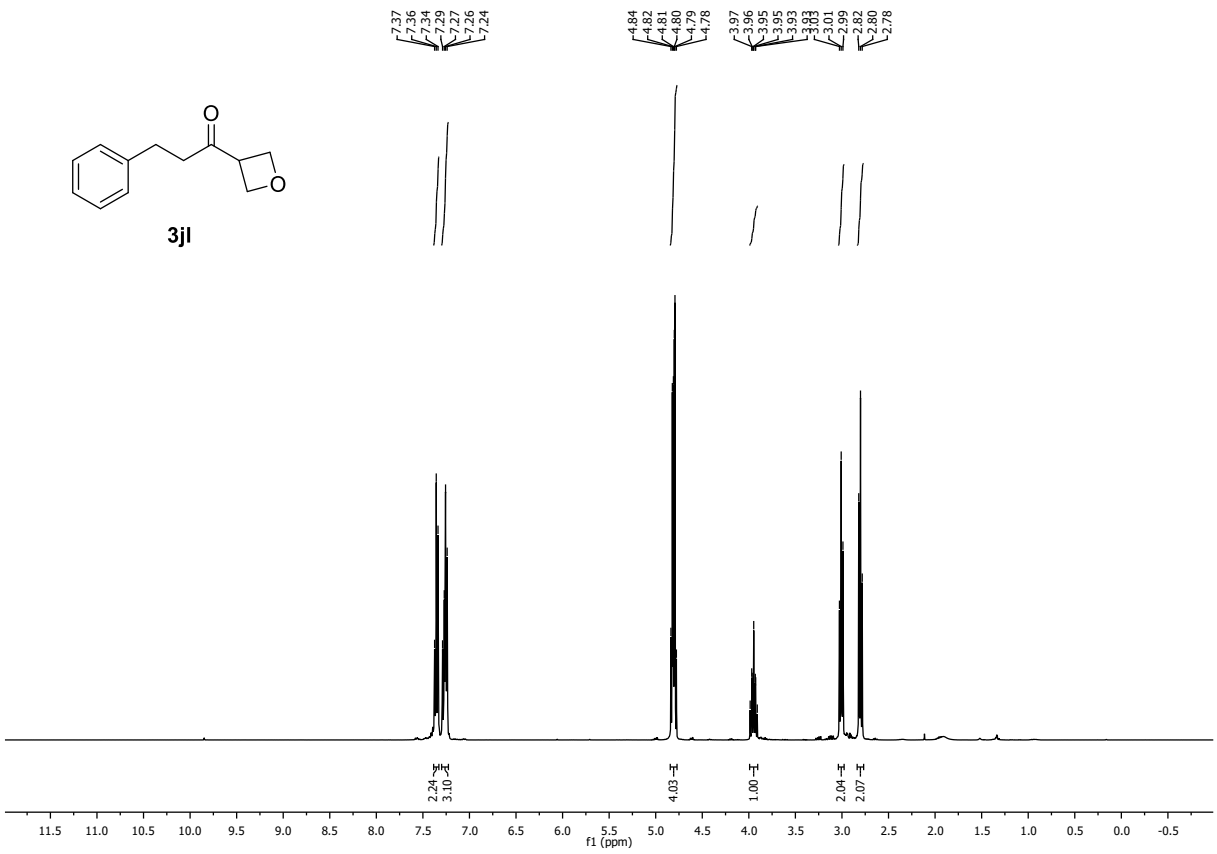

Figure S131. ^{1}H NMR spectrum (400 MHz, $CDCl_3$) of **3jl**.

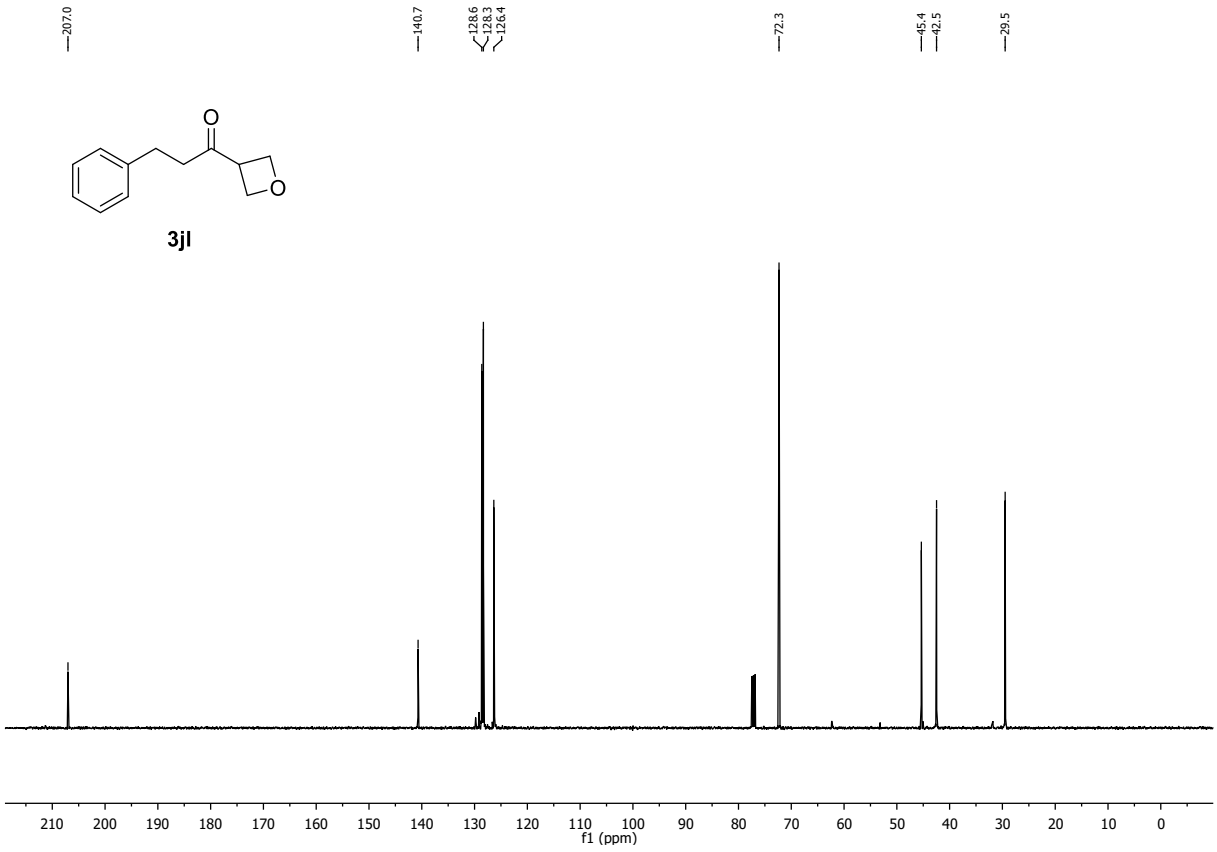

Figure S132. ^{13}C NMR spectrum (101 MHz, $CDCl_3$) of **3jl**.

1-Phenylpent-4-en-1-one (3an):

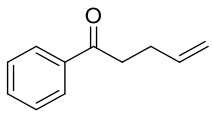

3an

$C_{11}H_{12}O$ (160.22 g/mol)

Following **GP-B**, **3an** was synthesized using *S*-phenyl benzothioate (**1a**) (214 mg, 1.0 mmol, 1.0 equiv.), (bromomethyl)cyclopropane (270 mg, 2.0 mmol, 2.0 equiv.), $NiCl_2 \cdot (H_2O)_6$ (23.8 mg, 0.1 mmol, 10 mol%), 4,4'-di-*tert*-butyl-2,2'-bipyridine (53.7 mg, 0.2 mmol, 20 mol%), zinc powder (131 mg, 2.0 mmol, 2.0 equiv.), sodium chloride (117 mg, 2.0 mmol, 2.0 equiv.) and pyridine (158 mg, 2.0 mmol, 2 equiv.). Purification by flash column chromatography (*n*-hexane/EtOAc gradient 100:0 to 90:10 over 10 CV) afforded **3an** (55 mg, 343 µmol, 34%) as colorless oil. Conforms to reported analytical data.[31]

R$_f$: 0.61 (*n*-hexane/EtOAc 90:10).

^{1}H NMR (400 MHz, $CDCl_3$, δ): 7.99 – 7.93 (m, 2H), 7.58 – 7.51 (m, 1H), 7.48 – 7.42 (m, 2H), 5.98 – 5.83 (m, 1H), 5.14 – 4.97 (m, 2H), 3.07 (t, *J* = 7.4 Hz, 2H), 2.55 – 2.44 (m, 2H).

^{13}C{^{1}H} NMR (101 MHz, $CDCl_3$, δ): 199.5, 137.4, 137.0, 133.1, 128.7, 128.1, 115.4, 37.8, 28.2.

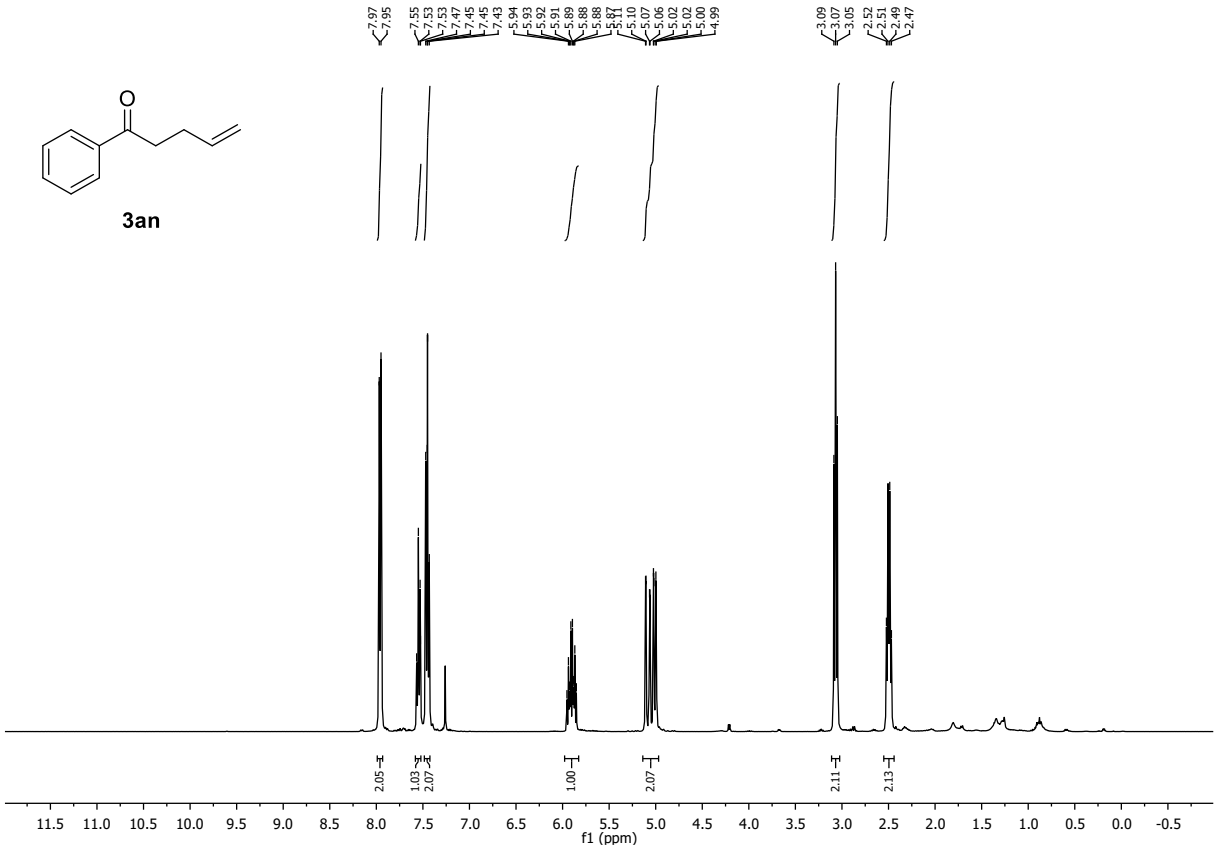

Figure S133. ^{1}H NMR spectrum (400 MHz, $CDCl_3$) of **3an**.

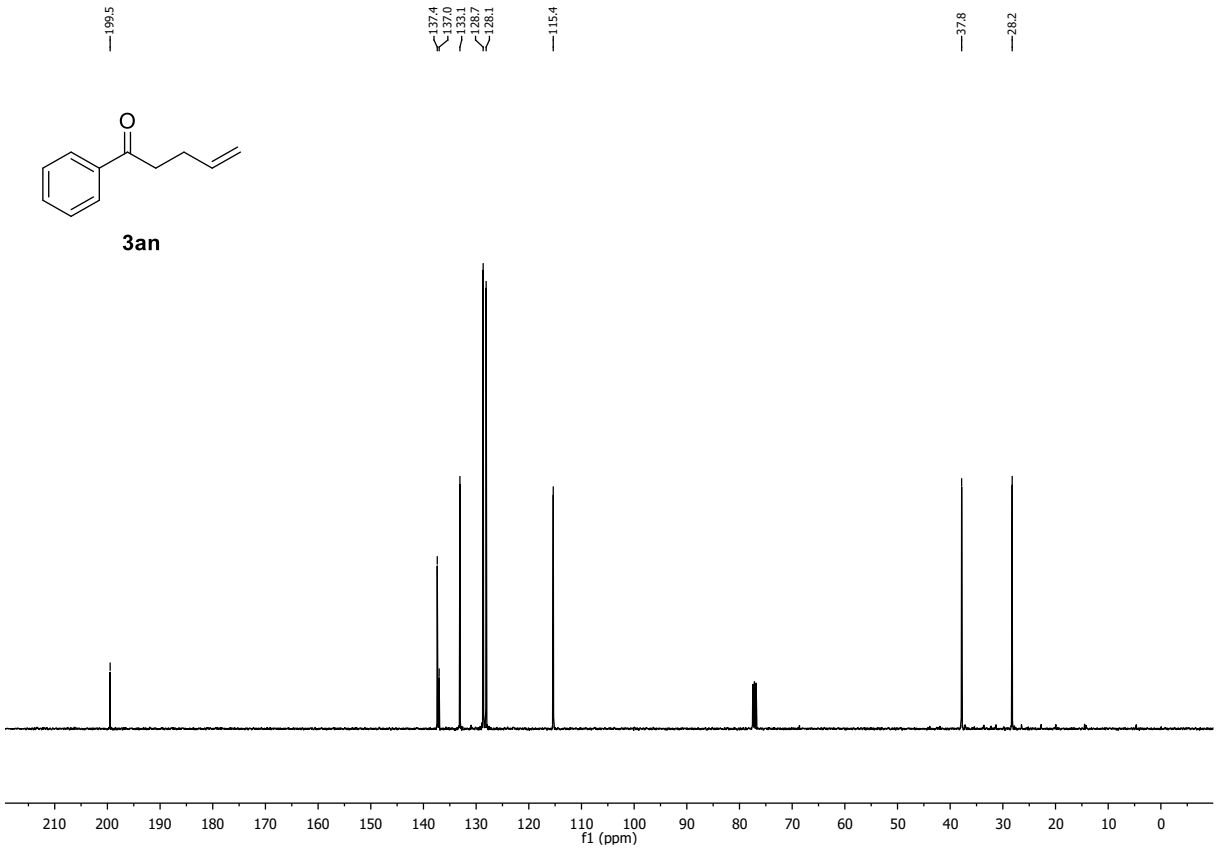

Figure S134. ^{13}C NMR spectrum (101 MHz, $CDCl_3$) of **3an**.

Ethyl 4-oxo-4-phenylbutanoate (5):

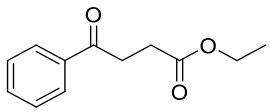

5

$C_{12}H_{14}O_3$ (206.24 g/mol)

5 was obtained from the mechanistic experiment, following **GP-B** (1 mmol scale), but adding ethyl acrylate (300 mg, 2.0 mmol, 2 equiv.) to the reaction. Purification by flash column chromatography (*n*-hexane/EtOAc gradient 100:0 to 80:20 over 10 CV) afforded **5** as colorless oil (67 mg, 325 µmol, 33%). Conforms to reported analytical data.[32]

R_f: 0.52 (*n*-hexane/EtOAc 80:20).

^{1}H NMR (400 MHz, $CDCl_3$, δ): 8.02 – 7.94 (m, 2H), 7.60 – 7.51 (m, 1H), 7.45 (m), 4.15 (q, *J* = 7.1 Hz, 2H), 3.30 (t, *J* = 6.6 Hz, 2H), 2.75 (t, *J* = 6.6 Hz, 2H), 1.25 (t, *J* = 7.1 Hz, 3H).

^{13}C{^{1}H} NMR (101 MHz, $CDCl_3$, δ): 198.2, 173.0, 136.7, 133.3, 128.7, 128.1, 60.7, 33.5, 28.4, 14.3.

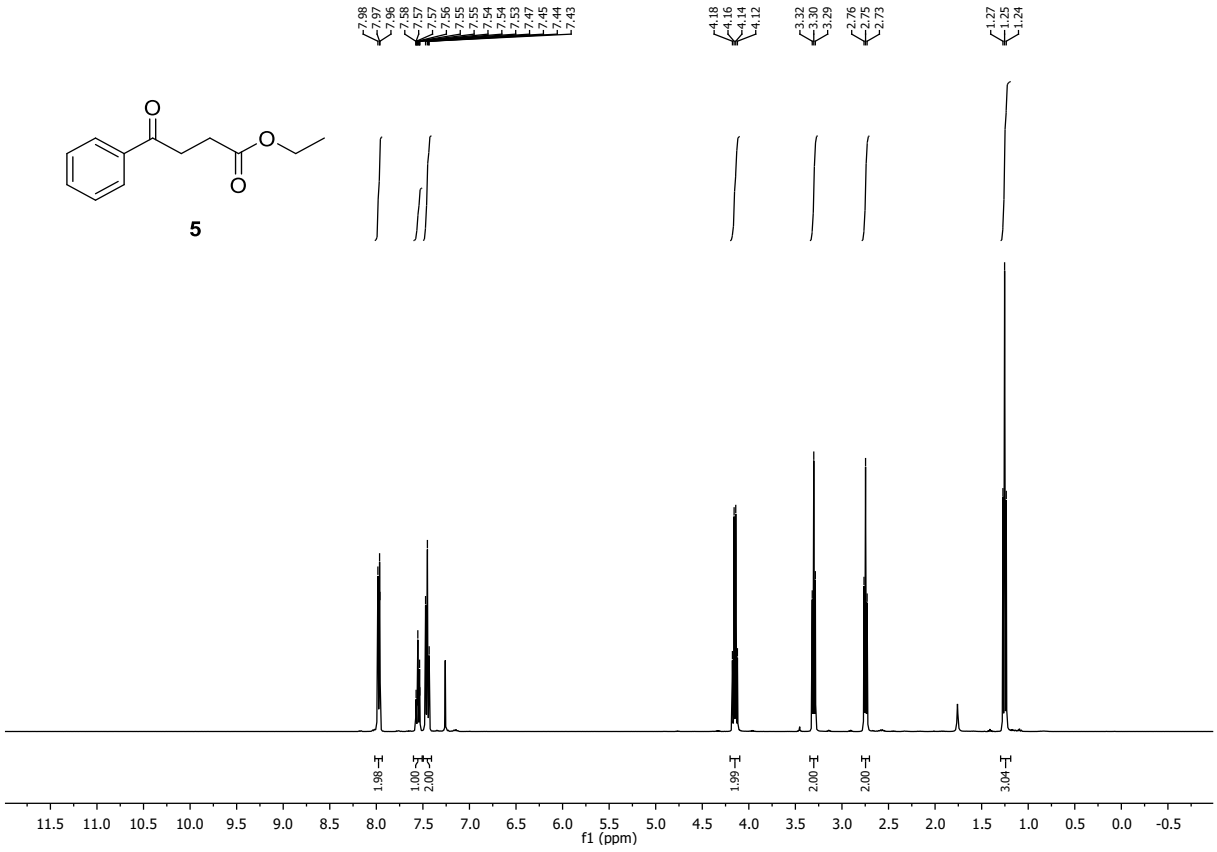

Figure S135. ^{1}H NMR spectrum (400 MHz, $CDCl_3$) of **5**.

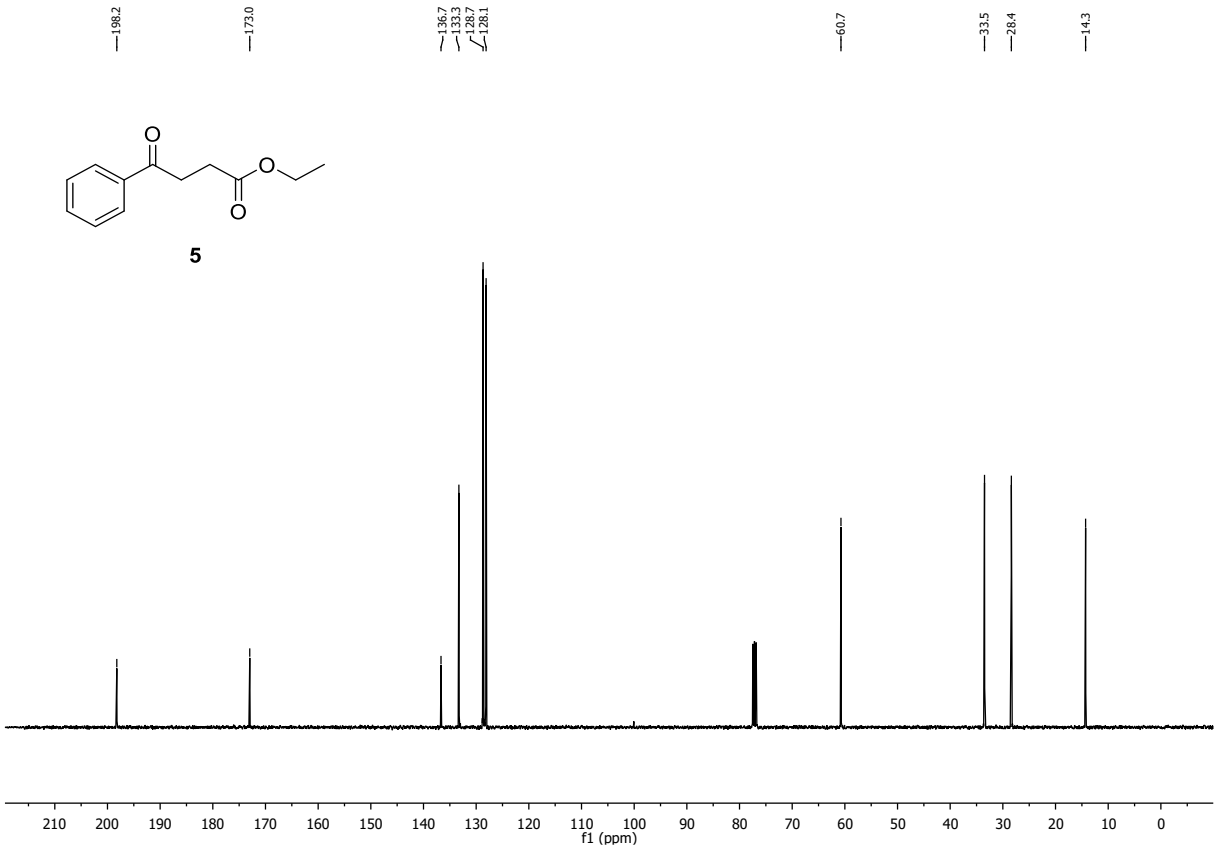

Figure S136. ^{13}C NMR spectrum (101 MHz, $CDCl_3$) of **5**.

6. Unsuccessful Substrates

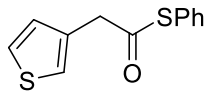

benzylic thioester
(many side products)

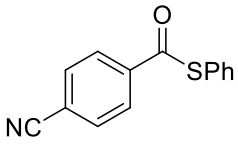

very electron-poor
(decarbonylation)

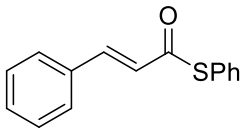

conjugated thioester
(side-reactions)

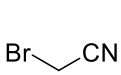

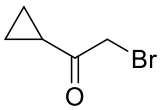

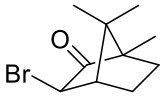

activated bromides

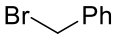

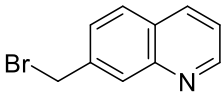

benzylic bromides

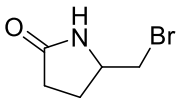

amides

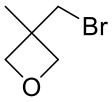

sterically hindered bromides

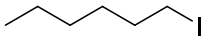

alkyl iodides
(homocoupling)

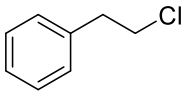

alkyl chlorides
(low conv.)
up to 25% yield with addition of NBu_4I (2 equiv.)

7. Crystallographic Data

Suitable crystals were selected in a glovebox and coated with perfluoropolyalkylether (1800 cSt). X-ray data were collected on a XtaLAB Synergy, Dualflex, HyPix diffractometer (Cu K_α (λ = 1.54184 Å)) at 149.99 K. The structures were solved with the ShelXT 2018/2 solution program[33] using dual methods and by using Olex2 1.5 as the graphical interface.[34] The model was refined with olex2.refine 1.5[35] using full matrix least squares minimization on $\boldsymbol{F^2}$.

Ni2a.

Suitable crystals were obtained by layering a THF solution of **Ni2** with n-hexane and placing the mixture in a glovebox freezer at -40 °C. A clear red block-shaped crystal of **Ni2a** with dimensions 0.07 × 0.06 × 0.04 mm was used for data collection.

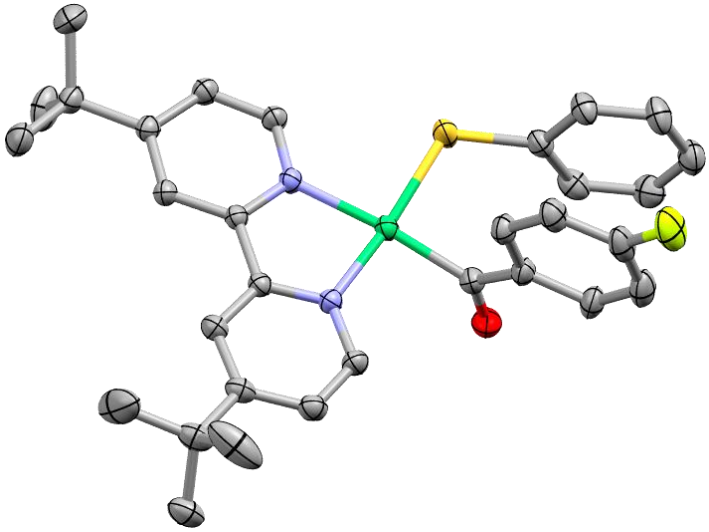

Compound	**IL190925V2**
Formula	$C_{31}H_{33}FN_2NiOS$
CCDC	2491069
$D_{calc.}$/ g cm^{-3}	1.339
μ/mm^{-1}	1.973
Formula Weight	559.378
Colour	clear red
Shape	block-shaped
Size/mm	0.07×0.06×0.04
T/K	149.99(11)
Crystal System	monoclinic
Space Group	$P2_1/n$
a/Å	11.9419(1)
b/Å	12.3816(1)
c/Å	18.7832(2)
α/°	90
β/°	92.574(1)
γ/°	90
V/Å^3	2774.48(4)
Z	4
Z'	1
Wavelength/Å	1.54184
Radiation type	Cu K_α
Θ_{min}/°	4.28
Θ_{max}/°	79.95
Measured Refl's.	65892
Indep't Refl's	6023
Refl's I≥2σ(I)	5517
R_{int}	0.0304
Parameters	632
Restraints	0
Largest Peak/eÅ^3	0.3744
Deepest Hole/eÅ^3	-0.3339
GooF	1.0428
wR_2 (all data)	0.0571
wR_2	0.0556
R_1 (all data)	0.0252
R_1	0.0222

8. GC-FID Calibration Data

The quantification of GC-yields was achieved by adding a standard compound (*n*-pentadecane) to reaction mixtures before quenching and applying the general formula:

$$\frac{\mathrm{A(compound)}}{\mathrm{A(standard)}} = R \times \frac{\mathrm{(compound)}}{\mathrm{m(standard)}}$$

R: Response factor of compound
A: Peak area determined by GC-FID
m: mass of compound

The R values were determined by GC calibrations of respective compounds with *n*-pentadecane in ethyl acetate and measuring different mass ratios.

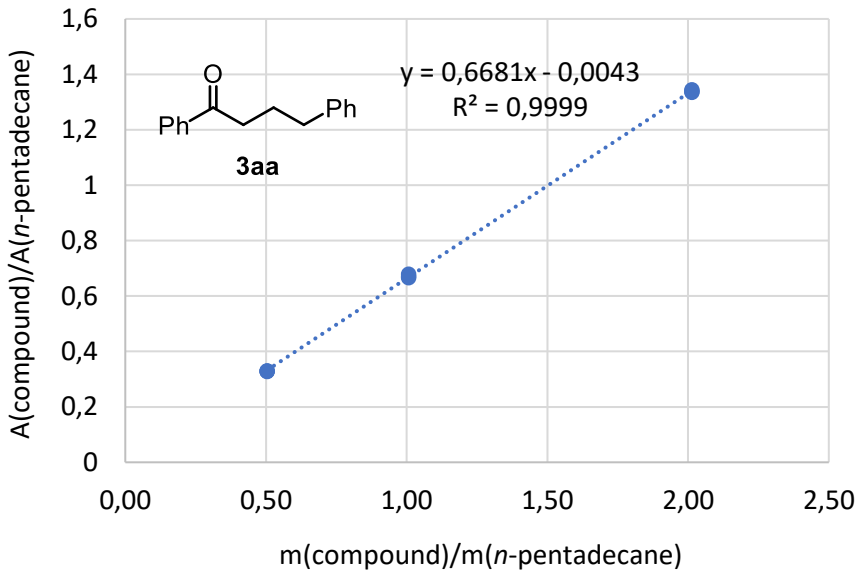

Entry	**m**(**3aa**) [mg]	**m**(standard) [mg]	**A**(**3aa**) [a.u.]	**A**(standard) [a.u.]
1	2.48	1.23	7449	5541
2	2.48	1.23	7636	5720
3	2.48	1.23	7806	5833
4	2.48	1.23	5665	8439
5	2.48	1.23	5702	8402
6	2.48	1.23	5736	8605
7	1.24	2.46	3828	11671
8	1.24	2.46	3834	11643
9	1.24	2.46	3853	11667

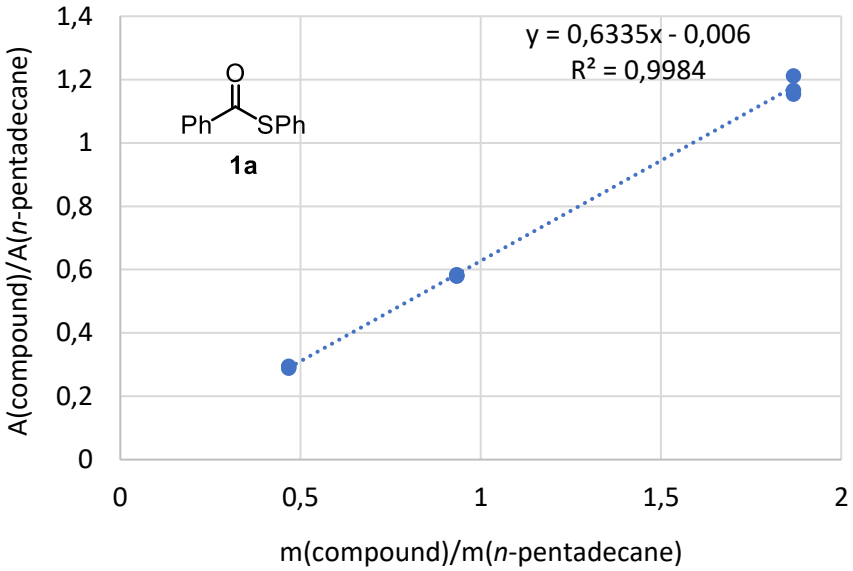

Entry	**m(1a)** [mg]	**m**(standard) [mg]	**A(1a)** [a.u.]	**A**(standard) [a.u.]
1	4.04	2.16	11437	9802
2	4.04	2.16	11700	9653
3	4.04	2.16	11765	10189
4	4.04	2.16	8435	14539
5	4.04	2.16	8392	14364
6	4.04	2.16	8488	14626
7	2.02	4.33	5556	19225
8	2.02	4.33	5734	19418
9	2.02	4.33	5552	18998

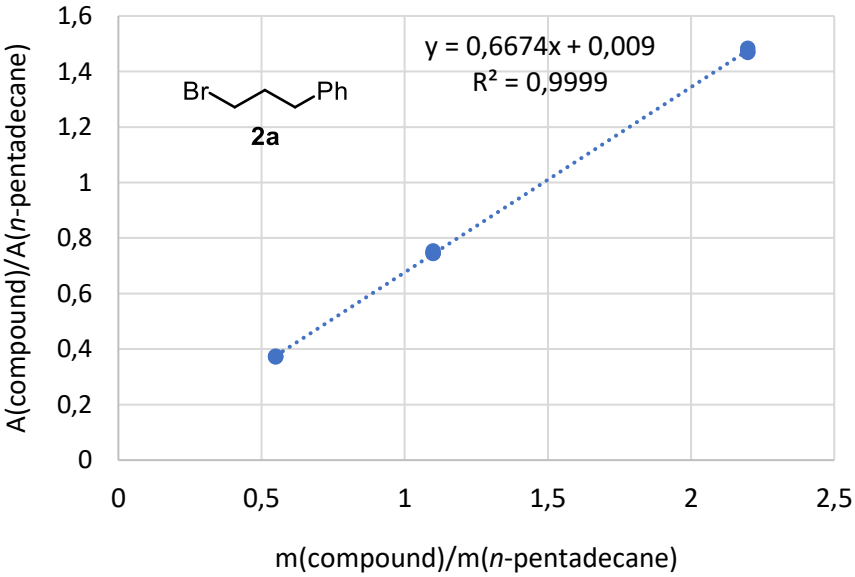

Entry	**m(2a)** [mg]	**m**(standard) [mg]	**A(2a)** [a.u.]	**A**(standard) [a.u.]
1	3.28	1.49	10241	6973
2	3.28	1.49	10141	6891
3	3.28	1.49	10414	7021
4	3.28	1.49	7598	10092

5	3.28	1.49	7552	10154
6	3.28	1.49	7585	10174
7	1.64	2.98	5153	13792
8	1.64	2.98	5148	13817
9	1.64	2.98	5117	13781

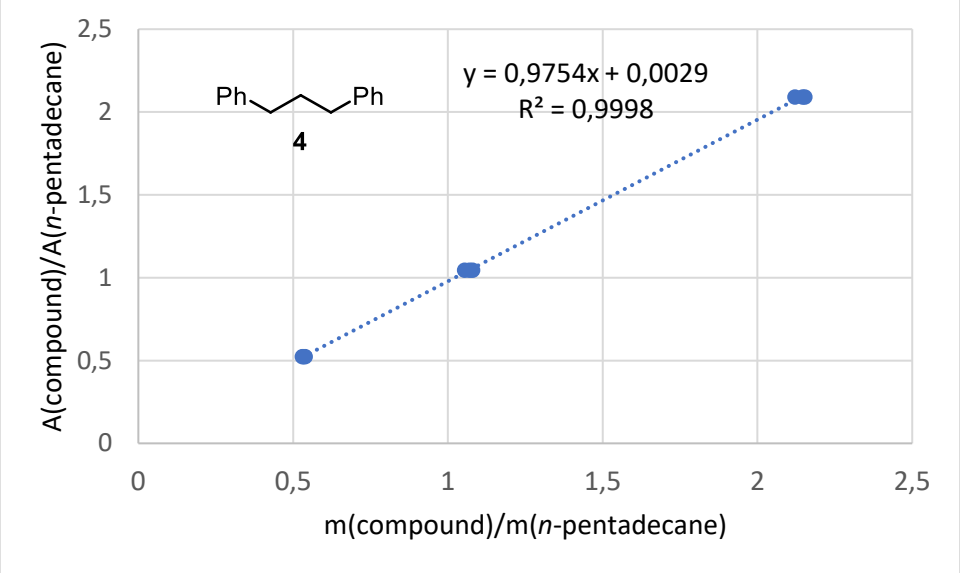

Entry	**m(4)** [mg]	**m**(standard) [mg]	**A(4)** [a.u.]	**A**(standard) [a.u.]
1	2.71	5.18	7067	13247
2	2.71	5.18	6864	12745
3	2.71	5.18	7354	13901
4	2.71	2.59	6610	6277
5	2.71	2.59	6915	6470
6	2.71	2.59	6561	6078
7	5.42	2.59	14176	6607
8	5.42	2.59	13872	6540
9	5.42	2.59	15661	7274

9. References

1. G. R. Fulmer, A. J. M. Miller, N. H. Sherden, H. E. Gottlieb, A. Nudelman, B. M. Stoltz, J. E. Bercaw and K. I. Goldberg, *Organometallics*, 2010, **29**, 2176-2179.
2. H. Cao, X. Liu, F. Bie, Y. Shi, Y. Han, P. Yan, M. Szostak and C. Liu, *J. Org. Chem.*, 2021, **86**, 10829-10837.
3. B. Neises and W. Steglich, *Angew. Chem., Int. Ed.*, 1978, **17**, 522-524.
4. D. C. Batesky, M. J. Goldfogel and D. J. Weix, *J. Org. Chem.*, 2017, **82**, 9931-9936.
5. L. S. Liebeskind and J. Srogl, *J. Am. Chem. Soc.*, 2000, **122**, 11260-11261.
6. C. N. Prieto Kullmer, J. A. Kautzky, S. W. Krska, T. Nowak, S. D. Dreher and D. W. C. MacMillan, *Science*, 2022, **376**, 532-539.
7. A. C. Jones, M. T. J. Williams, L. C. Morrill and D. L. Browne, *ACS Catal.*, 2022, **12**, 13681-13689.
8. J. Yin, R. T. Stark, I. A. Fallis and D. L. Browne, *J. Org. Chem.*, 2020, **85**, 2347-2354.
9. P. Blakskjær, B. Høj, D. Riber and T. Skrydstrup, *J. Am. Chem. Soc.*, 2003, **125**, 4030-4031.
10. P. H. Gehrtz, P. Kathe and I. Fleischer, *Chem. Eur. J.*, 2018, **24**, 8774-8778.
11. F. Bie, X. Liu, H. Cao, Y. Shi, T. Zhou, M. Szostak and C. Liu, *Org. Lett.*, 2021, **23**, 8098-8103.
12. J. Xu, F. Lu, L. Sun, M. Huang, J. Jiang, K. Wang, D. Ouyang, L. Lu and A. Lei, *Green Chemistry*, 2022, **24**, 7350-7354.
13. J. Su, A. Chen, G. Zhang, Z. Jiang and J. Zhao, *Org. Lett.*, 2023, **25**, 8033-8037.
14. S. Yang, X. Yu and M. Szostak, *ACS Catal.*, 2023, **13**, 1848-1855.
15. L.-W. Pan, N. Taniguchi, M. Hyodo and I. Ryu, *Eur. J. Org. Chem.*, 2024, **27**, e202400138.
16. C. Wang, S. Mavila, B. T. Worrell, W. Xi, T. M. Goldman and C. N. Bowman, *ACS Macro Lett.*, 2018, **7**, 1312-1316.
17. C. Guo, Z.-Y. Wang, W.-H. Liu, S.-Z. Liu, Y.-Z. Cheng, Q. Li and J. Dou, *Org. Biomol. Chem.*, 2025, **23**, 6100-6105.
18. W. Sun, L. Wang, Y. Hu, X. Wu, C. Xia and C. Liu, *Nat. Comm.*, 2020, **11**, 3113.
19. Z.-H. Xia, C.-L. Zhang, Z.-H. Gao and S. Ye, *Org. Lett.*, 2018, **20**, 3496-3499.
20. H. Chen, H. Yue, C. Zhu and M. Rueping, *Angew. Chem. Int. Ed.*, 2022, **61**, e202204144.
21. J. Zhuo, Y. Zhang, Z. Li and C. Li, *ACS Catal.*, 2020, **10**, 3895-3903.
22. Q.-Z. Li, M.-H. He, R. Zeng, Y.-Y. Lei, Z.-Y. Yu, M. Jiang, X. Zhang and J.-L. Li, *J. Am. Chem. Soc.*, 2024, **146**, 22829-22839.
23. J. Ni, X. Xia, D. Gu and Z. Wang, *J. Am. Chem. Soc.*, 2023, **145**, 14884-14893.
24. V. J. Geiger, G. Lefèvre and I. Fleischer, *Chem. Eur. J.*, 2022, **28**, e202202212.
25. B. D. W. Allen, M. D. Hareram, A. C. Seastram, T. McBride, T. Wirth, D. L. Browne and L. C. Morrill, *Org. Lett.*, 2019, **21**, 9241-9246.
26. G. A. Molander and L. Jean-Gérard, *J. Org. Chem.*, 2009, **74**, 1297-1303.
27. Y.-S. Hon, Y.-C. Wong, C.-P. Chang and C.-H. Hsieh, *Tetrahedron*, 2007, **63**, 11325-11340.
28. N. Iwasawa, S. Hayakawa, M. Funahashi, K. Isobe and K. Narasaka, *Bull. Chem. Soc. Jpn.*, 2006, **66**, 819-827.
29. H. Xin, X.-H. Duan, L. Liu and L.-N. Guo, *Chem. Eur. J.*, 2020, **26**, 11690-11694.
30. K. Miyashita and T. Satoh, *Tetrahedron*, 2005, **61**, 5067-5080.
31. J. C. L. Walker and M. Oestreich, *Org. Lett.*, 2018, **20**, 6411-6414.
32. A. Kondoh, K. Odaira and M. Terada, *Angew. Chem. Int. Ed.*, 2015, **54**, 11240-11244.
33. G. Sheldrick, *Acta Crystallogr. A*, 2015, **71**, 3-8.
34. O. V. Dolomanov, L. J. Bourhis, R. J. Gildea, J. A. K. Howard and H. Puschmann, *J. Appl. Crystallogr.*, 2009, **42**, 339-341.
35. L. J. Bourhis, O. V. Dolomanov, R. J. Gildea, J. A. Howard and H. Puschmann, *Acta Crystallogr A Found Adv*, 2015, **71**, 59-75.